The University Of Sheffield.

Experimental Process Development and Techno-economic Assessment of In-Situ Biomethanation of Carbon Dioxide in Biowaste Anaerobic Digesters

By

Arman **SASTRAATMAJA**

Supervisors:

Prof Mohamed Pourkashanian, Prof Derek Ingham,

Dr Davide Poggio, Dr Mark Walker

A Thesis submitted in accordance of the requirements for the degree of

Doctor of Philosophy

February 2022

ABSTRACT

Biomethanation of carbon dioxide has recently emerged as a competitive technology for upgrading biogas produced from the anaerobic digestion of biowastes. In this configuration, carbon dioxide in biogas is reduced to methane through a biological reaction with hydrogen, resulting in several benefits: increased carbon efficiency, decarbonisation of the natural gas grid and transport, and potentially storage of renewable electricity in the form of high-energy-density fuel.

In-situ biomethanation combines conventional biogas production from organic matter with the addition of H_2 to produce a higher quality biomethane gas through retrofitting existing anaerobic digestion (AD) infrastructure. However, process engineering challenges remain to the uptake of in-situ biomethanation especially surrounding its continuous operation, control, and economic viability, which are addressed by this research using lab-based and techno-economic studies.

An automated rig for the study of continuous in-situ biomethanation, including a monitoring and control system for control of the H_2 injection rate to maintain process stability, was designed, commissioned and operated across a series of experiments to study the dynamics and performance of in-situ biomethanation alongside AD of sewage sludge (SS) and food waste (FW). This configuration would correspond to the retrofit of existing industrial-scale AD reactors, maintaining the typical plants' operational strategies and gas storage characteristics (size and pressure).

Effects investigated experimentally included: H_2 injection systems, gas recirculation and stirring intensity, and variation of the organic loading rate (OLR). All results highlighted the rate-limiting effect of H_2 gas-liquid mass transfer, implied by a lack of evidence of biological limitation or inhibition and a relatively high equilibrium H_2 content (11-36 % vol.) in the headspace appearing requisite to the gas-liquid transfer.

Using a porous sparger as an improved injection system, a higher gas recirculation rate and mechanical stirring intensity improved the H_2 conversion and methane evolution rate (MER). In the case of sewage sludge, the highest MER achieved was 0.16 $LL^{-1}day^{-1}$, with H_2 conversion at 75 %, while in the case of FW, the highest MER was 0.23 $LL^{-1}day^{-1}$ with H_2 conversion at 66.3 %. The importance of the OLR on the achievable H_2 conversion was also highlighted and rationalised by its relationship with the gas Retention Time (RT). When operating the digesters at a reduced OLR of 1 gVS L^{-1} day^{-1}, higher H_2 conversion was achieved, up to 94 % for SS and 87 % for FW. However, that resulted in a trade-off with lower MER values, at 0.1 $LL^{-1}day^{-1}$ for SS and 0.16 $LL^{-1}day^{-1}$ for FW.

The techno-economic work modelled the economic viability of in-situ biomethanation in the current market conditions. The analysis considered a hypothetical consumer tariff linked to the wholesale (variable) electricity price, allowing scheduling of hydrogen production from lower-cost electricity. Scenarios were investigated using different electrolyser technologies, varying electrolyser sizes, and biomethane end-use. The economic assessment showed the sale price of biomethane ranging from £94-110 /MWh across all scenarios in current market conditions, with electricity price and electrolyser costs being the most influential parameters on the results.

ACKNOWLEDGEMENTS

I would like to express my gratitude to the supervisory team: Dr Davide Poggio, Dr Mark Walker, Prof Derek Ingham and Prof M. Pourkashanian for their support, dedication, guidance and knowledge of the subject in this research. Very much appreciation send to the technical support Dmitry Govorukhin and Chris Todd for their support and effort in building the experimental rig in the anaerobic digestion laboratory. The author also would like to express the greatest acknowledgement to Indonesia Endowment Fund for Education (LPDP) for their financial support in completing this PhD.

Special thanks and love to my wife, Titi, who has dedicated her time and never-ending support to the author for finishing this PhD; you have been amazing. Thanks also to my parents, families and friends in Indonesia who always send support and stories that make distance not really matter. Finally, to the Indonesian community in Sheffield for unforgettable memories in the past five years.

CONTENTS

LIST OF FIGURES

LIST OF TABLES

LIST OF ABBREVIATIONS

AD	Anaerobic Digestion
AEL	Alkaline Electrolysis
AM	Acetoclastic Methanogen
BA	Bicarbonate Alkalinity
BMP	Biomethane Potential
COD	Chemical Oxygen Demand
CSTR	Continuous Stirred Tank Reactor
FAN	Free Ammonia Nitrogen
GC	Gas Chromatography
HM	Hydrogenotrophic Methanogens
IA	Intermediate Alkalinity
LCOE	Levelised Cost of Energy
MER	Methane Evolution Rate
MFC	Mass Flow Controller
MS	Mass Spectrometry
NPV	Nett Present Value
PEM	Polymer Electrolyte Membrane
OFMSW	Organic Fraction of Municipal Solid Waste
OLR	Organic Loading Rate
PA	Partial Alkalinity
ROC	Renewable Obligation Certificate
RT	Retention Rime
RTFC	Renewable Transport Fuel Certificates
SCADA	Supervisory control and data acquisition
SOEC	Solid oxide electrolyzer cell
TA	Total Alkalinity
TAN	Total Ammonia Nitrogen
TS	Total Solid
UASB	Up flow Anaerobic Sludge Blanket
UK	United Kingdom
VFA	Volatile Fatty Acid
VS	Volatile Solid

LIST OF CHEMICAL FORMULA AND SYMBOL

CH_4	Methane
CO_2	Carbon Dioxide
H_2	Hydrogen
H_2O	Water
HCO_3^-	Bicarbonate ion
$k_L a$	Gas-liquid mass transfer coefficient
NH_3	Ammonia
NH_4^+	Ammonium Ion

1. INTRODUCTION

1.1 Anaerobic Digestion as a Renewable Energy Technology

Technological developments in the last two decades have made energy an essential part of our lifestyle. However, current energy use is one of the causes of global climate change because most of the energy comes from fossil fuels (coal, oil and natural gas). The International Energy Agency (IEA) statistical records show that more than 80 % of the global energy supply comes from fossil fuels, and the rest comes from nuclear and renewable energy (IEA, 2016). An impressive milestone in the global response against climate change occurred in 2016 when 120 countries ratified the Paris agreement that committed to reducing the use of fossil fuels (Remigijus Lapinskas, 2017). The agreement could be considered the most important commitment that the countries have taken on climate change since the Kyoto procedure agreement that was signed in 1997.

Renewable energy development has accelerated in the last few decades due to policymakers and governments in many countries implementing incentives for replacing the use of fossil fuels with renewable energy. The incentives, such as tax reductions by introducing special feed-in tariffs, have made the clean energy business promising for investors. In terms of the contribution of biogas to renewable energy supply, according to Pablo-Romero *et al.* (2017), 19 countries in Europe have applied some price incentives to promote the utilisation of biogas, 14 countries use the Feed-in Tariff, six countries use the Premium Tariff and one country use tenders. This benefit is reflected by the significant increase in the renewable energy global investment in renewable energy from only $46.6 billion in 2004 to $285.9 billion in 2015 (McCrone *et al.*, 2016).

As a renewable energy, anaerobic digestion (AD) not only produces biogas but also be one of the best solutions for waste management. The development of biogas in recent years shows an increase, as evidenced by the number of biogas plants that have increased each year. For example, in Europe, the European Biogas Association (EBA) recorded that more than 6,200 biogas plants were built in Europe in 2009, increasing to 18,202 in 2018 (Sustainable Agribusiness Forum, 2020), see Figure 1-1. The expansion number of biogas plants is still growing, with the total electricity produced from biogas being 63.5 terawatt-

hours in 2018 (Sustainable Agribusiness Forum, 2020). In Europe, Germany is still leading in the number of biogas plants installed, reaching more than 10,000 plants (Fletcher, 2017). In developing countries in Asia and Africa, anaerobic digestion has been implemented not only on a large scale, but also it has been built on low-cost, small-scale digesters in rural regions. Small-scale digesters give economic benefits to people who have energy issues (electricity or heat), especially in rural regions (Petersson and Wellinger, 2009; Bochmann and Montgomery, 2013).

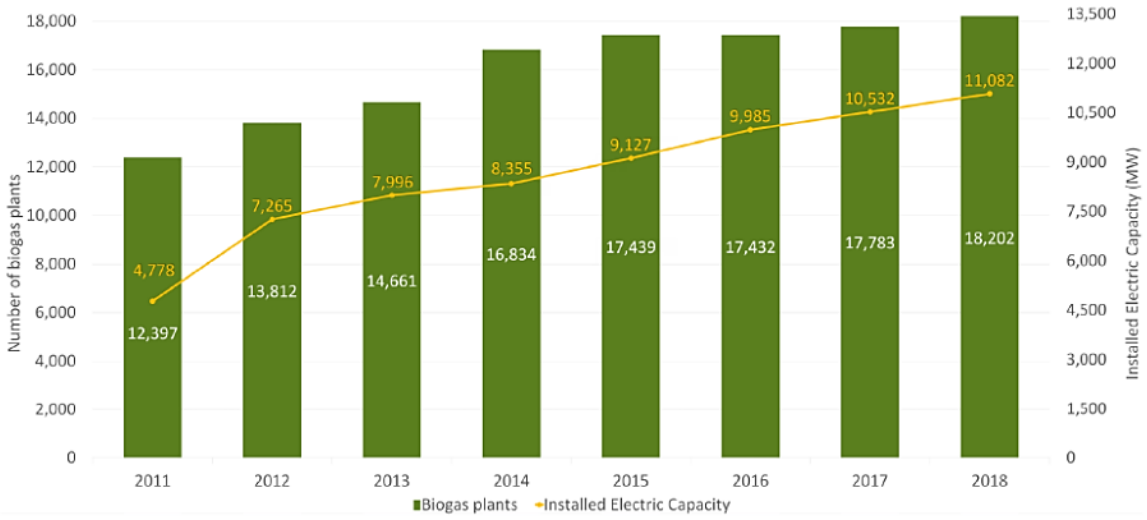

Figure 1-1 The growth of the number of biogas plants installed in Europe (Sustainable Agribusiness Forum, 2020).

1.2 Power to gas

Biological methanation of hydrogen and carbon dioxide, the overall chemical reaction of which is given in equation 1-1 and which is the topic of this thesis, can be applied as a "Power to Gas" concept where excess electricity produced by intermittent renewable energy power generation (solar, wind) is used to produce methane. The excess electricity can be utilised to produce H_2 via an electrolyser. Although hydrogen is a clean-burning gas, producing no direct GHG emissions from its combustion, the utilisation of hydrogen as an energy source is still very limited compared to methane due to technical and practical barriers. Hydrogen can be utilised as a vehicle fuel, but this would require hydrogen gas storage in a small and lightweight system (Durbin and Malardier-Jugroot, 2013); this is challenging, and the blending of hydrogen into the natural gas network is still under development (Kanellopoulos, Busch and M, 2022). However, some countries, such as

Germany, have implemented the injection of hydrogen into the natural gas grid (Rebecca Markillie, 2013a). Recently, Australia announced a trial on hydrogen injection into the gas grid (Chong, Subramaniam and Ng, 2015).

$4\ H_2 + CO_2 \rightarrow CH_4 + 2H_2O$ $\Delta G^o = -130.7\ kJ\ mol^{-1}$ Equation 1-1

In the United Kingdom (UK), the concept of blending hydrogen into the natural gas grid has been proposed in order to reduce carbon emissions (UK Houses of Parliament, 2017) and currently, it is running a feasibility study project for the implementation of this concept. Unfortunately, there are not currently adequate facilities that allow hydrogen to be injected into the gas grid on a large scale, and the progress towards this will take time until the concept is mature and ready to be implemented, especially regarding the facilities, technical and safety challenges. Alternatively, hydrogen can be utilised to produce biomethane by reacting the H_2 with CO_2 through a thermochemical and biochemical route, with the latter being possible inside existing anaerobic digestion reactors. Unlike hydrogen, biomethane injection into the gas grid has been implemented in the UK since 2010 (UK Houses of Parliament, 2017). In the UK, the biomethane network infrastructure and the regulations related to the injection of biomethane into the gas grid are more mature than hydrogen infrastructure and regulation. The UK Houses of Parliament (2017) recorded that the growth rate of the biomethane to the grid has been lower than their prediction, with the main issue being the quality of the biogas due to the feedstock (biomass) composition. The low quality of biogas has to be upgraded to meet the quality for injection into the gas network, which can be done by either removing the carbon dioxide (using several mature technologies) or converting the carbon dioxide into additional methane through biomethanation. Therefore, the excess electricity to produce hydrogen, and further utilisation of the hydrogen to produce biomethane, can be an alternative to producing low carbon renewable energy.

The wide range of utilisation of biogas may be the solution as an alternative fuel, and it is environmentally friendly. However, to meet the natural gas quality, the methane content needs to reach at least 90 % (Deublein and Steinhauser, 2008) or depend on the standard natural gas in each country for it to be connected to the natural gas grid. The methane content (% volume) obtained from conventional AD processes fluctuates between 50-75 %

(Bochmann and Montgomery, 2013), and it depends on the type, composition and quality of the digested substrates. Further, in order to obtain methane that meets the quality of natural gas, a post-treatment process is required in order to remove other gasses, such as CO_2 and H_2S. To remove the CO_2, the AD plant commonly uses a CO_2 scrubber to capture the CO_2 as part of the biogas upgrading technique.

On the other hand, the CO_2 can be utilised to produce CH_4 through a hydrogenotrophic methanogenesis pathway (Derbal Kerroum, Bencheikh-LeHocine Mossaab, 2012). In the anaerobic digestion biochemical process, the acetoclastic methanogen (AM) consumes acetate to produce methane, while hydrogenotrophic methanogen (HM) produces methane from carbon dioxide and hydrogen. Instead of releasing the CO_2 into the gas effluent, the captured CO_2 can increase the methane content of the biogas by conversion through hydrogenotrophic methanogenesis. However, the hydrogenotrophic methanogenesis process requires hydrogen as the electron donor, whereas the amount of hydrogen is insufficient to convert all CO_2 to CH_4 with conventional AD. The imbalance between hydrogen and oxygen content of the biodegradable fraction of the feedstock is the reason why the CH_4 produced from the hydrogenotrophic methanogenesis pathway is limited. The methane conversion from CO_2 can possibly be optimum if the additional H_2 is supplied from another source.

The methane production from carbon dioxide is not a new process. The catalytic methanation to convert CO_2 to CH_4 has been known since 1912, when Paul Sabatier introduced his invention (Leonzio, 2016). Further, biological methanation offered the advantages of lower energy requirements compared with catalytic methanation. However, the conversion of CO_2 to CH_4 by injecting the H_2 into the anaerobic digestion reactor still needs to be developed and to be better understood.

1.3 Biological methanation

On performing a literature review, it was found that many research groups have tried to find a better understanding of biological methanation of hydrogen and carbon dioxide from anaerobic digestion process, either by optimising the methane production (Luo and Angelidaki, 2013; Wahid and Horn, 2021) or by studying the microbiology of the process

(Agneessens *et al.*, 2017) or identifying process limit (Tao *et al.*, 2019). A critical issue is how to control the hydrogen injection into the reactor since the proportion of hydrogen that can be converted into additional methane within an anaerobic digester has to follow the stoichiometric reaction of the hydrogenotrophic methanation reaction (Equation 1-1). It has been posted that the control of the hydrogen supply will be easier if the only biomethanation reactions occur in a separate reactor because the amount of CO_2 would be equally controlled and known, in a process referred to as *ex situ* biomethanation. However, if the CO_2 biomethanation occurs in the same anaerobic reactor (known as *in-situ* biomethanation), then this would be challenging because the amount of CO_2 produced fluctuates due to feedstock and reaction rate variability and would need to be measured in real-time.

Some negative effects may occur if the proportion of the ratio H_2/CO_2 does not follow the stoichiometric ratio, excess hydrogen could increase the partial pressure of the hydrogen, and this could inhibit acetogenesis and fermentation reactions, causing VFA accumulation (Lee *et al.*, 2012; Agneessens *et al.*, 2017). On the other hand, at the lower H_2:CO_2 molar ratio, the conversion of CO_2 to CH_4 is not optimum because some of the CO_2 is not converted to CH_4 and will still appear in the biogas. Therefore, an estimation of the specific yield of carbon dioxide can be determined from conventional anaerobic digestion as a baseline operation. Then the amount of hydrogen requirement can be estimated (Bassani, Kougias and Angelidaki, 2016). However, introducing the hydrogen to the anaerobic digestion process may change the anaerobic digestion performance, especially in terms of influencing the microorganisms as the route of methanogenesis is shifted when hydrogen is injected into the reactor (Banks *et al.*, 2012a) and also change to the microbial population (Tao *et al.*, 2019). The changed biological process due to the hydrogen injection in the reactor may change the production of carbon dioxide, meaning the actual hydrogen requirement for biomethanation may also change.

Nevertheless, it is difficult always to know the actual carbon dioxide production in real-time during the biomethanation process, so an estimation and/or feedback is still necessary. Ideally, there is a system in a biomethanation reactor that can control and adjust the supply of hydrogen continuously based on the actual gas composition and the pH. In this study,

we propose an innovative system of hydrogen injection for in-situ biomethanation developed based on the real-time monitoring of CO_2 production from anaerobic digestion.

The amount of hydrogen is critical to be controlled; too much hydrogen injection will cause inhibition of the biological processes and the depletion of carbonate buffer, leading to high pH, whereas too little hydrogen injection will result in lower than targeted biomethane quality. In addition, the amount of required hydrogen depends on the available CO_2, which is variable and is influenced by the operation of the digester and the feedstock characteristics. For these reasons, injecting hydrogen into an in-situ biomethanation process is challenging, and more research is needed.

1.4 Project Aims and Objectives

This PhD project proposes a novel continuous hydrogen injection control with a feedback control approach to the in-situ biomethanation process and a supporting techno-economic assessment. The overall aim of the project was to study the application of in-situ biomethanation in terms of its governing parameters, implementation, operation and control, and financial viability.

The work is split into two major strands; (1) the experimental study and (2) the techno-economic study.

1.4.1 Experimental study:

This work aimed to investigate the governing parameters that could improve the gas-liquid mass transfer and improve methane enrichment using continuously controlled hydrogen injection in the in-situ biomethanation process. The objectives in order to meet this aim were as follows:

1) The development of a dedicated automated laboratory-scale biomethanation rig allowed the experimental work to run continuously and without continuous user attendance.
2) Studied the major parameters influencing the behaviour and performance of in-situ biomethanation; use of alternative hydrogen injection systems, gas recirculation, mixing, hydrogen injection rate, and the substrate feeding regime in the continuous

in-situ biomethanation process in order to achieve better hydrogen conversion and methane enrichment.

3) Based on the experimental work, gather information about the strategies to improve the gas-liquid mass transfer with controlled continuous hydrogen injection.

1.4.2 Techno-economic study:

This study aimed to simulate the application of in-situ biomethanation on a larger scale from the technical and economic points of view. The objectives in order to meet this aim were as follows:

1) Developed a technical and economic framework to model the application of an in-situ biomethanation system, including all major system components and all mass and energy flows
2) Produced a methodology for economic analysis taking into account the variability of electricity price depending on the supply and demand of the national gird allowing electrolyser scheduling strategies to be investigated
3) Designed application scenarios, relevant to the UK landscape for the techno-economic analysis that was employed in the assessment of the economic feasibility of the technology against key operational decisions
4) Gathered information on the most critical factors that influence the cost of energy in the production of biomethane through in-situ biomethanation
5) Investigated the sensitivity of the economic analysis to prevailing economic and technical conditions or modelling assumptions.

1.5 Thesis structure

The structure of this thesis is as follows:

Chapter 1: Introduction

This chapter introduces the current situation in anaerobic digestion and the project background. The project background led us to identify the knowledge gaps in the specifics

of the in-situ biomethanation. Then, the description of the research project, including the aims and objectives, is presented.

Chapter 2. Literature review

This chapter provides the fundamentals of anaerobic digestion in general and the current developments in the in-situ biomethanation, including a review of the previous studies in the literature that are relevant to this project. In addition, this chapter includes a detailed description of the knowledge gaps, which provides support for the novelty of this project.

Chapter 3. Methodology and experimental rig setup

This chapter presents the first results of the experimental investigation, providing an initial evaluation of some of the main relevant design and control parameters. The main conclusion of the chapter shows the impact on the biomethanation performance of using an improved hydrogen injection system, namely a porous sparger. In addition, this chapter also explained in detail the process of preparing the experimental rig and data collection. Finally, the results of the batch and semi-continuous experiment on conventional anaerobic digestion are also described in this chapter.

Chapter 4. In-situ biomethanation process control and monitoring with continuous H_2 additions

This chapter presents the results of the experimental investigation. In addition, this chapter also explained in detail the process of preparing the experimental rig and data collection. Finally, the results of the batch and semi-continuous experiment on conventional anaerobic digestion are also described in this chapter.

Chapter 5. Process optimisation of in-situ biomethanation with continuous H_2 additions

This chapter presents the main and most important results of the experimental investigation. The process optimisation mainly focused on increasing the gas-liquid mass transfer, which will lead to increased hydrogen conversion and methane enrichment. In addition, this chapter includes the result and discussion of the effects of the recirculation rate, additional sparger on the gas recirculation line, digester mixing rate, variable organic loading rate, onto the performance of the in-situ biomethanation.

Chapter 6. Techno-economic analysis of in-situ biomethanation: UK case study

This chapter presents the results of the techno-economic study in the application of the *in situ* biomethanation using the data in the UK as a case study. The results include the analysis of biomethanation implementation in different scenarios and determining the most influential factors from an economic point of view.

Chapter 7. Conclusions and future works

This chapter summarises all the results and discussions that have been presented in previous chapters and provides an overall conclusion of the work presented in the thesis. Also, some potential suggestions for possible future work are presented to support the continuation of this research work.

2. LITERATURE REVIEW

2.1 Anaerobic Digestion

Anaerobic Digestion (AD) is the process of organic material degradation to produce biogas. The organic material or biomass can be liquid manure, food waste, energy crops, waste from municipalities, industrial by-products, etc. (Bochmann and Montgomery, 2013). The anaerobic digestion process involves a consortium of microorganisms in a multistep process, such as hydrolytic-acidogenic bacteria, syntrophic-acetogenic bacteria and methanogenic archaea (Angelidaki *et al.*, 2011) without the presence of oxygen (anaerobic). The major components of biogas are methane and carbon dioxide, and theoretically, the potential of methane production can be estimated according to the Buswell equation (Buswell, 1936) as follows:

$$C_nH_aO_b + \left[n - \frac{a}{4} - \frac{b}{2}\right] H_2O \rightarrow \left[\frac{n}{2} - \frac{a}{8} + \frac{b}{4}\right] CO_2 + \left[\frac{n}{2} + \frac{a}{8} - \frac{b}{4}\right] CH_4 \quad \text{Equation 2-1}$$

where n, a and b are the number of carbon, hydrogen and oxygen elements, respectively. For instance, for glucose ($C_6H_{12}O_6$), the stoichiometric equation is given by:

$$C_6H_{12}O_6 \rightarrow 3CO_2 + 3CH_4 \quad \text{Equation 2-2}$$

An anaerobic digestion system can be as simple and cheap as a single fibreglass digester or as complex and expensive as an industrial-scale multi-digester system with moving parts with intelligent automatic control and monitor that supports the plant operation (Bilitewski *et al.*, 1997). The design of an AD plant should consider the type of waste to be treated, the availability, sustainability, and the climate of the region. These design considerations are the reason that makes the AD plant unique because the design has to consider many different parameters that are suitable in the particular region and may not necessarily be applicable in other regions, especially the types of feedstock availability. A wide range of biomass types can be used as a feedstock, with differences arising due to different contents of carbohydrates, protein, fats, cellulose and hemicellulose, and macro and micro-nutrients. However, some of the biomasses may have slower degradation, such as wood, since wood contains lignin as a cell wall, which is not easy to degrade.

2.1.1 Anaerobic digestion biochemical process

The anaerobic digestion process may be divided into four phases: hydrolysis, acidogenesis, acetogenesis and methanogenesis (Deublein and Steinhauser, 2008). A schematic pathway of anaerobic digestion is shown in Figure 2-1. Each stage in the anaerobic digestion process involves a consortium of microorganisms that have a specific role in organic material degradation. The synergy between microorganisms can create a better environment for the microorganisms to grow and stimulate the increase of the population of microorganisms.

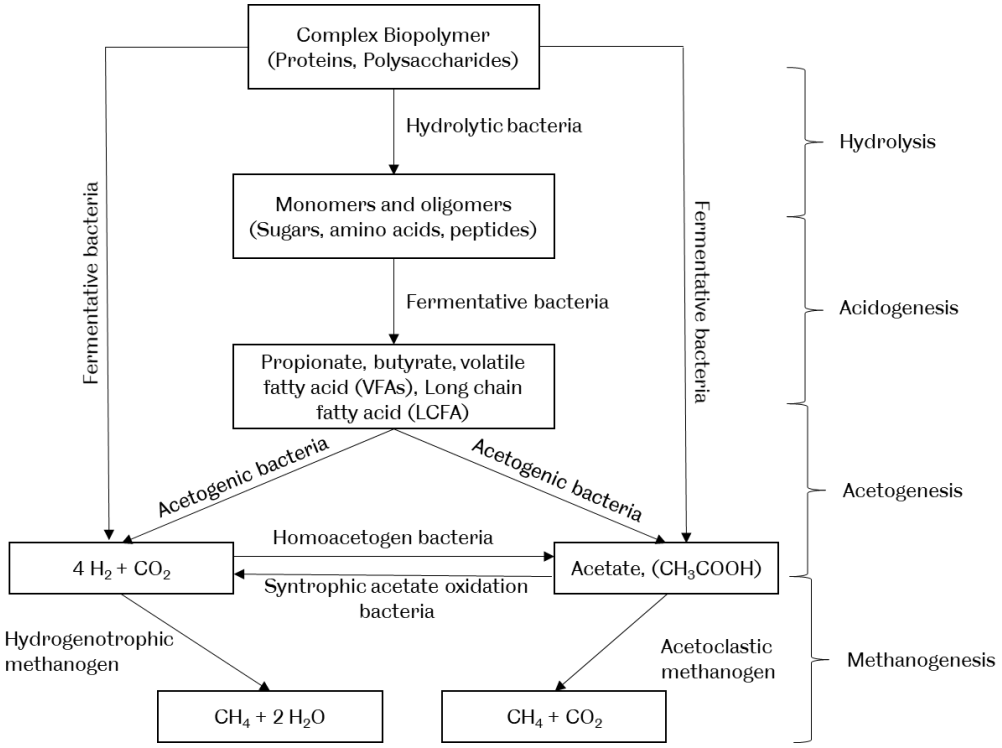

Figure 2-1 A schematic diagram of the anaerobic digestion processes (Derbal Kerroum, Bencheikh-LeHocine Mossaab, 2012).

The stages of the decomposition of the organic substrates and the active microorganisms at each stage are now described in the next section.

Hydrolysis

Hydrolysis is the solubilisation of the insoluble complex organic material that is broken down into simpler compounds. Hydrolysis is a crucial step because the microorganism cells cannot directly absorb insoluble particles as a substrate (Adekunle and Okolie, 2015). The biodegradation process involves extracellular enzymes, breaking the polymers' chemical

bonds into monomers or dimers. Hydrolysis involves a group of different enzymes, each of which has a specific task to degrade particular groups of polymers. The enzyme groups and their relevant functions are presented in Table 2.1. This enzyme converts complex organic matter (carbohydrates, proteins, and lipids) into monomers (sugars, amino acids and long-chain fatty acids) (Zhang *et al.*, 2014; Adekunle and Okolie, 2015).

The decomposition rate of the polymers depends on the type of the composition of the organic material, e.g. manure, food waste, agricultural residue, etc. The hydrolysis of the carbohydrates takes place in the order of hours, while the hydrolysis of the protein and lipids is within the order of days (Deublein and Steinhauser, 2008). Additionally, the groups of bio-fibres (cellulose, hemicellulose and lignin) degrade more slowly than the decomposition of proteins (Deublein and Steinhauser, 2008). The hydrolytic rate of bio-fibres depends on the material's structure and composition. Certain bio-fibres, such as those contained in straw, are relatively easier to degrade compared to those in wood. Wood has a high lignin content, and this makes its structure dense and difficult to degrade. For this reason, woody biomass usually does not process anaerobically (Ostrem, Millrath and Themelis, 2004).

Table 2.1 The groups of hydrolytic enzymes and their functions (Schunurer and Jarvis, 2009).

Enzymes	Substrate	Breakdown Products
Protease	Proteins	Amino acids
Cellulase	Cellulose	Cellobiose and glucose
Hemicellulase	Hemicellulose	Sugars, such as glucose, xylose, mannose and arabinose
Amylase	Starch	Glucose
Lipase	Fats	Fatty acids and glycerol
Pectinase	Pectin	Sugars, such as galactose, arabinose and polylactic

Acidogenesis

Acidogenesis, or the fermentation stage, consumes the components produced from the hydrolysis stage. The acidogenesis stage involves the action of acidogenic or fermentative and hydrolytic bacteria (Bochmann and Montgomery, 2013). The fermentable substrates include monosaccharides, amino acids, unsaturated fatty acids, glycerol and halogenated organics. Through various fermentation reactions, the products from the hydrolysis are

converted mainly into various organic acids (acetic, propionic butyric, lactic etc.), alcohols, hydrogen, carbon dioxide, ammonia (from amino acids), etc. (Mesbah and Wiegel, 2008; Derbal Kerroum, Bencheikh-LeHocine Mossaab, 2012; Adekunle and Okolie, 2015).

Acetogenesis

The acetogenic stage allows the transformation of acids that are produced from the acidogenesis stage into acetate, also producing both H_2 and CO_2, through the action of acetogenic bacteria (Derbal Kerroum, Bencheikh-LeHocine Mossaab, 2012). Syntrophic acetogenesis is the anaerobic oxidation process of propionate and butyrate to produce acetate and H_2 (Schunurer and Jarvis, 2009). with concomitant use of H_2 by hydrogenotrophic microorganisms, which is necessary to make the acetogenesis thermodynamically feasible. Homo-acetogenic bacteria can also form acetate from carbon dioxide and hydrogen, and homo-acetogenesis is the reduction of CO_2 with H_2 to acetate through the acetyl-CoA pathway (Diekert and Wohlfarth, 1994). The difference in the acetate reaction through syntrophic acetogenesis and homo-acetogenesis can be seen in the following reactions:

Acetogenesis:

$$Propionate^- + 3\ H_2O \rightarrow CH_3COO^- + HCO_3^- + 3\ H_2 \qquad \text{Equation 2-3}$$

$$Butyrate^- + 2\ H_2O \rightarrow 2\ CH_3COO^- + H^+ + 2\ H_2 \qquad \text{Equation 2-4}$$

Homoacetogenesis

$$4\ H_2 + 2\ HCO_3^- \rightarrow CH_3COO^- + 4H_2O \qquad \text{Equation 2-5}$$

Methanogenesis

The methanogenesis stage involves the transformation of acetate, hydrogen and carbon dioxide into methane. The microorganisms involved in this stage are identified from the domain archaea, which is different from the earlier stages performed by bacteria. Acetoclastic methanogen produces methane from acetate, while hydrogen and carbon dioxide produce methane through hydrogenotrophic methanogen (Deublein and Steinhauser, 2008; Adekunle and Okolie, 2015). During the methanogenesis stage, only 27-30 % of the methane is produced from the reduction of CO_2, while 70 % methane is

produced from acetate (Deublein and Steinhauser, 2008), although this proportion can vary depending on substrate concentration and reaction conditions.

2.1.2 Key parameters in anaerobic digestion

Temperature

Temperature is one of the most critical parameters that affect the AD process, and it affects not only the enzyme activity but also microbial activity. Additionally, the temperature also affects the effects of toxicity in the chemical elements and compounds, such as the formation of free ammonia (Zhang *et al.*, 2014).

The different types of bacteria and archaea can be divided into different groups depending on the optimum growing temperature, i.e. psychrophilic, mesophilic, thermophilic and hyperthermophilic (Mesbah and Wiegel, 2008; Latif, Mehta and Batstone, 2017). For example, psychrophilic methanogens can work in the temperature range of 4-25 ^{o}C, whereas the mesophilic methanogen works in the temperature range of 32-42 ^{o}C and the thermophilic temperature from 48-60 ^{o}C, while the temperature for the hyperthermophilic microorganism is above 65 ^{o}C (Deublein and Steinhauser, 2008; Latif, Mehta and Batstone, 2017).

In addition to energy efficiency, the stability of the process tends to be higher in the mesophilic temperature rather than the thermophilic (Labatut, Angenent and Scott, 2014). On the other hand, thermophilic methanogens have a faster growth rate compared to mesophilic and psychrophilic, see Figure 2-2. However, the optimum operating condition is very dependent on the microbial activity that is influenced by many factors; temperature is only one of them.

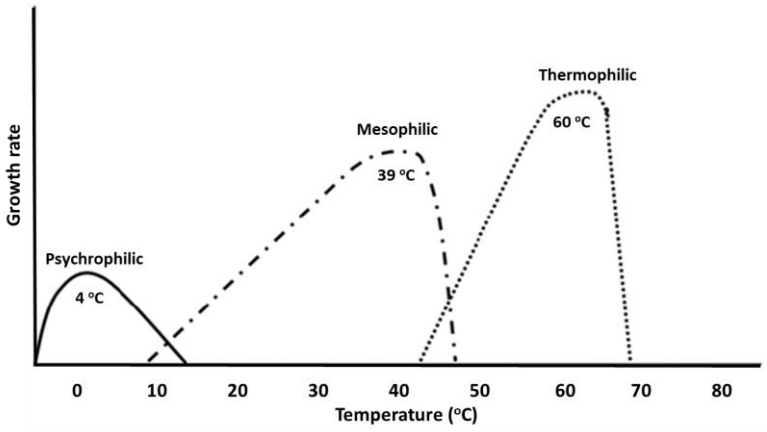

Figure 2-2 Schematic of the growth of microorganisms at different temperatures (Lettinga, Rebac and Zeeman, 2001).

pH and Alkalinity

In the anaerobic digestion process, pH is one of the most critical parameters that act as an indicator of a smooth process. This is because the microorganisms involved in the process are sensitive to the pH change, although some can adapt or be more tolerant to pH change (Horn *et al.*, 2003). The best biogas process usually runs at neutral pH or slightly above, between 7.0 and 8.5 (Bochmann and Montgomery, 2013), because the maximum growth of the methanogens is obtained in this range, and the population decreases when the pH is not in a favourable condition. For instance, as the pH decreases (pH 5-5.5), the methanogenic population decreases by more than 80 % compared to normal pH (Latif, Mehta and Batstone, 2017). The most important chemical compounds in an anaerobic digestion system that are affected by the pH are ammonia, VFA and CO_2 (Batstone *et al.*, 2002). Since there is a correlation between pH and microbial growth, pH is often used as one of the best references for monitoring the stability of the ongoing process, whether it works well or tends to cause a system failure.

Alkalinity, defined as the capacity of water/solutes to neutralise acid, and sometimes called the buffer capacity since it can prevent the rapid pH changes in the process (Ohrel and Register, 2006), is necessary in order to maintain the stability of the system and avoid the shock effects on the microbial activity. The ammonia and volatile fatty acids that are

released from the decomposition of the organic matter can change the pH of the system. Ammonia can also react with dissolved carbon dioxide to form ammonium bicarbonate.

The carbon dioxide that is produced from the anaerobic digestion process is partly released into the gas phase. However, the CO_2 is also soluble in water. The equilibrium equation for the carbon dioxide with carbonic acid and carbonates is given by equation 2-6 (Schunurer and Jarvis, 2009):

$$CO_2 + H_2O \leftrightarrow H_2CO_3 \leftrightarrow HCO_3^- + H^+ \leftrightarrow CO_3^{2-} + 2H^+ \qquad \text{Equation 2-6}$$

Low pH in AD may be due to the production of acid being too high; in fact, production of VFA consumes the carbonate alkalinity; when the buffer capability of the carbonate system is reduced, then the decrease of pH becomes more noticeable. For this reason, Hawkes et al. (Hawkes *et al.*, 1994) suggested that monitoring the alkalinity can be a good tool for early warning of organic overloading.

Organic loading rate (OLR) and hydraulic retention time (HRT)

Anaerobic digestion requires organic material to maintain biogas production. The quantity of substrate that supplies the reactor is defined by the organic loading rate (OLR). The OLR is the amount that indicates how much organic material is added to the reactor per unit of time (Schunurer and Jarvis, 2009), and it is calculated based on the Chemical Oxygen Demand (COD) or Volatile Solid (VS). OLR is the quantity that determines the amount of "food" for the microorganisms. If the OLR is too high, then it has a negative effect, which can lead to VFA accumulation that causes inhibition of the microorganism.

The retention time is defined as the time taken to replace all of the material in the digestion tank (Bochmann and Montgomery, 2013) on a volumetric basis. The hydraulic retention time (HRT) gives a proxy for the time that feed materials stay in the reactor, and it is defined differently for batch and semi-continuous operation. In the semi-continuous system, the retention time can be measured by dividing the working volume of the digester by the influent volumetric flow rate of the organic material, whereas in the batch reactor, there is no transfer in or out of the feed, and therefore the value remains steady at the length of time of the batch process.

The stable range of operational HRT depends on the substrate types. For example, in an anaerobic digestion plant, which uses complex substrates, such as manure or food waste, the typical HRT is about 10 to 25 days, but it may be longer (Mesbah and Wiegel, 2008; Derbal Kerroum, Bencheikh-LeHocine Mossaab, 2012). However, on the laboratory scale, the research studies that use a simpler substrate, such as glucose, the HRT could be in a couple of days or maybe hours. Therefore, the HRT is critical in order to ensure that for long periods, the organic materials can be mostly degraded, which is close to or similar to the value obtained by the BMP test.

Trace elements

Trace elements have an essential function in the cell metabolism of microorganisms, and the existence of a trace element can increase the stability of the anaerobic digestion system. The trace elements that have been found to improve the biogas production are iron (Fe), zinc (Zn), copper (Cu), nickel (Ni), molybdenum (Mo), tungsten (W), cobalt (Co), and selenium (Se) (Schunurer and Jarvis, 2009; Banks *et al.*, 2012a). The trace elements are essential constituents of the cofactor and enzymes in biogenic methane production, and adding trace elements in anaerobic digestion can improve the system's stability (Linville *et al.*, 2016). For instance, trace elements have a significant role in anaerobic digestion that operates at high ammonia concentrations. Banks *et al.* (2012a) found that the deficiency of selenium could be the reason that the process fails at high ammonia concentrations in food waste digesters, and this is because microorganisms require selenium and cobalt for interspecies electron transfer at high ammonia concentrations.

2.1.3 Inhibition

Process disturbances during the anaerobic digestion process can be related to the system's instability due to inhibition. The inhibition that is commonly present in the anaerobic digester process includes ammonia, sulphide, metal ions and organic ions (Chen, Cheng and Creamer, 2008). Inhibition can be a severe problem in the anaerobic digestion process. The impact of inhibition can be a gradual decrease in the performance that can be established from the biogas production or the pH profile. If the inhibition is continuously ongoing, it can be followed by a process failure (Angelidaki, Ellegaard and Ahring, 1993).

Ammonia

AD of substrates that contain a high concentration of protein can be potentially inhibited by ammonia, and this is because protein, urea and nucleic acids release ammonia as one of the products from their anaerobic degradation. At low concentrations, nitrogen is essential for the growth of anaerobic microorganisms (Kayhanian, 1999). But a higher concentration of ammonia might cause inhibition of the AD process (Rajagopal, Massé and Singh, 2013). Ammonia can form free ammonia (NH_3) and ammonium ion (NH_4^+), and the form of free ammonia is more toxic than the ammonium ion (Derbal Kerroum, Bencheikh-LeHocine Mossaab, 2012; Yenigün and Demirel, 2013). The combination between free ammonia and ammonium ion is called the total ammonia nitrogen (TAN).

One factor that can influence the shift of ammonia form is the temperature. As the temperature increases, the ammonia form is moved to form free ammonia (Schunurer and Jarvis, 2009). Thus, increasing the temperature provides a further impact on decreasing the CO_2 solubility, which increases the pH and pushes the equilibrium further towards the free ammonia (NH_3). Angelidaki and Ahring (1994) reported that when the ammonia concentration was high, the reduction of temperature from thermophilic to mesophilic results in an improved biogas yield and better stability of the process, thus resulting in a lower concentration of the VFA in the effluent. In this case, the ammonia may form an ammonium ion, which is less toxic than free ammonia.

The impact of increasing the temperature and pH is given as (Hansen, Angelidaki and Ahring, 1998):

$$NH_3 - N = \frac{Total\ Ammonia\ nitrogen}{\left(1 + \frac{10^{-pH}}{10^{-\left(0.09018 + \frac{2729.92}{T}\right)}}\right)} \qquad \text{Equation 2-7}$$

where NH_3-N is free ammonia-nitrogen, the total ammonia nitrogen is the sum of the concentration of the free ammonia and the ammonium ion, and T is the temperature in Kelvin.

There have been many investigations on the effect of ammonia on anaerobic digestion systems. However, the information on the maximum concentration of ammonia that can be tolerated before causing the inhibition varies. This could be attributed to many factors, such as the type of the substrate and inoculum and the digestion condition (temperature, pH, etc.) (Mahdy *et al.*, 2017). It is widely reported that the ammonia concentration in the high rate digester of around 1700-1800 mg L^{-1} of TAN could cause reactor failure (Yenigün and Demirel, 2013). However, the level of ammonia tolerance could increase by up to 5000 mg TAN L^{-1} by the acclimatisation of microorganisms in the ammonia environment, see Table 2.2 (Yenigün and Demirel, 2013). The acclimatisation can be achieved by introducing the bacteria to the ammonia concentration and gradually increasing the ammonia concentration. These study gives evidence that microorganisms have the ability to adapt to unfavourable environments.

Table 2.2 Ammonia inhibition in anaerobic digestion (Yenigün and Demirel, 2013).

Substrate	**Loading rate**	**Temperature (ºC)**	**pH**	**TAN (critical concentration or as specified)**	**FAN(critical concentration or as specified)**	**Acclimatisation**
Sludge	-	30	7.2-7.4	>5000 mg/L	-	Yes
Piggery manure	-	30	7.2-7.4	>3075 mg/L	-	Yes
MSW/Sludge	-	39	8.0	2800 mg/L		No
Synthetic wastewater	1.2 kg COD/m3.d	35	7.7-8.1	6000 mg/L	800 mg/L	Yes
Slaugtherhouse waste +OFMSW	3.7 kg VS/m3 d	34	7.5	4100 mg/L	337 mg/L	Yes
Sewage sludge	2.0 kg VS/m3 d	35	8.0	3000 mg/L	400 mg/L	Yes
Cattle manure	-	45	7.4-7.9	6000 mg/L	700 mg/L	Yes
Organic fraction of MSW	6.5 g VS/kg d	55	7.0	2500 mg/L (100% inhibition)	-	Yes
Non-fat dry milk	4 g COD/L/d	55	6.5	5.77 g/L (64% inhibition)	-	Yes
Pig manure	9.4 g VS/L d	51	8.0	1450 mg/L (50% inhibition)	1450 mg/L (50% inhibition	Yes

Mccarty and Mckinney (1961) proposed that the inhibition of ammonia is due to free ammonia rather than ammonium ion. As shown in Table 2.2, the limit of ammonia concentration is strongly influenced by the presence of free ammonia. The tolerated TAN level can be higher if the free ammonia concentration is low. In contrast, if the

concentration of free ammonia is high, the concentration of TAN that can be tolerated decreases. Additionally, the limit of the ammonia concentration that can be tolerated depends on the type of bacteria and archaea in the reactor and the acclimation period (Chen, Cheng and Creamer, 2008). The microbiological study shows that some species of methanogens are more robust to the ammonia concentration than the other species. *Methanothrix concilii* was reported to be completely inhibited at an ammonia concentration of 560 mg TAN L^{-1}, while *Methanosarcina barkeri* was not inhibited at 2800 mg TAN L^{-1} (Yenigün and Demirel, 2013). Additionally, the study using the pure culture was observed by Jarrel et al. (Jarrell, Saulnier and Ley, 1987), who investigated the effect of ammonia on *Methanobacterium barkeri, Methanobacterium thermoautotropicum, Methanobacterium fotmicicum and Methanobacterium hungatei*. Those methanogens were found to be resistant to the TAN concentration over 10000 mgL^{-1}, except the *Methanobacterium hungatei,* which experienced 50 % methanogenesis inhibition at 4200 mg TAN L^{-1}.

According to Kayhanian (Kayhanian, 1994), strategies to overcome the problems that are associated with ammonia inhibition can be corrected as follows:

(i) Diluting the contents of the digester to reduce the ammonia concentration.
(ii) Adjusting the C/N ratio of the feedstock (i.e. co-digestion with low-N feedstocks).
(iii) External ammonia absorption.
(iv) Acclimatisation.
(v) Trace element supplementation.

The Carbon-Nitrogen (C/N) ratio is one of the critical parameters that must be considered to minimise the ammonia inhibition effect. Adjusting the C/N ratio of the feedstock could reduce the concentration of ammonia (Bochmann and Montgomery, 2013). Many studies have indicated that the optimal C/N ratios in anaerobic digestion are about 25-30 (Tanimu *et al.*, 2014). The optimal C/N ratio has been studied by Wang *et al.* (2014) by comparing the performances of biogas production on dairy manure, chicken manure and rice straw, resulting in the optimal C/N ratio being 26.76 at 35 ^{o}C and 30.67 at 55 ^{o}C. The use of agricultural biomass can result in a high C/N ratio. However, the agricultural biomass is not always easy to digest because it contains lignocellulose, which must be pre-treated before

it is ready to digest. Lignocellulose consists of cellulose, hemicellulose, and lignin (Paudel *et al.*, 2017). The characteristic of lignocellulose is not soluble in water and has a rigid structure that is difficult to break either by mechanical stress or enzymatic activity (Taherzadeh and Karimi, 2008). Lignin is the most recalcitrant component of the plant cell wall; the lignin structure consists of phenylpropane that is linked in a three-dimensional structure which is difficult to biodegrade (Taherzadeh and Karimi, 2008). Although the agricultural biomass is very attractive to be used as the potential feedstock to control the C/N ratio, however, the lignocellulose content is one of the drawbacks in the use of lignocellulosic biomass where pre-treatment is needed to support the enzymatic hydrolysis.

Hydrogen Sulphide

Hydrogen sulphide is produced during the biochemical degradation of the protein (Tian *et al.*, 2020), and some of them involve sulphate-reducing bacteria (SRB) (Yang *et al.*, 2015; Dai *et al.*, 2017). Some microbial communities are very sensitive to the presence of hydrogen sulphide. The formation of the sulphide ion (S^{2-}) can be precipitated by the bonding with many metal ions, which has a negative impact on the availability of trace elements. According to Chen et al. (2008), the levels of the inhibition effect that are caused by the hydrogen sulphide are in the range of 50-400 mg L^{-1}.

Metal Ions

In small quantities, the metal ions, including light and heavy metal ions, do not affect the inhibition. However, according to Chen et al. (Chen, Cheng and Creamer, 2008), light metal ions, such as Na, K, Mg, Ca and Al, can become inhibitory agents at high concentrations. Light metals can be found from the breakdown process of organic materials; also, they can be found from chemical additives that are added to the reactor, for instance, the chemicals for pH adjustment such as sodium bicarbonate.

A similar situation occurs for heavy metal ions. Some heavy metal ions of trace elements are essential for microbial growth, but at high concentrations, they are toxic to the microbial environment (Bochmann and Montgomery, 2013).

Antibiotics and disinfectants

The effect of the presence of antibiotics and disinfectants in the digester is to cause inhibition or death of microorganisms (Bochmann and Montgomery, 2013). However, the presence of these two elements in anaerobic digestion is challenging to control and/or avoid, especially when using wastewater or food waste as substrates. In addition, disinfectants can be part of the wastewater from the industry, while antibiotics can be present in animal residues.

2.1.4 Biogas upgrading

Carbon dioxide is one of the main products of anaerobic digestion, in addition to methane that is released as a product at the fermentation and acetogenesis stages. The carbon dioxide content of the biogas can vary between 25-50 % (Bochmann and Montgomery, 2013). For this reason, CO_2 becomes the primary factor that has to be removed if the designed product gas is a high-quality biomethane. Biogas upgrading is the way to obtain a higher methane concentration so that the gas can be used as a vehicle fuel or supplied to the natural gas grid. Some countries in Europe have standardised the quality of biogas that can be injected or used as a vehicle fuel, see Table 2.3.

Table 2.3 Standard requirement for natural gas grid injection or utilization as a vehicle fuel (Petersson and Wellinger, 2009).

Compound	Unit	UK *)	France	Germany	Sweden	Switzerland		Austria	Netherland
						Lim Inject	Unlim. Inject		
Methane	Vol-%	95			95–99	> 50	> 96		> 80
Carbon dioxide	Vol-%		< 2	< 6		< 6		≤ 2[6]	
Oxygen	Vol-%	≤ 0.2	<0.01%	< 3		< 0.5		≤ 0.5[6]	< 0.5
Hydrogen	Vol-%	≤ 0.1	< 6	≤ 5		< 5		≤ 4[6]	< 12
CO_2+O_2+N_2	Vol-%				< 5				
Water dew point	°C		< 5[1]	<t[4]	<t[5] -5			< 8[7]	-10[8]
Relative humidity	ρ					< 60 %			
Sulphur	mg/Nm	≤ 50	< 100[2] < 75[3]	< 30	< 23	< 30		≤ 5	< 45

*) Source: Gas Safety (Management) Regulations 1996, Schedule 3, Part I,

[1]At maximal operating pressure downstream from the injection point, [2]Maximum permitted [3]Average content, [4]Ground temperature, [5]Ambient temperature, [6]Mole percentage, [7]At 40 bars, [8]At 10 bars.

Many methods/technologies have been proposed as strategies for biogas upgrading, and some of them are commercially available. Some of the technologies for biogas upgrading are as follows:

Pressure swing adsorption

The carbon dioxide is separated from the biogas by the adsorption on the surface under elevated pressure. The material that is used for this technique is usually activated carbon or zeolites (Petersson and Wellinger, 2009).

Absorption

The principle of the absorption technique is to take the benefits from the different solubility between carbon dioxide and methane. The biogas that meets the counterflow liquid is used in a column that is used as the separation chamber (Petersson and Wellinger, 2009). The absorption technology that is commonly used and commercially available is water scrubbing, organic, physical scrubbing and chemical scrubbing.

Membrane Separation

The principle of using a membrane for the biogas upgrading technique is to provide the material that can be permeable to carbon dioxide, water and ammonia (Petersson and Wellinger, 2009).

Cryogenic

The cryogenic technique is a new technology for biogas upgrading that utilises different boiling/sublimation points between carbon dioxide and methane. The biogas is cooled down until it reaches the sublimation point, then the carbon dioxide is found in liquid or solid form, whereas methane is still in the gas phase.

Biomethanation of H_2 and CO_2

Biomethanation is a new technique for biogas upgrading that is still under development. The principle is to inject the hydrogen into the anaerobic digester to provide an electron donor that can reduce the carbon dioxide to produce more methane through the action of hydrogenotrophic methanogens. The reaction upgrades the biogas' quality by increasing methane concentration (Durbin and Malardier-

Jugroot, 2013; Rebecca Markillie, 2013b; Chong, Subramaniam and Ng, 2015; UK Houses of Parliament, 2017).

2.1.5 Online monitoring and process control

Online monitoring and process control could improve productivity and quality and reduce analysis time (Dauwalder *et al.*, 2016). In anaerobic digestion applications, online monitoring of key parameters could give considerable advantages in order to improve biogas production or maintain process stability. Lots of online monitoring of AD parameters have been developed and implemented either from gas or liquid phases, such as online VFA monitoring based on headspace gas chromatography (GC) (Boe, Batstone and Angelidaki, 2007), alkalinity based on neural network models (Wang *et al.*, 2018), gas composition based on gas sensors (Li *et al.*, 2017), real-time pH monitoring, or even online monitoring of microbial activities using stable isotope analysis (Polag *et al.*, 2015). The implementation of online monitoring could give some benefits in process control, such as maintaining process stability and preventing process failure (Yu *et al.*, 2016)

To the best of our knowledge, online monitoring and control in the application of in-situ biomethanation are still not being developed.

2.2 In-situ biomethanation from the anaerobic digestion process

Methane production from carbon dioxide and hydrogen is a well-known process, and it was introduced by Paul Sabatier in 1912. Practically, the Sabatier reaction can be utilised in the carbon capture and storage (CCS) technology to reduce the emission of carbon dioxide and convert carbon dioxide into methane, which can give an economic benefit (Miguel *et al.*, 2015). The Sabatier reaction (equation 1-1) is commonly used to produce synthetic natural gas (SNG) using a catalyst, such as nickel, ruthenium, rubidium and palladium. Unfortunately, this conversion requires a high temperature (300 ^{o}C - 600 ^{o}C) and a high pressure above 10 atm (Lee *et al.*, 2012).

The biological methanation from H_2 and CO_2 involves hydrogenotrophic methanogens. Biological methanation (or biomethanation) can be achieved with less input energy because it does not need a high temperature or high pressure. In contrast, biomethanation requires low pressure, and the required temperature is the temperature where the

methanogen can grow (max 70 ^{o}C). However, the biomethanation process is challenging; The phase difference between the substrate (gas) and the methanogen (liquid/solid) makes the conversion effectiveness more complicated. Moreover, the solubility of the hydrogen in water is extremely low (1.47 mgL^{-1} at 30 ^{o}C 1 atm) (Jee *et al.*, 1987), and this makes the effective mass transfer between the gas and liquid to be a key focus for biomethanation development.

The biomethanation of CO_2 and H_2 under anaerobic conditions has been developed for over three decades. The early studies showed that the pure gas reaction of H_2 and CO_2 injected into the methanogenic cultures under anaerobic conditions can successfully produce methane (Jee *et al.*, 1987; Jee, Nishio and Nagai, 1988). This indicates that the biomethanation reaction could be applied in any anaerobic digestion configuration, where the CO_2 and H_2 are also produced in the anaerobic digestion process. Although methanogens are also present in the reactor, it is not always that methane production occurs from H_2 and CO_2. Generally speaking, the amount of H_2 produced from the anaerobic digestion is insufficient to react with all of the produced CO_2, hence why the biogas content always contains CO_2 as one of the primary products of anaerobic digestion. To overcome the limitation of the hydrogen availability in the reactor, an additional supply from outsources is required.

The study of biomethanation has provided evidence that the biochemical reaction between H_2 and CO_2 using methanogens can be achieved in pure methanogenic cultures or, more generally, within anaerobic digesters (Jee *et al.*, 1987; Luo *et al.*, 2012a). Several researchers have successfully converted H_2 and CO_2 completely by either using a pure culture in the fixed bed reactor (Jee, Nishio and Nagai, 1987; Lee *et al.*, 2012; Alitalo, Niskanen and Aura, 2015) or using a CSTR anaerobic digester (Luo *et al.*, 2012a; Wang *et al.*, 2013). The CO_2 conversion to CH_4 in an anaerobic digester can practically increase the methane content in the biogas to more than 90 % (Luo *et al.*, 2012a), which is close to the natural gas quality.

The reactor configuration of the biogas upgrading using the in-situ biomethanation technique is slightly different from the conventional AD plant. The difference lies in the additional line for the hydrogen injection into the digester. The technique of in-situ

biomethanation was proposed by Luo *et al.* (2012a), who investigated the possibility of converting hydrogen to methane within an anaerobic digester. Both the experimental results in batch and continuous reactors show positive results. The hydrogen consumption in the batch and the continuous reactor is more than 90 % and 80 % of the supply. The results are very promising, and hence this process should be developed further. Unfortunately, only a few studies have been published on this topic from 2012 to 2017. Current literature revealed the average number of publications on in-situ biomethanation is only about two papers per year, but it is anticipated that the number of studies will increase along with the development of the concept "Power to Gas". The application of biomethanation as part of the "Power to Gas" concept not only can be an alternative to solve the utilisation of the excess electricity issue, but also it can upgrade the biogas quality, which also opens the possibility of connecting to the natural gas grid.

2.3 Methanogenesis pathways

Anaerobic digestion has two main methanogenesis pathways; the pathway that forms methane from acetate and another from hydrogen and carbon dioxide (Deublein and Steinhauser, 2008), see Figure 2-3. However, the acetate from acetogenesis does not always form methane through acetoclastic methanogenesis, but there is also the possibility that the acetate oxidises to H_2 and CO_2 by syntrophic acetate oxidation bacteria (SAOB). On the other hand, there is also the possibility of the H_2 and CO_2 forming acetate through homoacetogenesis. In addition to the dominance of microorganisms, several factors such as acetate, VFA and ammonia concentration in the digester could influence the direction of the biochemical reaction pathways (Fotidis, Karakashev and Angelidaki, 2013).

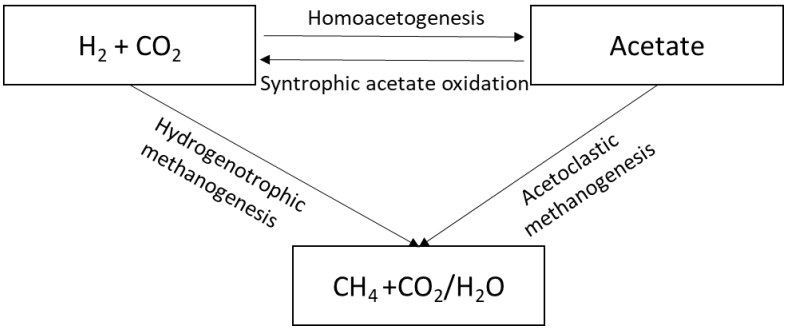

Figure 2-3 Two different methane production pathways from acetate or methane production from carbon dioxide (Schunurer and Jarvis, 2009).

It is widely reported that in the AD process, acetoclastic methanogen is more dominant in the contribution of methane production (Holmes *et al.*, 2015). In the methanogenesis stage, it is reported that 70 % of the methane formation is produced from acetate through acetoclastic methanogen, whereas the hydrogenotrophic pathways only cover 30 % of the methane production (Deublein and Steinhauser, 2008; Derbal Kerroum, Bencheikh-LeHocine Mossaab, 2012). The lack of a hydrogen source is a reason that methane production from CO_2 is not significant, but also the direction of methanogenesis pathways, determined by the role of syntrophic acetate oxidation and homoacetogen bacteria, which synergise with methanogens, could also contribute.

The biogas upgrading strategy in the in-situ biomethanation is to supply the additional hydrogen into an anaerobic digester. The hydrogen acts as an electron donor to form methane and for microbial growth (Costa, Lie and Jacobs, 2013). However, the addition of hydrogen increases the partial pressure of H_2, while the biochemical reaction in the acetogenesis (propionate and butyrate degradation) requires a low H_2 partial pressure (Schmidt and Ahring, 1993; Siriwongrungson, Zeng and Angelidaki, 2007). Therefore, the supply of hydrogen has to be controlled in order to maintain low H_2 partial pressure (Jürgensen *et al.*, 2015), or it can inhibit the VFA degradation and stimulate the acetogenesis via homoacetogen that utilises H_2 and CO_2 to form acetate (Siriwongrungson, Zeng and Angelidaki, 2007; Fotidis, Karakashev and Angelidaki, 2013). However, as long as that hydrogenotrophic methanogen can immediately consume the hydrogen, the partial pressure in the system can be maintained to be low.

In addition to the hydrogen partial pressure, other factors that can influence the direction of the methanogenesis pathways in biomethanation are the pH, temperature, VFA and ammonia (Fotidis *et al.*, 2013). These factors can influence the activity of methanogens. In some cases, some groups of methanogens are more tolerant to ammonia which can also trigger a change in the direction of the methanogenesis pathway.

The CO_2 conversion to CH_4 in in-situ biomethanation reduces the amount of CO_2 in the system. This is important as CO_2 also has a role in maintaining the pH as a bicarbonate buffer. This is why adding H_2 can increase the pH in the system (Luo and Angelidaki, 2013). Acetoclastic methanogens are very sensitive to the pH change when the pH increases; their

activity can be reduced or inhibited (Luo *et al.*, 2012a). On the other hand, hydrogenotrophic methanogens are reported to be more tolerant to the pH change (Horn *et al.*, 2003). Some studies have reported that hydrogenotrophic methanogens (HM) also could perform in an acidic environment (Horn *et al.*, 2003; Ju *et al.*, 2008). According to Hao et al. (Hao *et al.*, 2012), when the initial pH is 6-6.5, the methane production is primarily initiated through acetoclastic methanogens (AM). When the initial pH of the system was pH 5.5, the dominant pathways are shifted to SAO coupled with HM. Moreover, the role of methanogen can change from acetoclastic to hydrogenotrophic at a lower pH (Kotsyurbenko *et al.*, 2007).

The adaptability of HM applies to not only pH change but also extreme temperatures. The activity of HM reported increases at higher temperatures during the biomethanation process. Luo and Angelidaki (2012b) reported that the methane conversion obtained in thermophilic was 60 % higher than that compared to mesophilic. Additionally, in hyperthermophilic temperature (65 ^{o}C), the methane formation through HM can improve from 60 % to 100 % (Ho, Jensen and Batstone, 2014). Another evidence of the role of the HM in the higher temperature is that the hydrogenotrophic methanogen can be found to be higher at hyperthermophilic temperature compared to thermophilic (Demirel and Scherer, 2008). The robustness of the HM activities not only in the extreme high temperature but also in low temperatures, it was investigated by Garcia-Robledo *et al.* (2016). They compared the activity of HM at 20 ^{o}C and 38 ^{o}C. The results showed that higher activities might be found at higher temperatures. The effect of the temperature is more to influence the growth and activities of HM, and then the methanogenic population determines the direction of the methanogenesis pathways. In conclusion, the robustness of the activities of HM compared to AM can change the direction of methanogenesis pathways when the reactor changes to a higher working temperature (Fu, Song and Lu, 2015).

The shift in the methanogenic pathways between the acetoclastic methanogen and syntrophic bacteria, coupled with HM, is also influenced by the ammonia concentration (Schnürer and Nordberg, 2008; Hao *et al.*, 2012; Fotidis *et al.*, 2013). Ammonia can affect the acetoclastic methanogens activity at a particular concentration, while SAO and HM are

more tolerant to the ammonia concentration (Karakashev *et al.*, 2006; Westerholm, Levén and Schnürer, 2012; Wang, Fotidis and Angelidaki, 2015). Angelidaki and Ahring (1994) reported that the HM is more robust to the ammonia concentration than AM. On the other hand, the HM, which is more tolerant to ammonia, will replace the role of AM in producing CH_4. The change in the microbial activity can trigger changes in the methanogenesis pathway direction when the ammonia concentration increases to be more than a particular level (Banks *et al.*, 2012b) and additionally, when the working temperature is high (thermophilic or hyperthermophilic), the toxicity of ammonia will increase by the forming of free ammonia (Wang, Fotidis and Angelidaki, 2015). Many research groups have investigated the limit in the ammonia that can be tolerated by methanogen. The level of ammonia that can be tolerated by SAO, coupled with HM, is 2.8 - 4.57 g NH_4-L^{-1}, while the AM can still dominate at low ammonia levels < 1.2 g NH_4-L^{-1} (Fotidis, Karakashev and Angelidaki, 2013). The acclimatization of cultured microorganisms in the low concentration can increase the tolerance of methanogen to the ammonia level. This finding was reported by Fotidis *et al.* (2013). They showed that a methanogenic culture acclimatised to ammonia could tolerate up to 7 g NH_4-L^{-1}. The non-acclimatized methanogenic culture could only tolerate ammonia concentrations up to 5 g NH_4-L^{-1}.

2.4 Comparison of ex-situ and in-situ biomethanation

In general, the reactor configuration in the biomethanation study has focused on obtaining effective mass transfer and monitoring the microorganisms' activity. The study of the biomethanation of CO_2 and H_2 has two different approaches to adding H_2 into the digester. Hydrogen can be directly injected into the AD reactor, called *in-situ* biomethanation (Luo and Angelidaki, 2012b; Bassani, Kougias and Angelidaki, 2016; Agneessens *et al.*, 2017). On the other hand, the *ex-situ* biomethanation is where H_2 is injected into a separate reactor as post-treatment or as a standalone CO_2 consumption process, which contains the culture of the hydrogenotrophic methanogen (Lee *et al.*, 2012; Bassani *et al.*, 2015; Kim, Chang and Pak, 2015), see Figure 2-4.

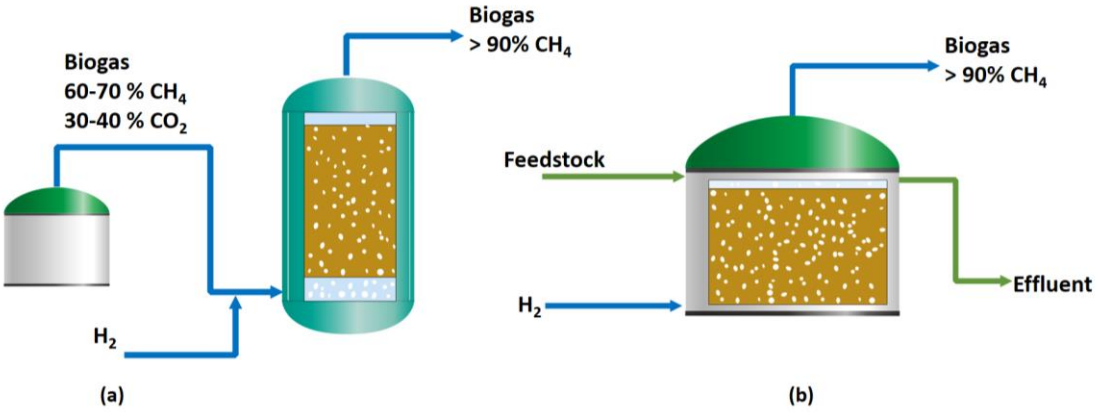

Figure 2-4 Schematic diagram of (a) ex-situ biomethanation and (b) in-situ biomethanation.

The principle of ex-situ biomethanation is to inject hydrogen and biogas or CO_2 into the reactor, which predominantly contains the hydrogenotrophic methanogenic culture, see Figure 2.5. The CO_2 that comes from the biogas is converted into CH_4, and this makes the methane content in the biogas, which previously contained only 60-70 %, and upgrades it to more than 90 % (Díaz *et al.*, 2015). In the in-situ biomethanation, hydrogen is directly injected into an anaerobic digester, which contains many groups of microorganisms, including hydrogenotrophic methanogen. The methanation process in in-situ biomethanation may be slightly competitive between the acetoclastic methanogen and hydrogenotrophic methanogen, while this does not occur in ex-situ. However, the methanation process in the in-situ can successfully upgrade the methane content from 55 % to more than 90 % (Luo and Angelidaki, 2013).

There are some advantages and disadvantages of using the in-situ or the ex-situ configurations. Since the methanation process of the ex-situ configuration occurs in the separate reactors, the methanation process can be simpler in terms of reactor design and control. The main process occurring in the ex-situ configuration is methanogenesis. In contrast, the in-situ configuration involves not only methanogenesis but also all of the other processes in an AD process, such as hydrolysis, acidogenesis and acetogenesis. Additionally, the hydrogen supply in the in-situ configuration must be adjusted to match the carbon dioxide production in order to follow the stoichiometric molar ratio (Lecker *et al.*, 2017), while in the ex-situ configuration, the CO_2 injection is controlled/measured and therefore is known and thus the amount of hydrogen supply can be easily determined. In

the ex-situ configuration, there is no limitation in the amount of CO_2 that can be reacted with the H_2, while in the in-situ configuration, the amount of hydrogen depends on the CO_2 produced (Lecker *et al.*, 2017). However, the ex-situ process requires an additional reactor for methanation, which increases the additional cost of the investment and the operational cost (Ahern *et al.*, 2015).

The biological methanation studies begin with the reaction of H_2 and CO_2 by a culture of hydrogenotrophic methanogens, or in the scope of biogas upgrading, this is called the ex-situ biomethanation. The studies on the ex-situ biomethanation have given much information on the principles of this process, and it has become the forerunner to the development of in-situ biomethanation. However, in the development of in-situ biomethanation, there are still many unexplored aspects, especially the monitoring of the methane production using the automatic system of hydrogen supply that can be adapted to the CO_2 production, which has led to the focus of this research work.

2.5 In-situ biomethanation reactor configurations and operations

The evaluation of the in-situ biomethanation has been studied in both batch and continuous reactors (Luo and Angelidaki, 2012b). Several reactor configurations exist in the in-situ biomethanation; in the continuous system, the Continuous Stirred Tank Reactor (CSTR) and Upflow Anaerobic Sludge Blanket (UASB) reactors are commonly used in the application of anaerobic digestion. In the case of in-situ biomethanation, in addition to the hydrogen injection line, the use of a sparger in the CSTR or UASB reactor is applied to obtain a better gas-liquid mass transfer. However, in prior works, most of the biomethanation parameters in a continuous experiment, such as gas composition, were monitored on a daily basis. Luo and Angelidaki (2013) proposed to use a gas bag in order to analyse initial and residual hydrogen on daily basis. This system was also adapted by Tao *et al.* (2019) with a gas recirculation loop that was also monitored on a daily basis. The limitation of those systems is that flexible gas storage is required to make a total conversion of hydrogen before the product biomethane/biogas can be discharged; this configuration may need substantial modifications in the operation of conventional AD reactors. The process monitoring using initial and residual gas could only analyse the process performance at the

beginning and the end of the day and for proper process design the information such as how the dynamic change of the process parameters such as pH, the behaviour of hydrogen conversion, etc. in the whole process would be required.

A model-based feasibility study for the biological methanation of hydrogen was investigated by Bensmann et al. (2014) based on a version of Anaerobic Digestion Model 1 (ADM1) (Batstone *et al.*, 2002) that has been extended to describe the hydrogen injection in anaerobic digestion. The results obtained using the model confirmed that the hydrogen could be methanised within the biogas plant. Overall, the modelling analysis showed that the biomethanation process might be influenced by two qualitatively different limitations, namely, either biological or mass-transfer limits.

2.5.1 Gas-liquid mass transfer

The gas-liquid mass transfer is still the major bottleneck in in-situ biomethanation (Szuhaj *et al.*, 2016). Therefore the design of the reactor has to take the effective mass transfer. Several ways have been evaluated in the literature in order to increase the gas-liquid mass transfer and, therefore, an effective hydrogen conversion.

The rate of gas-liquid mass transfer of the whole reactor is represented by the volumetric mass transfer coefficient, $k_L a$ (Pauss *et al.*, 1990). According to Jensen et al. (2021), the volumetric gas-liquid mass transfer can be determined with the following equation:

$$r_{g-l} = k_L a \,.\, (C_L^* - C_L) \qquad \text{Equation 2-8}$$

Where r_{g-l} is the volumetric gas-liquid mass transfer rate,

$k_L a$ is gas-liquid mass transfer coefficient

$(C_L^* - C_L)$ is the mass driving force

2.5.2 The use of a sparger

In order to obtain a higher gas-liquid mass transfer, the scheme of a bubbleless gas has been applied using a membrane (Luo and Angelidaki, 2013) or sparger (Bassani, Kougias and Angelidaki, 2016) to make smaller bubbles. Larger bubbles move upwards quickly and burst at the surface of the liquid. This situation is not productive because the activity of methanogens is in the liquid phase. To retain the H_2 in the liquid phase is difficult when the

H_2 comes in the form of larger bubbles, and this is the reason why the sparger is necessary to be applied in continuous biomethanation (Szuhaj *et al.*, 2016). Overall, the use of a sparger or membrane was able to increase the gas-liquid mass transfer and give a positive correlation to the hydrogen conversion. However, in the engineering application, the use of a sparger may not be required since the digester may be tall enough to dissolve the hydrogen despite a large bubble size (Amaral *et al.*, 2019). Further, the hydrogen bubbles may shrink and burst before the gas reach the liquid surface. Nevertheless, on the laboratory scale, the use of a sparger may be needed in order to cover the limitation of using a small-scale reactor.

2.5.3 Mixing rate

The distribution and dissolution of the gas are also influenced by the stirring intensity (Luo *et al.*, 2012a). The continuous stirring assists the gases in dissolving and thus makes contact with the bacteria on the liquid surface. From several studies in the literature, continuous stirring is required to be applied to the reactor in order to improve gas distribution. On the other hand, the stirring speed appears to affect methane production negatively; according to Peillex, Fardeau and Belaich (Peillex, Fardeau and Belaich, 1990), the optimum growth of methanogen occurs at low stirring rates, and in continuous systems, the methane productivity does not differ significantly when using 300rpm and 1200rpm (Peillex, Fardeau and Belaich, 1990).

A similar conclusion was obtained by Luo and Angelidaki (2012a), who found no significant difference in the CH_4 production when using mixing speeds of 150 rpm and 300 rpm. In another study, Szuhaj *et al.* (2016) experienced methane formation inhibition when the stirring speed was above 160 rpm. Continuous stirring is essential to provide a better distribution of the feed gas (H_2 and CO_2) and increase the contact with methanogens. However, it is essential not to run the reactor at a high stirring speed. According to Luo *et al.* (2012a), a lower stirring speed is required to keep the hydrogen partial pressure low, which is important for the VFA degradation process. Furthermore, a higher stirring speed requires more energy in the practical application, which significantly differs from the operational cost.

2.5.4 Gas recirculation

Gas-liquid mass transfer is the critical parameter for a biological methanation process (Luo *et al.*, 2012a; Bensmann *et al.*, 2014). Headspace gas recirculation is one of the strategies to increase the uptake of hydrogen by hydrogenotrophic methanogen. Gas recirculation has been applied to the biomethanation process on the laboratory scale in in-situ (Bassani, Kougias and Angelidaki, 2016), ex-situ (Kougias *et al.*, 2017) and also on a pilot-scale in-situ (Jensen *et al.*, 2018; Lebranchu *et al.*, 2019) and ex-situ (Alfaro *et al.*, 2018). It has been reported that gas recirculation increases the efficiency of hydrogen consumption (Jensen *et al.*, 2018) and has become a key parameter of the efficient biological methanation process (Bassani, Kougias and Angelidaki, 2016; Kougias *et al.*, 2017).

Many research groups have tried a variation of the gas recirculation rate from 2.5 L $L_{reactor}^{-1}$ day^{-1} (Jensen *et al.*, 2018), 5.7 L $L_{reactor}^{-1}$ day^{-1}, 8.6 L $L_{reactor}^{-1}$ day^{-1} (Bassani, Kougias and Angelidaki, 2016), 79 L $L_{reactor}^{-1}$ day^{-1}, 240 L $L_{reactor}^{-1}$ day^{-1} (Kougias *et al.*, 2017), and 200 L $L_{reactor}^{-1}$ day^{-1} (Alfaro *et al.*, 2018). In general, it was reported that higher recirculation rates increase the efficiency of hydrogen uptake in the biomethanation process (Bassani, Kougias and Angelidaki, 2016; Kougias *et al.*, 2017; Alfaro *et al.*, 2018). Additionally, Bugante *et al.* (1989) reported that the methane formation rate increased linearly as the gas recirculation rate increased. Bassani, Kougias and Angelidaki (2016) reported that 87 % of hydrogen injected was utilised and achieved a 37 % higher methane production rate by increased recirculation rate. Kougias et al. (2017) also showed a similar trend, who were able to increase the biomethane content from 73 % to 98 % by changing the gas recirculation rate from 79.2 L L_r^{-1} d^{-1} to 240 L L_r^{-1} d^{-1}. Voelklein, Rusmanis and Murphy (2019) could upgrade the methane formation to 94 % after increasing the gas recirculation rate up to 200 L L_r^{-1} d^{-1}. These results show that a higher recirculation rate positively correlates with the increased gas-liquid transfer.

From a microbial perspective, the reactor configuration using gas recirculation could enhance microbial activity (Bassani, Kougias and Angelidaki, 2016). Gas recirculation increases the amount of gas suspended in the liquid phase (gas hold-up). Therefore the value of the interfacial area between the gas and liquid phase, the hydrogen dissolution in the reactor, and finally, improves contact between hydrogen and hydrogenotrophic

methanogen. Although a higher recirculation rate could improve methane conversion rate, if the recirculation rate is run too high (in this case is more than 200 L L_r^{-1} d^{-1}), it will trigger high turbulence and foaming that will be an obstacle to the growth of microorganisms (Alfaro *et al.*, 2018) and cause practical operational issues.

On the other hand, the liquid recirculation configuration can slightly increase the methane content in the biogas (Bassani, Kougias and Angelidaki, 2016; Savvas *et al.*, 2017). The purpose of liquid recirculation is to maximise the methanogenesis of the substrate in the digestate, which has not been utilised yet. However, most of the organic content has been degraded and converted into methane during the anaerobic process, and this is the reason why the liquid recirculation produces an insignificant increase in methane production. In addition, in practical applications, liquid recirculation increases the operational cost, whose benefits may not be proportional to the additional methane produced.

A literature summary of different results from the different reactor configurations in the continuous system is presented in Table 2.4.

2.5.5 Hydrogen injection rate

Determining the injection rate of hydrogen to the AD reactor is critical since a too high injection rate may reduce the methane production due to the high hydrogen partial pressure and the following by VFA inhibition (Luo and Angelidaki, 2012b). According to the Sabatier reaction, the hydrogen that is injected into the reactor with a particular flow has to reach, or at least be close to the stoichiometry equation, with the H_2: CO_2 ratio being 4:1 (Bassani *et al.*, 2015; Kim, Chang and Pak, 2015). An increase in the injection rate increases the hydrogen partial pressure, which may lead to VFA accumulation (Fukuzaki *et al.*, 1990; Bassani *et al.*, 2015). Furthermore, H_2 injection that exceeds the stoichiometric ratio could result in the depletion of CO_2, leading to an increase in the pH (Luo and Angelidaki, 2012a), and too alkaline pH can interfere with the methanogenic activity (Luo and Angelidaki, 2013). However, Szuhaj et al. (Szuhaj *et al.*, 2016) show experimentally that the addition of CO_2 can recover the pH due to CO_2 depletion. On the other hand, the addition of CO_2 can increase the source of the carbon element, which can increase methane production (Tao *et al.*, 2019).

Leonzio (2016) investigated the effect of the temperature, injection rate, gas ratio, and reactor pressure on the performance of *Methanothermobacter marburgensis* through ANOVA analysis. The simulations showed that higher stability of the process is obtained at lower temperatures and higher injection rates.

Determination of hydrogen injection rate is the key in order to have the amount of hydrogen that is required. Another aspect that is also important is how the hydrogen is delivered; alternatives include constant flow (Bassani, Kougias and Angelidaki, 2016) or pulse injection (Agneessens *et al.*, 2017). With the limitation of hydrogen gas-liquid mass transfer, it is important to maintain the hydrogen rate according to its needs. Direct injection with a high rate would give a "flushing" effect causing hydrogen discharge without conversion and eventual contamination of the product gas. On the other hand, too low hydrogen injection rate will result in low CO_2 removal and low-quality biomethane product gas. From the author's point of view, a minimum flow rate and a continuous hydrogen injection corresponding to the stoichiometric requirement would be the best option. Low flow and continuous hydrogen injection would avoid the "flushing" effect and maximise contact time to allow hydrogen to be converted into methane. However, the exact amount of hydrogen requirement is difficult to know since the actual amount of carbon dioxide in the digester is relatively unknown. Therefore, a hydrogen injection should be adjusted according to the actual process parameters in real time. In the in-situ biomethanation, the key parameter that can be used are gas compositions and pH.

Table 2.4 The summary of the in-situ biomethanation in CSTR and UASB reactor configurations.

Reactor	Volume reactor (L)	Sparger/ medium	Temp (°C)	H2 Injection rate mL/(L day^{-1})	Mixing rate (rpm)	pH	CH_4 yield mL/(L day^{-1})	CH_4 content (%)	References
CSTR	4.5	Ceramic	55	686	65	8.3	453.6	65	(Luo *et al.*, 2012a)
CSTR	1	Ceramic	55	1700	150	7.89	885	75	(Luo and Angelidaki, 2012a)
CSTR	1	Hollow Fibre	55	930	150	7.61	680.5*	78.4	(Luo and Angelidaki, 2013)
CSTR	1	Hollow Fibre	55	1440	150	7.9	798.3*	90.2	(Luo and Angelidaki, 2013)
CSTR	1	Hollow Fibre	55	1760	150	8.31	860.1*	96.1	(Luo and Angelidaki, 2013)
CSTR	3	Hollow Fibre	37	960	200	8	435	98.8	(Wang *et al.*, 2013)
Two stage CSTR	3.5 each	Not mention	35	192	200	7.78	100	88.9	(Bassani *et al.*, 2015)
Two stage CSTR	3.5 each	Not mention	55	510	200	7.95	359	85.1	(Bassani *et al.*, 2015)
UASB	1.4	Rashig rings	55	3477	n.a	7.92	1528	40.4	(Bassani, Kougias and
UASB	1.4	Rashig rings	55	2636	n.a	7.90	1497	44.9	(Bassani, Kougias and
UASB	1.4	Ceramic	55	2629	n.a	7.93	1471	52.0	(Bassani, Kougias and
UASB	1.4	Ceramic	55	2144	n.a	7.64	1365	66.4	(Bassani, Kougias and
UASB	1.4	Ceramic	55	1834	n.a	7.85	1188	66.0	(Bassani, Kougias and
UASB	5	Acclimated	35	25	n.a	n.a	n.a	n.a	(Xu *et al.*, 2015)
UASB	5	Acclimated	35	25	n.a	n.a	n.a	n.a	(Xu *et al.*, 2015)

*) the CH_4 yield was calculated from the biogas yield and the methane content

2.5.6 H_2 and CO_2 ratio

The feed gas supply composition is an essential parameter to obtain the best process efficiency in the conversion of the feed gas. According to the Sabatier reaction, the feed gas ratio ideally follows the stoichiometric equation, in which the molar ratio of the H_2 and CO_2 should be 4:1 (Jee *et al.*, 1987; Kim, Chang and Pak, 2015; Kougias *et al.*, 2017). The effect of the molar ratio of the feed gas supply has been validated in many studies in the literature. In the very early stage of the biomethanation H_2/CO_2 study, Jee et al. (1987) reported that the maximum growth of methanogen is found to be optimum when the gas mix between H_2 and CO_2 is 80 %:20 % v/v, which is equal to the ratio 4:1. Also, Lee *et al.* (2012) obtained a higher methane conversion when the feed gas ratio (H_2/CO_2) was 4:1. The modelling study by Rittman et al. (2015) on the total gas inflow rate shows that only a 4:1 of the H_2/CO_2 ratio can convert 100 % of the methane, see Figure 2-5. Another simulation on the dynamic biogas upgrading was performed by Jürgensen *et al.* (2015). They found an optimal ratio for the production of methane was 3.4-3.7, which is close to the stoichiometric equation. Therefore, it is clear that the stoichiometric equation of the methanation reaction is the basis for the addition of feed gas to the methanogen cultures.

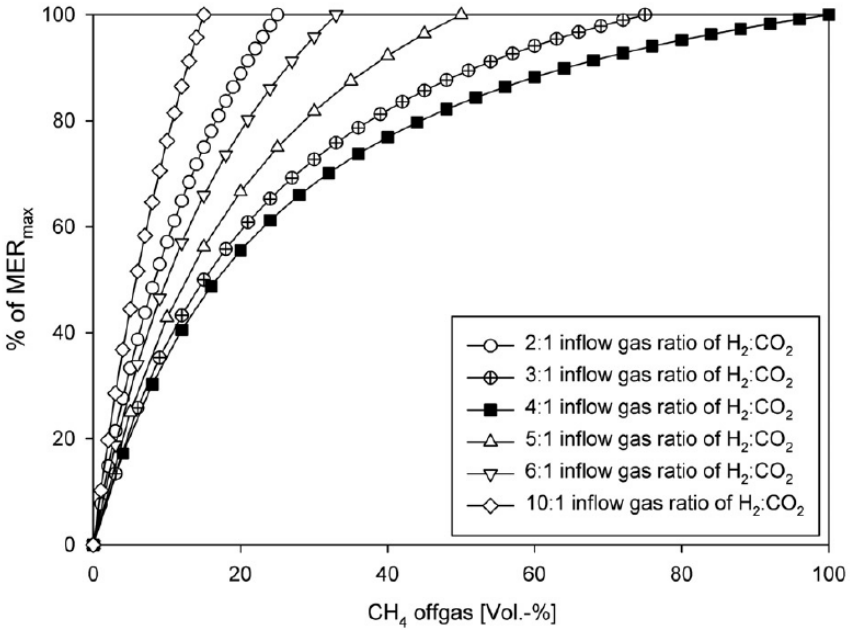

Figure 2-5 Conversion efficiency pattern of H_2 and CO_2 to CH_4 at different inflow gas ratios (MER – Methane Evolution rate) (Rittmann, Seifert and Herwig, 2015).

To determine the appropriate amount of hydrogen addition, some researchers have conducted methods to estimate the hydrogen requirement. Luo and Angelidaki (2012a, 2013) used two identical reactors; one was used as a control without adding hydrogen. In the experiment, the amount of hydrogen was determined based on the stoichiometric molar ratio calculated from the CO_2 production of the control reactor. The weakness of this method is the condition of biological reaction in two reactors is not identical due to natural variability, and the addition of hydrogen could change the path of the reaction. It could change the role of microorganisms, especially methanogens leading to different indigenous CO_2 production. Thus, the amount of CO_2 produced during the biomethanation reactor could be different. Other investigators, Bassani *et al.* (2015), used a two-stage CSTR reactor where the H_2 is injected into the second reactor, and the amount of H_2 is calculated from the amount of CO_2 produced in the primary reactor, similar to ex-situ biomethanation. In another experiment, Bassani et al. (2016) determined the amount of hydrogen by calculating the data recorded from the production of CO_2 before hydrogen is injected. The weakness of this approach is that the amount of CO_2 in the continuous system fluctuates, and the amount of CO_2 obtained at the beginning of the process cannot represent the CO_2 produced for the entire process. Determining the demand of additional hydrogen react with the amount of CO_2 produced is challenging.

An experimental study using various H_2:CO_2 ratios was investigated by Agneessens *et al.* (2017), who supplied the H_2:CO_2 molar ratio from 2:1 up to 10:1. The results show that the acetate accumulation occurred when the molar ratio of H_2: CO_2 exceeded 4:1. This demonstrates that it is essential to know the amount of CO_2, and then the amount of hydrogen can be set to follow the molar ratio. Furthermore, in a study by Agneessens *et al.* (2017), hydrogen was injected discontinuously in order to simulate the fluctuations of the hydrogen supply. The results show that the microorganism can immediately consume the hydrogen with an increase in the conversion rate, meaning the discontinuous supply of hydrogen could be a feasible application mode for in situ biomethanation. The control of the hydrogen supply is important for optimal CO_2 conversion since an excessive hydrogen supply can trigger process inhibition.

In summary, it is critical to control the amount of hydrogen corresponding to the stoichiometric ratio. The main issue in the continuous in-situ biomethanation process is that the amount of actual carbon dioxide in the reactor is unknown, then will make the hydrogen requirement difficult to know. The common approach is to use an estimation based on carbon dioxide-specific yield before hydrogen injection. However, the hydrogen addition to the anaerobic digestion can change the biochemical process making a prediction of the carbon dioxide production difficult. Therefore, the proposed hydrogen injection controlled based on gas composition and pH would be interesting to be explored.

2.5.7 Feedstock selection

Since the gas-liquid mass transfer is the main issue in the in-situ biomethanation process, feedstock selection was not a focus of study so far, and no comparative study of the effect of different feedstock. In the literature, the studies of biomethanation have mostly used manure-based or sewage sludge as inoculum and substrate source. In contrast, many AD plants have also used food waste as the inoculum and substrate. Feedstock-based study of in-situ biomethanation was performed by Luo and Angelidaki (2012a) by taking advantage of co-digestion manure and acid-whey since the whey has lower pH giving beneficial effects to avoid increasing pH as an effect of hydrogen injection. However, biomethanation studies have not focused on substrate variation.

To the best of the author's knowledge, no comparative study in in-situ biomethanation has evaluated the in-situ biomethanation process using different substrates and inoculums. This would be interesting because every substrate has a different characteristic of organic material. For example, using a substrate with low biogas potential may influence the amount of hydrogen requirement and work with a higher gas retention time. Another advantage is investigating potential inhibitors' influence, such as using feedstock with higher ammonia content. These investigations would give an insight into which element has the most influence on hydrogen conversion. Therefore, sewage sludge and food waste were selected to be used in this study.

2.6 Power to gas concept

The electricity generation from wind, wave and solar energy all depend upon the weather, which leads to fluctuating power production and eventually could result in excess electricity not being optimally utilised.

Electricity price is regarded as the most influential aspect affecting the economic feasibility of biomethanation projects (Götz *et al.*, 2016). The cost of electricity could reach 80 % of the total operational expenses (OPEX), which determines whether the project could be financially viable. Therefore, it is important to find approaches to reduce the cost of electricity that is required to produce the hydrogen used in biomethanation. Previous studies have mainly employed two different approaches. First, there are studies that have described the electricity price as a constant price with no seasonal or daily differences; this reflects situations where the operator would have a contract at a single tariff with an energy supplier (Götz *et al.*, 2016) or to describe the case of a power purchase agreement with local producers or renewable energy. Other studies have described the purchase of electricity with varied prices, depending on season and time of the day (Pääkkönen, Tolvanen and Rintala, 2018; Van Dael *et al.*, 2018; Michailos *et al.*, 2020). This approach allows the description of a variable tariff from the energy supplier for participation in the wholesale market. This approach is more realistic and can describe the characteristics of power to gas and power to methane systems in the future and their ability to use excess energy in the grid and, in turn, the potential income from the grid services.

2.6.1 Hydrogen production through the electrolyser

Hydrogen can be produced via an electrolyser using electricity. The ideal concept of power to gas is to utilise the excess electricity from renewable energy such as solar and wind, where the aim is to store the electrical energy that might otherwise not have been used.

Three types of electrolyser are considered to be used in power to methane application. There is Alkaline electrolyser (AEL), Polymer electrolyte membrane (PEM) and solid oxide electrolysis (SOEC). From those electrolysers, AEL is the most mature electrolyser technology for nearly a century. In accordance with the name of electrolyser, alkaline electrolyser requires an aqueous alkaline solution (KOH or NaOH) as an electrolyte. AEL is

operated at a temperature of 40-90 ^{o}C with pressure up to 30 bar (Smolinka, 2011). On the other hand, PEM electrolyser technology is still relatively new, although it is commercially available. PEM electrolyser is operated at a temperature of 20-100 ^{o}C with pressure up to 207 bar (Smolinka, 2011). Unlike the AEL and PEM electrolyser, the SOEC development is still at the laboratory stage and has to be operated at a high temperature (700 -1000 °C); it can cause fast material degradation, which is the biggest challenge of using this type of electrolyser. Also, by operating at a high temperature, the steam produced mixes with hydrogen, requiring an additional process to separate hydrogen and steam (Götz *et al.*, 2016). The summary of the operational parameter of the electrolyser can be seen in Table 2.5.

Table 2.5 Summary of an operational parameter of the electrolyser

	AEL	PEM	SOEC	reference
Temperature	40-90 ^{o}C	20 -100 ^{o}C	700 -1000 °C	(Smolinka, 2011)
Electrolyte	Alkaline solution	Solid polymer membrane	ZrO_2 ceramic doped with Y_2O_3	(Götz *et al.*, 2016)
Specific electricity consumption (kWh/m^3 H_2)	4.5-7	4.5-7.5	-	(Smolinka, 2011)
Electrolyser efficiency	63-71 %	60-68 %	100 %	(Böhm *et al.*, 2018)
Advantage	Mature and proven technology Lower CAPEX/OPEX	Less mature and proven technology Short respond time	Higher efficiency	(Götz *et al.*, 2016; Matute, Yusta and Correas, 2019)
Disadvantage	Long Cold start	Higher CAPEX/OPEX	Laboratory scale	(Matute, Yusta and Correas, 2019)

2.6.2 Wholesale electricity

In the United Kingdom (UK), electricity is traded in the N2EX Market. N2EX is the exchange-traded marketplace in Great Britain for day-ahead and the intra-day product as owned and operated by Nord Pool (2016). Day-ahead trading is the most common trading scheme where the participant could purchase and sell electricity for the following day. In the day-ahead market, the electricity can be traded in a single hourly order, while the intra-day

trading gives more flexibility by offering 15-minute, 30-minute, hourly and block trading. This study focuses on purchasing electricity from the day-ahead market. Two different bidding strategies can be placed in the day-ahead market for single hourly trading. First is the price-dependent order (PDO), where the trader can set the volume of electricity to be traded with a minimum and maximum bid price. Second is the price independent order (PIO), where the trader can set the volume of electricity to be traded at any price of electricity.

The PDO bidding strategy has been studied in applying power to gas by placing a maximum threshold price for purchasing electricity. For instance, Pääkkönen et al. (2018) evaluated the optimal operation of an electrolyser based on the fluctuating wholesale electricity prices for producing hydrogen in power to methane application. In their approach, the threshold was determined according to the target in the CH_4 production cost. In addition, Stavros et al. (Michailos et al., 2020) have studied a similar approach by varying the threshold price in purchasing the electricity to produce hydrogen through an electrolyser for the in-situ biomethanation process. In power to gas application, the electrolyser could be operated at the maximum load when the price of electricity is below the threshold. On the other hand, the electrolyser could be operated at the minimum load or can be operated on a standby mode, either hot or cold standby, when the price of the electricity is above the threshold.

The benefit of this PDO approach is that the hydrogen will be produced only when the electricity price is relatively low. However, there will be a risk that when the electricity price is higher, the amount of hydrogen produced is still not enough to cover the biomethanation process requirement. The PIO bidding strategy could be an option in order to guarantee that the hydrogen production is sufficient to fulfil the requirement of the biomethanation process. For both bidding strategies, it will be required to have an instant switch on and off or standby. To the best of the authors' knowledge, the implementation of the PIO from the N2EX spot market to the power to methane application has not previously been investigated.

2.7 Conclusion

In the biomethanation literature, most investigators have focused on the strategies to increase methane production by optimising the conversion rate of the CO_2 and hydrogen gas-liquid mass transfer in ex situ systems. However, the biomethanation of hydrogen and carbon dioxide is feasible to be applied to anaerobic digestion in an in situ process. The major constraint in the biomethanation process is the gas-liquid mass transfer. Many methods of injecting hydrogen have been applied to obtain a better gas distribution in the reactor. On the other hand, in applying the biomethanation process, it is important to supply hydrogen according to the stoichiometric ratio. In in-situ biomethanation, it would be difficult to measure carbon dioxide production and, at the same time, supply the required amount of hydrogen unless the system is able to record the actual data in a real-time situation. From the best of our knowledge, online monitoring and control in the application of in-situ biomethanation have not yet been developed. Therefore, this research focuses on combining the automated online process monitoring and control in order to simultaneously control the hydrogen injection and monitor the key parameters in the in-situ biomethanation process.

In the feedstock situation, no comparative study in the in-situ biomethanation has evaluated the influence of the substrate and inoculum. Each inoculum has a different population of microorganisms, and each substrate has different characteristics of the organic material. Therefore it is important to investigate the in-situ biomethanation using different types of inoculums and substrates, especially the complex substrates such as the organic fraction municipal solid waste (OFMSW) or other waste that would be useful in the practical applications of in-situ biomethanation.

Techno-economic studies mainly differ on the modality in which the electric market has been modelled. This directly influences the cost of electricity to run the electrolyser and, in turn, the dynamic and capacity factor of the electrolyser. Therefore, techno-economic studies need to be complex enough to capture this relationship between the demand of hydrogen for biomethanation, market bidding strategy, and the overall sizing of the system.

3. METHODOLOGY AND EXPERIMENTAL RIG SETUP

This chapter describes the materials and methods that were used in the experimental investigation. The experiment was prepared and operated in the Anaerobic Digestion Laboratory, Ella Armitage Building at the University of Sheffield.

3.1 Feedstock and inoculum

3.1.1 Feedstocks

Non-synthetic substrates were used for in-situ biomethanation laboratory reactors. Sewage sludge and food waste were used as feedstocks for the biomethanation experiments. This decision would allow the evaluation of the effect of different feedstocks, with different physical and biochemical characteristics, on the biomethanation process. For instance, the different feedstock will lead to different ammonia content, methane and carbon dioxide content in the produced biogas, methane and carbon dioxide flows, influencing the biomethanation process and its controls. Furthermore, substrate composition directly affects biomethanation performance, as it directly determines the dynamics and the amount of CO_2 production, the concentration of potential inhibitors such as ammonia, and hydrodynamic characteristics (viscosity) influencing gas-liquid transfer.

Sewage sludge

Sewage sludge is a residue originating from activated sludge wastewater treatment processes and is composed primarily by organic matter, water and active microorganism. Sewage sludge is usually composed of primary and secondary sludge: primary sludge is generated from chemical coagulation, sedimentation, and other primary processes, whereas secondary sludge is the activated waste biomass resulting from biological treatments (Jerry A. Nathanson, 2022).

The anaerobic digestion of sewage sludge is a major process in the practical application of wastewater treatment activities everywhere in the world. Compared to other sludge managements, the anaerobic digestion of sewage sludge offers many advantages, such as clean energy, reduction by 30 % to 50 % of the number of solids in the sludge, pathogen destruction, etc. (Gebreeyessus and Jenicek, 2016).

In this study, sewage sludge was collected from Stockport Waste Water Treatment Work (WWTW), and it was a mixture of both primary and secondary sludge on a roughly 50:50 basis. Once received, the TS and VS of sludge were analysed, and the rest was stored in the freezer until it was ready to use for feeding. When the time to used for feeding, the sewage sludge was defrosted and homogenised using a mixer. TS and VS were measured again before being used and taken into account in the calculation. The variation of the % TS and % VS was quite consistent on each batch of feed, with the variation of the % TS and % VS in the sewage sludge at ±7 % and the food waste was ±4 %.

Food waste

Food waste from the retail and hospitality sector was selected to represent the anaerobic digestion process using source-segregated food waste as the primary substrate. The composition of food waste that was used in the experimental investigations was made according to the types of food waste in the UK in accordance with the "*Household and drink waste in the UK*" report published by WRAP (Tom and Hannah, 2009). The compositions of the food waste sample used in this study are presented in Figure **3-1**.

A blended sample of food waste was then made using real food waste that was collected from various sources around the University of Sheffield; one collection point was from the university canteen, and the second source was from the student accommodations.

A representative sample was taken in a total of about 60-80kg of food waste that was taken from a waste bin at both locations. Food waste samples then were taken to the AD laboratory, and the contaminant packaging was removed.

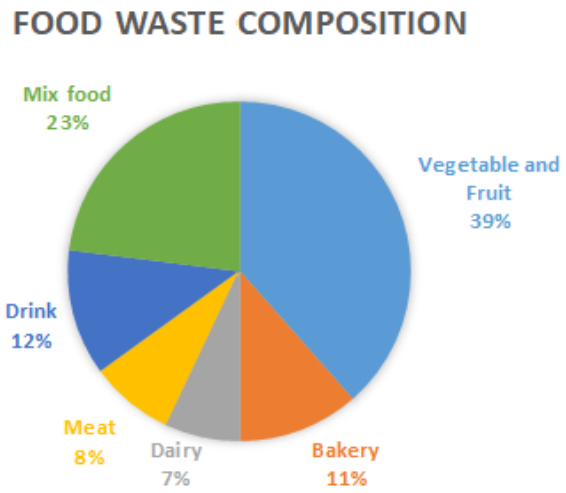

Figure 3-1 Food waste composition.

The waste was segregated according to the major categories of food waste, as described in the UK WRAP report (Tom and Andrew, 2017). The results categories used in this study are presented in Table 3.1.

Table 3.1 Food waste categories.

Categories	Content
Vegetable and fruit	Fresh vegetables and fruits, potato chips
Bakery	Bread
Dairy	Milk, yoghurt, butter
Meat	Chicken, pork, beef (raw meat and cooked)
Drink	Tea leaves residue, coffee residue, carbonated drinks
Mix food	Sandwich, ready meal products, cakes, spices, sauces, processed vegetables, etc.)

Each type of waste was weighed and then combined based on their categories, and about 40kg of the final weight of the food waste sample was used. The food waste sample was mixed in one large container and homogenised by ground and minced. The food waste was ground 2-3 times and minced at least twice through a 6mm cutting plate before being packed into a 2L container and then frozen to a temperature of -18 ^{o}C until it was used later. When the sample was ready for use, it was defrosted and made ready for use at room temperature. Once it has been defrosted, the food waste is prepared by adding 70 % (w/w) of DI water to reach a final desired TS concentration of 14 % and make it easier to pump during the feeding process. In order to further reduce the particle size and facilitate the

feeding through the peristaltic pump, the food waste was minced again using a 2 mm cutting plate before finally adding a trace element solution, see Figure 3-2. Grinding was done with kitchen equipment (Magimix 5200XL, France). Mincing was done with a meat electric mincer (Tritacarne No.12, Italy) using a 2 mm mincer plate.

In order to account for any variation of the feedstock composition in the different prepared batches, samples of both sewage sludge and food waste were taken before feeding for analytical characterisation; any variation in the VS content would be taken into account in order to maintain the desired OLR during the semi-continuous experiments.

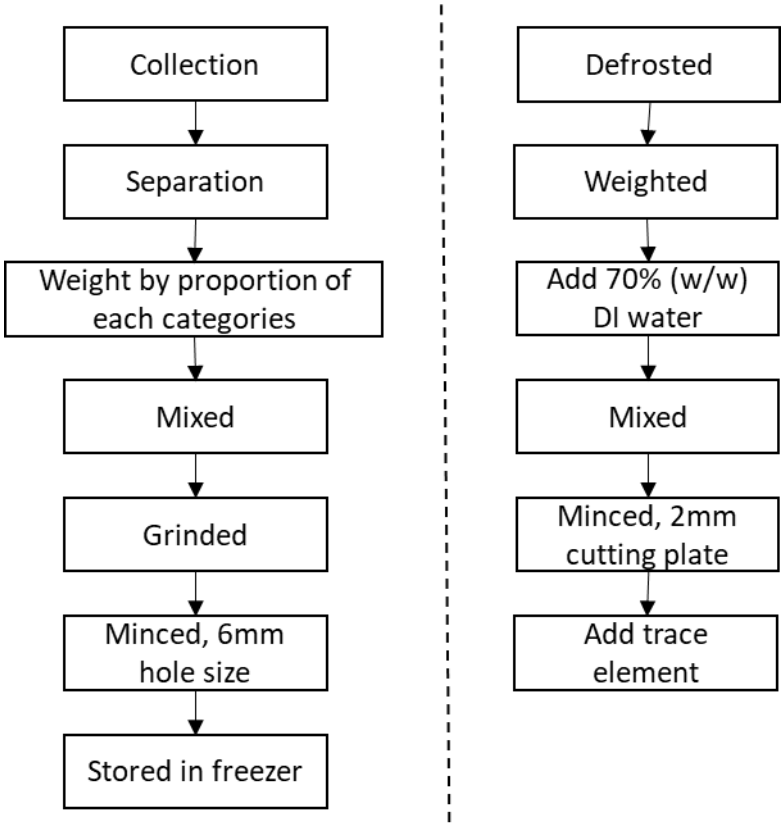

Figure 3-2 Food waste collection and preparation before stored (left) and food waste preparation before being used as substrate (right).

3.1.2 Inoculum

Two sources of inoculum were used in this project. The first inoculum was obtained from the Wastewater Treatment Works (WWTW) in Stockport (Greater Manchester). This inoculum was inoculum-adapted sewage sludge. It was used as an inoculum for a reactor

fed by sewage sludge. The second source of inoculum was obtained from an anaerobic digestion plant treating food waste in Doncaster (South Yorkshire), operated by the company namely ReFood. The second inoculum was inoculum-adapted food waste. It was used as an inoculum for a reactor fed by food waste. The inoculum was used immediately after collection for the experiment either batch or continue and was prepared by sieved through a 1 mm mesh before use in order to reduce the unwanted solid material in the sludge.

3.1.3 Trace Elements

Trace elements were added in this work to the prepared food waste and sewage sludge feedstocks. Indeed, trace elements have been shown to significantly impact the performance of food waste digestion (Demirel and Scherer, 2011; Facchin *et al.*, 2013). Furthermore, the addition of trace elements not only improves methane production but also increases the stability of the anaerobic digestion process (Banks *et al.*, 2012a).

A trace element (TE) mixture was prepared as a one-litre stock solution, and the composition of the trace element solution is presented in Table 3.2. One millilitre of TE per one litre of digestate (inoculum) in the digester was added at the beginning of the experiment as a one-off dose. Then the TE is added at the rate of one millilitre per one litre of feedstock for both the sewage sludge and food waste (Banks *et al.*, 2012b).

Table 3.2 The concentration of the trace elements in the stock solution.

Trace element	Compound used	Element concentration in the stock solution (g/L)
Molybdenum (Mo)	(NH4)6Mo7O24 · 4H2O	0.1
Nickel (Ni)	NiCl2.6H2O	1
Tungsten (W)	Na2WO4 · 2H2O	0.1
Selenium (Se)	Na2SeO3	0.1
Cobalt (Co)	CoCl2 · 6H2O	1

3.2 Analytical methods

The following analytical methods were used to measure different characteristics of the feedstocks and samples from the reactors. Reactors were sampled from a dedicated sample port and at different periods depending on the variable measured, as described in

the respective sections below. All reagents used were laboratory grade except where otherwise stated.

3.2.1 Total and Volatile Solid Analysis

The solid analysis consists of the total solid (TS) and volatile solid (VS). The solid samples are gravimetrically measured from the liquid effluent samples (digestate), and this procedure follows the standard method 2540 APHA (Arnold E. Greenberg, 1992). Samples were weighed in a dry ceramic crucible to a sensitivity of ±1 mg and then placed overnight in the oven (Heratherm OGS60, Thermo Scientific) at 105 ^{o}C. The dry samples were cooled to room temperature and then weighed again before ignition into a furnace (Elite BSF 12/10A), heated up to 550 ^{o}C for about 3 hours, the time count from the cold oven. The samples were cooled at room temperature and then weighed again.

The total solid and volatile solid were calculated according to the following equation:

$$\%\, TS \;=\; \frac{W_3 - W_1}{W_2 - W_1}\, x100 \qquad \text{Equation 3-1}$$

$$\%\, VS\ (wet\ weight\ basis) = \frac{W_3 - W_4}{W_2 - W_1}\, x100 \qquad \text{Equation 3-2}$$

$$\%\, VS\ (TS\ basis) = \frac{W_3 - W_4}{W_3 - W_1}\, x100 \qquad \text{Equation 3-3}$$

Where W_1 is the weight of an empty crucible (g);

W_2 is the weight of crucible containing fresh sample (g);

W_3 is the weight of crucible and sample after drying at 105 ^{o}C (g) and

W_4 is the weight of crucible and sample after heating at 550 ^{o}C (g).

3.2.2 Alkalinity

Alkalinity was measured using a titration method, according to APHA 2320 (Arnold E. Greenberg, 1992). First, the digestate was sampled, approximately 5g was transferred to a 100 ml glass beaker which was then placed on the analytical balance (weight of the samples was recorded), and then 50mL of deionised water was added. Then the sample was placed over a magnetic stirrer, and then the pH probe was immersed into the sample. The titration was performed using an automatic titrator (SI Analytic titrator Titroline® 5000) that is connected to a pH probe, and then a 0.25 N sulphuric acid solution was used as a titrant.

The titration was set to determine the volume that was used to reach a pH of 5.7 and 4.3, thus allowing the calculation of the total (TA), partial (PA) and intermediate alkalinity (IA) as follows (L. E. Ripley, 1986):

$$\boldsymbol{TA} = \frac{(\boldsymbol{V_{4.3}}+\boldsymbol{V_{5.7}})\boldsymbol{x\ N\ x\ 50000}}{\boldsymbol{Vs}} \quad \text{Equation 3-4}$$

$$\boldsymbol{PA} = \frac{(\boldsymbol{V_{5.7}})\boldsymbol{x\ N\ x\ 50000}}{\boldsymbol{Vs}} \quad \text{Equation 3-5}$$

$$\boldsymbol{IA} = \frac{(\boldsymbol{V_{4.3}})\boldsymbol{x\ N\ x\ 50000}}{\boldsymbol{Vs}} \quad \text{Equation 3-6}$$

Where the $V_{5.7}$ *and* $V_{4.3}$ are the volumes of titrants used to reach the endpoint pH 5.7 and 4.3, respectively; *N* is the normality of the sulphuric acid, and *Vs* is the volume of the sample.

3.2.3 Total Ammonia Nitrogen

The total ammonia nitrogen was measured based on the standard method 4500 NH_3 B and C (APHA, 2005). A digestate sample of approximately 3g was weighed into a 100 mL beaker glass, and then 50 mL of deionised water was added. Prepared samples were followed by adding about 0.3-0.4mL of sodium hydroxide 6 M. The pH was checked to ensure that the sample solution had a pH value above 9.5 to around 12. Then the sample was immediately placed into a distillation tube and placed on an automatic distillation system (VELP® Scientifica UDK 129); 50mL of boric acid solution (4 % weight/volume aqueous solution) (Scientific laboratory supplies, UK) was placed in a 250mL Erlenmeyer flask and then used to collect a distillate. The boric acid buffer contains an indicator which changes colour from pink to green around pH 4. The distillation was run for 5 minutes. The distillate was then titrated with an automatic titrator (SI Analytic titrator Titroline® 5000) using 0.25 N of sulphuric acid as a titrant until the pH reached 4, which is the initial pH of the boric acid solution. The change in the pH can also be visually seen by the colour change from green to pink. The calculation of *TAN* is based on equation 3-7.

$$\boldsymbol{TAN}\ \left(\frac{\boldsymbol{mg\ N}}{\boldsymbol{kg}}\right) = \frac{\boldsymbol{Vol\ titrant\ x\ N\ x14\ x1000}}{\boldsymbol{W_s}} \quad \text{Equation 3-7}$$

Where *Vol* titrant is the volume of titrant that is used to titrate the sample (mL), *Ws* is the wet weight of the samples (kg), and *N* is the normality of the titrant.

This method was tested and validated using a standard ammonia solution in order to ensure the method provides valid results.

3.2.4 Elemental analysis

An elemental analyser (Flash 2000, Thermo Scientific, Germany) was used to perform the CHNS analysis, and a standard tin capsule containing 10 mg vanadium pentoxide was used for the calibration. Reference samples were prepared with 10mg vanadium pentoxide and about 5 mg of BBOT (2,5- Bis (5-tert-butyl-benzoxazol-2-yl) thiophene).

The feedstock samples to be tested were prepared by placing them overnight at 105 ^{o}C in the oven in order to remove the moisture and then homogenised using a pestle and mortar. Three duplicate capsules were made for each feedstock sample with 10 mg vanadium pentoxide, and approximately 5 mg dried feedstock.

Hydrogen was used as the carrier gas and delivered at a flow rate of 200 mL min^{-1} and oxygen-enriched at a flow rate of 300 mL min^{-1}. The samples were heated to 900 °C for 700 seconds before being analysed with a flame ionisation detector and a capillary GC column.

3.2.5 Volatile Fatty Acids (VFA)

The sample was prepared by transferring 5 g of the digestate into a 50ml beaker that was placed on an analytical balance. After doing this, 0.5 mL of pure formic acid (5 % of the total volume) was added, and then this was topped up with deionised water until the total solution reached 10g. Formic acid was used to reduce the pH of the samples and ensure VFA volatilisation during the GC injection (Raposo *et al.*, 2013). Samples are then transferred to a microcentrifuge tube and centrifuged (Heraeus™ Pico™ 21 Microcentrifuge) for 30 minutes at 14,000 rpm. The supernatant was collected using a syringe and filtered using a 0.2µm microdisk into a 1.5 mL glass vial before finally being placed onto the GC autosampler.

The VFA analysis was measured by the gas chromatography (Thermo Scientific™ TRACE™ 1300), using a flame ionisation (FID) detector and a DB-FFAP column (length 30 m, ID 0.32 mm, film 0.25 µm) and Nitrogen was used as the carrier gas, and the carrier gas flow rate was 2.6 ml/min. The injector and detector temperatures used in this method were 250 ^{o}C

and 230 ^{o}C, respectively, with a split ratio of 40:1. The oven temperature was operated at 70 ^{o}C with 3 minutes hold, then increased to 180 ^{o}C, and the ramp-up temperature was 20 ^{o}C min^{-1}, and then 3 minutes hold at 180 ^{o}C.

A mix of the standard VFA solution containing acetic acid, propionic acid, isobutyric, butyric, isovaleric and valeric acids were prepared for standard calibration, and three different concentration standard solutions were made for this purpose at 10mM, 2.5mM and 1mM. The prepared samples were then analysed by using an autosampler.

3.3 Bio-methane Potential (BMP) test

The biomethane potential (BMP) test was used to investigate the methane produced that the feedstocks could potentially produce in ideal conditions. In this thesis, the BMP was performed using an AMPTS II (Bioprocess Control AB, Sweden) instrument. The system consists of fifteen anaerobic digesters units, each consisting of three main components (Figure **3-3**). First, a 500 mL stirred batch reactor placed in a water bath was used as temperature control. Second, a biogas scrubber containing a 3M sodium hydroxide solution with thymolphthalein indicator as an absorbing solution for the CO_2 and H_2S contained in the biogas. Addition, the third is a gas-measuring device, which works on the principle of an inverted tipping bucket immersed in the liquid. The system has a resolution of 10 ml methane produced and recorded at STP (0 ^{o}C, 1 bar, dry conditions). This system was controlled by the software user interface. The system also removes an overestimated methane gas due to the initial flushing gas in the headspace. For this purpose, an approximation of the initial biogas flow then is required. This can be done by using the Buswell formula (Buswell and Mueller, 1952), which can be calculated using the elemental compositions of the substrates. (Strömberg, Nistor and Liu, 2014)

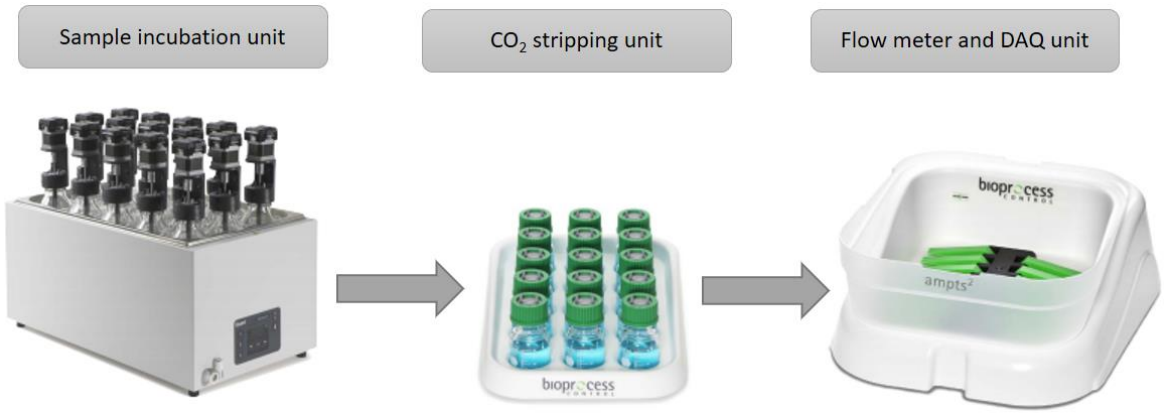

Figure 3-3 Schematic of the automatic methane potential test (AMPTS II).

The BMP was performed using AMPTS II with a working volume of 400 mL. Different inoculums were prepared depending on the types of substrate. Substrates for both sewage sludge and food waste were prepared in triplicate as well as blank as reactor control. The blank reactors were filled with inoculum without substrate addition, while the control reactors were filled with inoculum and used microcrystalline cellulose as a substrate. Inoculum and substrate ratio (ISR) was reported to have influence on increasing the methane production rate. Raposo *et al.* (2012) explained that high ISR could increase methane production rate and reduce the risk of the possible amount of VFA produced. They also recommended that the ISR ≥2 (VS basis) could be used as a standard BMP test. It is recommended to have VS inoculum that is higher than the VS substrate; according to Holliger *et al.* (2016), the recommended ISR ratio is between two and four. Therefore, in this study, the inoculum and substrate ratio (ISR) was selected at 3 $gVS_{inoculum}/gVS_{substrate}$.

After all reactors were filled with inoculum and substrate, the oxygen was purged by injecting synthetic biogas (60 % CH_4 and 40 % CO_2) into the digester for about 3 minutes to make an anaerobic condition. The temperature during the test was maintained at mesophilic temperature (38 ^oC) and stirred at 60 rpm. The incubation time was performed according to the daily methane production until the cumulative methane production was less than 1 % on three consecutive days (Holliger *et al.*, 2016).

3.4 In-situ biomethanation experiment setup

Theoretically, the biomethanation process could be designed as a combination of batch and continuous processes. For instance, substrate and the addition of hydrogen could be batch-fed and allow a suitable reaction time; substrate could be fed continuously and gas batch-fed, etc. However, no batch experiment is conducted in this study. Instead, the experimental work of this PhD implemented a configuration that would result from the retrofit of existing industrial AD reactors without affecting either the typical plants' operational strategies or gas storage characteristics. In other words, the AD reactor would receive the feedstock semi-continuously (i.e. a certain number of feedings per day). At the same time, a suitable injection system would deliver the hydrogen into the reactor in a continuous way.

In this study, the in-situ biomethanation rig was designed for continuous operation with a fully instrumented setup and was automated. The main principle of developing the rig is to proportionally control the injection of hydrogen to the anaerobic digester according to the composition of the biogas produced and indicators of the process stability. This strategy is required in order to control the desired biomethane quality. The biogas composition, biogas flow and pH are required to be monitored and programmed in order to communicate with the hydrogen injection system, in this case, the mass flow controller (MFC). Since the process involves hydrogen injection, a sound safety practice was critical in designing the system. A hydrogen sensor was installed to monitor the level of hydrogen in the atmosphere. For this purpose, the system configurations and automated process control were all designed and built specifically for this project.

The rig is designed to observe the in-situ biomethanation process in six independent reactors. Three reactors were fed with sewage sludge, and the other three were fed with food waste, while one of the three reactors was used as the reactor control without hydrogen injection.

A schematic diagram of the design of the experiment rig is presented in Figure 3-4. Hydrogen from a hydrogen gas cylinder is proportionally supplied to the anaerobic digester through a mass flow controller (MFC). The biogas composition is analysed by online gas

chromatography (GC). Once the required biogas composition was obtained, the information was sent to the MFC in order to supply hydrogen with a new flow rate proportionally. In order to increase the gas-liquid mass transfer, a gas loop was operated by a peristaltic pump that recirculates the biogas back into the reactor. Further, the volume of the biogas production was measured by a gas flow meter.

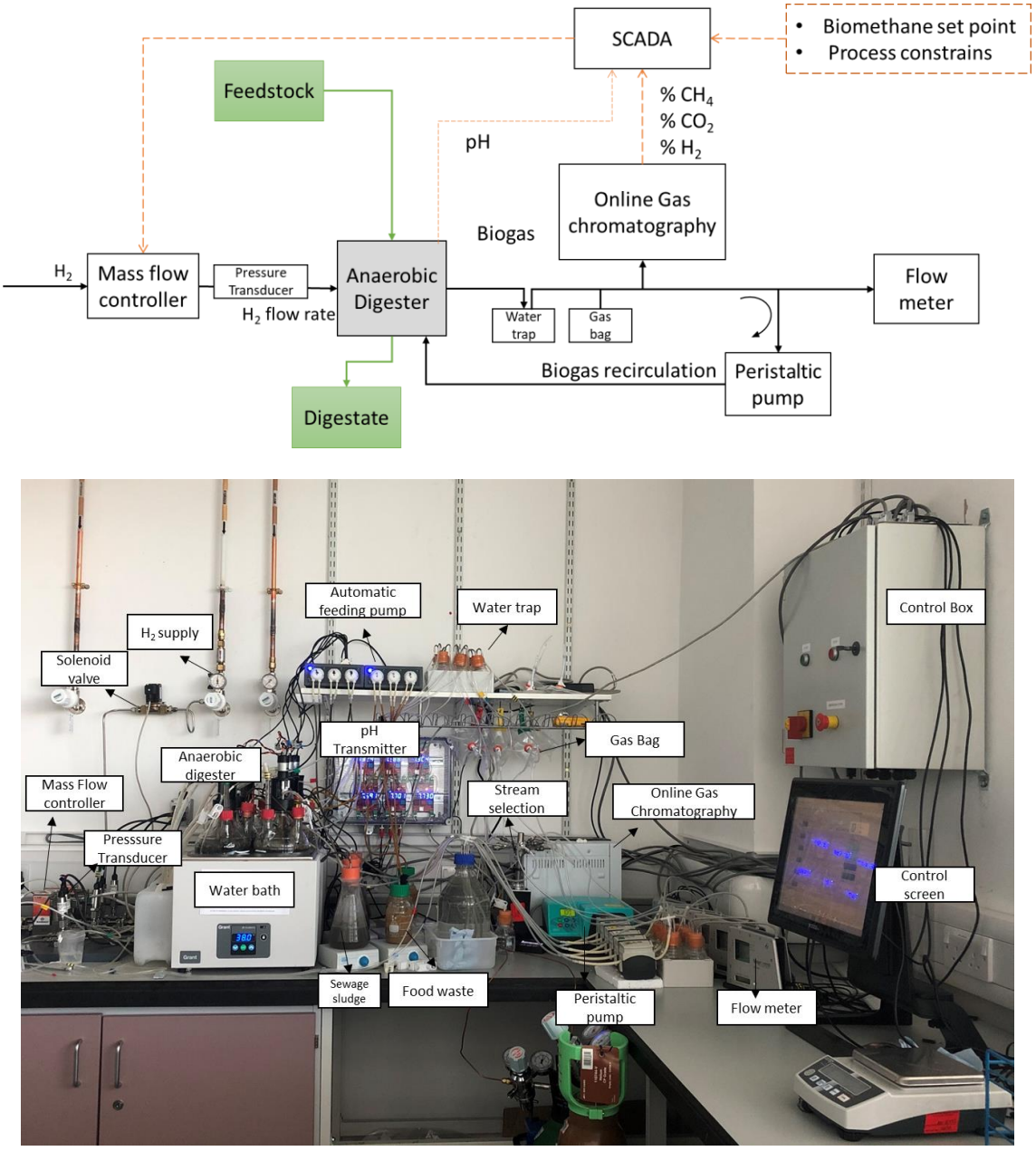

Figure 3-4 Schematic diagram of the design of the experimental setup (top) and a photograph of the in-situ biomethanation experimental rig (bottom).

A pressure transducer is installed to measure the pressure in the hydrogen injection line and to be used as a safety control to avoid pressure going too high. The water vapour produced in the system

may disturb the gas analysis result and could harm the lifetime of the gas chromatography, especially in filter and column. In order to avoid water vapour condensing and then flowing to the gas chromatography, a water trap made of 100mL beaker glass was installed between the digester and gas chromatography. The water trap is monitored periodically to ensure there is still enough space to collect condensed water. Gas compositions in the headspace were sampled and monitored continuously every 20 minutes, which will also reduce the volume of the headspace continuously. A 200 mL gas bag was installed before the gas chromatography as a gas buffer to avoid the vacuum effect of headspace volume reduction due to gas sampling by the gas chromatography.

3.4.1 Anaerobic digester

Single-stage continuous stirred tank reactors (CSTR) were used in this study. In in-situ biomethanation, CSTR has been found to be beneficial in order to provide a uniform distribution of hydrogen and increase the gas-liquid mass transfer as well as the distribution of the feedstock and temperature (Usack, Spirito and Angenent, 2012).

Six 2L identical CSTR (Bioprocess control AB, Sweden) were used, and the reactors are equipped with three ports (GL25 size). In this project, the ports were used to attach the pH probe and discharge the digestate, and one last port was used for feeding the inlet and the gas recirculation. A connector made of a 4 mm stainless steel tube was used for the gas recirculation and feeding inlet. The tubes were inserted into a rubber bung to ensure they fit the digester's port. The biogas produced was released through a metal tube attached to the rubber stopper lid and the hydrogen injection. A bent stainless steel rod covered by a Tygon rubber tube was used as a stirrer that was connected to a 12 V DC motor. In most of the experimental investigations, the stirring/mixing rate used was 60rpm, while in the higher stirring/mixing rate, the rate was increased to 110rpm. In most of the experiments, hydrogen was injected through a sparger. A stainless steel sparger with a 2 µm pore size was placed into the hydrogen injection line, and it was attached to the stirring rod. Finally, the temperature was controlled at 38 ^{o}C in a thermostatic water bath. An illustration of the reactor is presented in Figure **3-5**.

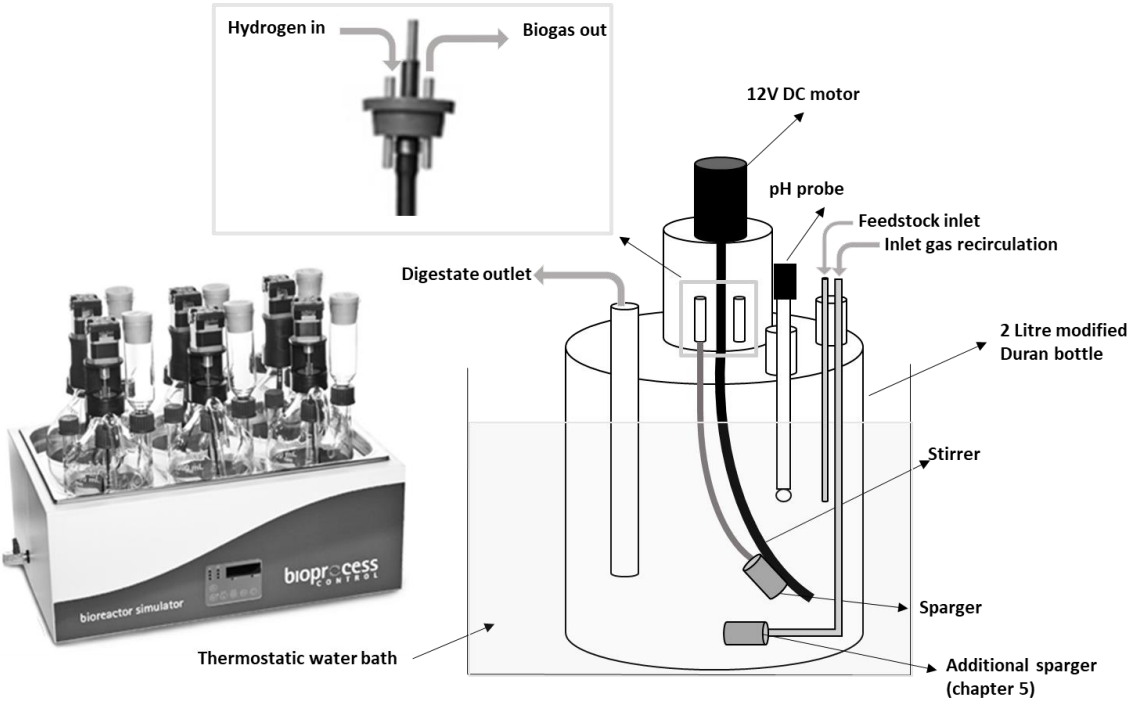

Figure 3-5 A schematic of the continuous stirred tank reactor design.

3.4.2 Real-time pH measurement

A pH transmitter (IXIAN, Atlas scientific) was used to monitor the pH during the experimental investigations, Figure **3-6**. Each pH transmitter for each digester was connected to the pH probe (Atlas scientific) and one temperature sensor (PT100, RS Pro, UK). The pH transmitter unit had a sensitivity of ± 0.001 pH unit and accuracy of ± 0.002 pH unit. The pH was calibrated by immersing the pH probe in a buffer solution at pH 4, 7 and 10. The calibration standard buffer solution was prepared from buffer pellets (Fisher Scientific) according to the supplier's instructions. The pH transmitter could read the pH 24-hour/ 365-day operation with no downtime. However, due to the heavy-duty operation, the pH probes were calibrated periodically every three months or at least before running a new experimental investigation. All the pH transmitters were connected to the SCADA system for data acquisition.

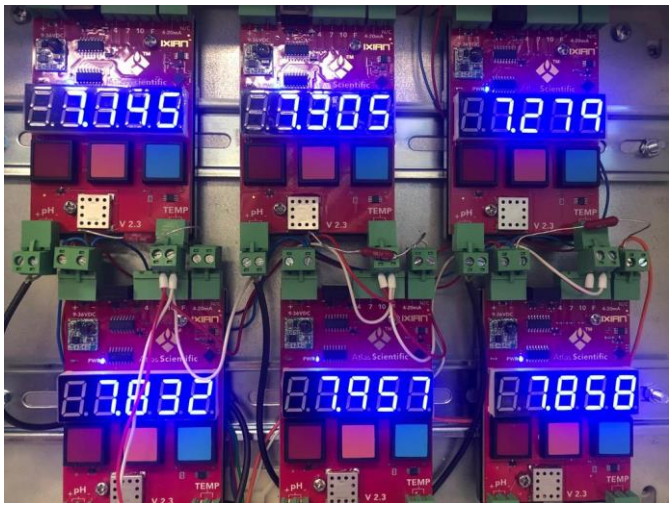

Figure 3-6 Photograph of the IXIAN pH transmitter for each reactor.

3.4.3 Automatic feeding system

The feedstock was supplied by a programmable dosing pump (D-DH2Ocean P4 Pro). Two unit feeding pumps with three head pumps are used for each unit pump to provide a sufficient feeding supply for each reactor, with one head pump for each feedstock. The feeding pump comes with the software (D-DH2Ocean) that can be downloaded at Playstore or Appstore to control and schedule the dosing time and dosing quantity. Each head pump was calibrated using dedicated feedstock, either sewage sludge or food waste. The calibration was achieved by pumping the feedstock using a 10 mL graduated cylinder for 15s, and the desired feeding volumes were registered to the software.

The feeding schedule simply registered the amount of the feed and the time for feeding. Up to 24 feeding times per day can be set when required with a fluid volume from 0.1-9999 mL. The feeding schedule for each feedstock type is different depending on the quantity of the daily feeding requirement.

In order to maintain the level of the working volume in each reactor, another two dosing pumps (Jebao DP 3) were used to discharge an effluent with approximately the same amount as that which is fed. Each discharge pump has three pump heads with almost the same pumping features as the pump used for feeding. In order to maintain the level of digestate in the reactor, the discharge effluent pump was scheduled to start 5 minutes before the schedule of the feeding pump.

Feeding for each reactor was prepared in a 100-500 mL feeding container and placed on a magnetic stirrer to maintain the homogenisation of feeding. The actual amount of feedstock fed by the peristaltic pumps might slightly deviate from the setpoint. Therefore, the overall amount of feedstock that enters into the reactor was recorded on a daily basis by weighting the feeding container before the start of the new cycle of feeding. It was then assumed that the overall amount was equally shared between the feeding events. An illustration of the automatic feeding system is shown in Figure **3-7**.

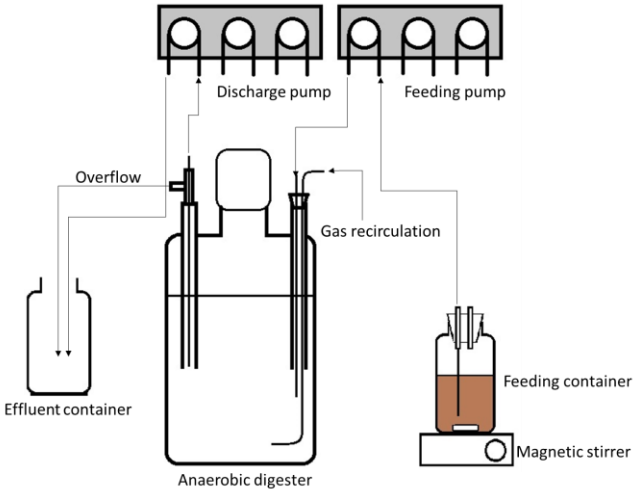

Figure 3-7 Schematic diagram of an automatic feeding system.

3.4.4 Hydrogen injection

Hydrogen was supplied from a hydrogen gas cylinder (BOC, UK) using a mass flow controller (EL-Flow select, Bronkhorst, UK). The mass flow controllers have a flow range of 0.6-30 ml min^{-1}, and the MFC with a lower flow range of 0.16-0.8 ml min^{-1} was used in the period where a lower injection rate is required. This MFC operated at 1 bar inlet pressure and 0 bar outlet pressure.

The SCADA system controls the flow of hydrogen supplied by the MFCs through MODBUS communication. Manufacturer software (Flow DDE and FlowPlot) were used to validate the implemented SCADA control system against a control via PC. MFC was connected directly to a flow meter (µFlow, bioprocess control, Sweden), the flow meter principle explained in section 3.4.6. Validation was done by measuring the flow during one-hour experiments at constant flow and comparing the expected requested flow from the MFC with the

measured flow. Another method to validate the flow rate was done with a gravimetric method by water displacement. This method has benefits, especially for a low flow rate that was difficult to be done using a flow meter. In the gravimetric method for validation, MFC was connected to the tube filled with water attached to the glass bottle. The flow was measured based on the weight of water out from the tube and time. Both methods gave confidence that the SCADA controller can control the MFC to send the requested flow with an average per cent error of 3.3 ± 0.4 % less compared to the value obtained using the manufacturer software. The error of the flow was then taken into account in the hydrogen injection flow calculation by adding the error percentage to the desired setting flow on the user interface. Therefore, the actual value obtained is in accordance with the expected value.

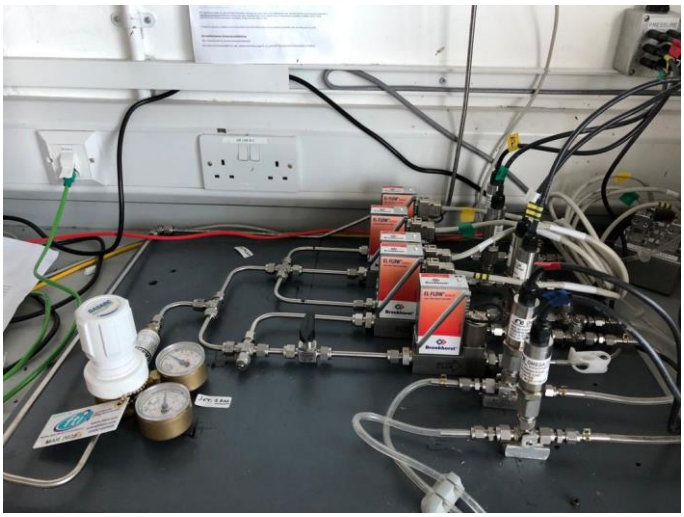

Figure 3-8 Photograph of the hydrogen injection system through the mass flow controller (MFC).

Hydrogen was injected via Tygon tube to the gas port on top of the reactor. In order to increase hydrogen gas-liquid mass transfer, stainless steel sparger (2µm) was installed at the end of the tube to reduce bubble size. In addition, a biogas recirculation was applied to increase gas-liquid transfer and gas uptake rate by microorganisms. The biogas then recirculates back to the reactor through a peristaltic pump (323/D Watson Marlow) at recycling rate between 20 and 280 rpm (or equivalent from 12 to 155 L L_r^{-1} day^{-1}) depending on the experiment (see Table 4.3). The peristaltic pump has six pump heads with one motor. Therefore, the recirculation rate was the same for all reactors.

3.4.5 Pressure transducer

A pressure transducer (PXM 309 0.035GI, Omega) was used to monitor the pressure and also used as a safety device that has a role in the emergency shutdown protocol. It has a detection range between 0-350 mbar. The pressure transducer was placed after the Mass flow controller as it measured the pressure in the hydrogen injection line. For the reactor's control, which is not connected to the MFC, the pressure transducer was connected to the recirculation line.

3.4.6 Biogas analyser

The instrument selection for the biogas analyser was quite challenging. First, the instrument needs to be able to measure all the biogas components (CH_4, CO_2, H_2, and H_2S) with excellent resolution and accuracy. Second, the instrument needs to analyse all six streams with the same condition and accuracy. Third, the instrument must be able to run continuously to provide feedback for the control of the hydrogen injection. For real-time measurements, the gas sensor (such as the infrared-based sensor) appears to be the best instrument to choose. However, the use of the sensor is specific to each gas, requiring at least three to four sensors for each stream, which would be challenging to keep the same condition and accuracy between each sensor. Therefore, the instrument is required to be one that can analyse all the gasses. Gas chromatography appears to be a perfect instrument to do this job, and it can run continuously with an autosampler.

In addition, this gas comes directly from the reactor, and there is no option to prepare the sample gas. However, a stream selector valve is available in the market and can be used for this job. The stream selector can select the stream alternately by continuously changing the connection from one stream to another. Nevertheless, the GC and the stream selector have to be able to communicate with each other and give the correct measurement for each stream. For this reason, online gas chromatography (490 Micro Gas Chromatograph, Agilent, US) and stream selector (VICI Valco® instrument, Canada) has been selected.

A stream selector or multi-position valve equipped with a micro-electric actuator that can switch each stream's position has been employed. There are many models of stream selector valves with different flow paths. In order to obtain a continuous flow to the biogas,

while one of the streams is being analysed but non-selected streams are flowing, a flow-through model (SF type) with ten ports was selected, as illustrated in Figure **3-9**. A stream selector has an individual inlet and outlet. However, the gas analysis in the GC takes about 3 minutes, and the flow on the selected stream will only flow to the GC.

The GC was sampling every 20 minutes for each stream. On each stream, the analysis was operated for about 3 minutes prior to sampling time. It was taken for about 30 seconds in order to ensure that all sampling line was properly flushed and that there was no contamination from another stream from the previous analysis. The sampling volume was measured and considered in the calculation as gas produced.

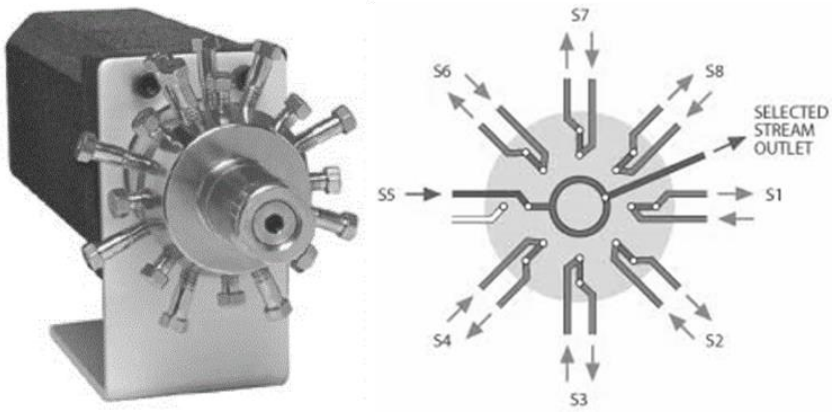

Figure 3-9**.** Valco® stream selector, flow-through model (SF type).

The GC has a dual cabinet equipped with a CP-Molsieve channel (Molsieve 5A PLOT 0.25 mm in, 20m) and a CP-PoraPLOT U channel (PoraPLOT U, 0.25mm, and 10m). The argon carrier gas was used for the CP Molsieve channel, and the helium carrier gas was used for the PoraPLOT channel. Both carrier gasses were supplied with a 5.5 bar of pressure according to the manufacturer's recommendation. In addition, the GC is equipped with a micro thermal conductivity detector (mTCD) that was used to analyse the gas from both channels. The CP-Molsieve channel analyses the permanent gases such as hydrogen, oxygen, nitrogen, methane and carbon monoxide, while the CP-PoraPLOT U channel was used to analyse the carbon dioxide and hydrogen sulphide.

All the setting parameters were set in the software (PROstation) that was provided by the manufacturer. During the continuous experiment, the GC analysis was set to be automatic

by following the order that was set in the sequence control. In the continuous GC analysis, the analysis starts by taking a sample from stream number 1, and the next analysis will be followed by stream numbers 2 to 6. After analysing stream number 6, the stream selector returns to take a sample from stream number 1. The analysis from the same stream is repeated approximately every 20 minutes, and an automatic analysis on the GC can be stopped anytime; in this case, the stream selector chooses the unused port. Therefore, no stream in the rig is connected to the GC inlet.

The GC has several interface options. In this project, A MODBUS TCP/IP procedure was used to communicate between the GC and SCADA. By using an internet connection, the GC status and the result of GC analysis could be accessed remotely.

3.4.7 Flow Meter

The biogas production was measured using a gas flow meter (µFlow^{TM} Bioprocess Control AB, Sweden), Figure **3-10**. The gas was measured on the principle of water displacement and buoyancy with the normalised gas condition (STP: 0 ^{o}C, 1 atm, dry conditions). A digital pulse was given with a 9mL resolution, and the flow meter provided a flow range with a resolution from 20 to 4000 ml h^{-1}. µflow instantly calculates the biogas flow based on the time interval between two consecutive pulses.

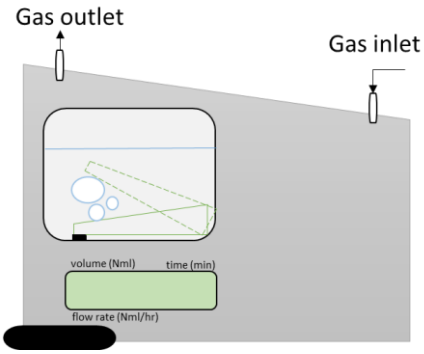

Figure 3-10 Sketch of the flowmeter (µFlow, Bioprocess control).

In order to monitor real-time gas volume production, all flow meters were connected to the SCADA controller. The SCADA controller was able to read an electric signal of 4-20mA from each flow meter and record it as an average.

3.5 Process control and data acquisition

The main goal of the process control in the in-situ biomethanation rig is to control the hydrogen injection, include the process monitoring and data acquisition, and ensure the experiment is running safely.

Supervisory control and data acquisition (SCADA) has been built using a National Instruments CompactRIO™ (cRIO-9045) controller consisting of an analogue and digital module. The cRIO controller has a memory card slot to store data logging and has the capability to remote monitoring via Ethernet connectivity. A custom-made LABVIEW™ application was carried out by a senior technician under the author's supervision. This SCADA system was used to control the injection of hydrogen and to monitor the real-time process parameters, such as pH, biogas flow rate, gas compositions and also some safety features.

A controller NI cRIO-9045 with an eight-module slot has been used to receive and send an electrical signal from all the devices. There are several inputs and outputs modules that were used. The MFCs were connected to modules NI9205 and NI9263 to control the voltage input and output. The MFC works based on a digital interface (RS232); the module NI9205 is also used to receive an input voltage from the pH transmitters. Another module, the NI9208, was used to receive a current input from the flowmeter and pressure transducer. Finally, a digital output module NI9472 was used to control several relay functions such as safety, solenoid, MFC, feeding pump and stirrers.

3.5.1 Feedback control relations for the operation of the H_2 Mass Flow Controller

The SCADA can control the MFC through a user interface (UI) with manual control, which can be controlled automatically by activating the feedback control. The manual control provided a constant flow depending on the input on the UI. On the feedback control, the hydrogen flow is determined based on the gas composition obtained from the GC and pH of the digestate in the digester.

The ultimate goal in the in-situ biomethanation upgrading process is to achieve as high as possible the carbon dioxide that can be converted to methane, meaning that the hydrogen needs to be maintained until the concentration of the biomethane reaches the targeted

concentration (e.g.>90 %). Therefore, the hydrogen flow rate on a feedback function can be expressed as a function of the methane set point (S_CH_4sp) as a targeted value according to equation 3-8. This approach was derived from the work of Bensmann *et al.* (2014), which introduced the use of Proportional and Integral (PI) control. However, in this work, the parameter was simplified to use only proportional control.

$$GH_2\_CH_4 = k\_CH_4 * (S\_CH_4sp - X\_CH_4) \quad \text{Equation 3-8}$$

Where,

- $GH_2\_CH_4$ is hydrogen flow rate related to methane concentration
- X_CH_4 is the measured methane value,
- S_CH_4sp is the desired methane set point
- k_CH_4 is the proportional constant.

From equation 3-8, it can be seen that the flow decreases linearly with the increasing methane concentration. However, the continuous injection of hydrogen does not always follow the CO_2/H_2 conversion to methane due to the limited gas-liquid transfer. Too much hydrogen would increase the pH and triggers the VFA accumulation. Additionally, CO_2 is required to maintain the chemical equilibrium in the AD system. Therefore, the constraint value of CO_2, H_2 and pH is necessary to limit the MFC in the sending of the hydrogen into the digester. The equations related to the constraints can be expressed as follows:

$$GH_2\_CO_2 = k\_CO_2 * (X\_CO_2 - S\_CO_2min) \quad \text{Equation 3-9}$$

$$GH_2\_H_2 = k\_H_2 * (S\_H_2max - X\_H_2) \quad \text{Equation 3-10}$$

$$GH_2\_pH = k\_pH * (S\_pHmax - pH) \quad \text{Equation 3-11}$$

Where,

- $GH_2\_CO_2$, $GH_2\_H_2$ and GH_2_pH are the hydrogen flow rate related to gas constraints.
- XCO_2, XH_2 and pH are the measured concentrations of CH_4, CO_2, H_2 and pH, respectively.
- S_CO_2min is the CO_2 constraint that will be the minimum acceptable CO_2 level in the biogas.
- S_H_2max is the H_2 constraint that will be the maximum acceptable H_2 level in the biogas.
- S_pHmax is the pH constraint that will be the maximum acceptable pH value in the reactors.
- While k_CO_2, k_H_2, and k_pH are the control parameters for CO_2, H_2 and pH, respectively.

The value of the flow that will be sent to the MFC is calculated as the smallest flow amongst all the feedback values, and the value of the setpoint is according to equation 3-12:

$$GH_2\_MFC = MIN(GH_2\_sp, GH_2\_CH_4, GH_2\_CO_2, GH_2\_H_2, GH_2\_pH) \quad \text{Equation 3-12}$$

There is a condition when the value of the measured methane (X_CH_4) is higher than the methane set point (S_CH_4sp) or the value of the measured hydrogen (X_H_2) is higher than the hydrogen constraint (S_H_2max), and when in this condition then this gives a result of negative flow. In this case, a negative flow is set as zero, meaning that there will be no hydrogen supplied to the digester.

3.5.2 Safety features

In order to be able to run the rig continuously and to be able to operate the rig unattended, several safety aspects were considered when the rig was built. The rig was equipped with safety devices that ensured the experiment would run safely, such as a flashback arrestor, solenoid valve, hydrogen sensor, and pressure transducer.

A shutdown procedure was controlled by SCADA as a safety precaution; therefore, the rig will automatically shut down safely. In addition, a shutdown procedure was made as a precaution against the risk that is triggered by a hydrogen leak and overpressure (Figure 3-11). A shutdown procedure is a procedure that will shut off the power of all the devices of the rig except the gas chromatography. The reason why the GC was excluded from this shutdown procedure was for maintenance purposes. If there is a sudden power going off, it will potentially shorten the GC column's lifetime. Also, the carrier gas cylinders will keep supplying the gases because no solenoid valve was installed for both the carrier gasses. Other devices, such as the solenoid valve, MFC, peristaltic pump, stirrer, feeding pump and feeding magnetic stirrer, will be shut off when the shutdown procedure is applied.

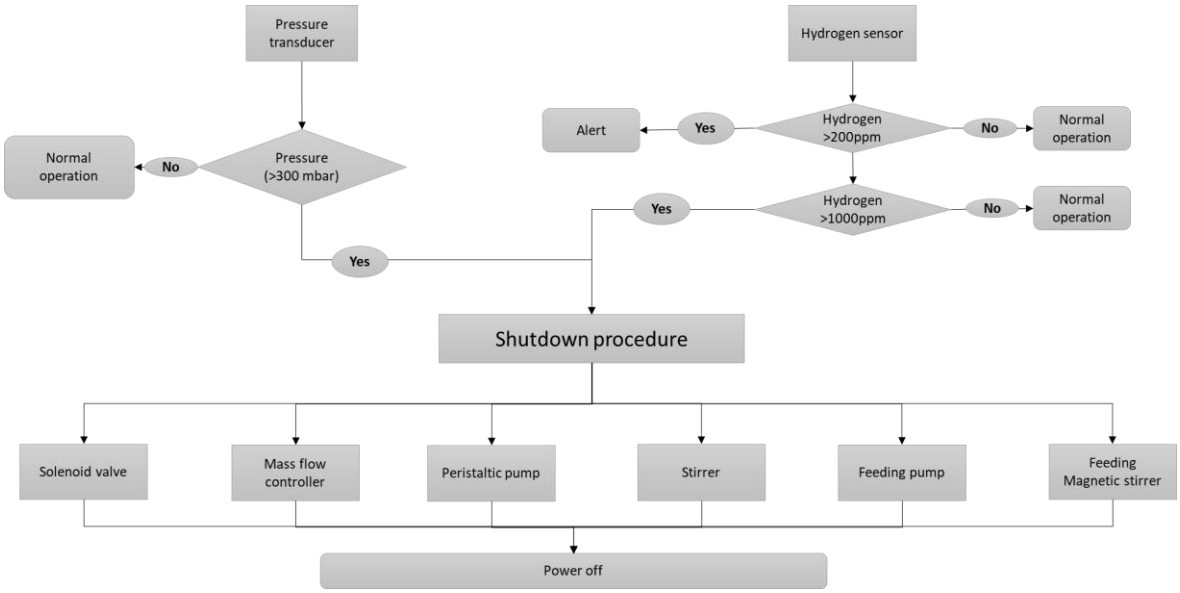

Figure 3-11 Schematic of the automatic shutdown procedure.

A dedicated hydrogen sensor (4H2-40000, Gasman) was installed to monitor the hydrogen concentration in the laboratory to control the risk of hydrogen leakage that will follow with the risk of explosion or fire. This sensor has a measurement range of 0-40000 ppm, corresponding to 0-100 % of hydrogen Low Explosion Limit (LEL) and has a resolution of 80ppm. Two-stage limit real-time monitoring was applied to control the hydrogen supply in the case of hydrogen leaking into the atmosphere. The first limit was set to 200 ppm as this level is enough to raise an alert that some hydrogen is leaking. An alert signal appears on the monitor (UI), but this does not shut down the rig until the accumulation of hydrogen continues to reach the second limit. The second limit was set to 1000 ppm, corresponding to 2.5 % of the hydrogen low-level limit. This setting was far enough from the hydrogen LEL as the risk of hydrogen accumulation in the headspace could cause severe consequences and catastrophic damage. Then the rig was designed to ensure that the system would be able to do a safety precaution to minimise the risk, even if the level of the detection is far from the hydrogen LEL.

The shutdown procedure closes the solenoid valve and the MFC, meaning there is no hydrogen supply to the digester when the shutdown procedure is activated. In the worst-case scenario, if the shutdown procedure fails, another hydrogen sensor (Xgard, Crowcon) was already installed in the laboratory. This sensor has higher sensitivity compared to a dedicated rig sensor. An Xgard sensor was connected to the solenoid valve that is

responsible for closing the supply of hydrogen from the hydrogen cylinder when the concentration of hydrogen in the atmosphere reaches 10000 ppm or 25 % of hydrogen LEL.

Another component that can trigger the shutdown procedure is overpressure. The pressure transducers (PXM309-0.035GI Omega, UK) were installed on each line and located after the MFC. Since the digester material was made from glass, there is a risk of breakage when the pressure is too high. For this purpose, the pressure in the system needs to be controlled as a safety measure, and this limit is set at 300 mbar.

3.6 Biomethanation performance parameters

3.6.1 Gas retention time

The gas retention time is an important process parameter which directly influences hydrogen conversion. The longer the hydrogen is in contact with the liquid phase, the higher the amount that will be dissolved and finally converted to methane. Contact to the liquid phase will happen in the different modalities in the reactor: after the injection and its ascension as bubbles through the slurry liquid until reaching the headspace; similarly, like bubbles from the gas recirculation injector; and at the interface of the gas headspace and the surface of the liquid slurry

Thema *et al.* (2019) proposed the gas retention time (RT) is calculated as the reactor volume divided by the average gas flow (equation 3-13).

$$\boldsymbol{RT_G = \frac{V_R}{Q_G}} \qquad \text{Equation 3-13}$$

Where Q_G is the average gas flow between gas in and gas out. In the in-situ system, the only gas input is hydrogen. Therefore, the main contribution of the gas retention time is the overall gas outflow, including the gas produced from the anaerobic digestion process and the hydrogen injected into the reactor. In this study, gas retention time is expressed in the unit of hours.

3.6.2 Hydrogen conversion

Interesting to see the relation between gas retention time and the conversion of hydrogen. Long retention time gives more time for the gas to have contact with the liquid, which leads

to the biomethanation process. So longer retention time might give higher hydrogen conversion.

Hydrogen conversion describes how much of the hydrogen injected is actually converted in the biomethanation process and is defined as in equation 3-14:

$$H_{2\ conversion} = \frac{H_{in} - H_{out} + \Delta HS}{H_{in}}\ x\ 100\ \% \qquad \text{Equation 3-14}$$

Where H_{in} is the total hydrogen injected into the reactor and H_{out} is the total hydrogen out from the reactor, while ΔHS is the variation of H_2 amount contained in the headspace in a given time interval, with a positive sign showing an accumulation of H_2 and a negative sign a depletion. For instance, H_2 accumulation in the headspace would result in lower H_2 outflow, which would not be accounted for as higher actual conversion. This definition of H_2 conversion, including the variations in the headspace, has been adopted in this thesis to better characterise the process during the dynamic periods of the experiment, such as at the beginning of the H_2 injection or during feedback control activation. H_2 amount can be defined either on a mass or molar basis or on a volumetric basis when all standardised to the same temperature and pressure conditions (as done in this Thesis). There will be a condition where some hydrogen will be used for anabolic activities. However, the proportion of hydrogen that was used for anabolic activities was small (between 0.28% and 0.43%) (Lecker *et al.*, 2017).

3.6.3 Relationship between H_2 conversion and retention time

A relationship between H_2 conversion (equation 3-14) and Retention Time (equation 3-13) will be attempted in chapter 5. To do so, a scatter plot of these two variables will be presented using average values across 6 hours intervals.

Previous literature (Choi *et al.*, 2010) has shown that in gas-liquid mass transfer limited bioprocesses, the relationship between RT and gas conversion would be as follow:

$$X_{gas} = \frac{K*RT}{1+K*RT} \qquad \text{Equation 3-15}$$

Where X_{gas} is the fractional conversion of gas, RT is the gas retention time as calculated in equation 3-13, and K is related to the gas-liquid mass transfer coefficient. This equation can

be derived from a mass balance in a CSTR, considering a first-order reaction. This chapter will use this curve as a trendline using equation 3-15 in the RT vs hydrogen conversion plots to identify potential improvements in the gas-liquid mass transfer. Trend lines were fitted with a Least Square Method implemented in OriginPRO, with equal weight to all data points.

3.6.4 Methane evolution rate

One indicator that expresses the increase of volumetric methane production rate over the methane production from anaerobic digestion resulting from the in-situ biomethanation process is methane evolution rate (MER).

The methane evolution rates (MER, [L Lr^{-1} day^{-1}]) were calculated using equation 3-16.

$$MER = \frac{\frac{H2in - H2\ out + \Delta HS}{4}}{Vr}$$ Equation 3-16

The MER of in-situ biomethanation was reported within a range from 0.08 to 0.39 L/Lr day (Luo *et al.*, 2012a; Lecker *et al.*, 2017; Alfaro *et al.*, 2019).

3.6.5 Biomethanation extent

While the MER describes the increase in volumetric methane production, biomethanation also allows for higher biogas quality. Another indicator to express the additional methane as a product of biomethanation is to measure the biomethanation extent. This is expressed as a fraction of methane to the sum of methane and carbon dioxide, as seen in equation 3-17.

$$Biomethanation\ extent\ = \frac{\%\ CH_4}{\%CH_4 + \%CO_2}$$ Equation 3-17

The biomethanation extent considers only methane and carbon dioxide content. The methane will increase during biomethanation as carbon dioxide and hydrogen are converted into methane. Equation 3-17 shows that in the cases of all carbon dioxide being converted, the methane enrichment would give 100 %. On the other hand, if there is no conversion of CO_2 in relation to no additional methane as a product of the biomethanation

process, the biomethanation extent value will show a similar value as biogas (CH_4 and CO_2) produced without hydrogen addition. Another indicator that can be used to express the methane enrichment is the CH_4/CO_2 ratio, where the value of the CH_4/CO_2 ratio will increase along with the methane enriched.

3.6.6 Gas-Liquid mass transfer coefficient

The gas-liquid mass transfer rate is usually expressed using the following formula, derived from the two-film theory (Díaz *et al.*, 2015; Jensen, Ottosen and Kofoed, 2021)

$$\dot{m}_{G/L} = V_R k_L a (C_l^* - C_l) \qquad \text{Equation 3-18}$$

Where $\dot{m}_{G/L}$is the mass transfer rate (mol/d), V_R is the volume of the liquid phase in which the gas-liquid transfer happens (L), $C_l^*$is the concentration of the dissolved gas in equilibrium with the gas concentration in the bulk gas phase (mol/L), C_l is the concentration of the dissolved gas concentration in bulk liquid (mol/L). $k_L a$ is the gas-liquid transfer coefficient (d^{-1}).

C_l is challenging to be determined experimentally. In this Thesis, it was assumed that the concentration of the dissolved H_2 in the bulk liquid phase (digestate slurry) would be negligible, as its consumption by the microbial population would be relatively fast. This is equivalent to the assumption that the Gas-Liquid transfer rate of H_2 is the limiting step of the biomethanation reaction. This assumption was validated by the results and conclusion shown in chapter 5. Díaz et al. (2015) also assumed a similar assumption in their studies on biomethanation. Therefore:

$$C_{H2,l} \approx 0 \qquad \text{Equation 3-19}$$

C_l^* can be evaluated knowing the concentration of the gas in the bulk phase C_g (mol/m^3), via the Henry relation

$$C_l^* = \frac{C_g}{H} \qquad \text{Equation 3-20}$$

Where H is the dimensionless Henry constant for the gas; in the case of H_2, it would be equal to 50 (molH_2/L_gas)/(molH_2/L_water) at 35 °C (Díaz *et al.*, 2015).

In the case of our experimental study, the concentration of the gas in the bulk phase, C_g depends on both the concentrations of H_2 in the inlet gas (injection, i.e. 100 % H_2) and in the outlet gas (headspace, i.e. 0-40 % of H_2). Due to this non-constant concentration gradient throughout the reactor, it has been recommended to use a mean logarithmic concentration (Jensen, Ottosen and Kofoed, 2021)

$$C_g = \frac{C_{g,injection} - C_{g,headspace}}{\ln(C_{g,injection}) - \ln(C_{g,headspace})}$$ Equation 3-21

A mass balance can be made for the H_2 on the gas phase, considering steady-state conditions (no variation in the headspace):

$$\dot{m}_{IN} = \dot{m}_{OUT} + \dot{m}_{G/L}$$ Equation 3-22

Combining the previous equations, it is possible to calculate the value of $k_L a$, for the H_2 gas-liquid transfer, as follows:

$$k_L a = \frac{(\dot{m}_{H2,IN} - \dot{m}_{H2,OUT})}{V_R * C_l^*}$$ Equation 3-23

3.7 Conclusion

This chapter has explained in detail the materials and analytical procedures, as well as the rig development of the suitable experimental setup that has been used in this study. The author designed and prepared the experimental rig setup with the support of laboratory technicians, electricians, academics and engineers from the instrument manufacturer. The part of the experimental setup that has been developed, including

- Sizing and selection of components
- Online and high-frequency measurement of gas composition, gas flow, pH, temperature and pressure.
- Monitoring and control system implemented in Labview
- Safety measures in case of H2 leak or excessive pressure

The rig, consisting of four biomethanation reactors, two control anaerobic digesters, and the monitoring and control system, was successfully built and commissioned during the PhD work. The rig has been successfully tested and operates properly according to the design and concept needed to support this study.

This experimental setup and program were dedicatedly built for the application of this study. Nevertheless, there is still room for improvements and modifications that may be needed to support further applications.

4. IN-SITU BIOMETHANATION PROCESS CONTROL AND MONITORING

The in-situ biomethanation process involves the injection of hydrogen into an anaerobic digester in order to convert the available carbon dioxide into methane. The hydrogen is produced through electrolysis, which ideally is powered by excess renewable electricity. The amount of hydrogen injected is critical to be controlled in the in-situ biomethanation process. Too much hydrogen injection could cause a blending issue that will affect the biomethane quality. However, it will give an advantage as the hydrogen concentration will enhance the gas-liquid mass transfer through the headspace. From the biological process point of view, too much hydrogen injection will cause the inhibition of the biological processes and the depletion of the carbonate buffer, leading to high pH (Luo and Angelidaki, 2012b; Lecker *et al.*, 2017).

On the other hand, too little hydrogen injection could result in low hydrogen and carbon dioxide conversion as well as low biomethane quality (Alfaro *et al.*, 2018). The amount of hydrogen required depends on the available CO_2, which is variable and is influenced by the digester's operation and the feedstock characteristics. For these reasons, injecting hydrogen into an in-situ biomethanation process is challenging; therefore, more research is required.

Continuous hydrogen injection will significantly increase the hydrogen concentration if the conversion of CO_2 and H_2 does not perform as expected. Furthermore, continuous hydrogen injection without control increases the hydrogen partial pressure and theoretically could lead to acetogenesis inhibition and VFA accumulation, then leading to an overall process imbalance (Luo *et al.*, 2012a). On the other hand, the control of hydrogen concentration is required in order to follow the blend limit of hydrogen that is allowed in the natural gas grid. In this study, the hydrogen was controlled by setting the constraint limiting hydrogen concentration in the headspace. A lower hydrogen content will allow the direct injection into the natural gas grid, reducing the need for costly downstream treatment of the produced biomethane to remove excess H. According to IEA (IEA, 2020),

in the UK, the limit on the hydrogen that is allowed to be blended in the natural gas grid is limited to 0.1 %, while in Germany, the limit on the hydrogen content can reach 10 %. However, in the future, it is predicted that hydrogen blended in the natural gas grid could reach up to 20 % as safety aspects and technology will be further developed.

This chapter presents the result of implementing the developed process control and monitoring system in the application of in-situ biomethanation described in the previous chapter (Chapter 3). The purpose of being achieved in this experimental investigation is as follows:

- To evaluate the effect of different spargers on gas-liquid transfer and biomethanation performance
- To evaluate the effect of gas recirculation rate
- To evaluate the effect of control parameters, in particular, the constraint on H_2 content

In this chapter, a biological methane potential (BMP) test was performed to evaluate the potential methane production of sewage sludge and food waste as a substrate as well as their adapted inoculum. A semi-continuous experiment was then performed after the BMP test of sewage sludge and food waste had been obtained. A comparison between a BMP test and a semi-continuous test will be useful in order to monitor any variations due to the process imbalances that possibly will happen during the semi-continuous. For instance, the methane production from the BMP test could give an insight into how much methane production should at least be obtained in the continuous experiment. Suppose the methane or biogas obtained in the semi-continuous experiment is far from the BMP test. In that case, it can be suspected that the process in the semi-continuous experiment is disturbed. The profile gas composition obtained from a semi-continuous experiment will be used as a baseline for the biomethanation experiments.

An in-situ biomethanation experiment was performed using pulse hydrogen injection, which means that the hydrogen injection will be only ON with the same flow rate or fully OFF. The experiment was divided into four periods based on different hydrogen injection rates, gas recirculation rates and hydrogen constraints. A hydrogen constraint was placed from 5% to 10 % to observe the response of the pulse hydrogen injection as part of the

control process. In addition, this chapter shows the potential and characteristic biogas in the feedstock that is important to obtain an estimation of the amount of hydrogen required. A detailed experimental design and results will be discussed in the following sections.

4.1 Biological methane potential test

A biological methane potential (BMP) test was performed to evaluate the extent of the degradation of the feedstock in ideal conditions and compare it to the values achieved during the semi-continuous biomethanation processes.

Both feedstocks were tested using different sources of inoculum that are specifically adapted to each feedstock. For example, sewage sludge BMP was tested using the sewage adapted inoculum from a local wastewater treatment plant, while the food waste was tested using the food waste adapted inoculum from a local anaerobic digester plant (for more details, see Chapter 3).

Table 4.1 Composition of the inoculums.

Inoculum	Unit	Sewage sludge-adapted inoculum (SSI)	Food waste-adapted inoculum (FWI)
TS	%	3.04	3.97
VS	%	2.00	2.74
pH		7.20	7.50
Ammonia	gTAN/kg	1.43	6.42
PA	gCaCO3/kg	3.26	18.40
IA	gCaCO3/kg	1.24	6.13
Total alkalinity	gCaCO3/kg	4.51	24.52
IA/PA		0.38	0.33

The sewage sludge and food waste samples were prepared, and the VS content was measured to give the correct inoculum substrate ratio (ISR) based on the VS value. The ISR determination for the BMP test is essential even though there are no rules for applying the optimum ISR. However, a poor decision on the ISR determination could lead to inhibition. A low ISR ($r_{I/S}$ <1) could potentially disturb the stability of the digestion process due to the excessive production of VFA as an intermediate (Raposo *et al.*, 2006), especially with rapid

fermentation of the easily degradable fraction. To avoid acidification or inhibition problems, it is recommended that the portion of the VS of the inoculum should be greater than VS of the substrate. Therefore for most substrates, the ISR should be between two and four (Holliger *et al.*, 2016), and, in this experiment, the ISR was set to be 4 for both the sewage and food waste, as these substrates present a relatively high rate of degradation.

On the other hand, the cellulose was set to have an ISR of 3, as cellulose has a relatively slower degradation rate. The TS, VS values and the elemental analysis composition of the substrates are presented in Table 4.2. The elemental analysis composition is presented in per cent of weight of the substrates.

The BMP test was performed using cellulose as the substrate control for both the feedstock sewage sludge and food waste, as well as two different inoculums adapted to the feedstocks as blank (without substrate). Sewage-adapted inoculum (SSI) was used for the sewage sludge, and the food waste adapted inoculum (FWI) was used for the food waste. Also, both inoculums were tested using cellulose, which was employed as a positive control to validate the measurements. The theoretical methane potential of the cellulose can be calculated using the Buswell equation. By assuming the total conversion of organic matter, the theoretical BMP of cellulose is 414 mlCH_4/gVS at STP. However, in the experiment, a potential error could appear in the measurement devices or could be due to the non-ideal experimental conditions, such as the low activity of inoculums. The range of cellulose BMP has been reported to be in the range between 354-370 mlCH4/gVS (B. Wang *et al.*, 2014), and if the result of the BMP is <352 or >414 mlCH4/gVS, then the result of the BMP is recommended to be rejected (Holliger *et al.*, 2016).

Table 4.2 Compositional analysis of sewage sludge and food waste.

Feedstock	Unit	Sewage sludge	Food waste
% TS	%	3.97±0.03	15.96±0.05
% VS	%	2.89±0.06	15.20±0.10
Elemental Analysis			
Carbon	% w	39.80±0.84	49.92±0.31
Hydrogen	% w	5.98±0.22	6.77±0.77
Oxygen	% w	26.58±1.51	35.27±0.63
Nitrogen	% w	4.80±0.56	3.35±0.08
Ash	% w	22.3±0.01	4.7±0.01

Where %w is the percentage by mass of the total solid (TS) sample.

The BMP was tested using the AMPTS II equipment, in triplicate for blank, control and substrates, and run for 38 days for the sewage sludge and 31 days for the food waste. The duration of the experiments was determined according to Hollinger (Holliger *et al.*, 2016); the BMP test can be terminated when the daily methane output for three days in a row is less than 1 % of the accumulated methane volume. The resulting curve shows a similar shape for all the substrates for both sewage sludge and food waste. However, cellulose shows a slow degradation at the beginning of the process, either using SSI or FWI: this is potentially due to the initial inoculum acclimatisation to cellulose, adsorption of bacteria on the cellulose, and the lag in the production of the enzyme (Lebaz *et al.*, 2015). In Figure **4-1**, the methane potential of the cellulose as a positive control using SSI and FWI gives acceptable values, which are 370.61 mlCH4/gVS and 374.09 mlCH4/gVS and these are equivalent to 89.5 % and 90.4 %, respectively, compared to the theoretical value.

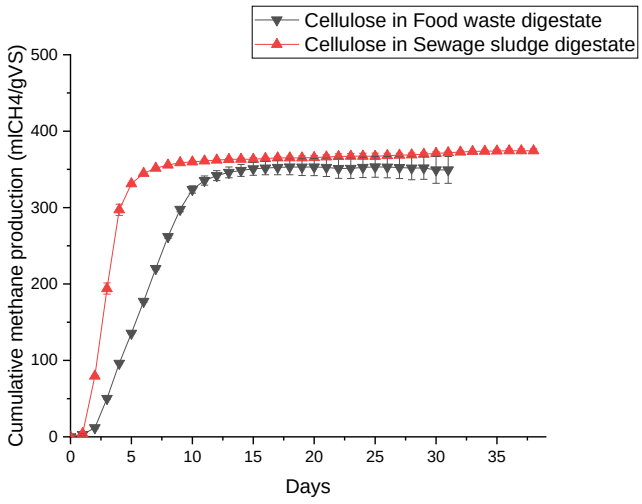

Figure 4-1 The methane production as a function of time for the biological methane potential tests of cellulose using food waste and sewage sludge digestate.

The average methane production of the sewage sludge and food waste during the BMP test is presented in Figure **4-2**. The BMP of the sewage sludge is 402.43±4.79 $mlCH_4/gVS$, while the BMP of the food waste is 471.22 ±19.97 $mlCH_4/gVS$. As a reference, the range in the methane yield of the sewage sludge is reported to be between 220-460 $mlCH_4/gVS$ (Huiliñir *et al.*, 2017; Grosser, 2018; Chow *et al.*, 2020), and for food waste, the methane yield is reported to be between 460-530 $mlCH_4/gVS$ (Voelklein *et al.*, 2016; Zamanzadeh *et al.*,

2016; Xu *et al.*, 2018). Therefore, the methane yield results, either the sewage sludge or the food waste, are within the range of methane yield expected according to the literature.

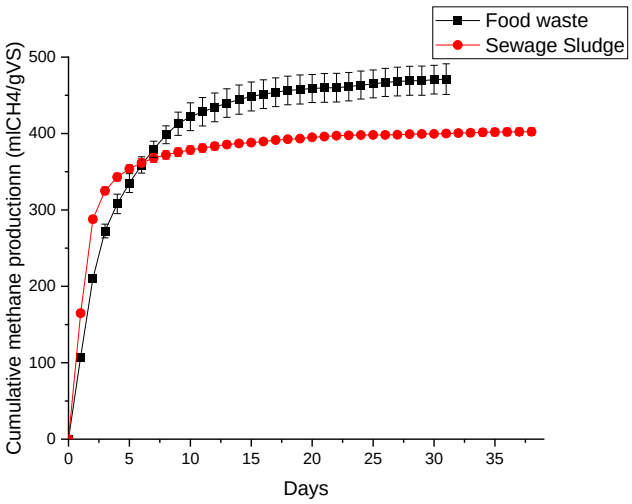

Figure 4-2 The methane production as a function of time for the biological methane potential tests of cellulose, sewage sludge, and food waste.

To further validate the BMP results, the theoretical BMP was calculated using elemental analysis data (CHNS), where it is assumed that the volatile solids only consist of C, H, O, N, and S. Due to the limitations in the equipment, the S element was not recorded, and its content was assumed to be negligible, which is true for most food waste and sludges (TNO Biobased and Circular Technologies, 2022)

Therefore, the theoretical methane potential is calculated using equation 4-1 (Buswell and Mueller, 1952):

$$C_aH_bO_cN_d + \left(a - \frac{b}{4} - \frac{c}{2} - \frac{3d}{4}\right)H_2O \rightarrow \left(\frac{a}{2} + \frac{b}{8} - \frac{c}{4} - \frac{3d}{8}\right)CH_4 + \left(\frac{a}{2} - \frac{b}{8} + \frac{c}{4} + \frac{3d}{8}\right)CO_2 + d\,NH_3$$

Equation 4-1

Using the values of the elemental composition of sewage sludge and food waste (Table 4.2), the following equations are obtained:

$$C_{10.15}H_{18.09}O_{5.40}N + 3.68\,H_2O \rightarrow 5.61\,CH_4 + 4.54\,CO_2 + NH_3$$ Equation 4-2

$$C_{17.38}H_{28.06}O_{9.22}N + 6.51\,H_2O \rightarrow 9.52\,CH_4 + 7.86\,CO_2 + NH_3$$ Equation 4-3

As a result, the theoretical methane potential of the sewage sludge is 529.06 $mlCH_4/gVS$ (equation 4-2), with a methane concentration of 55.53 %. In comparison, food waste has a methane potential of 535.59 $mlCH_4/gVS$ (equation 4-3) with a methane concentration of 54.77 %. Theoretical BMP assumes a complete degradation and conversion of the volatile solids to biogas; however, this is not achievable in the case of complex substrates due to the presence of recalcitrant matter and, to a lesser extent, the production of new microbial biomass during the digestion process (Angelidaki and Sanders, 2004). In this case, the experimental BMP of the sewage sludge produced 76.04 % methane compared to the theoretical BMP of the sewage sludge, while the food waste was 87.95 %. Comparing the theoretical and experimental BMP shows that sewage sludge is less degradable than food waste. This is due to the specific composition of the sewage sludge and, in particular, the hard cell walls and complex floc structures which hinder anaerobic hydrolysis (Khanh Nguyen *et al.*, 2021). On the other hand, the components of the food waste contained bread, sugar, starches and meat, which are easier to be degraded.

4.2 Feeding regimes and pattern

The feeding regimes in anaerobic digestion can influence the quality and quantity of biogas production. However, in the literature, the influence of the feeding regimes is still unclear. For example, a larger quantity of biogas is provided by less feeding frequency (Mulat *et al.*, 2016). In contrast, Svensson (Svensson *et al.*, 2018) found the opposite result that higher biogas was achieved when the feeding frequency was high.

When coming to in-situ biomethanation, the increase in the daily feeding frequency may be beneficial for the following considerations. The benefit of increased feeding frequency is to achieve a more uniform biogas flow and avoid a “flushing effect” after each feeding. In fact, the rate of biogas production increases rapidly after feeding for both the sewage sludge and food waste (Figure 4-3). The carbon dioxide production is relatively higher after each feeding due to the alkalinity consumption from the pH drop and the VFA production, as the rate of fermentation is higher compared to methanogenesis. The biomethanation rate may not be high enough to convert the rapid production of CO_2. As a result, a relatively high amount of carbon dioxide would be flushed out of the reactor before being converted into methane.

The profile for the feeding schedule and the relation to the change in the gas production is shown in Figure 4-3. In order to show the relation of the feeding regime to the biogas flow, the rolling average was performed in one-hour intervals. The data in Figure 4-3 is the record of one-day gas production for the control reactor control, without H_2 injection, for both the sewage sludge and food waste digestion: the flow behaviour of these profiles is similar throughout the experiment. However, the feeding regimes differed for sewage sludge and food waste digester. Sewage sludge reactors were fed 12 times per day, while the food waste reactors were fed four times per day. The difference was due to the different VS content on each feedstock. Sewage sludge has a lower VS compared to food waste. Hence, it required more volume of feedstock, which is needed to maintain the same OLR in all the reactors. The multiple feeding approach is to be in line with industrial practice.

It is clearly shown there is a regular pattern, with biogas flow increasing after each feeding event and the peak reached approximately one hour after the feeding. In the case of food waste, the magnitude of the peak was higher than in the sewage sludge digestion, which is due to the higher degradability of food waste and fewer feeding events.

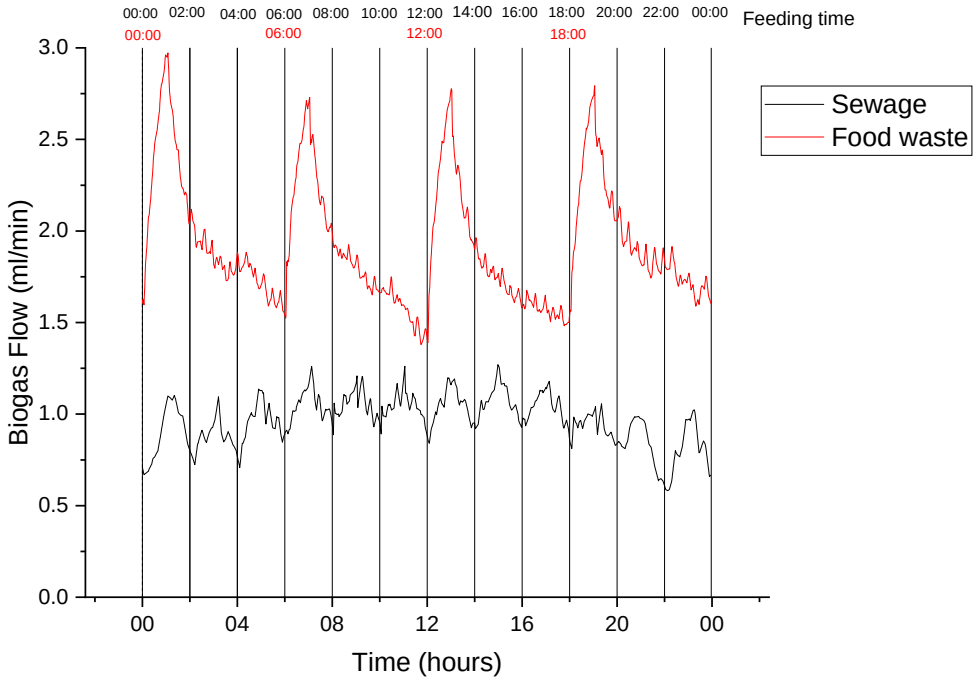

Figure 4-3 Biogas flow as a function of time for the sewage sludge and food waste.

Another influence on biogas production is the value of the OLR. Each experiment was designed with a specific average OLR. The daily fluctuations around the OLR setup could occur due to stratification effect, viscosity and technical issues due to partial or total blockage of the feeding. Therefore, after each day, the exact amount of feeding was recorded, and it was possible to monitor any daily change in the OLR.

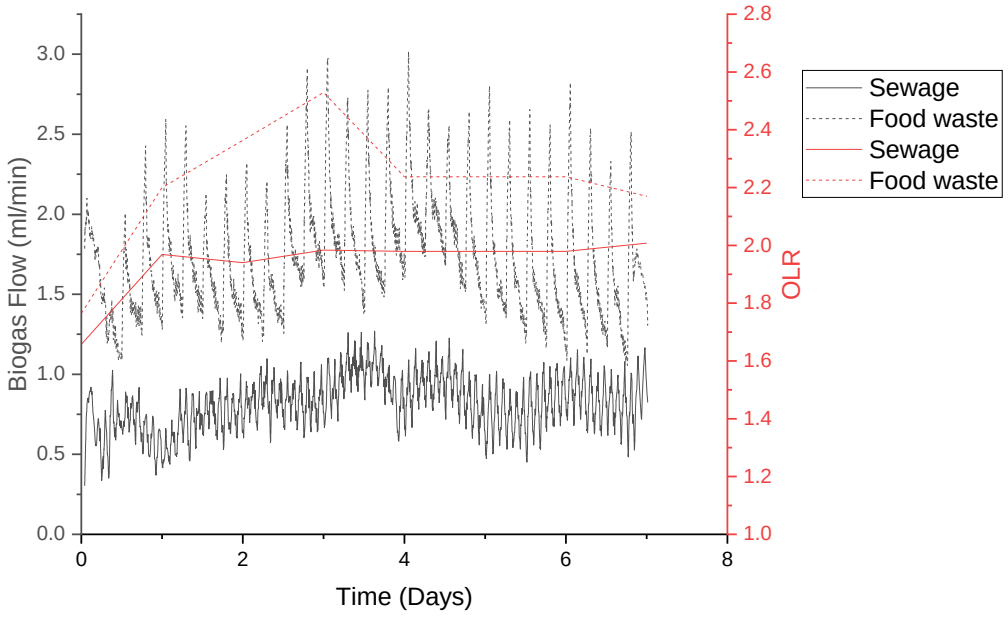

Figure 4-4 Biogas flow as a function of time for the sewage with the fluctuation of OLR.

Figure 4-4 shows the effect of these OLR daily fluctuations on the biogas flow. It is still evident that a similar pattern of peaks at each feeding event as described previously. However, superimposed on this pattern, it can be seen how the average flow tends to follow the variations in the daily OLR, with increased flows following OLR increases. Later in the thesis (Chapter 5), it will be discussed how these daily fluctuations in the OLR and biogas production affect hydrogen conversion and biomethanation performance.

4.3 Data collection frequency

The SCADA system on the in-situ biomethanation rig was set up to take measurements from each device, such as the mass flow controllers, pH meters, pressure transducers, and flow meters. Approximately 500 data samples were taken every 3 seconds, and their average was displayed immediately. The software can then automatically average these

measurements over the desired time interval, then display them on the UI and save these values on a peripherical memory. For all the experiments, the raw data was set to be averaged and saved at one-minute intervals; these values have been used in the data analysis of the biomethanation process in this chapter and also in Chapter 5. However, in the case of the biogas flow, a further averaging of the data was performed to improve the plotting clarity, which is shown in Figure 4-5. Every cell in the excel was displayed every one minute, and the averaging method that is used in this study is the average for a certain time on a minute basis. For instance, for one hour average, every point in the average represents the average for 60 cells, which is one hour; and the next point in the average represents the following 60 cells. No rolling average was used in this study.

With no averaging, the raw data in Figure 4-5a presents all the instantaneous variations in the biogas flow, as measured by the flowmeter; the plot is crowded, and it is not easy to detect visually any trend or pattern in the biogas production. With larger averaging intervals (Figure 4-5a and b), the instantaneous variations are smoothed, and the pattern due to the feeding events become more evident. At the other extreme, at 6 hours averaging intervals (Figure 4-5c), the smoothing becomes excessive, and details are lost. Therefore, as a balance between data fidelity and readability, the average interval of 2 hours has been selected for the biogas flow plots in this thesis. Using the average data for every 2 hours will give a clear relation between the change in organic loading rate in relation to the flow of biogas. This will further will give benefit in explaining the relation between hydrogen conversion and gas retention time.

Biogas production was calculated by multiplying the gas output recorded with the actual gas compositions. The gas output flow was recorded on a minute basis. The gas composition was assumed to be the same until the new gas composition was measured (in 20 minutes).

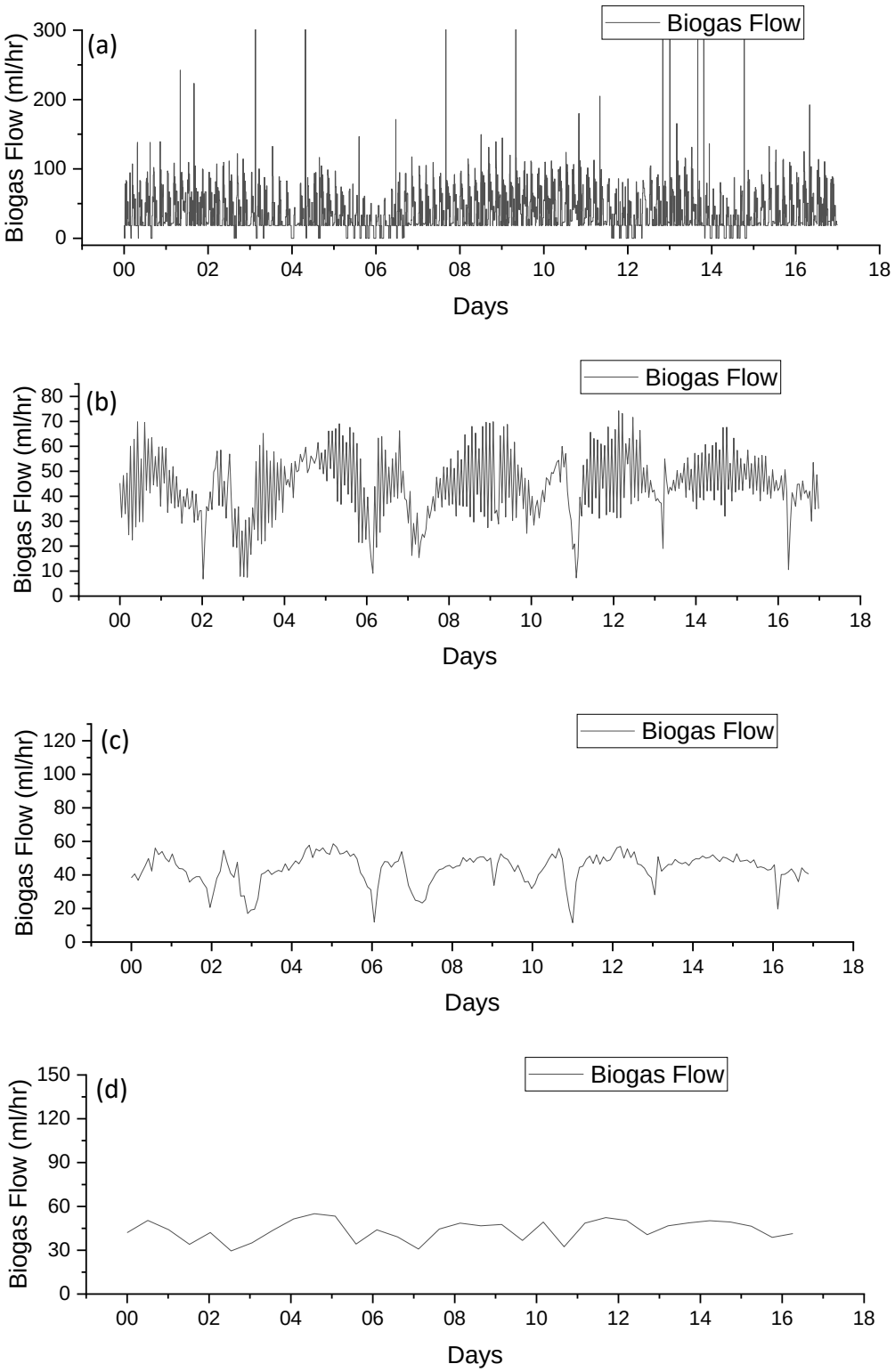

Figure 4-5 Biogas flow with different plotting and averaging (a) 1 minute, (b) 1 hr, (c) 2 hr and (d) 6 hr.

4.4 Semi-continuous anaerobic digestion of sewage sludge and food waste

Anaerobic digestion of sewage sludge and food waste was evaluated before the injection of hydrogen in order to achieve similar process conditions and performance in all the reactors. In addition, the evaluation is very important in order to identify any disturbances or instabilities in the anaerobic digestion process before the hydrogen injection, as well as to evaluate the values of the biogas production and CH_4 and CO_2 specific yields in a semi-continuous reaction (and compare them with the previous BMP results). Furthermore, the knowledge of the CO_2 specific yield allows the estimation of the stoichiometric amount of H_2 needed for a complete biomethanation of CO_2. This H_2 stoichiometric value will be used in this chapter as a comparison to the amount of H_2 that could be injected into the biomethanation reactors.

The semi-continuous experiment was monitored for about 13 days in order to obtain an average biogas yield and the average gas compositions. Three reactors were prepared on each feedstock type. Namely, control SS and control FW act as reactor controls, without hydrogen injection. On the other hand, SS1, SS2, FW1 and FW2, where SS represents a reactor fed with sewage sludge and FW represents a reactor fed with food waste. For the digesters fed with the sewage sludge as the substrate, the overall average methane composition in the control SS, SS1 and SS2 was 65.22 %, while carbon dioxide was 34.17 % (Figure 4-6). The methane and the carbon dioxide specific yields are 0.24 L g^{-1} VS and 0.12 L g^{-1} VS, respectively. On the other hand, the controls FW, FW1, and FW2, which are fed by the food waste, have an overall average methane composition of 59.63 % and 39.70 % of carbon dioxide (Figure 4-7), while the average methane-specific yield was 0.42 L g^{-1} VS and the carbon dioxide was 0.28 L g^{-1} VS.

The gas composition in all the reactors was recorded to be stable during the monitoring days and have identical composition on each type of substrate. This semi-continuous experiment's stability was essential to identify the disturbance that may appear in the in-situ biomethanation process. Therefore, any disturbance that may appear is not influenced by the conventional anaerobic digestion process.

Table 4.4. Average biogas composition and average specific yield in each reactor.

Reactor	Feedstock	% CH_4	% CO_2	specific methane yield (L g VS^{-1})	specific carbon dioxide yield (L g VS^{-1})
Control SS	Sewage Sludge	65.38±0.01	34.02±0.00	0.25±0.13	0.13±0.06
SS1	Sewage Sludge	65.32±0.00	34.26±0.00	0.24±0.02	0.12±0.01
SS2	Sewage Sludge	64.97±0.01	34.22±0.01	0.23±0.06	0.12±0.03
Control FW	Food waste	59.96±0.01	39.62± 0.01	0.44±0.09	0.29±0.05
FW1	Food waste	59.34±0.01	39.56±0.01	0.42±0.05	0.28±0.03
FW2	Food waste	59.57±0.01	39.90±0.01	0.41±0.13	0.27±0.07

Compared with the BMP result, the digesters fed by the sewage sludge have a specific methane production (SMP) of 57.60 % of the BMP, while the digester fed by the food waste has SMP of 86.60 % of the BMP. As shown in Table 4.2, due to the lower VS value of the sewage sludge, the digesters control SS, SS1 and SS2 were operated at a lower HRT (15 days) compared to the digesters control FW, FW1 and FW2 (71 days). A higher HRT could result in higher degradation of the substrates, which is closer to its BMP value. Voelklein *et al.* (2016) reported that the SMP of food waste has 0.32 L g^{-1} VS with 16 days of HRT, which corresponds to 64.60 % of the BMP that they reported.

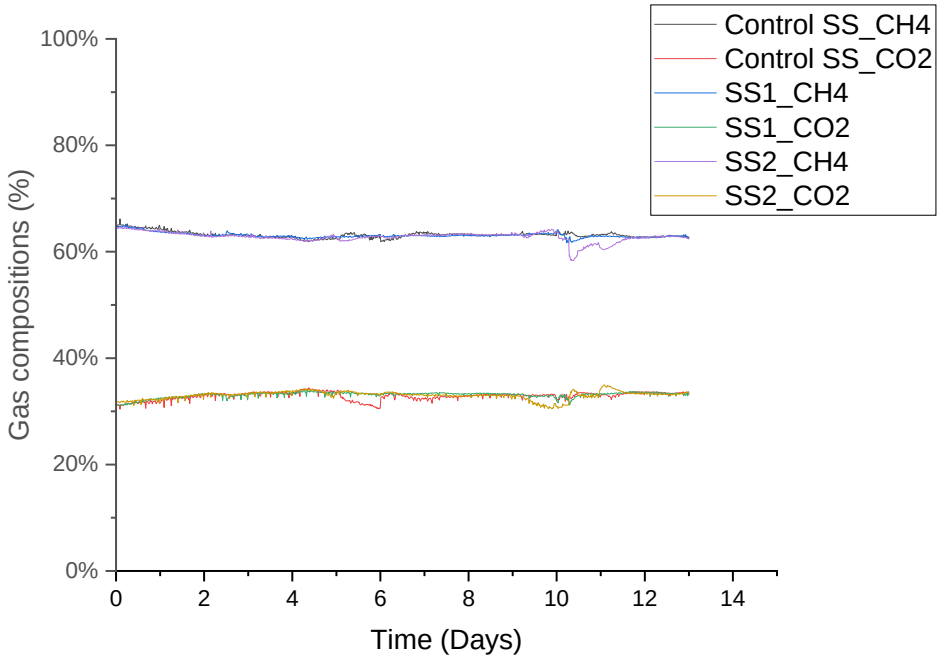

Figure 4-6 Biogas composition as a function of time for the sewage sludge.

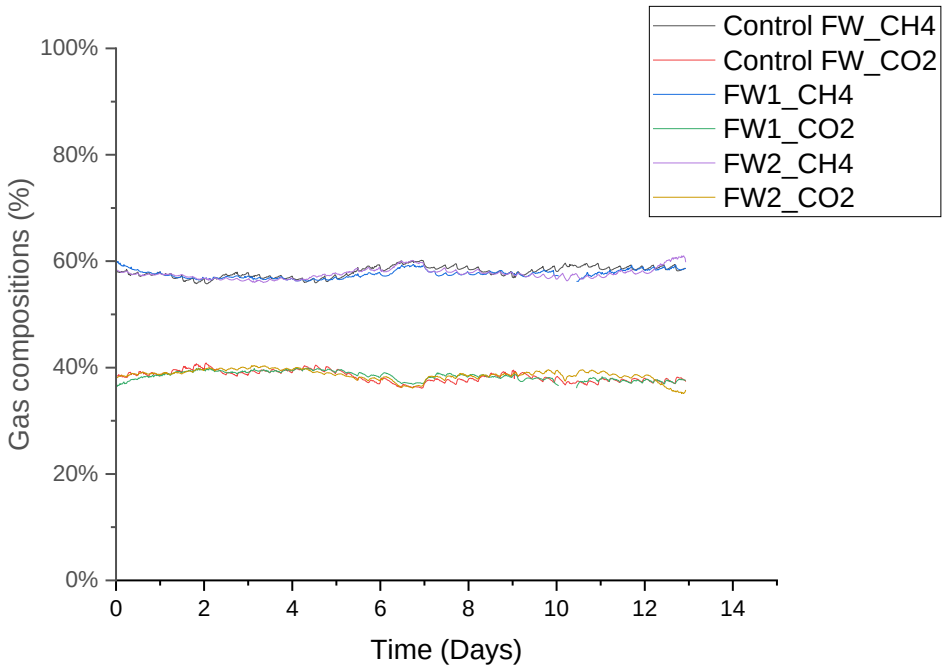

Figure 4-7 Biogas composition as a function of time for the food waste.

During the experiment, the alkalinity ratio (IA/PA) for both the digesters was relatively stable, being around 0.40 (SSD) and 0.38 (FWD)), respectively. The alkalinity ratio is slightly higher than the recommended alkalinity ratio of well-maintained anaerobic digestion, which is between 0.1 to 0.35 (Bochmann and Montgomery, 2013).

4.5 Controlled pulse hydrogen injection in the in-situ biomethanation rig

Knowing the specific yield of CO_2 is essential in order to know how much amount of hydrogen is required according to the stoichiometric value. The objective of the experiment is to compare the effect of the use of the sparger and the simple injector tubing on the hydrogen injection. The hydrogen injection is based on the set of hydrogen injection rates and the constraint value set on the SCADA system. This constraint gives the pulse ON/OFF injection based on the actual gas composition and pH. On the other hand, the exact knowledge of the CO_2 specific yield is the key to controlling an in-situ biomethanation process.

4.5.1 Experimental setup and operation

The experimental investigation was conducted in continuous stirred tank reactors (CSTR), using a modified 2L glass bottle with a 1.7 L working volume, incubated at the mesophilic temperature of 38±1 ^{o}C. Six reactors were set for the two different feedstocks: three reactors were fed with sewage sludge (control SS, SS1, and SS2), and the other three with food waste (control FW, FW1, and FW2). The digesters were fed automatically through peristaltic pumps 12 times per day for the sewage sludge and four times per day for the food waste, with an average OLR of 2 gVS L^{-1} day^{-1}.

Hydrogen was injected directly into the reactor via a mass flow controller that was controlled by a supervisory control and a data acquisition (SCADA) system. This experiment evaluated the effect of using different hydrogen injection systems. Two options were explored: direct injection through a simple stainless steel tubing with a 2.7 mm internal diameter (SS1 and FW1); and a stainless steel sparger with a 2 μm pore size (SS2 and FW2). The control SS and control FW acted as a reactor control without hydrogen injection.

In this experiment, hydrogen was controlled based on the actual gas composition and pH without the proportional feedback control being activated, which is mentioned in Section 3.5. Instead, the feedback control was based on the pulse injection (ON/OFF) approach that is controlled by the SCADA system. The SCADA system works based on the gas compositions of the produced biogas and the pH of the digestate. In this experiment, the constraint was set to ensure process stability and blending limit. The details of the setting for the H_2 injection pulse, gas recirculation, and H_2 constraint are presented in Table 4.3.

The hydrogen concentration constraint was inspired by the limit of the hydrogen blending in the natural gas that is allowed in some countries in Europe (Altfeld and Pinchbeck, 2013; McDonald, 2020). Therefore, the hydrogen constraint was set to be less than 5 % in the periods PS1-PS3, which then increased to 10 % in period PS4.

Table 4.3. Hydrogen injection setting and gas recirculation.

	Unit	PS1	PS2	PS3	PS4
H2 injection pulse	ml/min	3	1	1	1
Gas recirculation rate	L $L^{-1}day^{-1}$	25	67	115	115
Max H_2 constraint	%	5	5	5	10
Min H_2 constraint	%	2.5	-	-	-
Min CO_2 constraint	%	4	4	4	4
Max CH_4 setpoint	%	80	80	80	80
pH constraint	%	8.5	8.5	8.5	8.5

The gas compositions on each reactor were measured every 20 minutes using the online GC and stream selector, while the pH was measured continuously. Every time the SCADA system acquires a new measurement, the pulse ON/OFF status of the hydrogen injection is determined by the feedback control based on the process outputs and constraints. If any of the process outputs are outside the values allowed by the constraints, the status of the H_2 injection is set to OFF, and the injection remains stopped until the constraint becomes satisfied again.

4.5.2 Pulse hydrogen injection

The experiment varied the proportion of the hydrogen injection between the sewage sludge reactors and food waste reactors in order to explore the effect of the hydrogen injection. The hydrogen was injected at a rate of 3 ml/min in the beginning period (Period PS1). If the hydrogen were able to be injected continuously, the amount of hydrogen injection in the sewage sludge reactor would be three times higher than the amount of the hydrogen requirement based on stoichiometric, while the proportion in the food waste was 1.5 times higher than the stoichiometric.

The proportion of the hydrogen injection in the PS1 with a hydrogen injection rate of 3 ml/min was set to be higher than the amount of hydrogen, based on stoichiometric, to compensate for the pulse hydrogen injection. However, the profile of the pulse injection was still unknown at the beginning of the experiment. Therefore, the amount of hydrogen injected may end up below stoichiometric.

In the period PS1, the control hydrogen injection was set with upper and lower limits due to the high injection rate. The hydrogen injection will respond to stop when the hydrogen content in the headspace reaches the upper limit, which is 5 %. The hydrogen will start injecting again when the hydrogen content is below 2.5 %. This high amplitude causes a wider amplitude in the hydrogen concentration. Because the hydrogen will return for injection when the hydrogen content is below 2.5 %, this causes a lower injection frequency than in other periods. With this setting, high hydrogen flow rate set point and wider constraint in the hydrogen control results in a wider amplitude in the profile of the hydrogen content in the headspace. This causes low hydrogen injection frequency, thus resulting in less amount of hydrogen being injected.

For this reason, in the periods PS2, PS3 and PS4, the hydrogen injection setpoint is reduced to 1 ml/min, and the lower constraint is no longer used. By reducing the hydrogen injection rate to 1 ml/min, the amount of hydrogen injection will reach 100 % stoichiometric in the sewage sludge reactor and 50 % stoichiometric in the food waste digester. This amount could be achieved if the hydrogen was able to be injected continuously, meaning that the gas compositions and pH would be able to be maintained below the constraint.

In period PS2, with no lower constraint used, the hydrogen injection will respond to the one hydrogen constraint. For instance, in period PS2, when the hydrogen content reaches more than 5 %, the hydrogen injection will stop. Then, as soon as the new gas composition is updated and hydrogen is detected below 5 %, the hydrogen injection will be activated immediately. A comparison of the hydrogen injection profile of both settings PS1 and PS2 can be seen in Figure 4-8.

Figure 4-8 shows an example of the pulse hydrogen injection behaviour in reactor SS1 in the periods PS1 and PS2. It shows that the hydrogen content in PS1 reached up to more than 10 %. In comparison, when the hydrogen injection rate was reduced to 1 ml/min in the period PS2 the overshoot was able to reduce the maximum to around 7 %. Also, with no lower constraint then, the range of hydrogen content was narrowed to around 3 % compared to 8 % in period PS1. The narrower range of gas composition was not only for hydrogen but also it was observed in the methane and carbon dioxide content. As discussed before, the gas composition was updated for approximately 20 minutes. The higher rate of

hydrogen injection results in a higher hydrogen content in the headspace as a consequence of the blending effect. Also, the hydrogen conversion process was limited by the gas-liquid mass transfer. Therefore, the hydrogen that is injected into the reactor is required some time to be able to be 100 % converted.

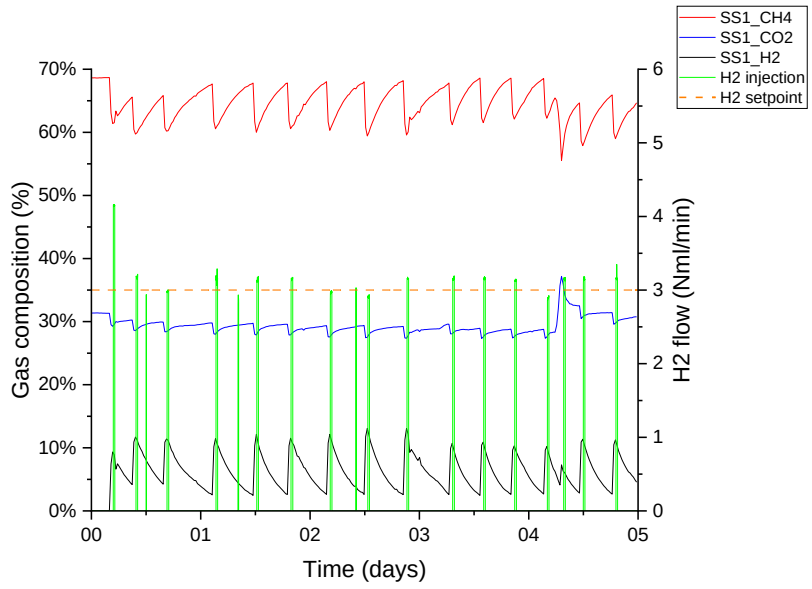

(a)

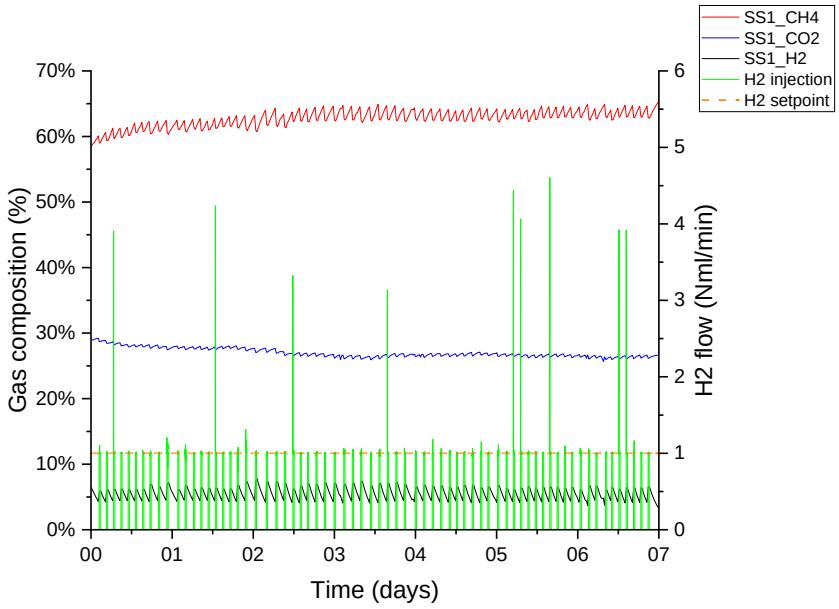

(b)

Figure 4-8 Pulse hydrogen injection in relation to gas composition ion SS1 on the period (a) PS1 and (b) PS2. Hydrogen setpoint refers to pulsed injection rate a) 3 mL/min – b) 1 mL/min

4.5.3 Process performance

The hydrogen injection rate and the hydrogen constraint affected the amount of hydrogen injection in each period. Even though in period PS1, the hydrogen injection was a third times higher than in other periods, the hydrogen injection in PS1 was often limited by the upper and lower constraints compared to the other periods with only one hydrogen constraint (upper constraint), as can be seen in Figure 4-9. It shows that the amount of hydrogen injected in the period PS1 was the lowest compared to the other periods. This was due to the delay in the injection as the hydrogen will start being injected again when the hydrogen in the headspace becomes less than 2.5 %. Therefore, the time of the hydrogen injection in the period PS1 was the lowest compared to the other periods, with only 6 % (sewage sludge digesters) and 11 % (food waste digesters) of the duration of the experiment. On the contrary, the highest amount of hydrogen injection was achieved in PS4 when the hydrogen constraint was increased from 5 % to 10 %. This increase of hydrogen injection increased from 12 % stoichiometric to 39 % stoichiometric for sewage sludge and 9 % to 25 % for food waste.

Overall, the reactor with a stainless steel sparger (SS2 and FW2) has a higher amount of hydrogen injection compared to the reactor with a simpler open tubing injector (SS1 and FW1). The amount of desired hydrogen injection was nearly achieved by the reactor with a sparger as SS2 could reach H_2:CO_2 of 3.8 and FW2 could reach 1.9 (Figure 4-9) as this corresponds to 95 % of the amount of hydrogen when the hydrogen could be able to be injected continuously. This could indicate that the sparger could increase the gas-liquid mass transfer by producing smaller hydrogen bubbles, which will increase the surface area of the contact between the gas and liquid phases (Bassani, Kougias and Angelidaki, 2016), leading to a higher hydrogen conversion.

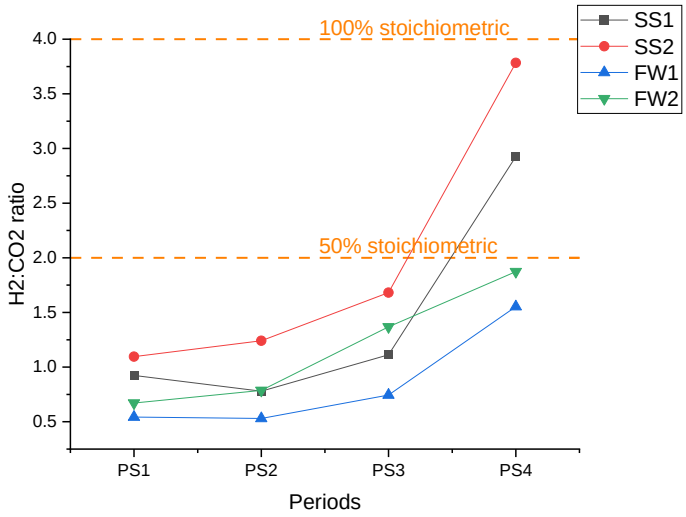

Figure 4-9. Hydrogen injection in each period, as a proportion of the stoichiometric H_2:CO_2 ratio.

In most cases, the feedback control of the hydrogen injection was working based on the hydrogen constraint. Hydrogen content is the most dynamic parameter compared to other parameters since hydrogen content is influenced by the rate of biomethanation and the rate of hydrogen injection as external parameters. The gas composition in periods PS1, PS2, PS3 and PS4 can be seen in Figure 4-10 and Figure 4-11. The biomethanation extent was calculated based on the proportion of methane to methane and carbon dioxide discussed in section 3.6.5.

In the period PS1, the hydrogen content oscillated over a wider range compared to the other periods, which was observed to be above the hydrogen constraint limit. This is related to the pulse injection, where in period PS1, there is a higher injection rate. Also, the low constraint limit caused the hydrogen to start injecting when the hydrogen content was less than 2.5 %. In fact, having a lower hydrogen constraint gives more time for the hydrogen in the headspace to be converted by hydrogenotrophic methanogens. Having higher hydrogen injection rates could give a rapid increase in the hydrogen content in the headspace.

Nevertheless, having a higher hydrogen content could give an advantage as the hydrogen content in the headspace is a driving force in the gas-liquid mass transfer. This means that having a higher hydrogen content could increase the gas-liquid mass transfer (Díaz *et al.*, 2015). However, the higher injection rate and the wider hydrogen constraint caused the

wider range of gas composition, making the biomethanation quality more challenging to control. In relation to the practical application, it is essential to be able to maintain the quality of biomethane production by having consistency in the biomethane quality.

(a)

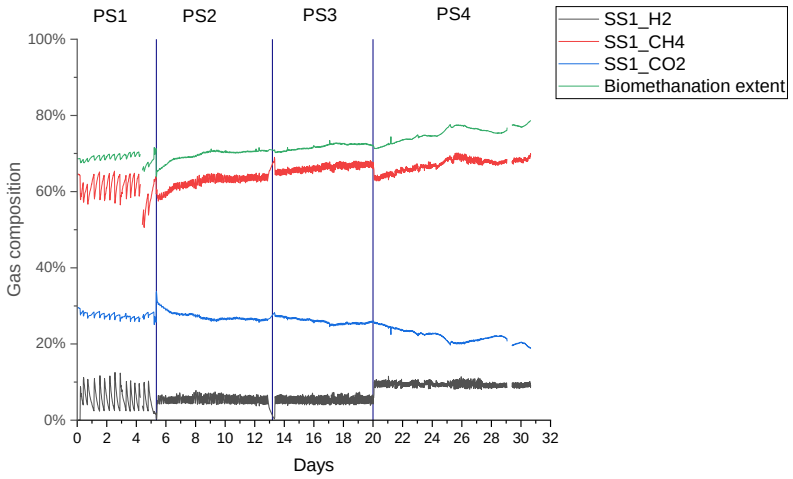

(b)

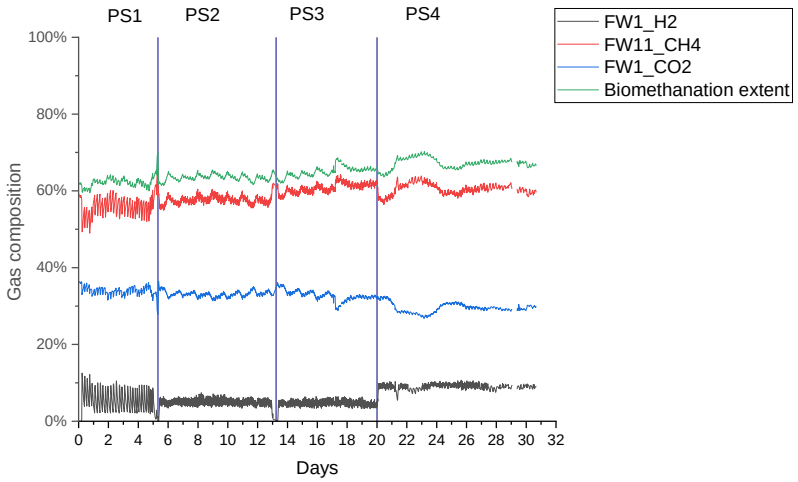

Figure 4-10 The gas composition as a function of time on the reactors with simple open tubing injectors SS1 (a) and FW1 (b).

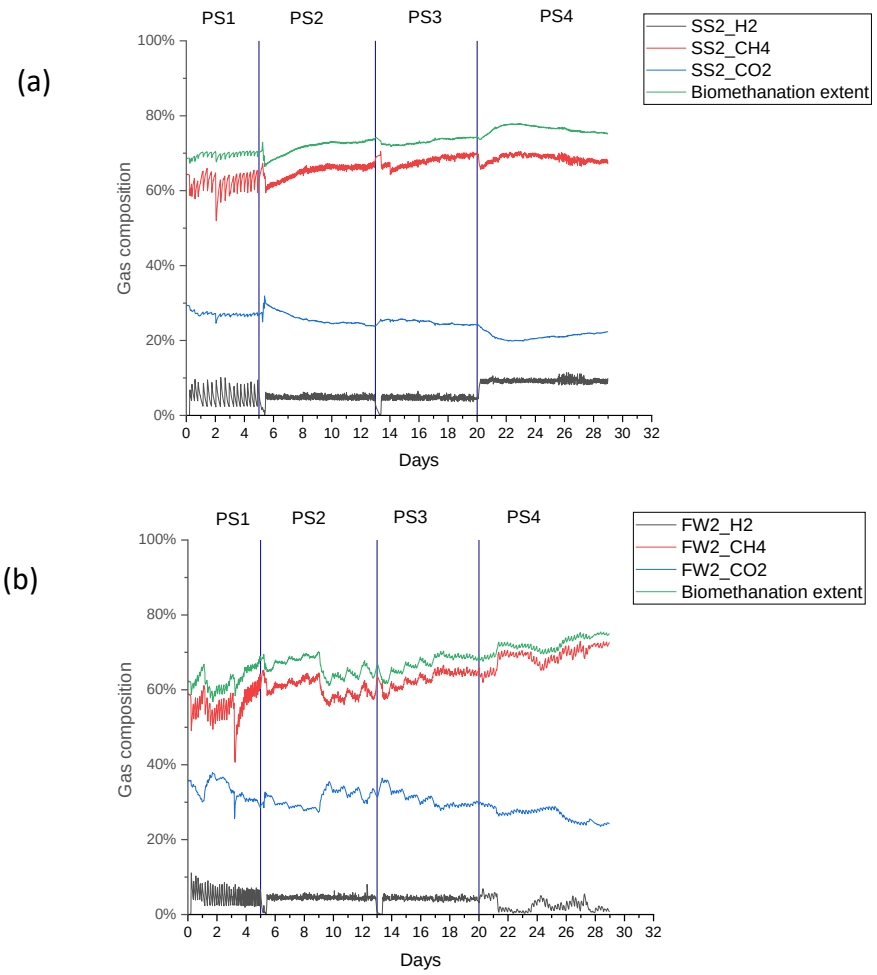

Figure 4-11 The gas composition as a function of time on the reactors with sparger on (a) SS2 and (b) FW2.

Having enough hydrogen injected by reducing the hydrogen injection rate was able to increase the hydrogen conversion (section 3.6.2). As a result, the hydrogen conversion in period PS2 was higher compared to PS1 in the sewage sludge and the food waste digester. Several factors make the hydrogen conversion in PS2 to be higher than in PS1. First, an improvement in the hydrogen conversion was attributed to the higher gas recirculation rate, thus allowing the hydrogen to have more contact with the microorganism (namely, a larger gas hold-up). Second, the lower hydrogen injection pulsed rate in PS2 could make smaller bubbles that could further increase the surface area of contact with the hydrogenotrophic methanogens. Third, a “flushing” effect may occur due to the higher injection rate in period PS1, which makes the hydrogen discharged before it can be converted.

In Figure 4-11 (b), the hydrogen content on FW2 fluctuated in period PS4, with the average hydrogen content only 2.3%. On the other hand, the hydrogen content in the PS4 for SS2 was observed to be stable within the hydrogen constraint limit (10%). The hydrogen injection was recorded stable and continuous in the period PS4 for both SS2 and FW2. The hydrogen content in FW2 dropped to 0.6% only one day after the hydrogen had been injected. No significant difference in OLR or biogas flow was recorded between the first and second days after hydrogen injection. There was also no air contamination recorded in this period. The methane content was recorded to increase while hydrogen content decreased; it concludes that the decrease of hydrogen content in period PS4 is due to higher hydrogen conversion.

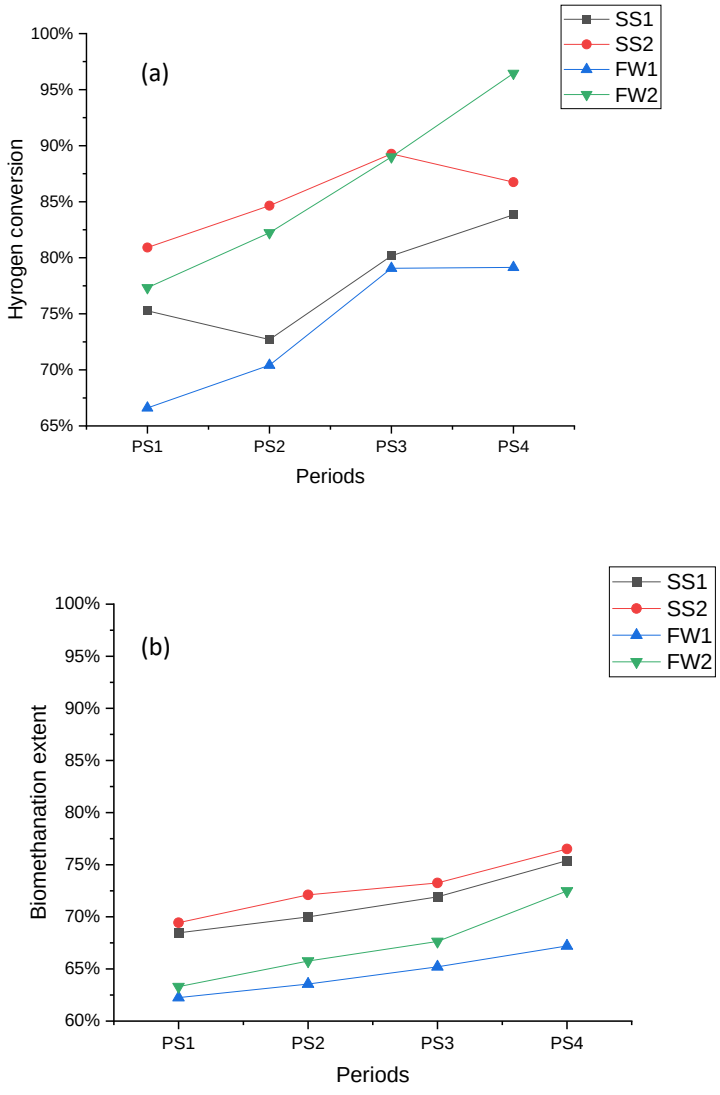

Figure 4-12 The H_2 conversion rate (a) and increased methane production relative to the control (b).

The increase in the gas recirculation rate has a positive effect on increasing the hydrogen conversion and biomethanation extent. For instance, in Figure 4-12, it was observed that the hydrogen conversion in reactor SS1 increases from 72 % in period PS2 (recirculation rate 120 rpm) to 80 % in period PS3 (recirculation rate 280 rpm). Also, the biomethanation extent tends to increase along with the reincrease of gas recirculation rate, as seen in Figure 4-12b. For instance, the biomethanation extent in FW2 increase from 65% in PS2 to 67% in PS3 when the gas recirculation increase from 120 rpm to 280 rpm. This corresponds to the previous study that reported the influence of the higher recirculation rates in order to improve the gas-liquid mass transfer, and this can lead to an increase in the H_2 and CO_2 conversion into methane (Bassani, Kougias and Angelidaki, 2016; Bassani *et al.*, 2017; Wahid and Horn, 2021).

A further increase in biomethane extent also occurred in period PS4 when the hydrogen constraints were increased, allowing more hydrogen to be injected into the reactor. In period PS4, a biomethanation extent was relatively higher than in period PS3, with an average (SS1 and SS2) of 72 % in the sewage sludge digester and 66 % in the food waste digester (FW1 and FW2) in period PS3. In comparison, in period PS4, the average biomethanation extent for sewage sludge and food waste were 76 % and 69 %, respectively. Also, the highest methane content was achieved in period P4 on SS2, and FW2, with the methane concentration, increasing from 63 % (control) to 70 % CH_4 with the sewage sludge and from 58 % (control) to 73 % CH_4 with the food waste.

A porous sparger improved the biomethanation performance compared to a simpler tubing injector. In particular, the reactor with porous sparger achieved higher methane production values across all experiments, which were 45 % and 66 % higher in the sewage sludge and the food waste digesters than the simple tubing injector. This can be justified by increased gas-liquid interfacial area due to smaller bubbles diameter achieved when hydrogen is injected through a porous sparger.

The pH in the biomethanation reactor was recorded to have increased in all the reactors. The pH value was related to the hydrogen and carbon dioxide conversion. The higher hydrogen and carbon dioxide conversion is reflected in the higher pH value as an effect of bicarbonate consumption.

In all the periods, higher hydrogen conversion and methane enrichment were achieved in the reactor with the hydrogen injected through the metallic sparger than the reactor with a simple open tubing injector. This result corresponded with the previous study that reduced the bubble size of the hydrogen improved the gas-liquid mass transfer and led to increasing hydrogen conversion (Luo and Angelidaki, 2012a; Bassani *et al.*, 2017). Smaller bubbles in the hydrogen increase the contact time between the gas and microorganism, in this case, the hydrogenotrophic methanogen. On the other hand, larger bubbles in the hydrogen have a higher rising in reaching the surface and thus make less contact with the microorganism.

The use of sewage sludge and food waste gives a slightly different effect in terms of the hydrogen conversion rate. Food waste has a higher baseline biogas production rate that will influence the amount of hydrogen that is required based on the stoichiometric ratio. A combination between the higher biogas production rate and the higher rate of hydrogen injection results in a lower gas retention time, which gives a disadvantage to hydrogen conversion. This will be further explored in chapter 5. It can be seen that in Table 4.4 and Table 4.5, even though the food waste reactor has a lower hydrogen conversion than the sewage sludge digester, the food waste digester has double the hydrogen consumption rate than the sewage sludge reactor, and this is due to the higher average injection rate. The overall higher hydrogen injected in the food waste digesters was due to the gas dilution that gives rise to the lower chance of the hydrogen to be in between the hydrogen constraints, producing a higher intensity in the hydrogen pulse injection.

Gas output in biomethanation reactors is the overall gas output, including biogas produced from the conventional anaerobic digestion process and the product from the biomethanation process. This will contribute to overall gas out consisting of biomethane, unconverted hydrogen, and unconverted carbon dioxide. On the other hand, in reactor control (without hydrogen injection), gas output comes from only biogas production from the conventional anaerobic digestion process. For this reason, the gas output in the reactor control was lower than that in biomethanation reactors (with hydrogen injection). The proportion of gas output in biomethanation at each stage depends on the amount of hydrogen injection that is influenced by the activation of feedback control. For instance,

the gas output on the biomethanation reactor can have lower gas output if the hydrogen injection is interrupted by the activation of feedback control.

The methane evolution rate was calculated according to equation 3-16, as discussed in section 3.6.4.

Table 4.4 Summary of the process performance indicator in the sewage sludge digesters.

		Period PS 1			Period PS2			Period PS3			Period PS4		
		Control	SS1	SS2	Control	SS1	SS2	Control SS	SS1	SS2	Control	SS1	SS2
Hydrogen pulse Flow rate	ml min^{-1}		3	3		1	1		1	1		1	1
Average OLR	gVS L^{-1} day^{-1}	1.99	1.84	2.04	1.93	1.90	1.92	1.95	1.84	1.91	1.99	1.93	1.82
Average actual Hydrogen Injection rate	L day^{-1}		0.25	0.30		0.21	0.34		0.31	0.46		0.81	1.05
Gas output	L g^{-1} VS	0.33	0.36	0.35	0.25	0.36	0.35	0.24	0.37	0.32	0.21	0.40	0.47
Specific CH4 production	L g^{-1} VS	0.21	0.22	0.22	0.15	0.23	0.23	0.20	0.24	0.22	0.14	0.27	0.29
Specific CO_2 in output gas	L g^{-1} VS	0.09	0.10	0.09	0.07	0.09	0.09	0.09	0.09	0.08	0.06	0.09	0.09
Hydrogen conversion rate	L day^{-1}		0.20	0.25		0.15	0.29		0.25	0.41		0.69	0.93
H2 Conversion	%		75.27	80.92		72.70	84.65		80.17	89.28		84.59	88.00
Average pH	%	7.35	7.47	7.43	7.36	7.51	7.47	7.41	7.48	7.50	7.38	7.56	7.61
Methane evolution rate	L $L^{-1}day^{-1}$		0.03	0.04		0.02	0.04		0.04	0.06		0.10	0.13

Table 4.5 Summary of the process performance indicator in the food waste digesters.

		Period PS 1			Period PS2			Period PS3			Period PS4		
		Control	FW1	FW2	Control	FW1	FW2	Control SS	FW1	FW2	Control	FW1	FW2
Hydrogen Flow rate	ml min^{-1}		3	3		1	1		1	1		1	1
Average OLR	gVS L^{-1} day^{-1}	2.18	2.26	2.12	2.10	1.82	2.18	2.08	2.03	2.11	1.90	1.84	1.72
Average actual Hydrogen Injection rate	L day^{-1}		0.41	0.51		0.40	0.60		0.57	1.04		1.19	1.43
Gas output	L g^{-1} VS	0.59	0.66	0.69	0.63	0.93	0.70	0.61	0.72	0.76	0.68	0.77	0.90
Specific CH_4 production	L g^{-1} VS	0.35	0.37	0.39	0.38	0.54	0.42	0.37	0.44	0.48	0.41	0.46	0.68
Specific CO_2 in output gas	L g^{-1} VS	0.21	0.22	0.22	0.22	0.31	0.22	0.23	0.23	0.31	0.25	0.23	0.25
Hydrogen conversion rate	L day^{-1}		0.28	0.41		0.28	0.49		0.45	0.93		0.98	1.38
H2 Conversion	%		66.61	77.33		70.42	82.23		79.06	89.00		81.05	96.67
Average pH	%	7.76	7.98	7.96	7.78	8.02	7.98	7.77	8.06	7.99	7.81	8.12	8.08
Methane evolution rate	L $L^{-1}day^{-1}$		0.04	0.06		0.04	0.07		0.07	0.14		0.13	0.20

4.6 Conclusion

The application of the controlled hydrogen injection was able to manage the pulse of hydrogen injection proportionally based on the biogas compositions produced. In all the periods, the hydrogen content is the main parameter responsible for the decision-making in the pulse hydrogen injection.

This study shows that the biomethanation process is affected by the gas-liquid mass transfer limitations. An increase in the hydrogen concentration in the headspace due to the hydrogen injection may increase the gas-liquid mass transfer through the headspace. However, it could cause a blending issue where the methane and carbon dioxide concentration decreases to compensate for an increase in the hydrogen content. On the other hand, having a higher gas-liquid mass transfer could increase the hydrogen and carbon dioxide conversion into methane. This could impact the carbon dioxide depletion that will increase the pH, as shown in this study.

Having a higher injection rate and two constraint limits in the period PS1 results in a wider range in the gas composition and a lower injection frequency. As a result, this gives rise to an impact on the insufficiently supplied hydrogen. Furthermore, a higher injection rate in period PS1 would give rise to a lower hydrogen conversion for several reasons; a higher injection rate could create bigger bubbles that make a smaller contact area between the gas and the hydrogenotrophic methanogen; and also a higher injection rate may give a *flushing* effect that makes the hydrogen to discharge before it can be converted. In addition, the lower conversion rate in period PS1 was due to the lower gas recirculation rate that will affect the gas retention time in the reactor.

An increase in the gas recirculation rate was able to improve the gas-liquid mass transfer. A higher gas recirculation rate allowed more contact between the gas and the hydrogenotrophic methanogen, leading to a higher hydrogen conversion. Another improvement in the gas-liquid mass transfer was shown in the reactor with the stainless steel sparger (SS2 and FW2). The conversion of hydrogen in the reactor with hydrogen injection through the stainless steel sparger was observed to be higher in all the periods

compared to the reactors with a simpler tube injector. For this reason, only the stainless steel sparger will be used in chapter 5.

This initial study provides valuable insight into the strategies that can improve the gas-liquid mass transfer while maintaining the process stability; this is very useful for further investigations, as described in chapter 5.

5. PROCESS OPTIMISATION OF IN-SITU BIOMETHANATION WITH CONTINUOUS H_2 ADDITIONS

This chapter assessed the process optimisation to improve hydrogen conversion by exploring the factors that can increase the hydrogen gas-liquid mass transfer. This experiment involved the exploration of various approaches to improve the performance of the process:

- Increasing the gas recirculation rate;
- adding a sparger on the gas recirculation line in order to further improve the gas transfer into the liquid (as demonstrated in chapter 4 for the hydrogen injection);
- increasing the mechanical mixing rate of the reactor
- reducing the organic loading rate (OLR).

Two types of substrates were used in parallel and with the same reactor configurations: this will also allow investigation of the effect on the biomethanation process of substrates with different characteristics, such as nitrogen content, CH_4 and CO_2 specific yields, and rate of degradation. For each substrate, the biomethanation reactor was run in duplicate, while a single control reactor with no hydrogen injection was used as a control to monitor the effect of OLR changes on biogas production.

In this experiment, the hydrogen injection is no longer controlled using the pulse hydrogen control (ON/OFF), as was done in the previous experiment (chapter 4). Instead, hydrogen injection is controlled by SCADA using a feedback control approach based on gas compositions and pH, which is able to change the injection rate proportionally, depending on how close the process outputs are to the process constraints. This was intended to avoid the oscillating and overshooting behaviour of a pure ON/OFF feedback control, as seen in chapter 4.

Two stages of experiments were provided using sewage sludge and food waste as a substrate. In the first stage, the study was focused on the effect of recirculation rate in in-situ biomethanation. In this experiment, the gas recirculation was varied into three different recirculation rates at 20, 120 and 280 rpm or equivalent to 12, 67 and 155 L L_r^{-1}

day^{-1}. In the second stage, the process optimisation was carried out by modifying an operation condition, including an additional sparger on the recirculation line, a higher mixing rate and operating in a lower organic loading rate (OLR). These two stages of the experiment were done using one reactor control (without hydrogen injection) and two biomethanation reactors (with hydrogen injection). The detail of the experiment will be discussed in the following sections.

A liquid sample was taken twice a week to analyse the biological process indicators, such as TS, VS, alkalinity, ammonia and volatile fatty acids. An average value was taken during the experiment period by including the point when hydrogen began to be injected and when hydrogen was stopped.

In this chapter, the experiment was carried out by monitoring the biogas production before hydrogen is injected. This monitoring was done for at least one week or until stable biogas production was obtained. This is essential to know that the level of gas production and composition in each period was not significantly different, meaning that it was shown that there was little effect of adaptation during the time. Therefore, once the biomethanation experiment is complete and hydrogen injection stopped, the remaining hydrogen is allowed to be fully converted until a similar baseline is obtained to be used for the next period of the experiment.

5.1 Hydrogen injection with feedback control enables

The feedback control implemented in this chapter has the benefit of delivering the flow proportionally, based on the values of the process outputs (gas composition and pH) and the selected process constraints. The logic of this feedback control is explained in section 3.5.1; its implementation is as follows and resumed in the schematics in Figure **5-1**.

Firstly, the estimated daily hydrogen injection requirement is calculated according to expected carbon dioxide production, calculated as a function of the measured CO_2 specific yield in the control reactor, the OLR and the stoichiometric hydrogen requirement. The carbon dioxide in the liquid is important to maintain the stability of the pH. Therefore, it was considered that the stoichiometric proportion of hydrogen was not necessary to be 100 % stoichiometric, as Tao et al. (Tao *et al.*, 2019) reported that the biomethanation

process was not sustained when the proportion of hydrogen injected was 100 % stoichiometric due to a lack of bicarbonate buffering that was indicated by the pH increase then lead to VFA accumulation. For this reason, the proportion of hydrogen injection will be set to be 90 % of the stoichiometric. This daily hydrogen requirement is then converted to mL/min units according to the settings of installed MFCs; this value constitutes the injection flow rate set point (GH_2_sp) of the feedback control.

The value of hydrogen flow injected in the digester, GH_2_MFC, is then calculated following the algorithm. The feedback control is looking for the minimum flow either based on setpoint or constraints, meaning that the hydrogen flow will change proportionally only if the feedback hydrogen flow on the MFC (GH_2_MFC) has a lower value than the initial setpoint. The hydrogen constraint (GH_2_sp) was set to be maximum (at 40 %) in order to avoid the hydrogen content reaching above the threshold while waiting for the subsequent measurement of the gas composition, as happened in the previous experiment (chapter 4, period PS1). GH_2_lower limit was a minimum limit of hydrogen maintained in the headspace, with the opposite operation than the hydrogen constraints, which means that when the hydrogen content reaches lower than the lower limit (GH_2_lower limit), the hydrogen injection will start. There was a condition where GH_2_MFC was lower than the lower limit. However, the MFC could not accommodate the flow beyond its flow rate range. The MFC has a working flow range from 0.6-30 ml/min. For instance, if the feedback control provides the value of GH2_MFC 0.5 ml/min, the MFC cannot deliver the exact flow rate as shown based on the proportional feedback control flow rate, or the flow rate delivered was not accurate. For this reason, the SCADA was programmed to send the flow of 0 ml/min (GH_2_MFC =0) if the flow requested by the feedback control is between 0 - 0.6 ml/min.

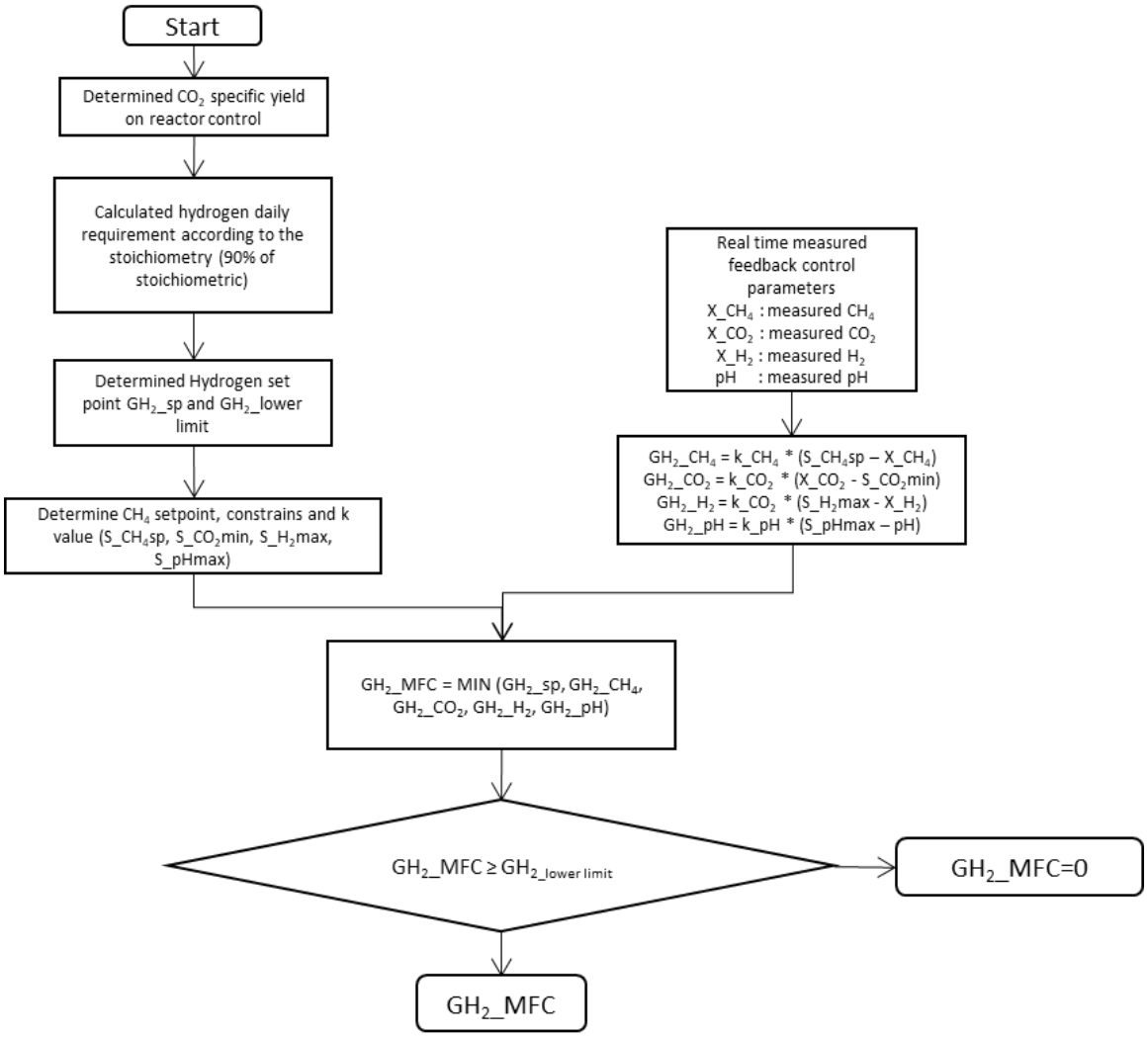

Figure 5-1 Decision-making algorithm for the hydrogen injection flow, using a feedback control based on real-time gas composition measurement and pH value.

5.2 General characteristics of the biomethanation experiments

This section gives a preliminary overview of the qualitative effects of hydrogen injection in the in-situ biomethanation reactors, focusing on the variations in gas composition and pH before, during, and after the injection.

In general, for each experimental phase, before the hydrogen injection, it was ensured that all replicates had a similar baseline in terms of gas composition, gas content, pH and alkalinity ratio. The hydrogen was then injected into the reactor in accordance to the specific experimental design of each period. The following sections will present the results for each of these periods, focusing on the results after the beginning of the injection. It

shows the complementary results of the baseline values before hydrogen injection and the conditions after it stopped.

In order to simplify the discussion, an example was taken corresponding to the experimental phase of biomethanation with food waste at a recirculation rate of 20 rpm (R_{20}_FW). Figure 5-2 shows the variations of the gas content in the headspace. During the baseline period (days 0 -3), the biogas composition returns to the expected composition for food waste digestion (around 60 % CH_4 and 40 % CO_2). As soon as the hydrogen is injected (on day 3) into the reactor, the level of methane and carbon dioxide in the headspace diminishes due to the higher hydrogen content, displacing and diluting the "original" biogas in the headspace. Hydrogen content then reaches a peak (around day 8-10), and a condition of quasi-equilibrium is achieved between hydrogen injection rate and hydrogen conversion via biomethanation. In fact, the gas-liquid mass transfer of hydrogen is proportional to the concentration "driving force", which in turn also depends on the hydrogen partial pressure in the headspace. During the first days after injection, the concentration of hydrogen in the headspace increases as the hydrogen injection rate is higher than its conversion. This increase in the concentration of hydrogen causes an increase in the mass transfer between the headspace and the liquid and between the gas recirculation bubbles and the slurry; finally, the mass transfer approaches the value of the microbial conversion, and this results in a plateau of the hydrogen concentration value until the end of the experiment.

On the other hand, methane content slowly increases after the hydrogen peak due to further enrichment via biomethanation. Following the onset of the hydrogen concentration, it can be noticed that the methane content shows a rate of diminishment that is relatively higher than carbon dioxide. This is due to the buffering effect from the bicarbonate buffering system in the liquid (both soluble CO_2 and bicarbonate), which acts effectively as latent storage of carbon dioxide. Each reduction of CO_2 partial pressure in the headspace is partially compensated by the buffer. Overall, this explains the different trends in the CO_2 content curve, which monotonically decreases.

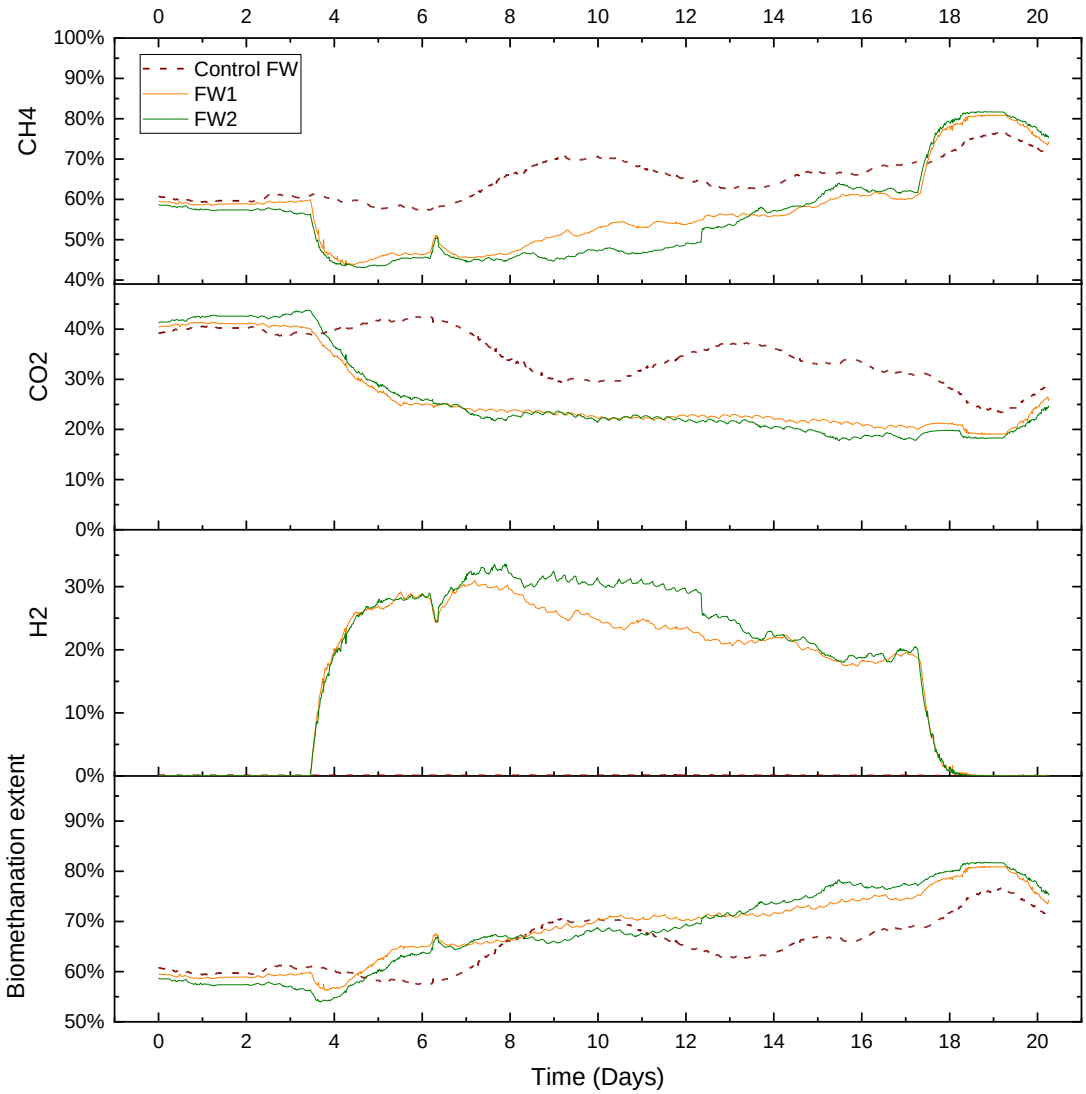

Figure 5-2 Effect of hydrogen addition to gas compositions

Once hydrogen injection stopped on day 17, it can be seen how the hydrogen content is rapidly consumed and reaches a value of zero in only about a day. Simultaneously, methane content shows a further rapid increase from the biomethanation of the residual hydrogen. Biogas composition will then slowly return to baseline levels, with methane and carbon dioxide production determined solely by feedstock digestion characteristics.

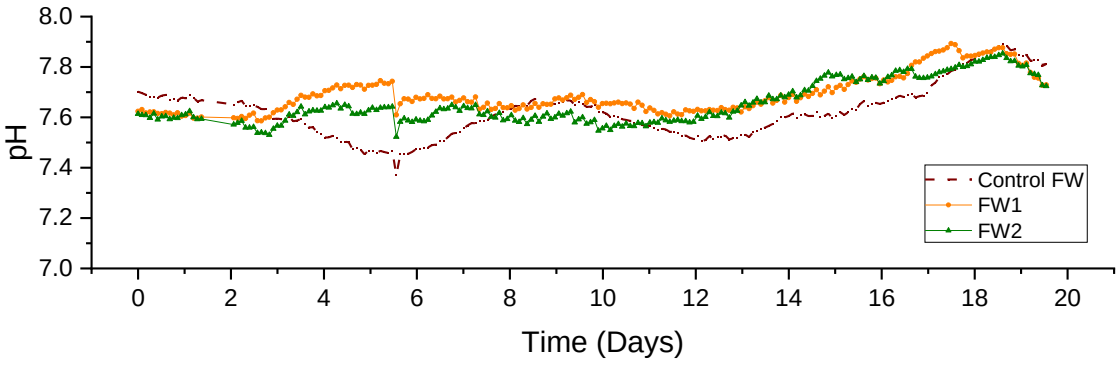

Figure 5-3 Effect of hydrogen addition to pH

Another general characteristic of biomethanation is the effect on pH influenced by the conversion of carbon dioxide. Generally, the pH in anaerobic digestion systems is influenced by different buffering systems, such as bicarbonate, VFA, ammonia, sulphides, and phosphates (Batstone *et al.*, 2002). In our experiments, the ammonia level in the food waste digesters was higher than in sewage sludge, resulting in a different pH value (higher in food waste than in sewage sludge). In the case of biomethanation, the consumption of the bicarbonate buffer directly influences the pH (Luo and Angelidaki, 2012a). Figure 5-3 shows how the pH in the biomethanation reactors increases together with the start of hydrogen injection and reaches a maximum at the end of the injection, following the decrease of the CO_2 partial pressure. Once hydrogen injection stops (day 22), the pH returns to the previous baseline values, in accordance with the increase of the carbon dioxide partial pressure.

5.3 In-situ biomethanation using sewage sludge at a different recirculation rate

The effect of gas recirculation in the in-situ biomethanation process was investigated using three different recirculation rates, namely at 20, 120 and 280 rpm or equivalent to 12, 67 and 155 L L_r^{-1} day^{-1}. In the literature, the effect of gas recirculation in the in-situ biomethanation has been explored at a low recirculation rate, 2.5 L L_r^{-1} day^{-1} (Wahid and Horn, 2021), 6-9 L L_r^{-1} day^{-1} (Bassani, Kougias and Angelidaki, 2016), and 23 L L_r^{-1} day^{-1} (Tao *et al.*, 2019). On the other hand, the effect of recirculation rate at a high rate was investigated at the ex-situ biomethanation system 156 L L_r^{-1} day^{-1} (Díaz *et al.*, 2015), 240 L

L_r^{-1} day^{-1} (Kougias *et al.*, 2017). The effect of gas recirculation at a higher flow rate in the continuous in-situ biomethanation system has not been fully investigated.

The reactor configuration is the same as in the previous experiments. However, since the experiments in chapter 4 demonstrated a higher performance of the hydrogen sparger with a 2µm pore size compared to the simple injector, both biomethanation reactors were operated with the hydrogen sparger for the experiments presented in this chapter 5.

This chapter also presents a different approach to the constraint of H_2 in the headspace. In chapter 4, it was demonstrated how a higher value of allowed H_2 (from 5 % to 10 % vol.) led to a higher amount of hydrogen injected and hence to higher CO_2 methanation (e.g. Figure 4-9). In the following experiments, a higher value of the H_2 constraint was used to further increase the gas-liquid transfer through increased driving force and explore the system's performance at higher H_2-CO_2 conversion and CH_4 enrichment values.

As with previous experiments, the hydrogen injection is compared to the expected stoichiometric requirement to achieve a high conversion of the available carbon dioxide. To estimate the available CO_2, anaerobic digestion of both substrates was monitored before hydrogen injection in order to determine the specific yield of carbon dioxide. The average carbon dioxide specific yield of the sewage sludge over 30 days was estimated as 0.12 LCO_2 $gVS^{-1}L_r^{-1}$. Based on this value, and considering an OLR of 2 gVS $L^{-1}day^{-1}$, the stoichiometric daily hydrogen requirement was calculated as 1.6 LH_2 day^{-1}. Considering to avoid excessive fall in bicarbonate buffering due to reducing CO_2 partial pressure (Tao *et al.*, 2019), the actual H_2 injection was then set as 90 % of the theoretical stoichiometric requirement. Therefore, the hydrogen setpoint (GH_2_sp) was set at 1.02 ml/min.

The fluctuation of OLR provides different biogas production flow that will influence the gas retention time in the headspace. The gas retention time will influence the gas-liquid mass transfer that will lead to hydrogen conversion. For this reason, the variations of the daily feeding allow the investigation of the effect of OLR on the biomethanation performance and process control as we found the correlation between the fluctuation of OLR and the hydrogen conversion that will be discussed later in the next section.

The setpoint and constraints for all the experimental phases can be seen in Table 5.1.

Table 5.1 Constrains and setpoint setting for feedback control parameters.

	Unit	Setpoint and constraints	k (proportional control parameter)
CH_4	%	90.0	0.3
CO_2	%	5.0	0.3
H_2	%	40.0	0.3
pH		8.2	5.0

The methane setpoint was set to reach a maximum concentration of 90 % (vol.) during the biomethanation process. Carbon dioxide was maintained to have at least 5 % in the headspace in order to keep the bicarbonate buffering system that could lead to pH increasing beyond the optimum range of process (Tao *et al.*, 2019); while the pH constraint was set at 8.2, lower than maximum operational pH for food waste anaerobic digestion that is being reported by Tao *et al.*, (2020).

The values of the k constant parameters determine the proportional band in which the feedback control is active; their actual values depend on the units of the respective process outputs, and they influence the process output intervals in which the hydrogen injection is controlled (analogously to the proportional band, in control terminology). For instance, in the case of H_2, based on the feedback control algorithm in Figure 5-1 and information in Table 5.1 and the GH_2_sp of 1.02 mL/min, the feedback control will be activated caused by H_2 content in the headspace if the concentration of H_2 in the headspace higher than 36.6 % as the value of GH_2_H_2 when H_2 content reaches 36.6 % is similar to the GH_2_sp (1.02 mL/min). Therefore, when the H_2 content has been higher than 36.6 %, the value of GH_2_H_2 will be lower than GH_2_sp, and then the feedback control will choose a lower value to deliver a new hydrogen injection flow rate. However, if the value of GH_2_H_2 is lower than the minimum flow range of the MFC, in this case, is 0.6 ml/min, the hydrogen injection will set the flow rate to 0 ml/min as the hydrogen flow rate below 0.6 ml/min will not be accurate.

At each gas recirculation value, the experimental periods lasted until the experimental conditions were evaluated to be in steady-state. Then, the hydrogen injection was interrupted at the end of each experimental period. The residual hydrogen is let to be fully

consumed to reach a similar baseline again before the following experimental phase (as explained in Section 5.3).

5.3.1 In-situ biomethanation using sewage sludge as substrate at a recirculation rate of 20 rpm (equivalent to 12 L $Lr^{-1}day^{-1}$) (R_{20}_SS)

In this experiment, in-situ biomethanation using sewage sludge at a gas recirculation rate of 20rpm (12 L $Lr^{-1}day^{-1}$) was monitored for about 17 days. Due to the technical issue of data acquisition, the biogas flow in the reactor biomethanation SS1 on day 9 is not presented. The OLR was set to have a constant value of 2 gVS L^{-1} day^{-1}; variations in the daily feeding, as shown in Figure 5-4, were due to a certain variability in the actual daily amount pumped by the automatic peristaltic pump. The average OLR during the experiment for control SS and biomethanation SS1 and SS2 were 1.91, 1.88 and 1.92 gVS L^{-1} day^{-1}, respectively.

Hydrogen injection remained fairly stable at its setpoint value (equivalent to about 1.36 NL day^{-1}), excluding short interventions of the feedback control on days 0 and 9 and a technical problem on day 6 – all of which will be explained below.

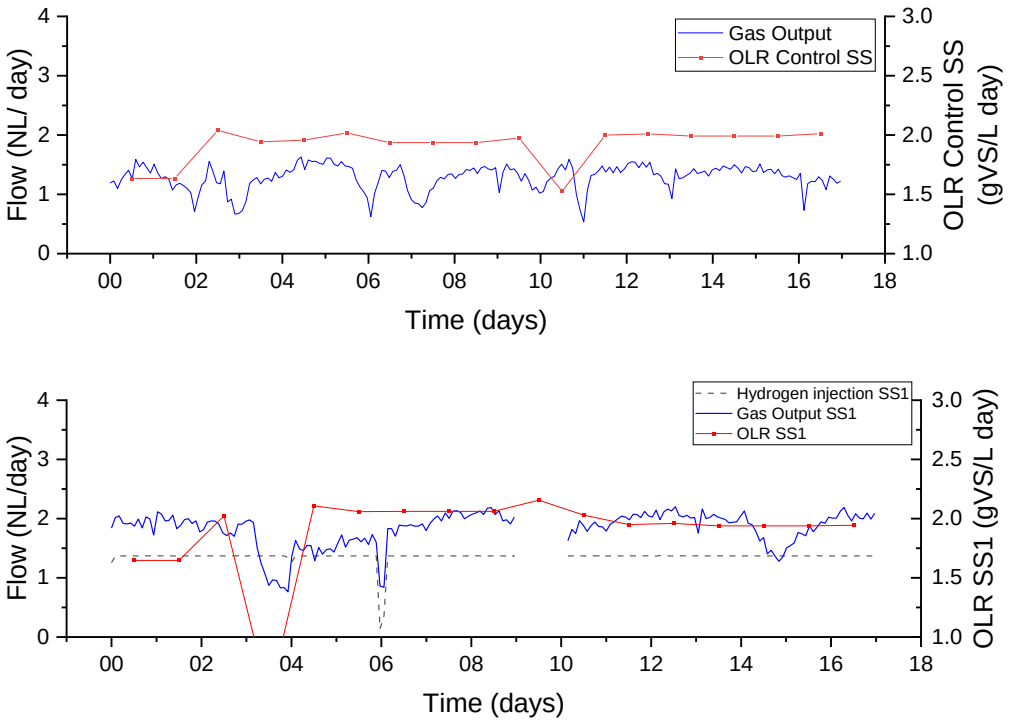

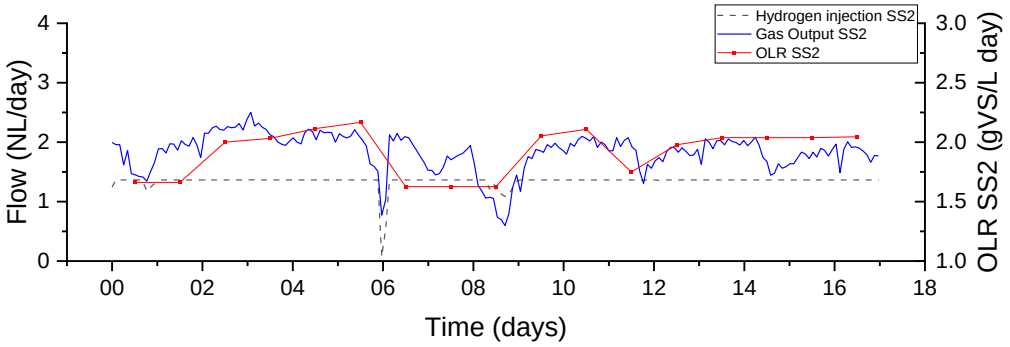

Figure 5-4 Gas flows, OLR, and hydrogen injection rate from in-situ biomethanation of sewage sludge, at gas recirculation rate of 20rpm. SS: control reactor; SS1 and SS2 duplicate biomethanation reactors.

The initial pH, in all reactors, at the beginning of the experiment was around 7.1 (Figure 5-5). The pH in the reactor SS1 and SS2 increased immediately after the addition of hydrogen. The increase of the pH due to hydrogen addition is expected and well known due to bicarbonate consumption (Luo *et al.*, 2012b). Both duplicates showed an almost similar pH profile, with average values for SS1 and SS2 of 7.41 and 7.44, respectively. On the other hand, the pH in the reactor control SS remained around pH 7.20.

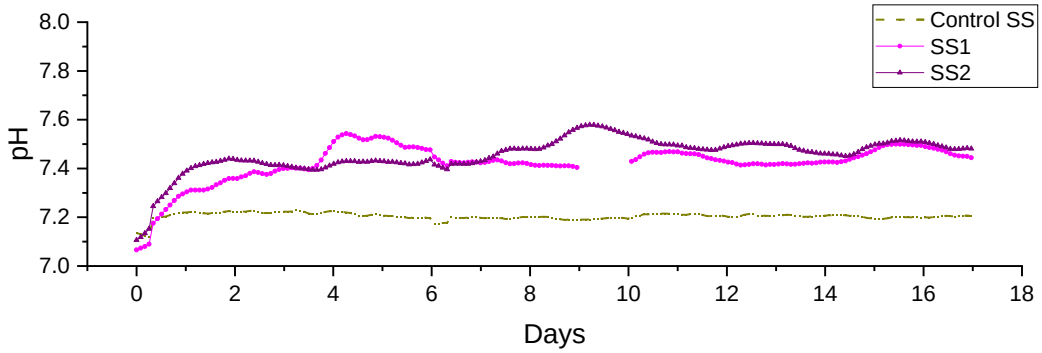

Figure 5-5 pH profile during in-situ biomethanation of sewage sludge at recirculation at 20 rpm

Both duplicate reactors showed a certain extent of biomethanation, which reached a value of around 80 %, compared to the control at about 70 % (Figure 5-6c); while H_2 conversions were between 50-70 %, with an average of 64.1 and 58.5 % for SS1 and SS2 respectively. CO_2 content decreased to around 15 % in both biomethanation reactors, compared to a 30 % level in the reactor control. Methane too decreased in the biomethanation reactors, reaching an average of 56.1 % and 54.3 % in SS1 and SS2, due to the dilution by hydrogen in the headspace, which reached the maximum hydrogen content of 33.1 % and 36.1 %, respectively.

A feeding pump failure on day 3 on reactor SS1 (Figure 5-4) caused the feeding not to be delivered properly. This feeding failure caused an evident drop in biogas production, while the flow of hydrogen injection remained at its constant setpoint value. Lower biogas production and constant hydrogen injection caused an increase in hydrogen concentration up to 37 %, while methane and carbon dioxide concentrations dropped to 49.5 % and 13.5 %, respectively. In addition, the reduction in biogas production resulted in a higher retention time, leading to higher H_2 conversion, evident at around days 3-4 in Figure 5-7a.

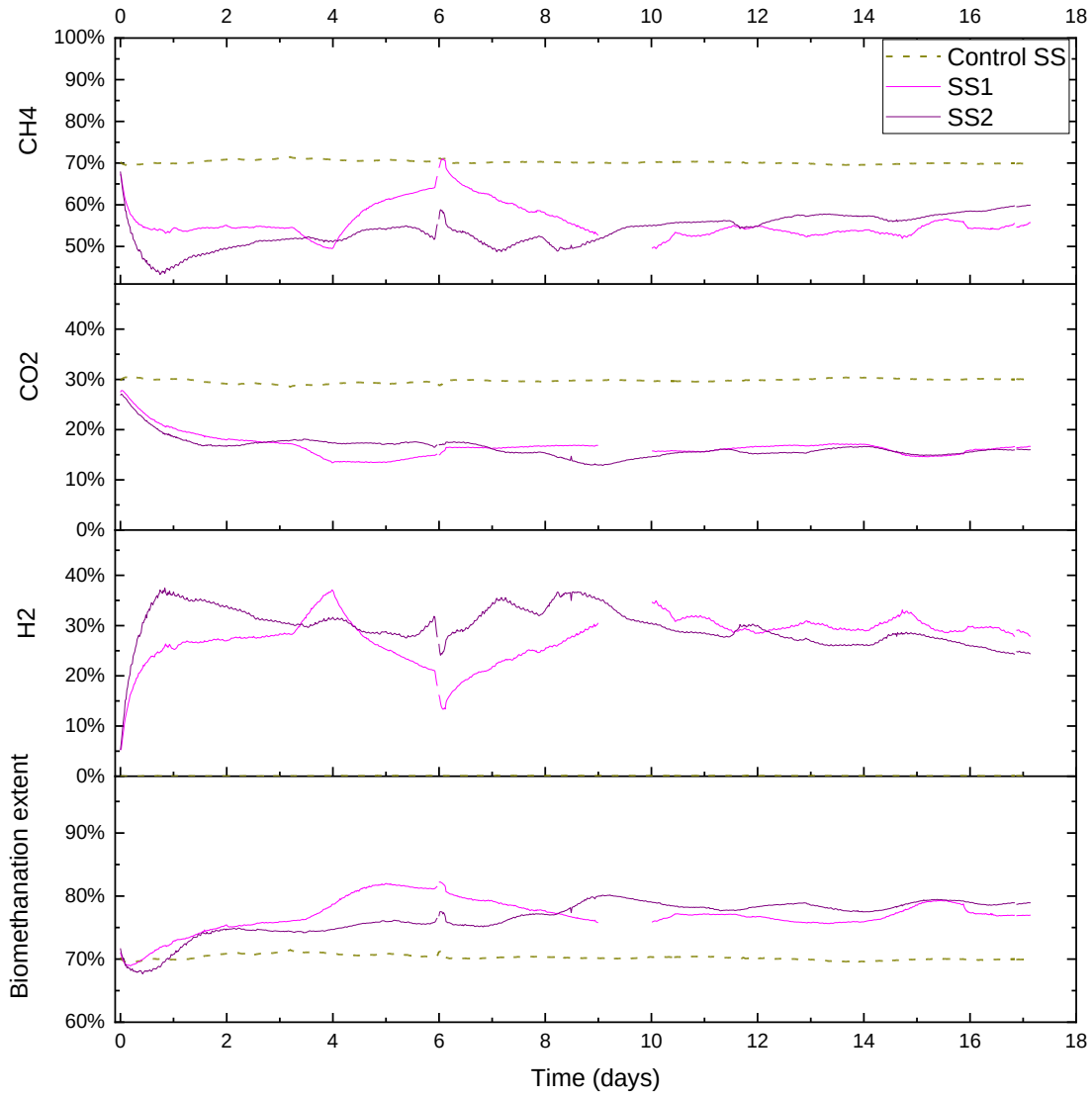

Figure 5-6. Gas composition and biomethanation extent during in-situ biomethanation of sewage sludge at gas recirculation at 20 rpm.

Abrupt changes in hydrogen injection also influence the process performance; this can be seen on day 6 in both reactors SS1 and SS2 when hydrogen had to be stopped for about five hours due to a technical problem on the rig. Gas outflow immediately follows the change in hydrogen injection, as a similar reduction can be seen (Figure 5-4b and c); this leads to a reduction in the gas flow and increases in gas residence time (RT), to which a higher hydrogen conversion follows. Resulting changes in gas composition can be seen in Figure 5-6b and c: hydrogen concentration diminishes, and methane increase towards the value of the baseline; on the other hand, carbon dioxide has a slower response, and its content in the headspace remains more stable, due to the buffering capacity in the liquid phase.

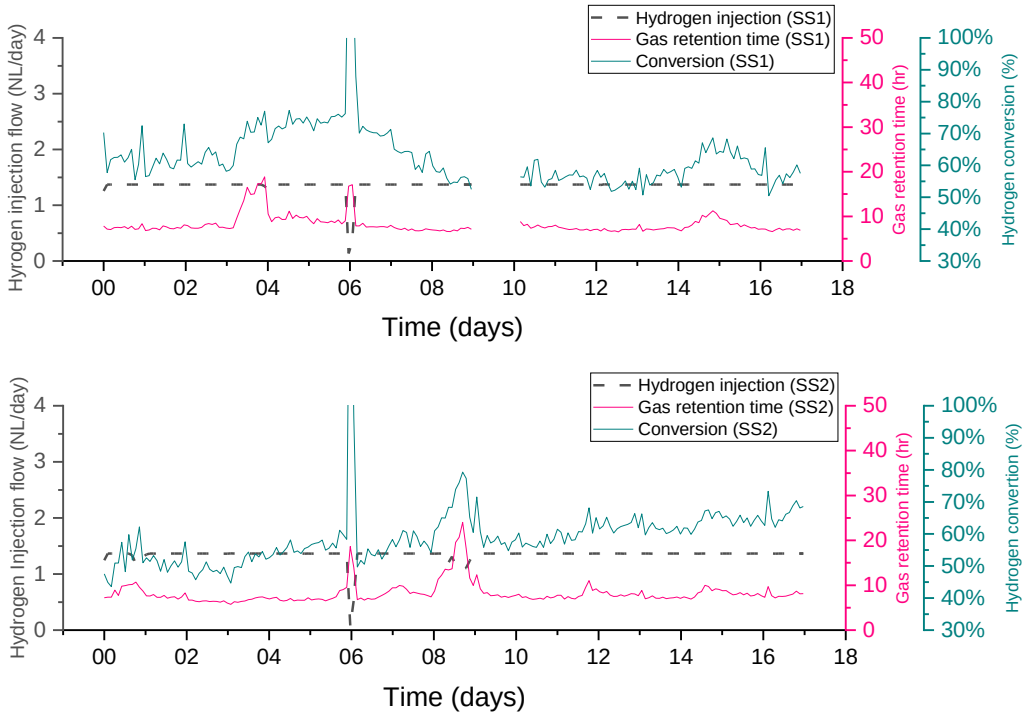

Figure 5-7. Hydrogen conversion in relation to gas retention time and hydrogen injection rate during in-situ biomethanation of sewage sludge at recirculation 20 rpm.

The feedback control was activated on days 0 and 9 on the reactor SS2, as shown as a small drop in the hydrogen injection flow, Figure 5-7. The gas composition of methane and carbon dioxide is still far from the constraints, while the hydrogen is near the constraint value. According to the algorithm in Figure 5-1 and the constraints and proportional k

values in Table 5.1, the value of hydrogen injection requested to the MFC (GH_2_MFC) will decrease from the setpoint GH_2_sp when the hydrogen concentration reaches more than 36.5 %. At this point, the value of GH_2_H_2 would be less than GH_2_sp. Therefore, the feedback control was activated based on hydrogen concentrations when the hydrogen content reached 37.4 % on day 0 and 36.7 % on day 9.

The hydrogen conversion tends to increase from 50 % at the beginning to 70 % at the end of the experiment in both reactors (Figure 5-7). This trend is also confirmed by the gas composition data (Figure 5-6), where on the final six days, methane content was observed to slightly increase in reactor SS2 along with a decrease in hydrogen content. The H_2 conversion trend could therefore be explained by microbial acclimation and growth of the hydrogenotrophic population during the experiment. Microbial activity can in fact, increase the gas-liquid mass transfer rate compared to the purely physical process in abiotic liquid by converting the absorbed gas into the stagnant liquid layer surrounding the gas bubble, thereby increasing the diffusional gradient. This phenomenon is reported in the literature as microbial enhancement of the gas-liquid mass transfer (Jensen, Ottosen and Kofoed, 2021).

5.3.2 In-situ biomethanation using sewage sludge as substrate at recirculation rate 120rpm (equivalent to 67 L $Lr^{-1}day^{-1}$) (R_{120}_SS)

The experiment of in-situ biomethanation using sewage sludge at 120 rpm (equivalent to 67 L $L_r^{-1}day^{-1}$) was monitored for 12 days. The OLR profile is quite stable, with less variability compared to the previous experiment (Figure 5-8). The average OLR is similar in all reactors, with average values for the control SS and biomethanation reactors SS1 and SS2 at 1.93, 1.89 and 2.03 gVS L^{-1} day^{-1}, respectively. Hydrogen injection remained constant at its setpoint (equivalent to 1.35 NL day^{-1}), with no activation of the feedback control as all process outputs remained below the respective constraints.

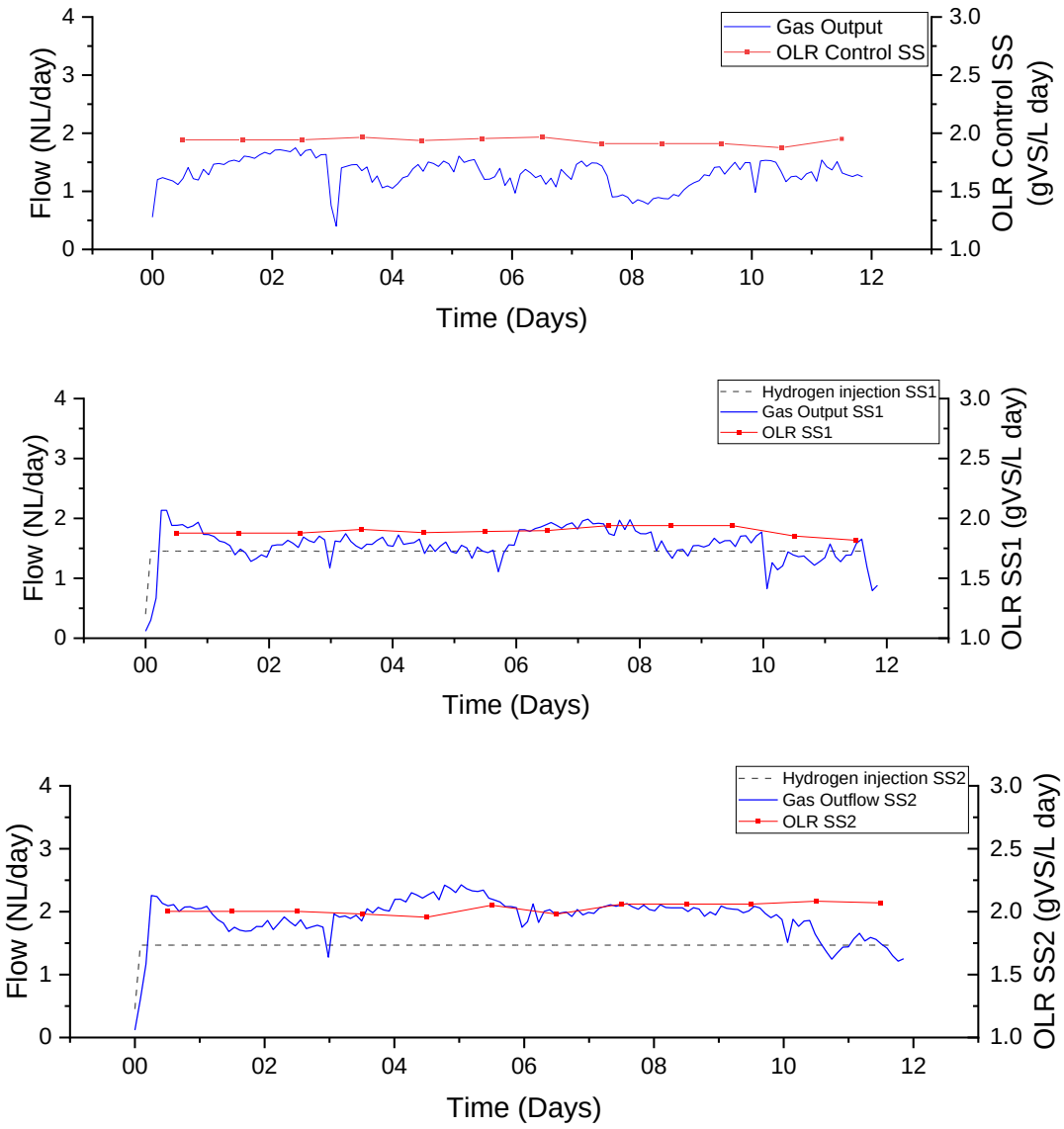

Figure 5-8 Gas flows, OLR, and hydrogen injection rate from in-situ biomethanation of sewage sludge, at gas recirculation rate of 120rpm. SS: control reactor; SS1 and SS2 duplicate biomethanation reactors.

In Figure 5-8, on around day 3, it can be seen how the biogas flow decreased in all reactors. On that occasion, digestate samples were collected in all reactors, reducing the volume of gas in the headspace as well as the gas in the buffer bags. In the control reactor SS, biogas flow dropped quite significantly from 1.6 NL day^{-1} to 0.4 NL day^{-1}, while in both biomethanation reactors, the flow still decreased, but to a lesser extent and around 1.2 NL day^{-1}. Hydrogen injection helps recover gas lost from the buffer bags, while in reactor control SS, the gas recovery relies solely on biogas production.

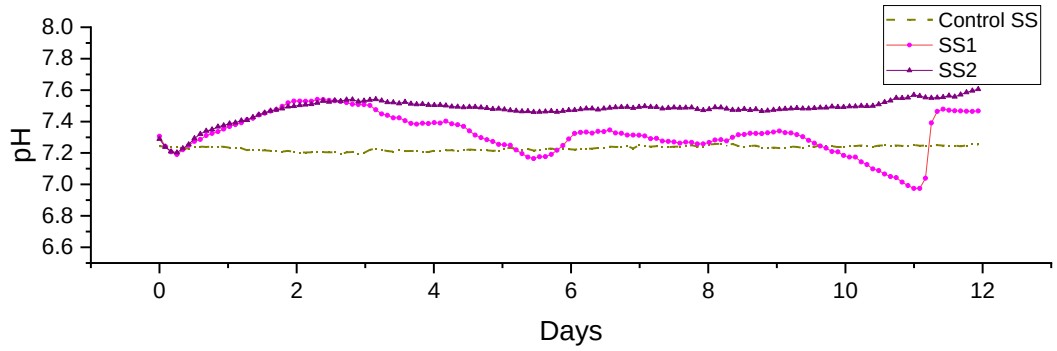

Figure 5-9 pH profile during in-situ biomethanation of sewage sludge at recirculation at 120 rpm

In Figure 5-9, the pH in reactor control SS remained fairly constant around an average value of 7.2, similarly to the pH in the previous experiment at gas recirculation 20rpm. On the other hand, the pH in biomethanation reactor SS2 had an average pH of 7.5, reaching a maximum around pH of 7.6 at the end of the experiment; these values are slightly higher compared to the previous experiment at recirculation of 20 rpm. Unfortunately, the pH monitoring on reactor SS1 had to be stopped at around day 3 due to a sudden large drift caused by previous long use. A similar disturbance also happened in the reactor using food waste (will be discussed later). In these cases, the pH probe had to be replaced or reconditioned before the next experiment.

The extent of biomethanation reached values around 81 % for both biomethanation reactors, compared to control at about 70 %: this shows the effective conversion of CO_2 through biomethanation.

In reactors SS1 and SS2, hydrogen content increased immediately after the start of the injection. It kept increasing until reaching a maximum in about two days, before a fairly constant decrease to about 23 % towards the end of the experiment (Figure 5-10). The maximum hydrogen content was 35.9 % on SS1 and 31.5 % on SS2. As mentioned in Section 5.4.1, with the implemented feedback control settings, the minimum hydrogen content that activates the feedback control is 36.5 %. As a result, the hydrogen injection remained continuous at the hydrogen setpoint flow.

Methane reached a minimum value of about 54 % in the biomethanation reactors, around day 1, in correspondence with the hydrogen maximum. The methane content then slowly increased to around 49 % in both biomethanation reactors. The average methane

composition observed stable on SS1 and SS2 were around 62 % and 60 %, while the methane content in the reactor control remained fairly constant at around 69 %.

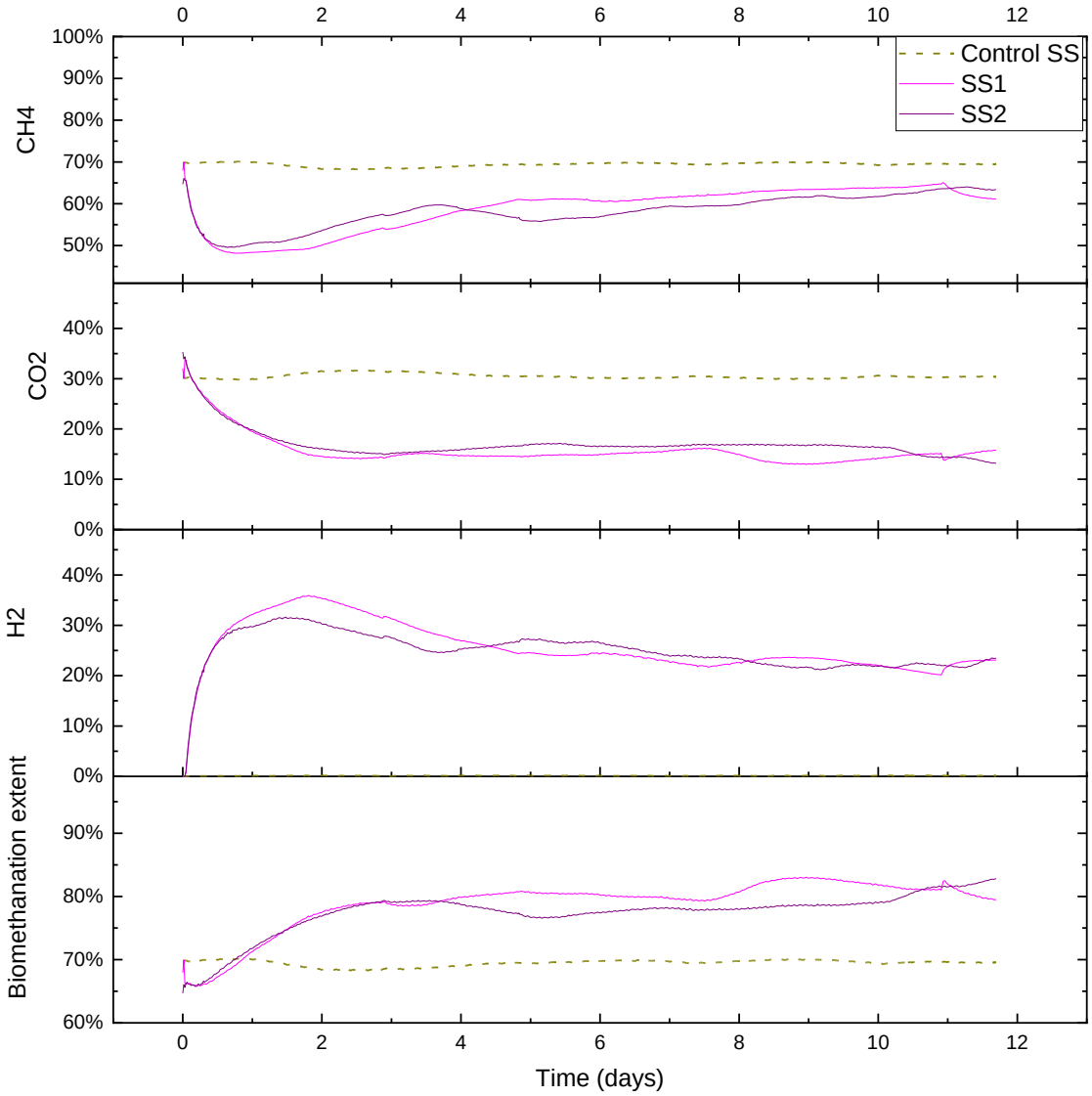

Figure 5-10. Gas composition and biomethanation extent during in-situ biomethanation of sewage sludge at gas recirculation at 120 rpm.

The hydrogen conversion on the SS1 increased from 40 % at the beginning of the experiment to a maximum of 87 % at the end of the experiment, with an average of 71.2 %, Figure 5-11. In addition, the hydrogen conversion on SS1 was higher than in SS2, with an increase in hydrogen conversion from 40 % to around 80 % at the end of the experiment.

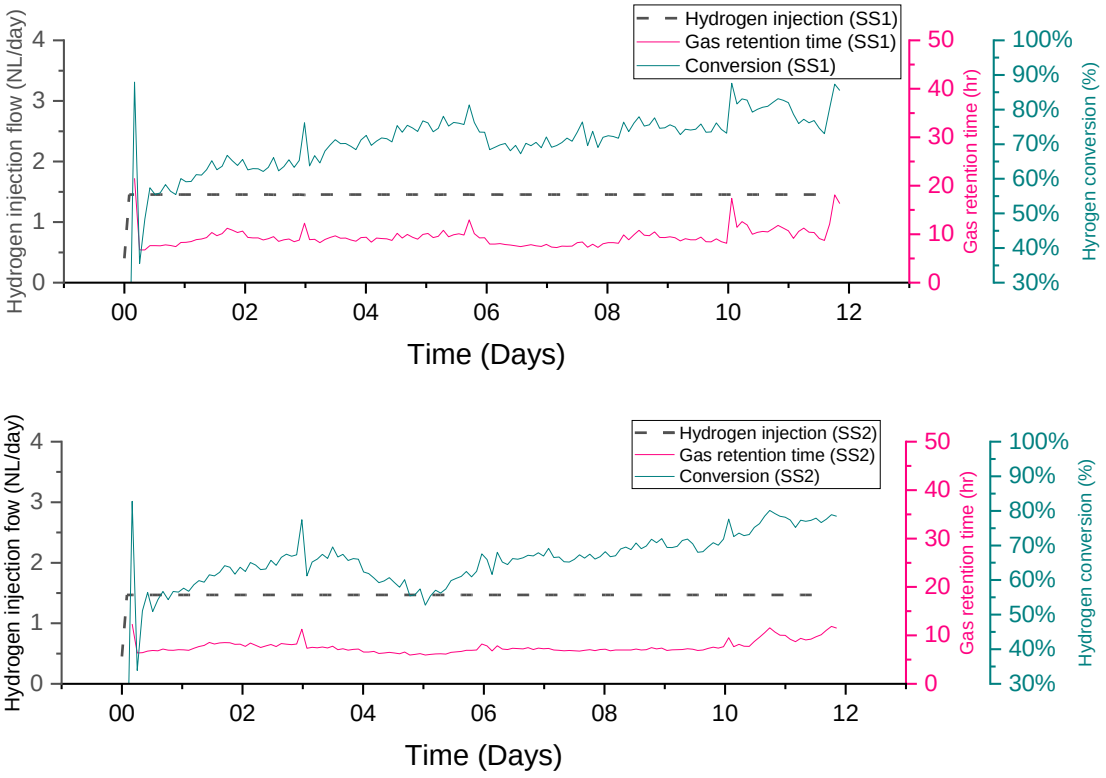

Figure 5-11 Hydrogen conversion in relation to gas retention time and hydrogen injection during in-situ biomethanation of sewage sludge at recirculation at 120 rpm

5.3.3 In-situ biomethanation using sewage sludge as substrate at recirculation rate 280rpm (equivalent to 115 L $Lr^{-1}day^{-1}$) (R_{280}_SS)

The experiment for the in-situ biomethanation using sewage sludge at 280 rpm (equivalent to 115 L $Lr^{-1}day^{-1}$) was monitored for 21 days. The feeding rate was able to be maintained close to the intended OLR, except less feeding occurred on the reactor control SS at the end of the experiment. The average OLR during this experiment for the reactor controls SS, SS1 and SS2 are 1.87, 1.97 and 2.04 gVS L^{-1} day^{-1}, respectively. The average gas outflow in the reactor biomethanation SS1 and SS2 is almost similar with 1.75 and 1.83 NL day^{-1}, while the average gas outflow on reactor control SS is much less than 1.23 NL day^{-1}. Hydrogen injection is relatively stable throughout periods, with the average injection flow rate in both reactors being 1.46 NL day^{-1}. The feedback control was activated in the middle of day 1, which will be explained below.

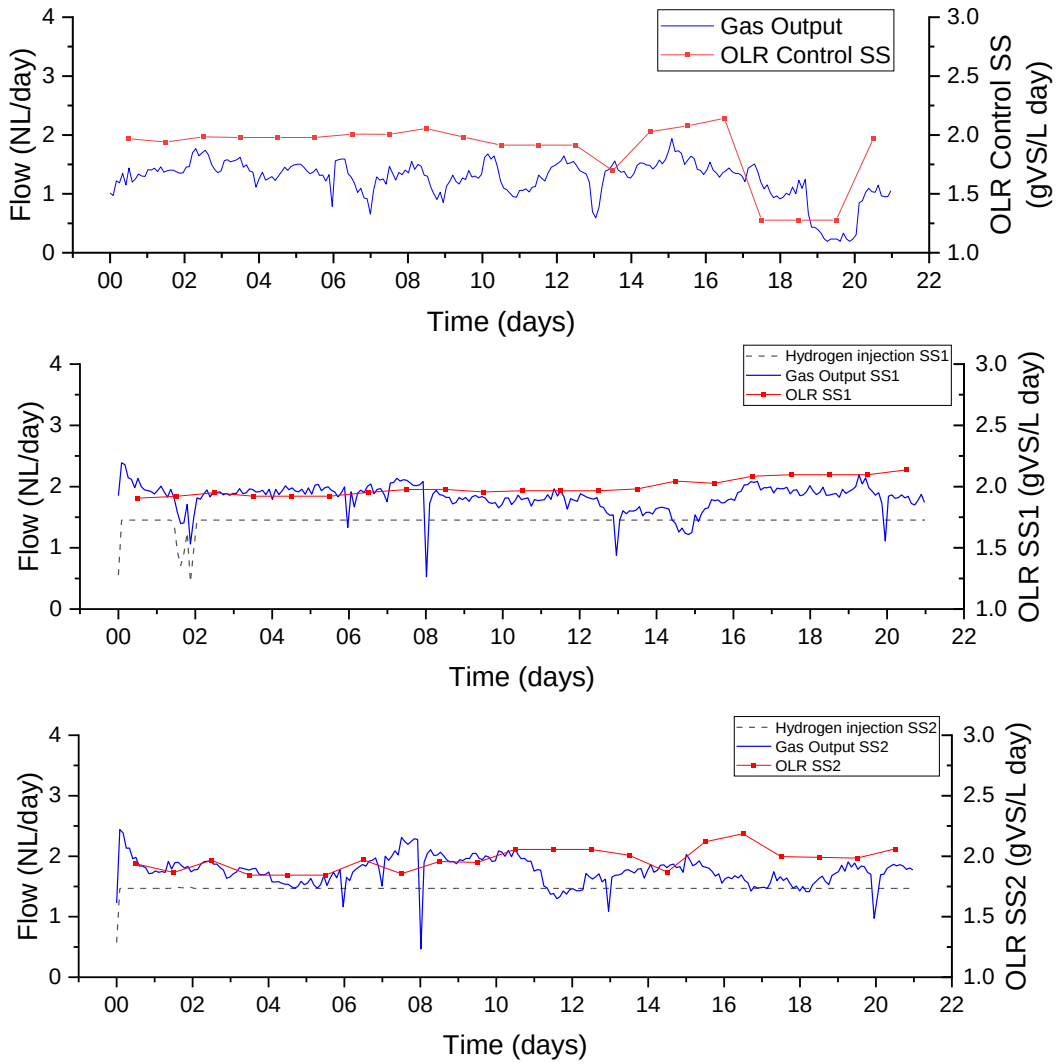

Figure 5-12 Gas flows, OLR, and hydrogen injection rate from in-situ biomethanation of sewage sludge, at a gas recirculation rate of 280rpm. SS: control reactor; SS1 and SS2 duplicate biomethanation reactors.

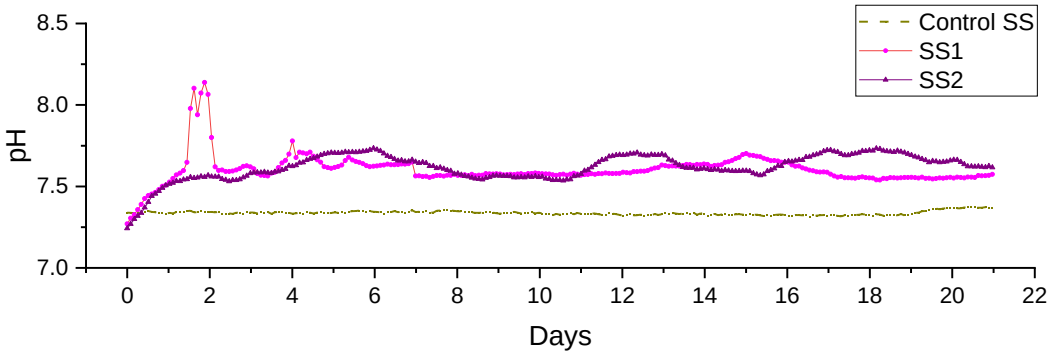

Figure 5-13 The pH profile during in-situ biomethanation of the sewage sludge at recirculation at 280 rpm.

The initial pH before the hydrogen injection was similar in all the reactors, around 7.3, Figure 5-13. The pH increases immediately when the hydrogen is injected into the reactor. The average pH in this period for both reactors was quite similar, being around 7.6. On day 1, the pH value was interrupted by the reading error in the data acquisition caused a spike in the pH value that interfered with the hydrogen injection due to feedback control adjustment.

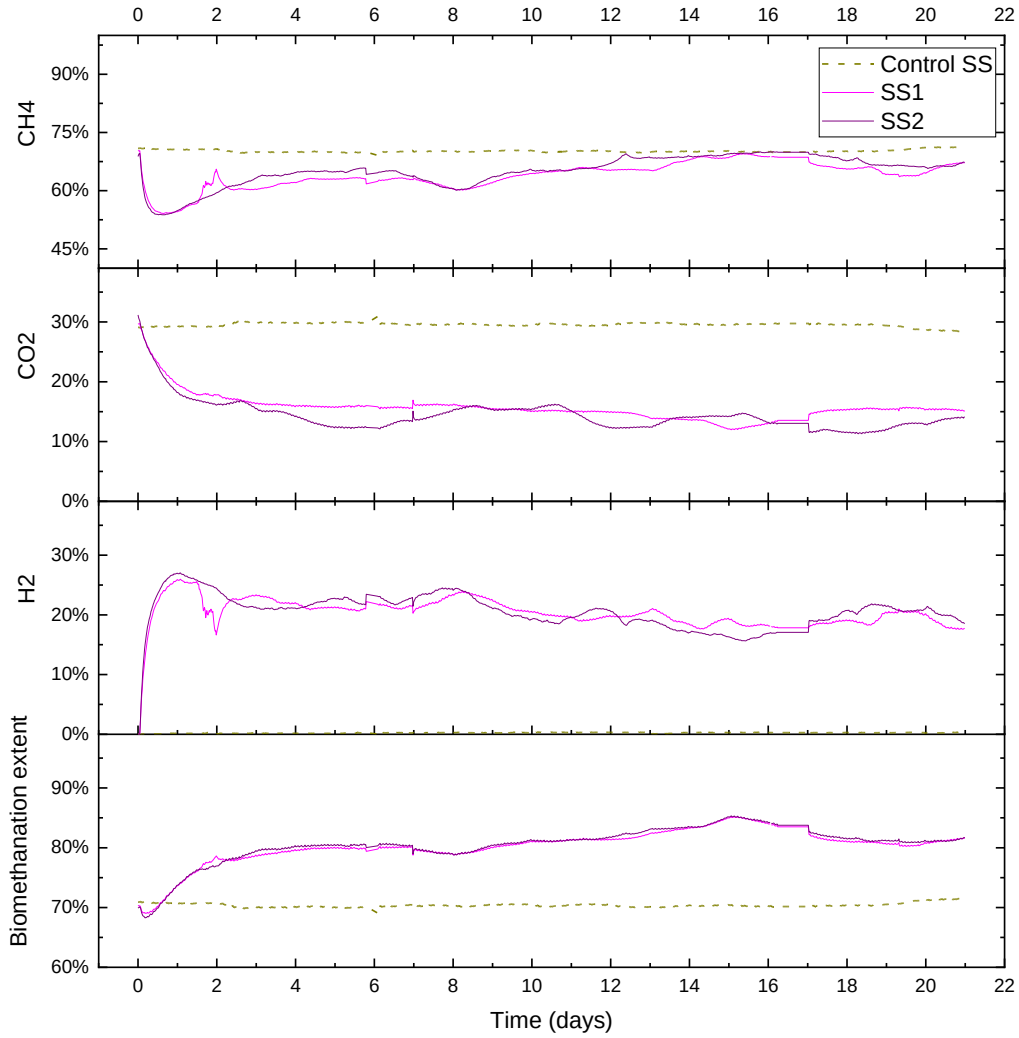

Figure 5-14. Gas composition and biomethanation extent during in-situ biomethanation of sewage sludge at gas recirculation 280 rpm.

In Figure 5-14, the methane content in both biomethanation reactors decreases as soon as hydrogen is injected and reaches a minimum of 54 %. The methane content in biomethanation reactors showed a similar trend of methane enrichment, with the maximum methane content able to reach the methane content in the reactor control (70

%) on day 14. The carbon dioxide content in biomethanation reactor SS1 looks stable after day 2 at 16 %, while in biomethanation reactor SS2 reactor has slightly oscillated between 12 % and 16 %. The average hydrogen content for both reactors is almost the same, where SS1 has an average hydrogen conversion of 73.93 %, and SS2 was 75.26 %. In addition, the proportion of hydrogen conversion is in line with the average methane content, where SS2 has a slightly higher average methane content (64.72 %) than SS1 (63.65 %). The biomethanation extent shows the enrichment to a maximum of 85 % or 15 % higher relative to the reactor control.

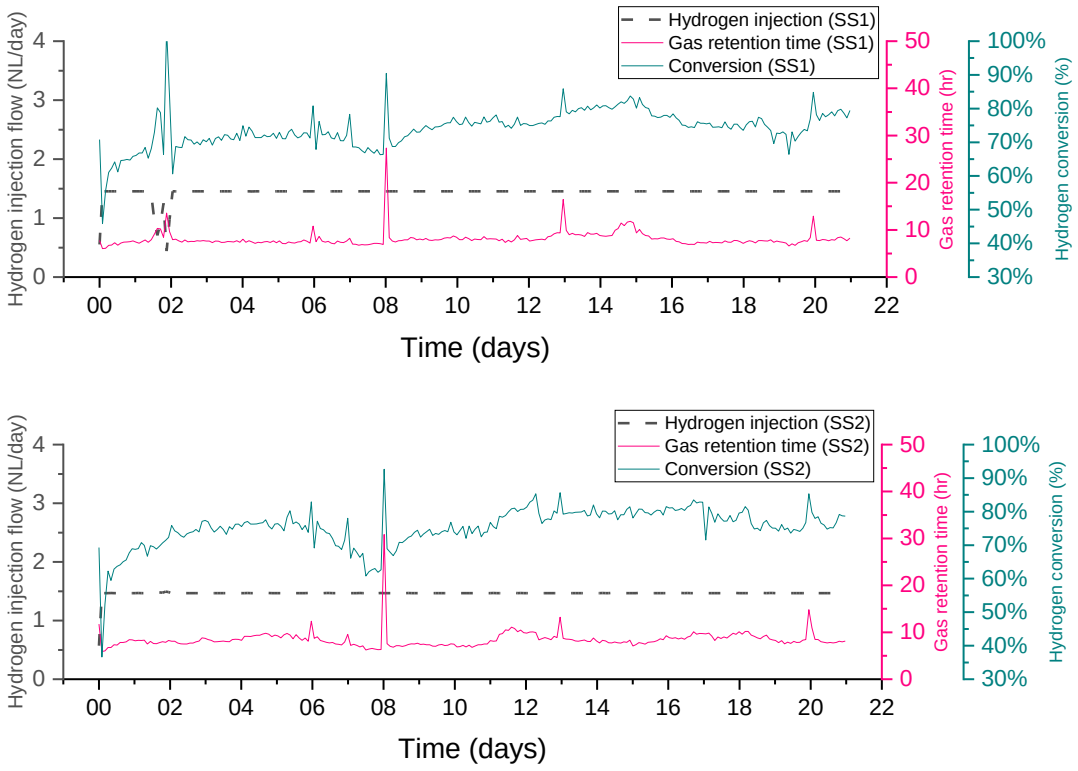

Figure 5-15. Hydrogen conversion in relation to the gas retention time and hydrogen injection during in-situ biomethanation of sewage sludge at a recirculation of 280 rpm.

In Figure 5-12, the hydrogen injection in the SS1 reactor begins to decrease on day one. The hydrogen composition at that time was 25.1 %, methane 56.8 % and carbon dioxide 17.7 %. According to the gas compositions, the feedback control should not be able to be activated because the GH_2 of those gases are still higher than the hydrogen injection set point GH_2_sp. However, in Figure 5-13, we can see a spike in the pH on day one. At that time, the pH constraint was set at 8.2, with the k value being 10. According to this setting, the feedback control is activated when the pH reaches a value greater than 8.1. Having

seen the gas composition, Figure 5-14 shows an increase in methane content in line with the decrease in the hydrogen content. In order to avoid the feedback control controlled by the pH value, the constraint was increased to 8.7, and the k value for the pH was 15 (the same change was also applied to the food waste digesters). With the new setting of the pH constraint, the feedback control is corrected by the pH when the pH reaches a value above 8.6, which also what is reported by Tao et al. (Tao *et al.*, 2020), that stable pH during the biomethanation process in the food waste in-situ biomethanation is around 8.6.

5.3.4 The effect of the recirculation rate on the in-situ biomethanation using sewage sludge

As previously described in the literature review, the key to successfully implementing the in-situ biomethanation process is to increase gas-liquid mass transfer (Luo *et al.*, 2012b). The gas recirculation could give rise to a positive correlation on increasing the gas-liquid mass transfer (Bassani, Kougias and Angelidaki, 2016).

The summary of the in-situ biomethanation of sewage sludge at different recirculation times can be seen in Table 5.2. The average data in the summary table was calculated based on the value obtained during the experiment, including the average OLR, injection rate, gas retention time, and gas composition. The gas retention time was calculated based on equation 3-13, as discussed in section 3.6.1. A single point value of gas retention time was obtained and calculated from the raw data that was recorded every minute; then, the average was taken from the day when the beginning of hydrogen injection until the day when hydrogen injection was stopped. A similar method was provided to calculate an average value of hydrogen conversion.

The average hydrogen injection rate in R_{20}_SS is lower compared to the R_{120}_SS and R_{280}_SS; this is due to the feedback control activation and some technical problem. However, in general, the hydrogen injection rate in all periods is quite stable, meaning that the hydrogen on continuous injection into the digester and the activation of the feedback control only occurred on some occasions as the hydrogen reaches a value close to the constraint (at period R_{20}_SS) or a rapid increase of pH (at period R_{280}_SS).

The recirculation rate has improved the hydrogen conversion rate along with an increase in gas recirculation rates. On average, the hydrogen conversion increased from 61.30 % in the R_{20}_SS to 68.87 % at R_{120}_SS and continues to increase to 74.60 % at R_{280}_SS. This increased the specific methane production rate by up to 26 % relative to the reactor control at R_{280}_SS. The hydrogen conversion rates constituted with the hydrogen injection rate in all periods ranged from 64.5 % to 75 %, where the highest value was achieved at R_{280}_SS. This conversion rate was lower than what Bassani et al. (2016) obtained, achieving 86.8 % by using a UASB reactor and ceramic sponge sparger. On the other hand, the value of the conversion rate is still far better compared to the large-scale reactor that was investigated by Jensen *et al.* (2018), which was only able to achieve 10-26 %.

The highest biomethanation extent was achieved at R_{280}_SS. In this period, the average methane content in the reactor with hydrogen injection, the SS1 and SS2, were 63.65 % and 64.72 %, respectively. Both the methane contents are less than the methane content in the reactor control, 68.64 % or, on average, around 6.5 % less relative to the reactor control. The methane content in the period R_{280}_SS was higher than R_{20}_SS and R_{120}_SS. However, even though the methane content in the biomethanation reactor is less than the control, the specific methane production was detected to be higher than the control in all periods.

In comparison, the actual specific methane production is higher compared to the theoretical specific methane yield based on the stoichiometric value of 0.25 $LCH_{4\ enrich}/LH_2$. In Table 5.2, the proportion of methane enrichment increased along with the increased recirculation rate. At R_{20}_SS, the ratio of the relative methane enrichment with hydrogen converted was 0.11 $LCH_{4\ enrich}/LH_2$. With this value, it appears to require more than four moles of hydrogen to produce one mole of methane. However, hydrogen is required for microbial growth (Díaz *et al.*, 2015; Alfaro *et al.*, 2018). At R_{120}_SS, the methane enrichment ratio was slightly improved to 0.18 $LCH_{4\ enrich}/LH_2$ and even closer to the stoichiometric at R_{280}_SS, with the ratio being 0.22 $LCH_{4\ enrich}/LH_2$.

Interestingly, the sum of the theoretical CO_2 from the biomethanation (calculated from converted H_2) and the volumetric CO_2 from the output gas in all periods is 35 %-39 % higher compared to the CO2 produced in the reactor control. In this case, the extra CO_2 might

have come from the bicarbonate consumption as the pH increases. Bassani, Kougias and Angelidaki (2016) also obtained a similar result.

Table 5.2 Summary of in-situ biomethanation using sewage sludge at different recirculation rates.

		Recirculation at 20 rpm			Recirculation at 120 rpm			Recirculation at 280 rpm		
	Unit	Control	SS1	SS2	Control	SS1	SS2	Control	SS1	SS2
Time	Days	17	17	17	12	12	12	21	21	21
Hydrogen injection flow setpoint	ml min^{-1}		1.02	1.02		1.02	1.02		1.02	1.02
Average OLR	gVS L^{-1} day^{-}	1.91	1.88	1.92	1.93	1.89	2.03	1.87	1.99	1.97
Actual hydrogen Injection supplied	L day^{-1}		1.37	1.36		1.44	1.45		1.45	1.48
Total gas out	L gVS^{-1}	0.40	0.55	0.57	0.39	0.49	0.56	0.39	0.54	0.52
Specific CH_4 production rate	L gVS^{-1}	0.28	0.31	0.31	0.27	0.28	0.32	0.27	0.34	0.34
Specific CO_2 in output gas	L gVS^{-1}	0.12	0.09	0.09	0.12	0.08	0.10	0.08	0.05	0.04
Hydrogen consumption rate	L day^{-1}		0.88	0.79		1.03	0.96		1.07	1.11
H_2 Conversion	%		64.09	58.5		71.41	66.3		73.93	75.26
Average retention time	hr		10.86	8.22		9.42	7.63		8.08	8.43
Methane evolution rate (MER)	L/L_r day		0.13	0.12		0.15	0.14		0.16	0.16
Average pH		7.21	7.43	7.46	7.23	7.32	7.48	7.34	7.6	7.62
Average CH4	%	69.91	56.16	54.2	68.50	59.47	58.8	68.64	63.65	64.72
Average CO2	%	29.58	16.78	16.5	29.63	15.56	16.8	28.89	15.59	14.28
Average H2	%	0.07	27.91	30.2	0.11	25.28	24.6	0.24	20.23	20.38
Average TS	%	2.41	2.59	2.48	2.34	2.38	2.53	2.51	2.76	2.57
Average VS	%	1.54	1.56	1.54	1.30	1.47	1.58	1.46	1.73	1.57
Average Ammonia	gTAN kg_{sub}^{-1}	1.61	1.55	1.49	1.46	1.36	1.56	1.46	1.56	1.52
Average Alkalinity ratio		0.45	0.42	0.40	0.37	0.38	0.31	0.33	0.31	0.31
Average Acetate	g kg_{sub}^{-1}	0.25	0.25	0.08	0.38	0.25	0.12	0.68	0.23	0.21
Average total VFA	g kg_{sub}^{-1}	2.81	2.02	0.72	3.34	2.55	2.35	2.17	1.38	1.13

The average pH value on the SS1 and SS2 were increased compared to the pH at the reactor control. The average pH tends to increase along with the increase in the recirculation rate. The highest pH was observed at R_{280}_SS, increasing to pH= 7.6. However, this is still categorised as a healthy digester. The maximum stable pH during in-situ biomethanation was reported by Tao et al. (Tao *et al.*, 2020) to be around 8.6, whereas pH values higher than 8.5 will lead to the inhibition of the methanogenesis process (Angelidaki *et al.*, 2018). The average alkalinity during the experiment in SS1 and SS2 was improved along with the increasing recirculation rates. The average alkalinity ratio (IA/PA) on recirculation rates 20, 120 and 280 are 0.41, 0.35 and 0.28, respectively, while a healthy digestate was reported at an IA/PA ratio of 0.3 (L. E. Ripley, 1986).

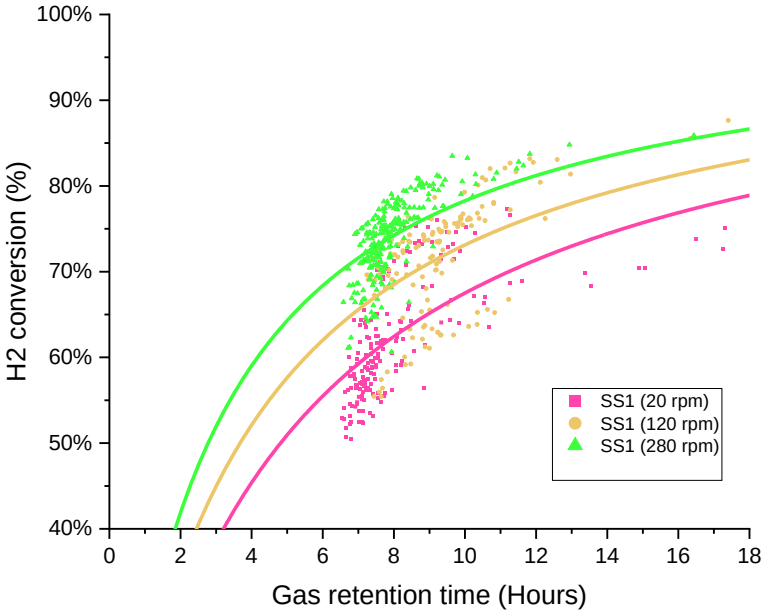

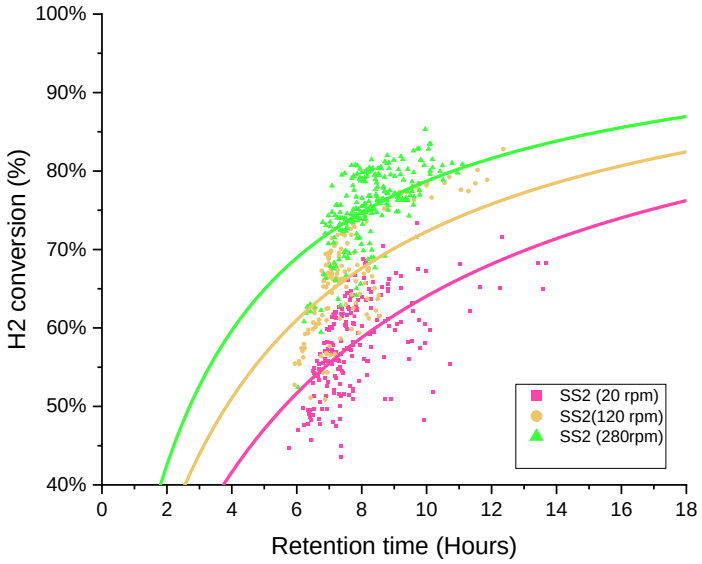

Figure 5-16. Scatter plot of the retention time and hydrogen conversion on different retention times on the SS1 and SS2

In Figure 5-16, the data distribution on the gas retention time (section 3.6.1) in relation to the conversion (section 3.6.2) is presented. The trendline In Figure 5-16 was shown a relationship between H_2 conversion and gas retention time, as discussed in section 3.6.3. In general, the data distribution shows the same trend that the hydrogen conversion increases along with the increase in the recirculation rate. This is an indication that the recirculation rate is able to improve gas transfer and biomethanation performance. The trend lines are also "ranked" in the graph following the same, from lowest to highest recirculation rates.

The effect of the gas recirculation rate improves the conversion of the H_2, and a similar result has been reported by Alfaro et al. (2018). The increasing biogas recirculation rate also improves the methane evolution rate (MER) on both reactors from 0.12 L L_r^{-1} day^{-1} at R_{20}_SS to 0.15 L L_r^{-1} day^{-1} at R_{280}_SS, with the maximum conversion being achieved of up to 75 % at R_{280}_SS. The value was lower compared to the study by Wang et al. (2013), which could achieve quite a high MER up to 0.75 L L_r^{-1} day^{-1}. However, the study was performed at OLR 1 gVS L^{-1} day^{-1} and also the use of a hollow membrane as a sparger could make a significant difference. In general, the MER of the in-situ biomethanation is in the range of 0.08 to 0.39 L L_r^{-1} day^{-1} (Luo (Lecker *et al.*, 2017).

5.4 In-situ biomethanation using food waste at a different recirculation rate

The effect of the recirculation rates was also observed using food waste as a substrate. The anaerobic digestion of the food waste has an 80 % higher biogas-specific yield compared to the sewage sludge. Therefore, one of this study's advantages in determining the effect of the recirculation rate at lower gas retention times.

A similar configuration and feedback control setting has been used to study the effect of the recirculation rates using food waste as the substrate, see Table 5.1. A similar set of recirculation rates was investigated at 20, 120 and 280rpm (equivalent to 12, 67 and 155 L $L_r^{-1}day^{-1}$). The intended organic loading rates (OLR) were set at 2 gVS L^{-1} day^{-1}. However, the ammonia content of the inoculum was recorded to be high at 6.3 gTAN/kg. The high ammonia content could cause instability in biogas production and lead to system failure (Rajagopal, Massé and Singh, 2013). Therefore, to reduce the risk of system failure, a baseline investigation was performed with a lower OLR at OLR 1 gVS/L for about 25 days, and the ammonia was monitored twice per week. After 25 days of monitoring, the ammonia level could be reduced from 6.3 to 5.6 gTAN/kg substrate. Using the low OLR is one strategy to tackle ammonia inhibition by avoiding the increasing C/N ratio (Polizzi, Alatriste-Mondragón and Munz, 2018; Christou *et al.*, 2021). On the other hand, the hydrogenotrophic methanogen is more tolerant to the higher ammonia content (Schnürer and Nordberg, 2008; Garcia-Robledo *et al.*, 2016). For this reason, at the beginning of the experiment, at the recirculation rate of 20 rpm, the OLR was set at 1.5 gVS $L^{-1}day^{-1}$ in order to avoid process failure due to inhibition. Then on recirculation at 120 and 280 rpm, the setting was set back to 2gVS $L^{-1}day^{-1,}$ and the hydrogen injection set point (GH_2_sp) was adjusted on each period based on the daily hydrogen requirement following the set of OLR.

The average CO_2 specific yield before starting the hydrogen injection in period R_{20}_FW was recorded at 0.174 LCO_2 g^{-1}VS L^{-1} day^{-1}. Then, the hydrogen set point was set at 1.1 ml min^{-1} by taking into account 90 % of the daily hydrogen requirement (as described in Section 5.3). In the period $R_{120,}$ the biogas production was recovered with an ammonia content recorded at 3.6 gTAN kg^{-1}, which was significantly reduced from the previous period (average TAN level was 4.2 gTAN kg^{-1} in period R_{20}_FW). This resulted in an increase in the

CO_2 specific yield with 0.215 LCO_2 $g^{-1}VS$ L^{-1} day^{-1}. Therefore, it can explain why in the period R_{20}_FW, the CO2 specific yield was recorded lower compared to CO_2 specific yield in the period R_{120}_FW and R_{280}_FW. However, the CO_2 specific yield in periods R_{120}_FW was similar to the value obtained in the previous experiment (see Chapter 4, Table 4.5). Therefore, the calculation of hydrogen requirement was adjusted with the value of CO_2 specific yield at 0.215 LCO_2 $g^{-1}VS$ L^{-1} day^{-1}. In periods R_{120} and R_{280}, the hydrogen injection flow rate then increased to 1.9 ml min^{-1} as OLR was set to be 2 gVS L^{-1} day^{-1}.

5.4.1 In-situ biomethanation using food waste at a recirculation rate of 20rpm (R_{20}_FW)

The experiment of in-situ biomethanation using food waste at 20 rpm (equivalent to 12 L $L_r^{-1}day^{-1}$) was observed for 14 days. Less feeding appeared in the reactor control FW due to feeding pump malfunction. No extra feeding was given as compensation for the less feeding. On the other hand, the OLR in both biomethanation reactors were record stable. The average OLR of the reactor control FW, FW1 and FW2 was 0.94, 1.35 and 1.31 gVS L^{-1} day^{-1}, respectively Figure 5-17.

The hydrogen injection was interrupted on day 3 in biomethanation reactor FW1 and FW2 and on day 9 on reactor FW2 due to feedback control activation. As a result, the average hydrogen injection rate in reactor biomethanation FW1 and FW2 were recorded at 2.31 and 2.25 L day^{-1}, respectively.

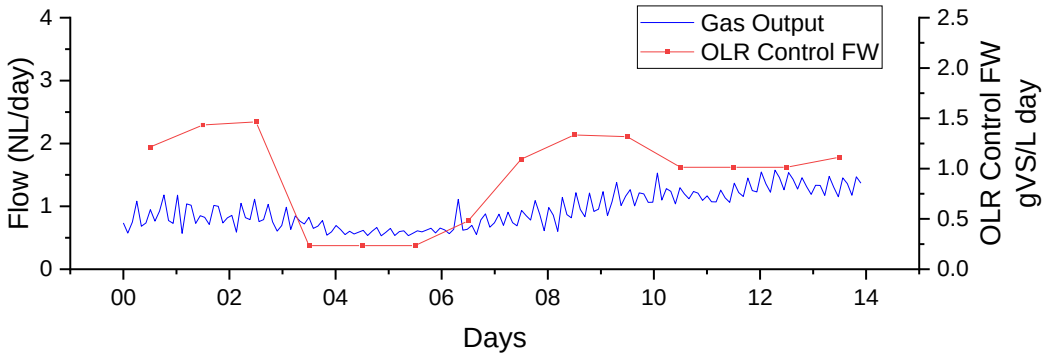

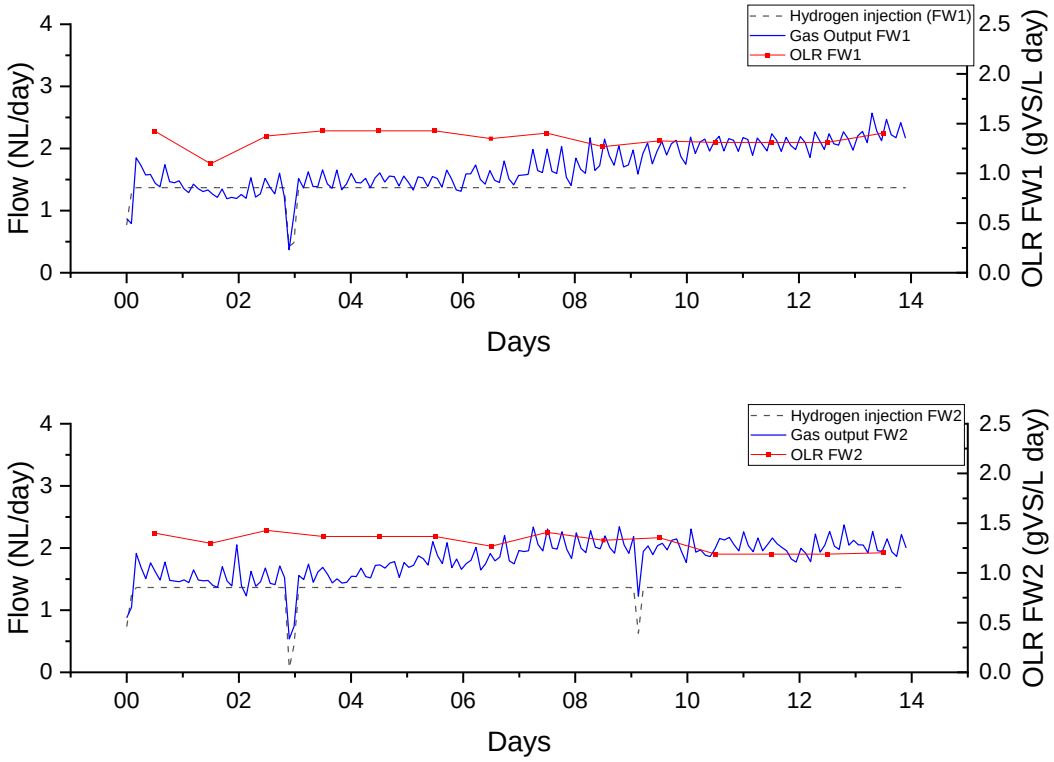

Figure 5-17 Gas flows, OLR, and hydrogen injection rate from in-situ biomethanation of food waste, at gas recirculation rate of 20rpm. FW: control reactor; FW1 and FW2 duplicate biomethanation reactors.

The average gas output flow tends to increase after six days, see Figure 5-17. For example, the average gas output flow on the first six days is 1.4 NL day^{-1} for FW1 and 1.5 NL day^{-1} for FW2; then, after six days, the average increases up to 1.9 NL day^{-1} for FW1 and 2.0 NL day^{-1} for FW2.

The initial pH for all the reactors before the hydrogen injection was recorded to be around 7.6. However, the pH on the reactor control FW was decreased to 7.4 in the first three days, see Figure 5-18. The pH of reactors FW1 and FW2 oscillated around 7.6, and by the end of the experiment, the pH in both reactors was recorded at 7.75 (FW1) and 7.77 (FW2).

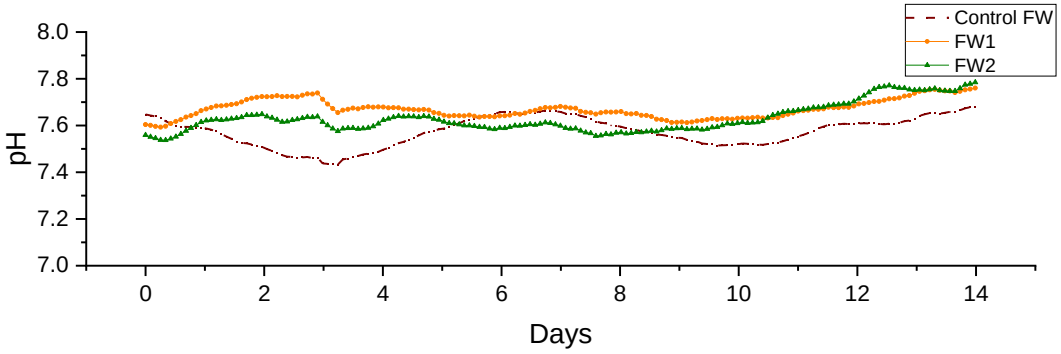

Figure 5-18 The pH profile during in-situ biomethanation of food waste at gas recirculation at 20 rpm.

The methane content decreased immediately as soon as hydrogen started injected from around 60 % to around 43 % in just one day of injection, Figure **5-19**. On the other hand, hydrogen content in both reactors looks flattering at around 28 % on day 2. Similar to the period R_{20}_SS, there was some technical problem on day 3 that required hydrogen injection to be stopped for about five hours. As a result, the hydrogen content dropped by around 4 % along with the increased methane content with a similar proportion, while CO_2 was not affected by the temporary stop of hydrogen injection due to the bicarbonate buffering system.

The methane content tended to increase during the experiment and for both reactors (FW1 and FW2) after reaching minimum methane content (45 %) due to hydrogen dilution in both reactors. The maximum methane content in biomethanation reactor FW1 and FW2 was 63 % and 64 %, respectively. Unlike methane, the carbon dioxide content tended to be stable at 26 %. The hydrogen content in both reactors was recorded to have a similar value at the end of the experiment, around 18 %. The biomethanation extent in the FW1 and FW2 was recorded at 75 % and 77 %, or 7 % and 9 % relative to the reactor control, respectively.

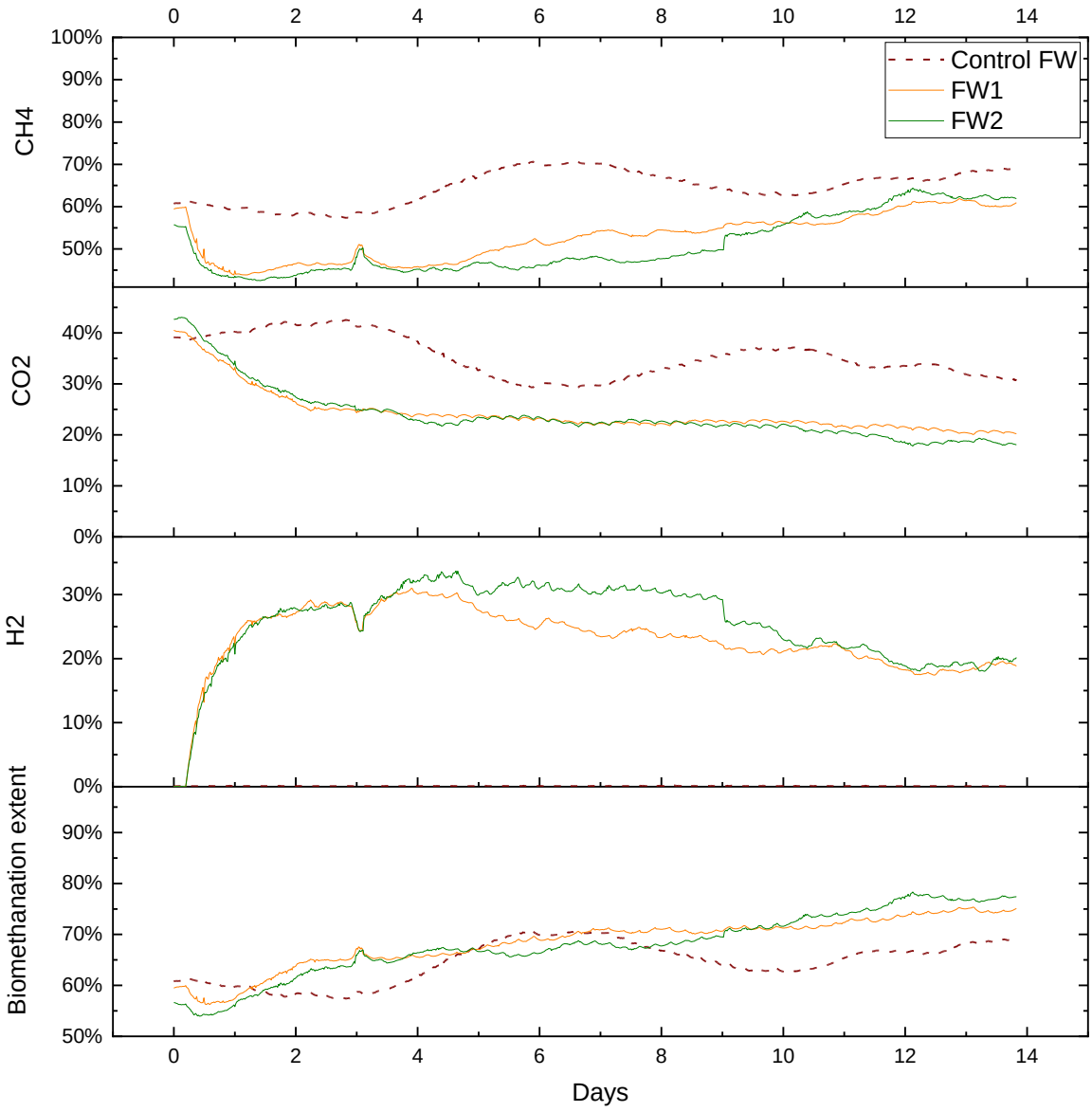

Figure 5-19. Gas composition and biomethanation extent during in-situ biomethanation of food waste at gas recirculation 20 rpm.

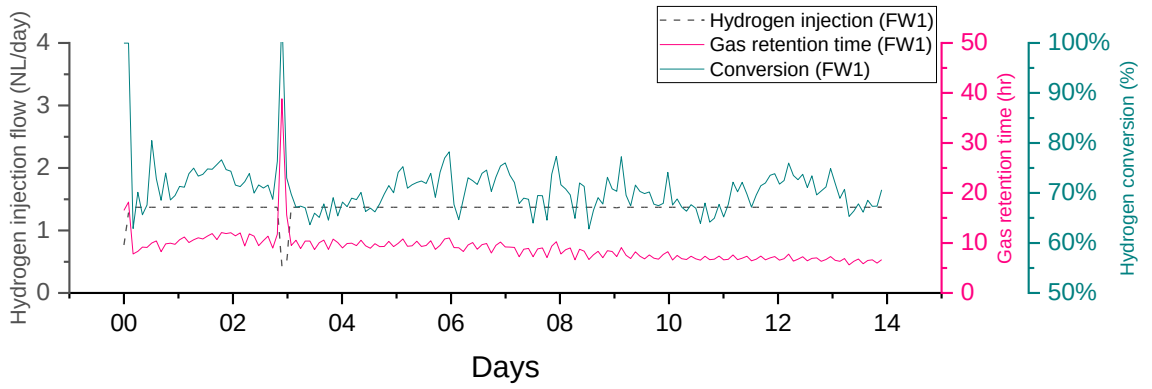

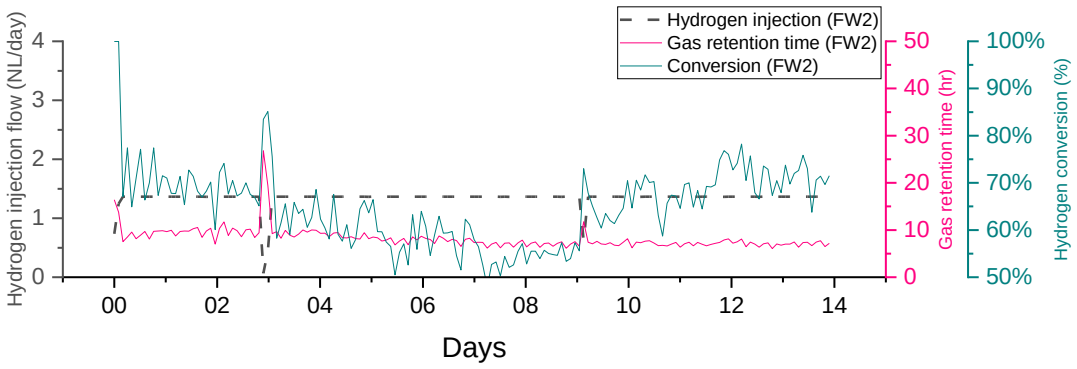

Figure 5-20. Hydrogen conversion in relation to gas retention time and hydrogen injection during in-situ biomethanation of food waste at gas recirculation 20 rpm.

In Figure 5-20, around 70.6 % (FW1) and 64.6 % (FW2) of hydrogen are consumed during this period, and by the end of the period, the hydrogen content was recorded at 18.8 % (FW1) and 20.2 % (FW2) with the methane contents being 60.9 % (FW1) and 61.9 % (FW2). This is interesting because even though FW1 has a higher hydrogen conversion and a lower hydrogen level at the end of the period, the methane content in the FW1 is lower than in the FW2. This is because the average OLR on FW1 was slightly higher than the FW2, making higher biogas production compared to the FW2. Therefore, the amount of CO_2 produced in FW 1 was higher than in FW2, making a higher chance of hydrogen conversion in FW1 as H2 content was recorded lower in FW1 than FW2. A slightly higher methane content on FW2 may be due to the dilution effect as lower hydrogen conversion resulting higher hydrogen unconverted, contributing to overall gas composition in the headspace.

5.4.2 In-situ biomethanation using food waste as substrate at a recirculation rate of 120rpm (R_{120}_FW)

This experiment was run for nine days, and there was a technical problem on FW1 on day 4 that resulted in the experiment being unable to be continued. For this reason, the report of FW1 was only based on the data in the first 4 days.

The ammonia level at the end of the previous period (R_{20}_FW) was recorded at 4 gTAN kg^{-1} on the reactor control FW, and it was found to be even lower on the reactor with the hydrogen injection at around 3.6 gTAN kg^{-1}. As a reference, the ammonia level of the digestate in the previous experiment (Chapter 4) was found to be stable at around 3.6 gTAN kg^{-1}. Referring to the ammonia level at the end of the previous period (R_{20}_FW), the OLR

then increases to 2gVS L^{-1} day^{-1}. By increasing the OLR, the daily hydrogen requirement also has to be increased; an increase of OLR results in the average specific carbon dioxide yield increasing to 0.215 LCO_2 gVS^{-1} $L^{-1}day^{-1}$. This makes the hydrogen injection setpoint (GH_2_sp) have to be set at 1.9 ml/min.

The average OLR on each reactor was recorded at 1.70 gVS L^{-1} day^{-1} (reactor control FW), 1.88 gVS L^{-1} day^{-1} (FW1), and 1.63 gVS L^{-1} day^{-1} (FW2), see Figure 5-21. The average gas output flow was recorded at 1.6 NL day^{-1} on the reactor control FW, while in the biomethanation reactor, FW1 and FW2 have a higher gas outflow with 18-19 % higher compared to the reactor control FW. The feedback control influenced the hydrogen injection rate with an average flow of 2.31 and 2.25 NL day^{-1} on FW1 and FW2, respectively. Nevertheless, the hydrogen being injected still covers around 90 % of the desired amount of hydrogen injection.

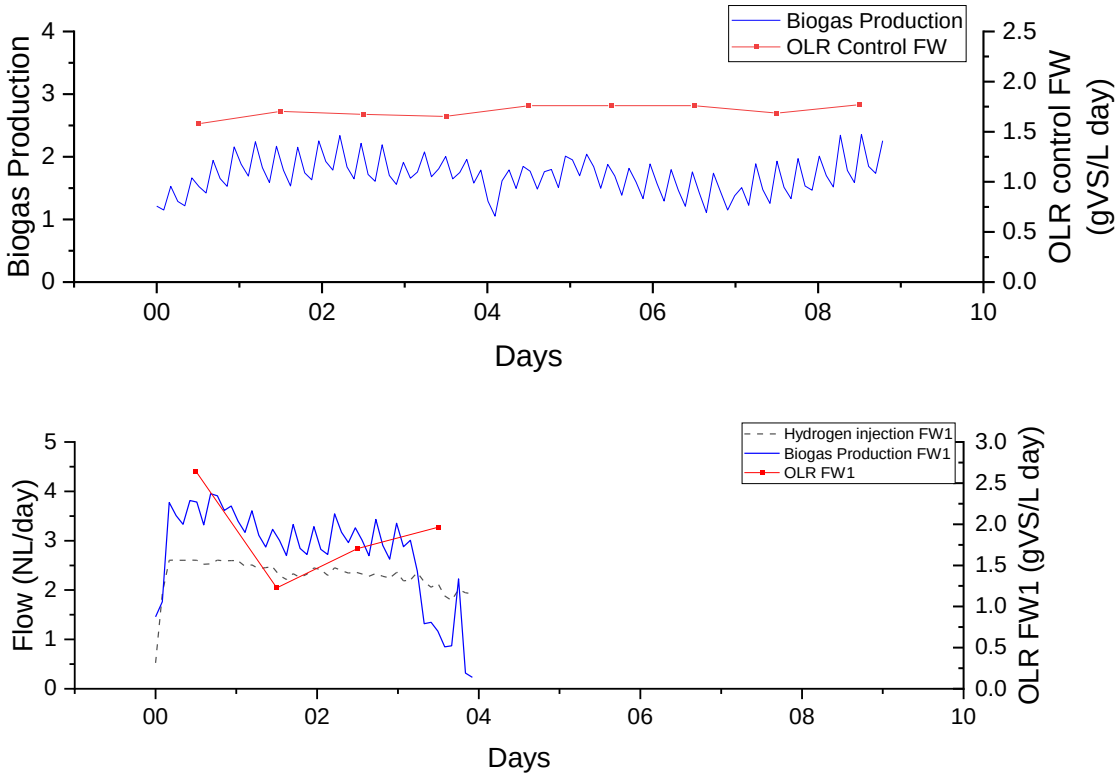

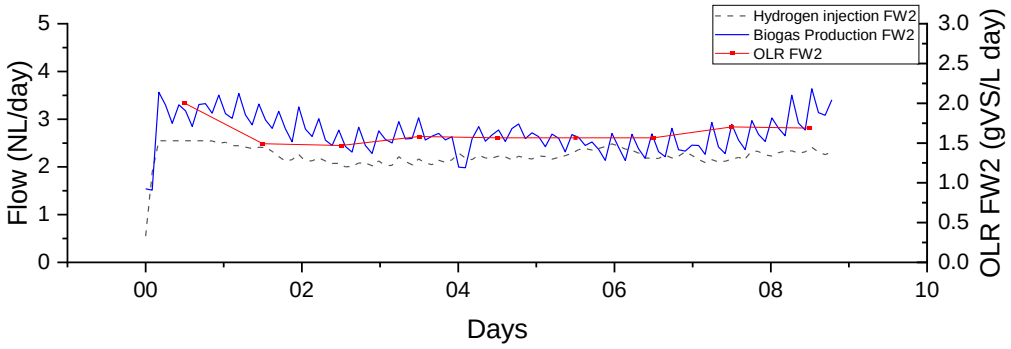

Figure 5-21. Gas flows, OLR, and hydrogen injection rate from in-situ biomethanation of food waste, at a gas recirculation rate of 120rpm. FW: control reactor; FW1 and FW2 duplicate biomethanation reactors.

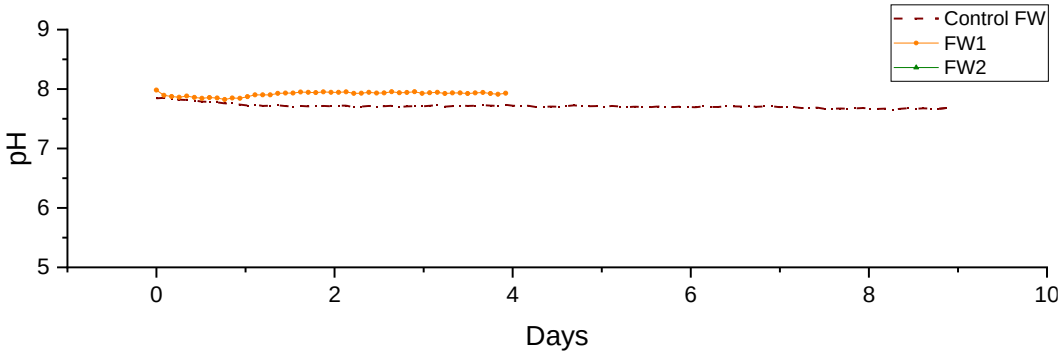

Figure 5-22**.** The pH profile during in-situ biomethanation of food waste at a gas recirculation 120 rpm.

In Figure 5-22, the pH value is more stable in this period when compared to the previous period at 20 rpm. The pH of the control FW was stable at pH 7.71; as expected, the pH with hydrogen injection was higher than the reactor control FW. The pH on reactor FW1 was stable at pH 7.86. Unfortunately, the pH data on reactor FW2 cannot be shown due to inaccurate reading. The investigation by the end of the experiment shows that the pH probe was covered by the biofilm that substantially affected the reading. However, the manual pH measurement shows that the pH on the FW2 was quite similar to the pH on the FW1, around 7.8.

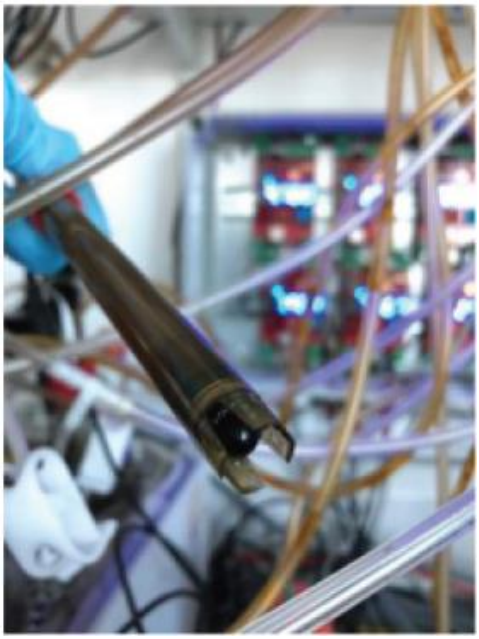

Figure 5-23. Photograph of the pH probe covered by the biofilm on the FW2 at period R_{120}_FW

Even though the FW1 was run for a very short period, the performance of the gas compositions shows to be stable and almost similar to the gas composition on the FW2. The gas compositions in the controls FW, FW1 and FW2 appear to be stable during the observation, with an average methane composition of 47.96 % (FW1) and 49.67 % (FW2), see Figure 5-24. The hydrogen content in the headspace is observed to be close to the limit of the constraint. The average concentration of hydrogen in the headspace in the FW1 was recorded at 32.82 %, and in the FW2 at 33.56 %, it was found that hydrogen concentration in both reactors was stable at around 33 %. As seen in Figure 5-21, the hydrogen injection flow was oscillating in both reactors, which means that the feedback control was activated. The first sign of the activation in the feedback control was detected on the FW1 when the hydrogen content reached 33.7 %. According to the feedback control formula, the feedback control will be activated when the hydrogen in the headspace becomes more than 33.6 %. The activation of the feedback control due to the pH will only be activated when the pH reaches 8.01 (k_pH value 10). On the other hand, it can be confirmed that the hydrogen injection that was influenced by the feedback control on the FW2 was only influenced by the change of hydrogen content since the pH is shown to be very low due to the pH probe malfunction, Figure 5-23.

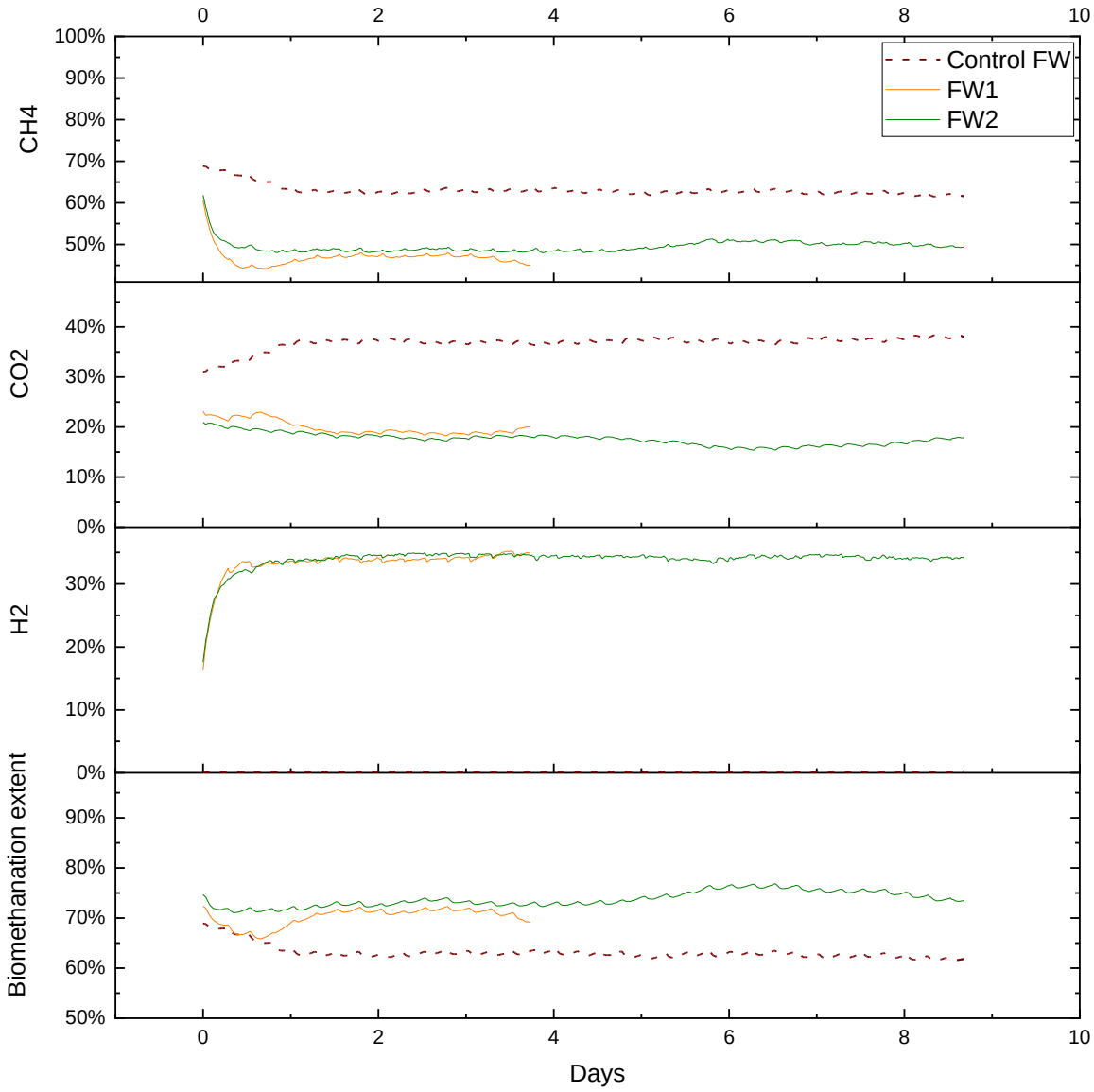

Figure 5-24 Gas composition and biomethanation extent during in-situ biomethanation of food waste at gas recirculation 120 rpm.

The methane content dropped to around 50 % in FW1 and around 45 % in FW2 since hydrogen was being injected. The methane content remained relatively stable at around 50 % in both reactors. The stability of the methane content corresponds to the hydrogen and carbon dioxide content, which were stable at around 20 % and 34 %, respectively. The maximum biomethanation extent on reactor FW1 reached 75 %, or around 15 % higher compared to the reactor control.

Figure 5-24 shows that the biomethanation extent was around 11 % on average on the FW2 and only 9 % on the FW1. On the other hand, the hydrogen conversion rate in the FW2 was maintained in a range between 50-70 %, with an average conversion of 59.71 %, see Figure 5-25. There is no significant change to the biogas flow and the gas retention time appears to be stable at 0.4 days.

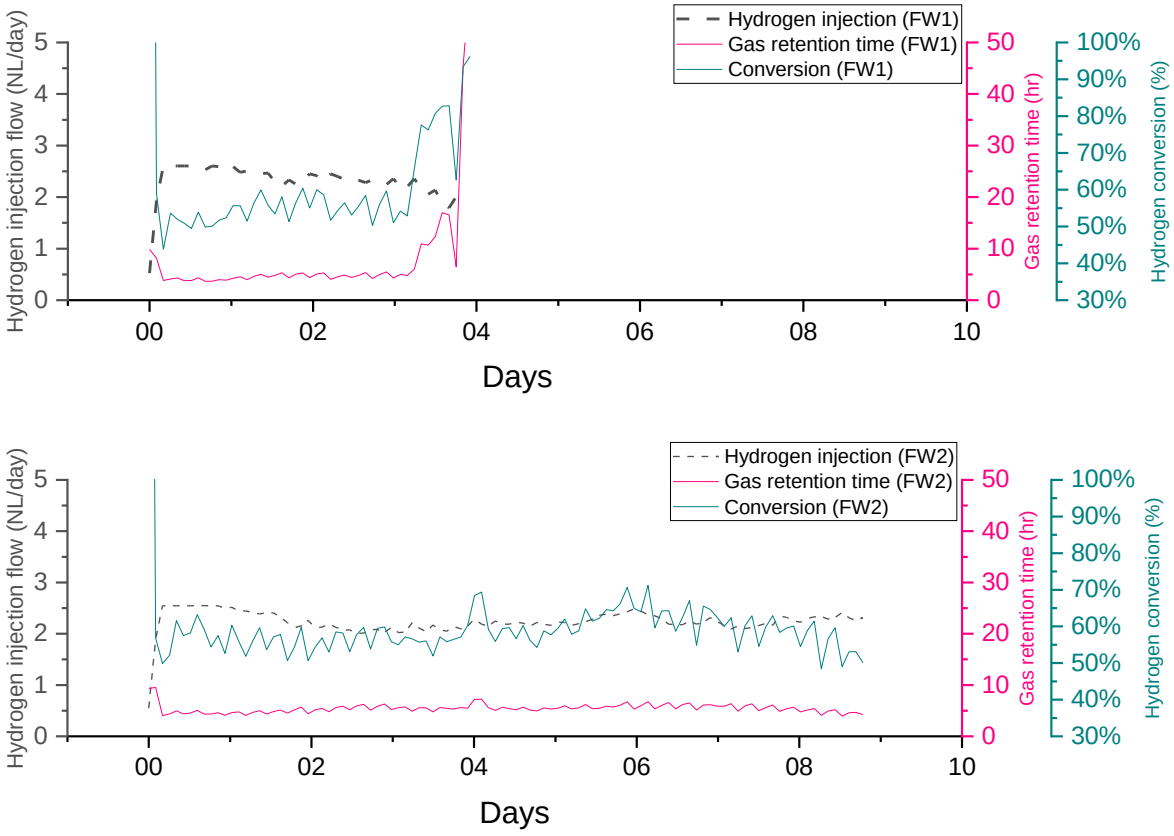

Figure 5-25 Hydrogen conversion in relation to gas retention time and hydrogen injection during in-situ biomethanation of food waste at recirculation 120 rpm

5.4.3 In-situ biomethanation using food waste as substrate at a recirculation rate of 280 rpm (R_{280}_FW)

The experiment in the period of recirculation rate 280rpm was observed for 21 days in all the reactors. The average OLR in reactor control FW and reactor biomethanation FW1 and FW2 were 2.04, 1.97 and 2.00 gVS L^{-1} day^{-1}, respectively. In Figure **5-26**, the gas output flow tends to be stable in all the reactors, with an average gas outflow of 2.47 NL day^{-1} (control FW), 3.47 NL day^{-1} (FW1), and 3.36 NL day^{-1}(FW2).

The average hydrogen injection rate in reactor biomethanation FW1 and FW2 were recorded at 2.49 and 2.54 NL day^{-1}. The hydrogen injection in reactor FW1 dropped on day 16 due to feedback control activation.

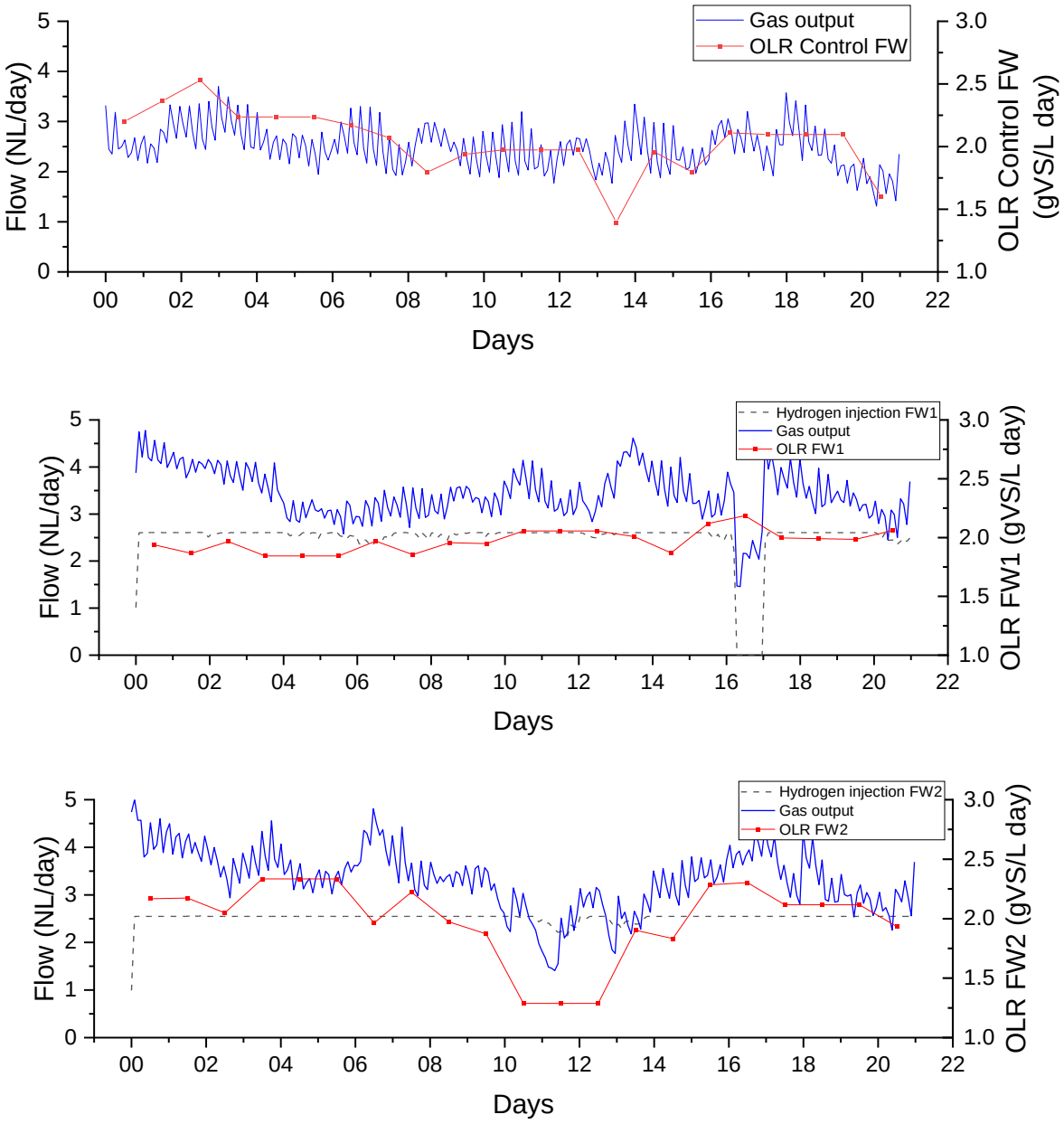

Figure 5-26 Biogas production of in-situ biomethanation in relation to gas retention time and hydrogen injection during in-situ biomethanation of food waste at a circulation of 280 rpm.

The pH profile was observed to increase relatively fast compared to the previous periods, see Figure 5-27. The initial pH in all the reactors was recorded to be around 7.7, and on the FW2, the pH increased from 7.7 to 8 in just one day. With this behaviour and the pH constraint of 8.2, the feedback control was possibly controlled by the pH, which is

undesirable. The pH constraint then increased to 8.7, and the kpH increased to 15 in order to allow the feedback control only to be controlled by the gas composition. With this constraint, the feedback control will be activated by the pH if the pH reaches at least 8.5. The maximum pH on the FW1 was recorded to be 8.07 and 8.39 on the FW2. According to the maximum pH on the FW1 and FW2, it shows that the pH did not control any hydrogen injection adjustment due to the feedback control.

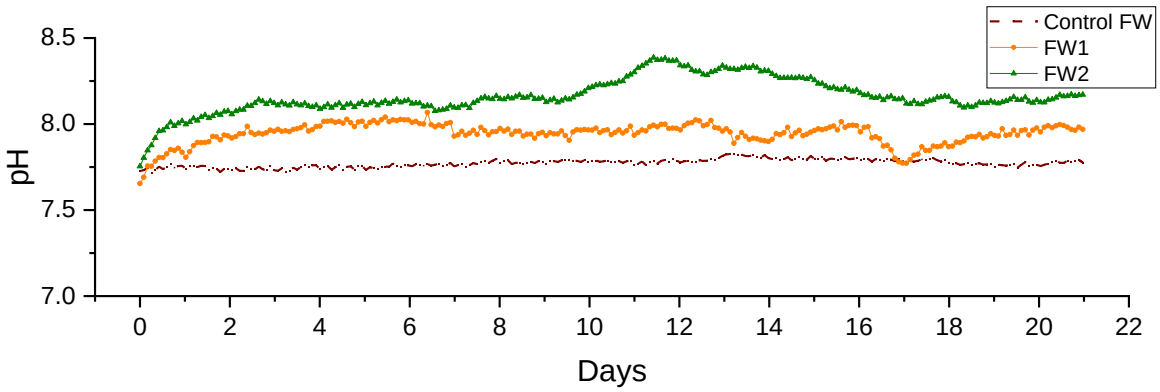

Figure 5-27 The pH profile during in-situ biomethanation of food waste at recirculation 280 rpm.

In this period, the methane and hydrogen content were observed to flatten out in less than one day since the hydrogen started to be injected into the reactors, see Figure 5-28. This behaviour was very similar to the previous period. The average methane content in the FW1 was slightly lower than in the FW2, while the hydrogen content was observed to behave the opposite way. The average methane content was recorded at 48.4 % on the FW1 and 53.2 % on the FW2. On the other hand, the average hydrogen content was recorded at 28.15 % on the FW2, while the average hydrogen content on the FW1 was 32.1 %. At some moment, the high hydrogen content proportionally changed the hydrogen injection flow by activating the feedback control. According to the feedback control setting parameter, the hydrogen injection flow was activated when the hydrogen content reached 33.6 %.

The hydrogen content on the FW1 was recorded to be quite high since the hydrogen was injected. This is only required for two days on the FW1 to activate the feedback control when the hydrogen in the headspace reaches 33.65 %. On the FW2, the hydrogen injection was able to be maintained at the setpoint until the feedback control was activated on day 11. The level of the hydrogen content in the FW1 appears to be stable, but unfortunately,

it is near to the hydrogen constraint. Therefore, the hydrogen injection was observed to fluctuate more when compared to the FW2.

On day 16, for some reason, the SCADA could not read the gas analysis on each stream, and this was the same situation that happened at R_{280}_SS. Therefore, the gas composition could not be updated for almost one day. Unfortunately, this produced an error in the reading function of the SCADA, which stopped the hydrogen injection on the FW1. According to the feedback control parameter, there are no reasons why the feedback control was activated according to the last gas composition read by the SCADA. The last hydrogen content read by the SCADA on the FW1 was 33.11 %, and with this value, the feedback control should not be activated, moreover was set to zero. With no hydrogen injection, was resulting hydrogen reduced to 0.99 %, CO_2 increased to 27.99 %, and CH_4 increased to 70.95 %. An increase in CO_2 signified that the amount of H_2 could not keep up with the amount of CO_2. One day after the hydrogen injection restarted, the gas compositions were returned to almost similar gas compositions as those before hydrogen stopped being injected.

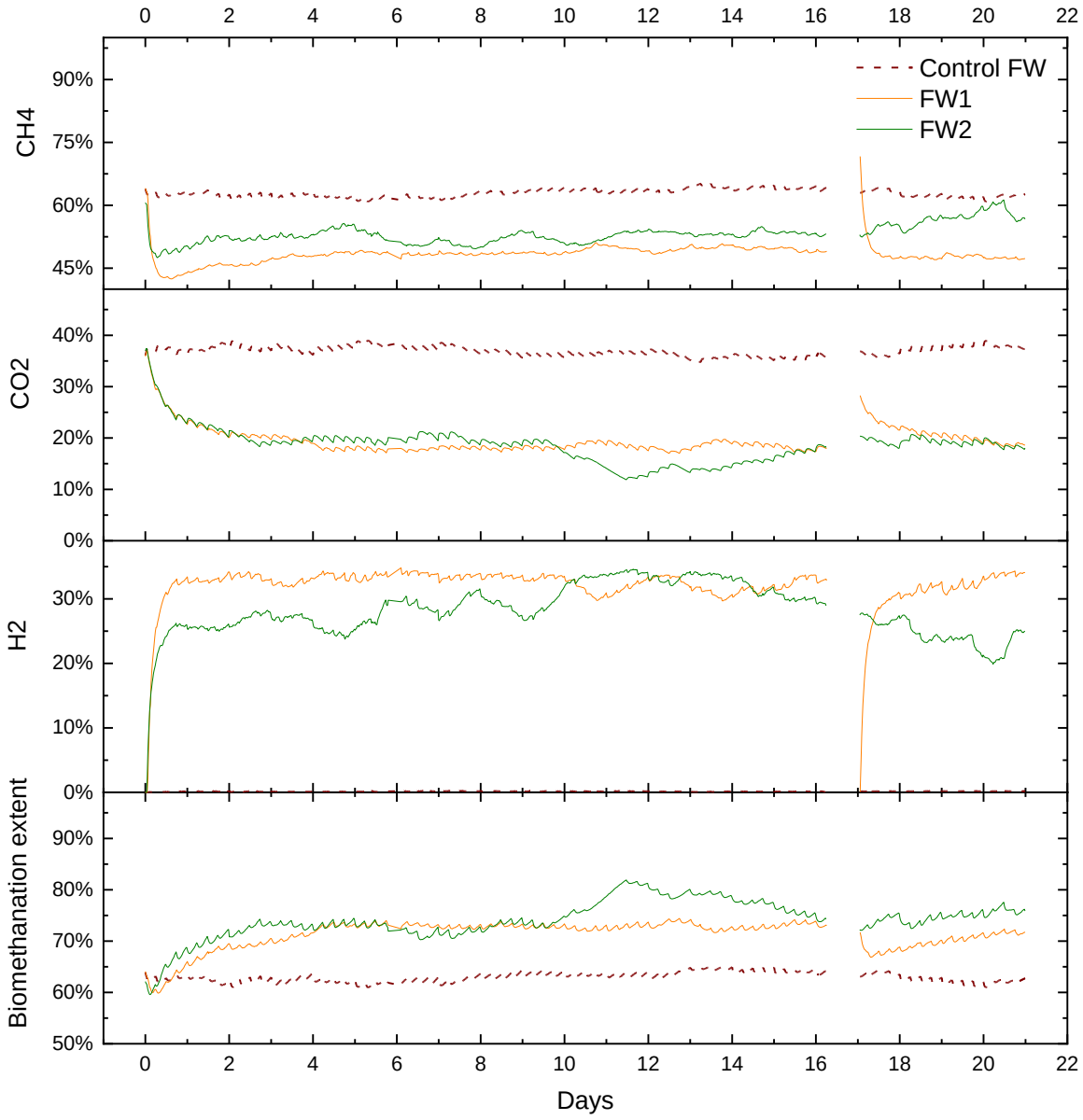

Figure 5-28 Gas composition and biomethanation extent during in-situ biomethanation of food waste at gas recirculation 280 rpm.

The hydrogen conversion was observed to be stable and maintained within a range of 45 % to 80 % for both the reactors, with an average conversion of 54.5 % on the FW1 and 63.5 % on the FW2, see Figure 5-29. The hydrogen conversion on the FW2 was higher compared to that on the FW1. This trend can also be seen in the biomethanation extent related to the methane enrichment, where the average biomethanation extent on the FW1 is 68.8 %, and on the FW2, it was 72.9 %.

The maximum hydrogen conversion on the FW 1 reached 66 %. However, more than 100 % conversion was achieved when the hydrogen injection was restarted. For most of the time, the retention time in both reactors was very similar.

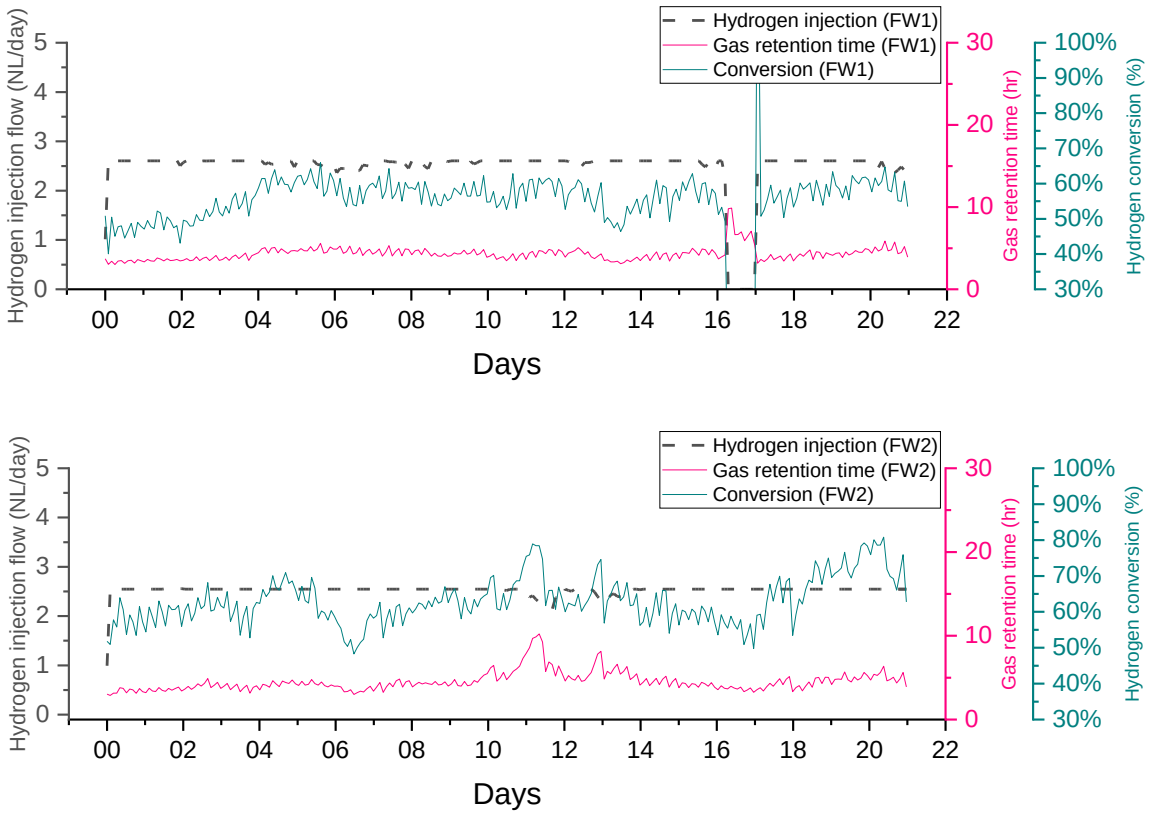

Figure 5-29 Hydrogen conversion in relation to gas retention time and hydrogen injection during in-situ biomethanation of food waste at a recirculation of 280 rpm.

5.4.4 The effect of recirculation rate on in-situ biomethanation using food waste

A summary of the in-situ biomethanation using food waste at different recirculation times can be seen in Table 5.3. In general, there are no differences in the effect of the recirculation rate on the in-situ biomethanation process between the sewage sludge and food waste.

In this set of experiments, the result in the in-situ biomethanation process was slightly influenced by the ammonia inhibition at the beginning of the experiment. However, it was found to be at a stable level by the end of the period R_{20}_FW. The ammonia level may influence the performance of the in-situ biomethanation, as Banks et al. (Banks *et al.*, 2012a) reported that the hydrogenotrophic methanogens could replace the role of the acetoclastic methanogen when the ammonia level reaches more than 500 mg/L. On the

other hand, it was reported that the synergetic between the syntrophic acetate oxidation and the hydrogenotrophic methanogens are more robust on acetate degradation at high ammonia levels (Wang *et al.*, 2013; Krakat *et al.*, 2017). Even though the process was slightly influenced by higher ammonia content, it can be seen that the effect of increasing the recirculation rate can be observed clearly. Similar to the sewage sludge, the positive result of improved hydrogen conversion was also shown in the increasing recirculation rate.

The hydrogen content was observed to be stable at a higher level in the food waste digester compared to the sewage sludge digester. The feedback control often makes an adjustment to the hydrogen injection flow in order to reduce the hydrogen level and increase the methane content. Overall, the hydrogen is maintained at a level that is very close to the hydrogen constraint, namely around 30 %, for most of the time in all periods. On the other hand, the methane was down at around 48 % from around 62 % before the hydrogen injection. This is quite significantly different from the result when using sewage sludge, where the methane in the reactor with hydrogen injection reached almost similar to the methane content in the reactor control.

The average hydrogen conversion in the R_{20}_FW was relatively higher compared to the R_{120}_FW and R_{280}_FW. This is because the OLR in the period R_{20}_FW was lower than in other periods, which increases the retention time in period R_{20}_FW, which also increases the contact time between the gas and microorganism and leads to the hydrogen conversion. For example, in Figure 5.3, it can be seen that the retention time in the R_{20}_FW is 26 % higher than in period R_{120}_FW.

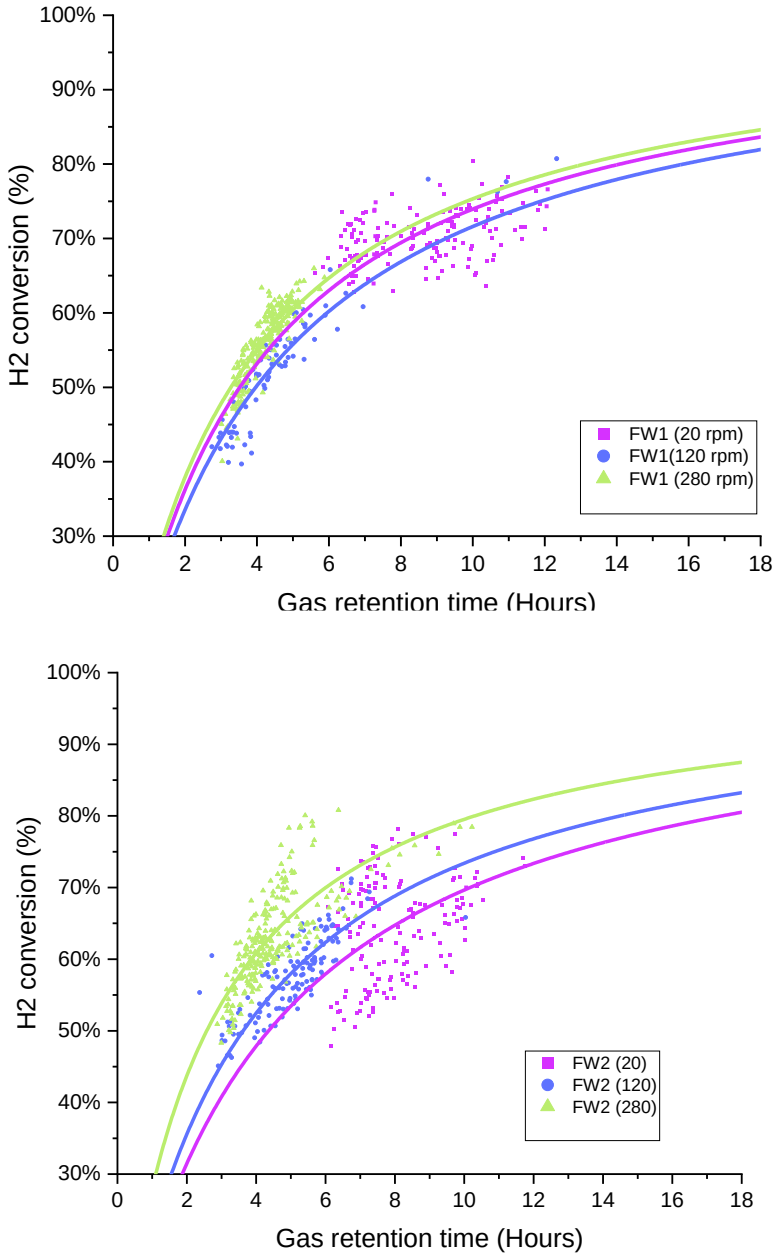

Figure 5-30 Scatter plot of the retention time and hydrogen conversion on different retention times on the FW1 and FW2.

A side-by-side comparison between R_{120}_FW and R_{280}_FW shows that the increase in the retention time does not give a significant improvement in the hydrogen conversion or the methane evolution rate (MER). However, increasing the recirculation rate increased retention time as an effect of higher conversion of hydrogen, which can be seen in Figure 5-30. The distribution of the retention time on the R_{120}_FW was higher than R_{280}_FW for both FW1 and FW2. Ideally, a higher retention time increases the hydrogen conversion. In

this case, the improvement in the increasing recirculation rate was not as high as observed in the sewage sludge, see Figure 5.13. However, with a shorter retention time, a higher retention time at 280rpm could give a similar conversion with the recirculation at 120 rpm. The performance between the R_{120}_FW and R_{280}_FW was not influenced by the different ammonia levels because the ammonia content was monitored to be stable at around 3.6 gTAN kg^{-1} in both periods.

The intake of bicarbonate due to injection is not too significant in the R_{20}_FW as the pH in the FW1, and FW2 was slightly increased compared to the control. The highest increase in the pH was observed at R_{280}_FW, where the pH was able to reach more than 8.

In Table 5.3, the biogas production or total gas out in periods R_{280}_FW was higher than in periods R_{20}_FW and R_{120}_FW. As discussed in section 5.4.1, at the beginning of the experiment in period R_{20}_FW, the digestate experienced high ammonia content that caused inhibition in the biogas production as confirmed by the value of alkalinity ratio and total VFA in period R20_FW is the highest compared to other periods. The inhibition may slightly influence period R120_FW as biogas production is not significantly different compared to period R20_FW as confirmed by the average alkalinity ratio, which is still around 0.5, while the healthy anaerobic digestion process was recommended to be able to maintain the alkalinity ratio around 0.3 (Martín-González, Font and Vicent, 2013).

Table 5.3 Summary of in-situ biomethanation using food waste at different recirculation rates.

		Recirculation at 20 rpm			Recirculation at 120 rpm			Recirculation at 280 rpm		
		Control	FW1	FW2	Control FW	FW1	FW2	Control FW	FW1	FW2
Time	Days	14	14	14	9	4	9	21	21	21
Hydrogen injection flow setpoint	ml/min		0.96	0.96		1.79	1.79		1.79	1.79
Average OLR	gVS/ L day^{-1}	0.94	1.35	1.31	1.70	1.88	1.63	2.04	1.97	2.00
Actual hydrogen Injection supplied	L day^{-1}		1.36	1.35		2.31	2.25		2.49	2.54
Total gas out	L/gVS	0.59	0.75	0.83	0.58	0.89	0.99	0.71	1.04	0.99
Specific CH_4 production rate	L/gVS	0.38	0.40	0.42	0.36	0.42	0.48	0.45	0.50	0.53
Specific CO_2 in output gas	L/gVS	0.20	0.17	0.19	0.21	0.42	0.48	0.24	0.18	0.18
Hydrogen consumption rate	L day^{-1}		0.96	0.87		1.39	1.35		1.38	1.60
H_2 Conversion	%		70.6	64.66		60.02	59.71		56.26	63.7
Average retention time	hr		11.1	10.15		7.83	5.29		9.88	10.23
Methane evolution rate (MER)	L/L$_r$ day		0.13	0.12		0.20	0.20		0.19	0.22
Average pH		7.6	7.66	7.63	7.71	7.86	n.a	7.77	7.94	8.16
Average CH4	%	63.83	52.7	50.86	62.45	47.96	49.67	61.82	48.45	53.18
Average CO2	%	35.09	24.2	23.82	36.33	20.26	17.67	36.36	19.56	18.64
Average H2	%	0.10	23.1	25.50	0.12	32.82	33.56	0.16	32.11	28.15
Average TS	[gTAN/kg$_{sub}$	4.43	4.25	4.13	3.8	3.62	3.50	3.66	3.69	3.60
Average VS	%	2.73	2.80	2.73	2.38	2.29	2.24	2.82	2.46	3.14
Average Ammonia	%	1.44	1.88	2.05	1.59	1.55	1.58	2.02	1.69	1.75
Average Alkalinity ratio		0.63	0.77	0.78	0.39	0.35	0.34	0.33	0.29	0.28
Average Acetate	g kg$_{sub}^{-1}$	0.64	1.31	1.53	0.47	0.53	0.51	0.37	0.34	0.48
Average total VFA	g kg$_{sub}^{-1}$	1.30	2.07	2.26	0.80	0.86	0.83	0.89	0.86	0.98

5.5 Process optimisation of in-situ biomethanation to improve the gas-liquid mass transfer on the sewage sludge digester

Further improvement in the process optimisation is still focused on increasing the gas-liquid gas transfer. In the next periods, another strategy explored was the employment of an additional sparger on the recirculation line, thus increasing the mixing rate and reducing the OLR.

The process optimisation evaluation was divided into three periods on sewage sludge and food waste digesters, with one reactor control and two reactors with hydrogen injection. The overall configuration is still similar to the previous experiment but with a little modification or change. In all the periods, the reactor was set to have a similar recirculation rate of 120 rpm.

The use of the sparger, as discussed in chapter 4, shows that adding the sparger to the hydrogen injection could increase the hydrogen conversion and lead to higher methane evolution rates. In the previous experiment, the sparger was placed only at the hydrogen injection line, while on the recirculation line, it only used a simple tubing without the sparger. Therefore it was realised that this is something that could be improved to increase the gas-liquid mass transfer. For that reason, in the first period (OP1), an additional sparger with a 10 µm pore size was placed at the end of the recirculation tube in order to reduce the bubble size on the recirculation line. In the second period (OP2), the effect of increasing the mixing rate was explored as another strategy to improve the gas-liquid mass transfer. Therefore, the mixing rates were increased from 60 rpm to 110 rpm during OP2 in order to increase gas-liquid mass transfer. The higher biogas flow and hydrogen injection could give a flushing effect, where the hydrogen or biogas are flushed out before they are converted. For that reason, another strategy was to reduce the OLR in order to reduce the biogas production flow as well as the hydrogen injection flow rate. With the lower flow, the gas retention time increases, which was expected to produce a higher conversion rate of hydrogen. Therefore, in the third period (OP3), the OLR in all the reactors were reduced to 1 gVS L^{-1} day^{-1}. In brief, the detailed settings in each period are presented in Table 5.4

Table 5.4 Experiment parameters in the process optimisation.

	OP1_SS	OP2_SS	OP3_SS	OP1_FW	OP2_FW	OP3_FW
Feedstocks	Sewage	Sewage	Sewage	Food	Food	Food
Recirculation rate	120 rpm	120 rpm	120 rpm	120 rpm	120 rpm	120 rpm
Additional sparger	10µm	10µm	10µm	10µm	10µm	10µm
Mixing rate	60rpm	110rpm	110rpm	60rpm	110rpm	110rpm
OLR gVS L^{-1} day^{-1}	2	2	1	2	2	1

There was no significant difference in CO_2 production in this period compared to the previous periods. In addition, the hydrogen injection and feedback control parameters were set to be almost at the same value as mentioned in Table 5.1. The only update was the constraint on the pH value by increasing the constraint to 8.7, and the k value was 15, as seen in Table 5.5. This setting is also applied to the reactor that uses food waste as a substrate. The average biogas production before the hydrogen injection was recorded at 0.492, 0.433 and 0.474 L/gVS, and the average methane concentration in all the reactors was around 68.5 % and 29.5 % for the carbon dioxide.

Table 5.5 Update of the feedback control parameters.

	Unit	Setpoint and constrains	Proportional control parameter (k)
CH4	%	90	0.3
CO2	%	5.0	0.3
H2	%	40	0.3
pH		8.7	15

5.5.1 Effect of an additional sparger on the recirculation line using sewage sludge (OP1_SS)

The experiment was observed for 19 days. The average OLR on the reactor control was 1.94 gVS $L^{-1}day^{-1}$, Figure 5-31. The feeding supply was relatively stable in all reactors, except for one moment when the OLR dropped to 1.5 gVS L^{-1} on the SS1 and 1 gVS L^{-1} on the SS2, due to feeding pump malfunction. The average OLR was recorded at 1.85 gVS $L^{-1}day^{-1}$ (SS1) and

1.79 gVS $L^{-1}day^{-1}$ (SS2). The hydrogen injection remained fairly stable at its setpoint value. The hydrogen injection was influenced by the feedback control on day 13 in biomethanation reactor SS2, which resulted in the average hydrogen injection in reactor SS2 being slightly lower than reactor SS1 with 1.44 L day^{-1}, while in reactor SS1 was 1.46 L day^{-1}.

The feedback control was activated due to the carbon dioxide level. The carbon dioxide content was recorded at 8.69 %, and according to the feedback control parameter for the CO_2, the feedback control was activated when the carbon dioxide level fell below 8.76 %. The effect of the feedback control activation was shown when the hydrogen content decreased on day 13. In Figure 5-33, the hydrogen content is observed to decrease as the effect of the reducing flow of hydrogen injection, along with the methane content being increased.

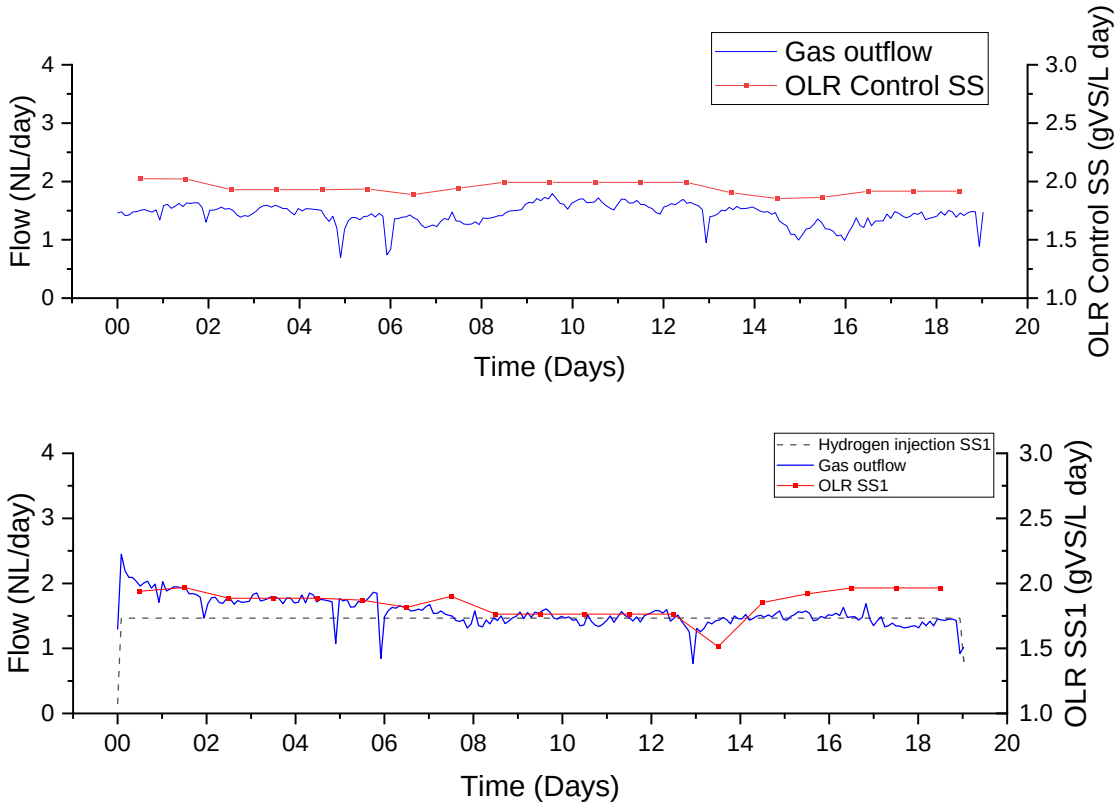

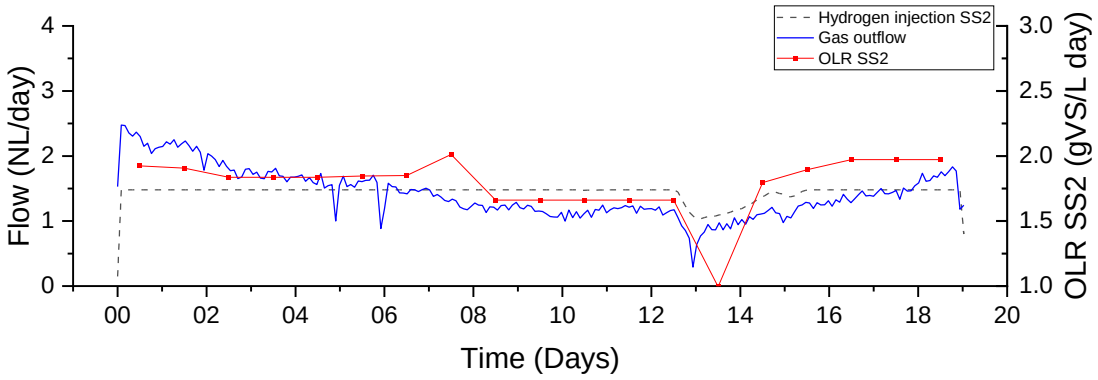

Figure 5-31 Gas flows, OLR, and hydrogen injection rate from in-situ biomethanation of sewage sludge, at gas recirculation rate of 120rpm and with additional sparger on recirculation line. SS: control reactor; SS1 and SS2 duplicate biomethanation reactors.

The initial pH in reactor control SS and biomethanation reactor SS1 were around 7.4. The initial pH on the SS2 was slightly higher at a value of 7.5 see Figure **3-2**. The pH increased shortly after the start of the hydrogen injection. The pH value on reactor SS2 was recorded higher than reactor SS1 throughout the experiment and reached the maximum pH at 8.2 on reactor SS2, while in reactor SS1 was 8. The higher pH value on reactor SS2 was also reflected by the slightly lower CO_2 content than in the reactor SS1.

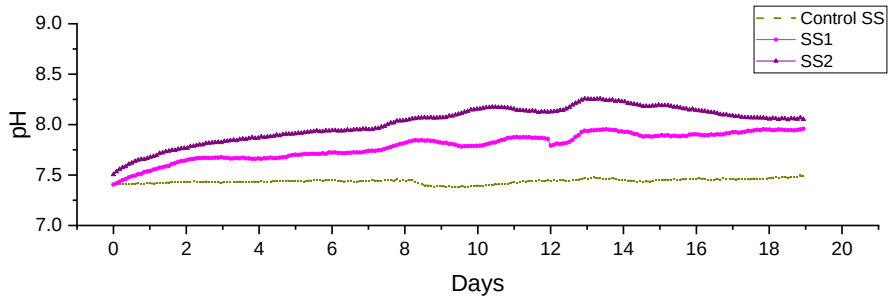

Figure 5-32 The pH profile during the in-situ biomethanation of sewage sludge on the additional sparger

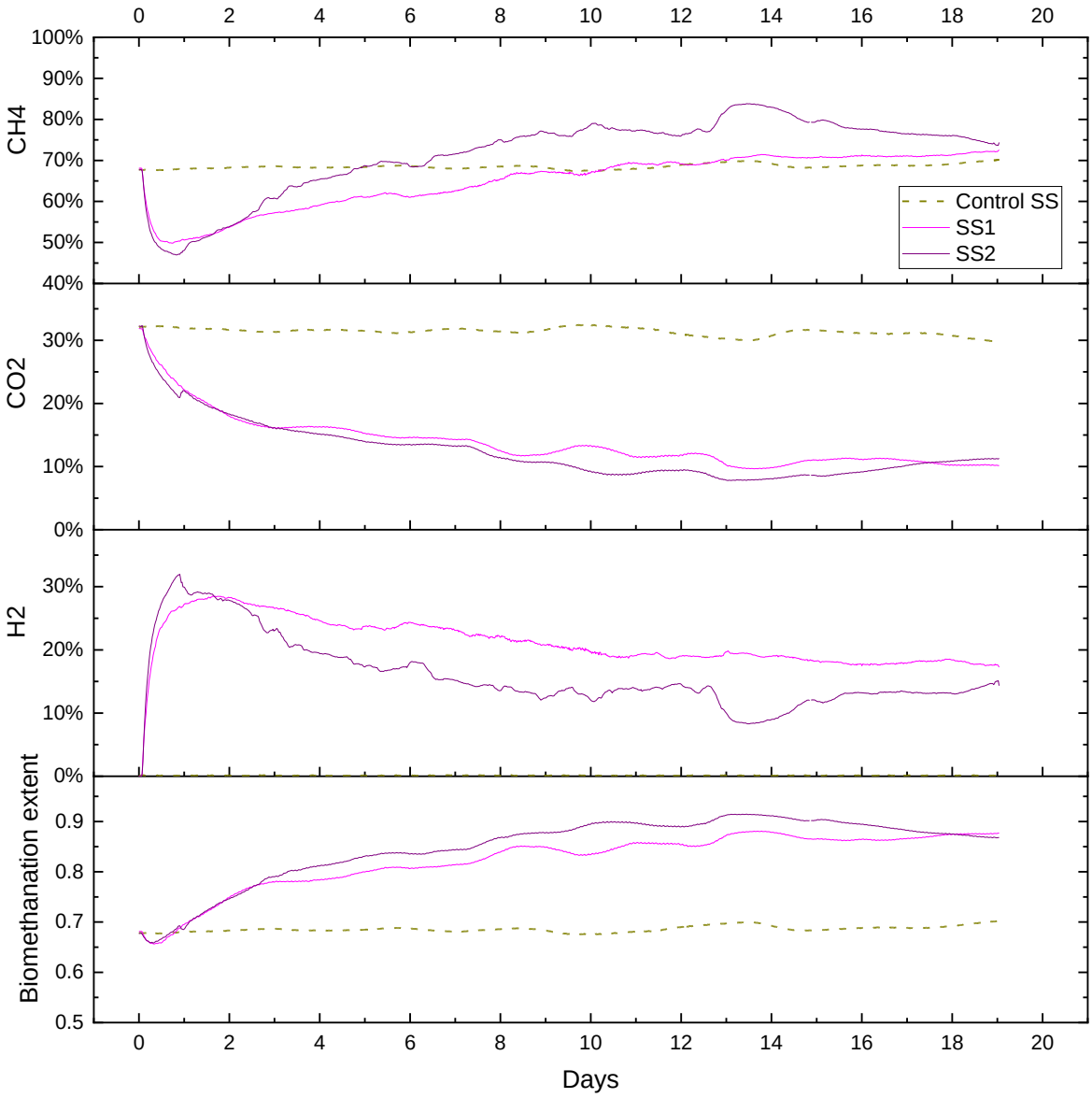

Figure 5-33. Gas composition and biomethanation extent during in-situ biomethanation of sewage sludge with additional sparger.

The biogas composition in the reactor control SS was stable during the experiment, and it maintained the methane content at an average of 68.5 % and the CO_2 at 31.3 %, see Figure 5-33. When the hydrogen was injected into the reactor, the hydrogen content increased straight away, reaching 31 % on the SS2 in less than one day before it slowly decreased. In the reactor SS1, the maximum hydrogen that could be achieved was around 28.5 % between day one and day two. The hydrogen content then was observed to be faster on the SS2 compared to the SS1, along with the increase in the methane content. However, there was not much difference in the carbon dioxide content, and the carbon dioxide was

stabilised in both the reactors after day 10. The biomethanation extent value shows that the effect of the additional sparger on the recirculation line could enrich the methane up to 17.5 % on the SS1 and 20.4 % on the SS2 compared to the reactor control with the biogas extent found similar in both biomethanation reactors at 87 %.

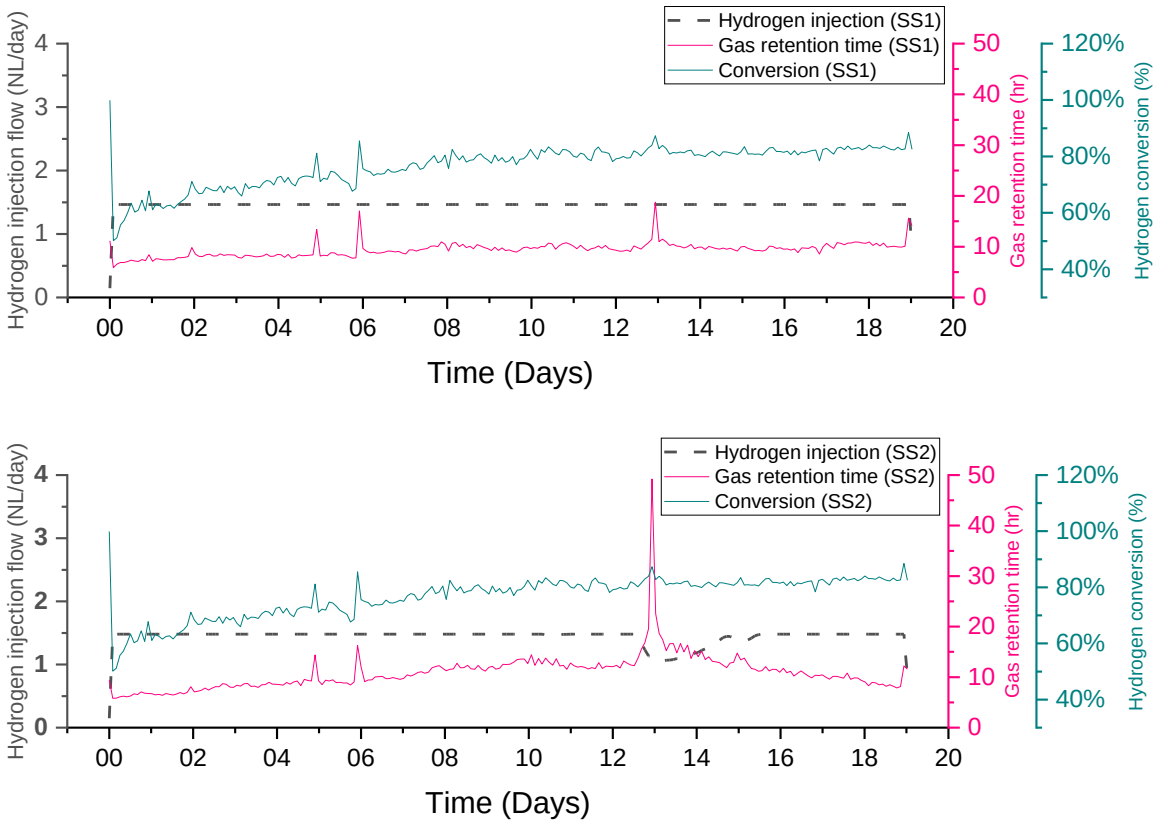

Figure 5-34 Hydrogen conversion in relation to the gas retention time and hydrogen injection during the in-situ biomethanation of sewage sludge with the additional sparger.

Having a higher methane enrichment on the SS2 was also confirmed by the higher conversion that was recorded. In the last seven days, the average hydrogen conversion on the SS2 was 88 %, with a maximum hydrogen conversion that was able to be achieved is 97 %. On the other hand, the average hydrogen conversion on the SS1 was 82 %, with a maximum of 88 % (see Figure 5-34).

5.5.2 Effect of additional sparger on the recirculation line and increased mixing rate using sewage sludge (OP2_SS)

Another strategy to improve the gas-liquid mass transfer is to increase the mixing rate in the reactor. In this period, the mixing rate was increased from 60 rpm to 110 rpm in order

to explore the effect of the higher mixing rate. The experiment was operated for 20 days. The feeding was quite stable during the experiment, with an average loading rate of 2.21 gVS $L^{-1}day^{-1}$ (control SS) and 2.07 gVS $L^{-1}day^{-1}$ (SS1). Unfortunately, the reactor SS2 experienced high alkalinity on day 7, with the alkalinity ratio (IA/PA) increasing to 0.8. The initial alkalinity ratio on the SS1 and SS2 was slightly higher than the control, which was 0.35 for the SS1 and 0.41 for the SS2.

In order to reduce the potential failure due to the high alkalinity ratio in the reactor SS2, the OLR was reduced to 1.5 gVS L^{-1} day^{-1}. Unfortunately, the alkalinity recorded the next day did not improve, and the alkalinity ratio increased to a value greater than 1. The OLR was then reduced again to 1 gVS L^{-1} day^{-1} and maintained at this value for about two days. On day 10, the alkalinity ratio was not recovered and was stable at 0.9. For this reason, we decided to terminate the hydrogen injection and maintain the OLR with 1 gVS/L for system recovery. However, until the end of the period, the alkalinity ratio on the SS2 did not improve, and it was only able to decline to 0.6. Therefore, the SS2 data that is shown in the summary table was for the data on the first ten days. Due to this issue, the data in biomethanation reactors cannot be performed in duplicate. Therefore, in the comparison summary, the data shows only used the data obtained on reactor SS1.

The hydrogen injection in reactor SS1 was relatively stable, with an average hydrogen injection rate of 1.45 L day^{-1}. On the other hand, the hydrogen injection was stopped on reactor SS2 on day 9.

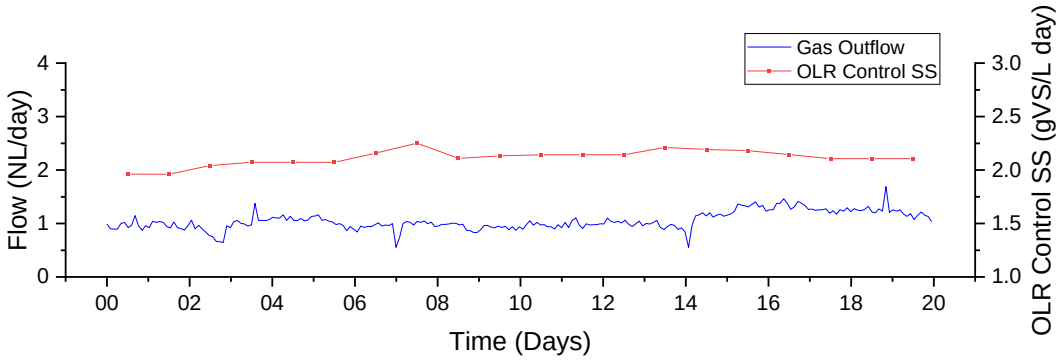

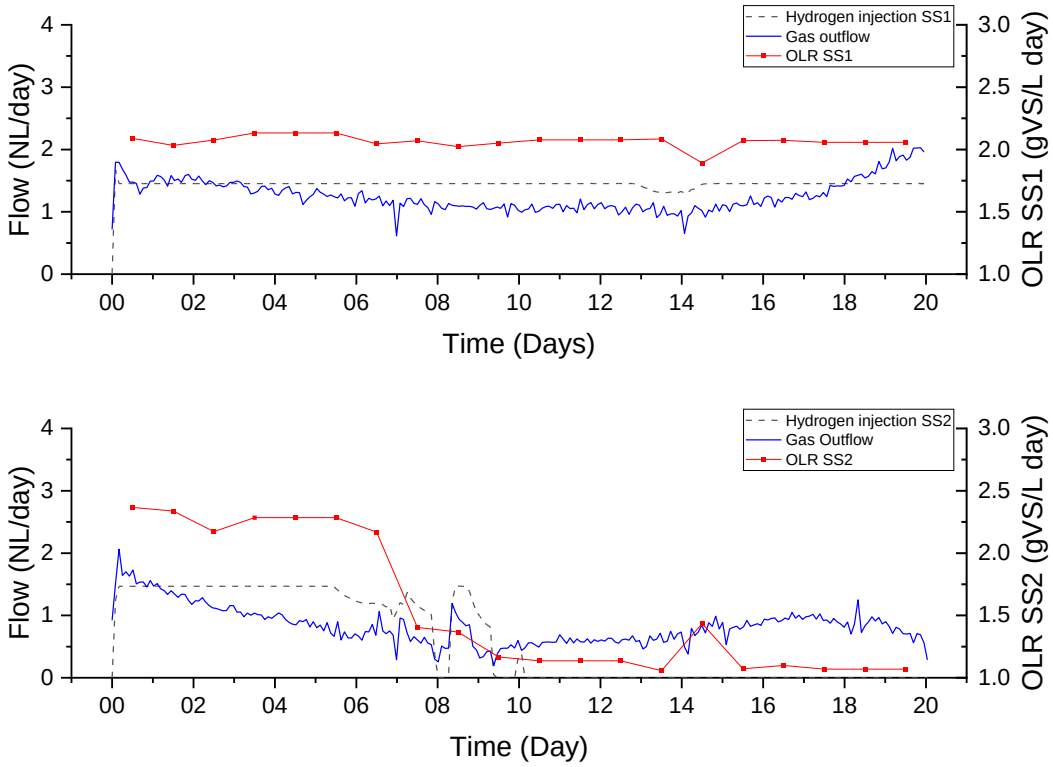

Figure 5-35 Gas flow, OLR and hydrogen injection from in-situ biomethanation of sewage sludge, at gas recirculation rate of 120rpm and with additional sparger on recirculation line, and higher mixing rate. SS: control reactor; SS1 and SS2 duplicate biomethanation reactors.

In Figure 5-37, the hydrogen content in the SS2 declined faster than the SS1, in line with the higher hydrogen conversion during that time as the methane content also increased. Due to the bicarbonate buffering system, the level of carbon dioxide did not change rapidly, but it continued to reduce down to 8 % on day 6. From the pH point of view, the pH on the SS2 increased as soon as the hydrogen injection started but was still lower than the control value. Regarding the high alkalinity ratio at the beginning of the experiment, it was expected that the digester was influenced by the high acetate accumulation Table 5.6 and also indicated by the low pH profile on the SS2. The hydrogen injection into the reactor may increase the instability in the system due to the high consumption of carbon dioxide, as we can see from the higher conversion on the SS2 compared to the SS1.

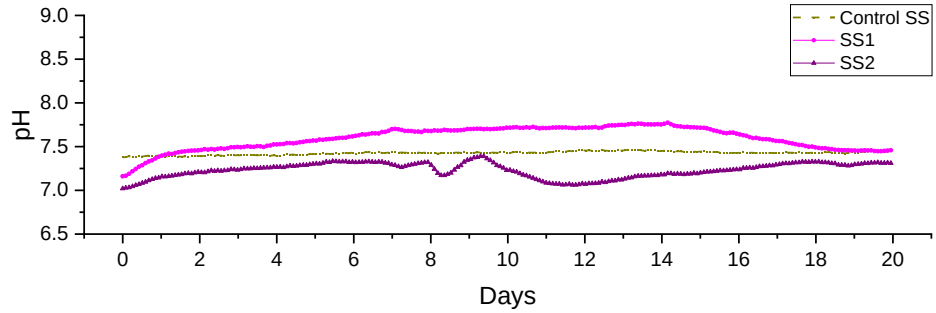

Figure 5-36 The pH profile during the in-situ biomethanation of food waste on the additional sparger and higher mixing rate.

The initial pH for the SS1 and SS2 was slightly higher than the control SS, see Figure 5-36. The pH profile on the control was stable during the experiment, with the average pH being 7.42. The pH on SS1 increased gradually to the maximum pH of 7.7 but then slowly declined to a similar level to the pH on the control SS. The decrease in the pH on day 14 on the SS1 was also in line with the gas composition profile, where the CO_2 and the hydrogen contents increased along with the decrease in the methane content. In Figure 5-37, it can be seen that the hydrogen conversion also started decreasing during that time. This could be due to the system experiencing VFA accumulation as it was found that the alkalinity ratio was recorded as 0.46 on day 15, and this increased to 0.53 at the end of the experiment.

The methane content in both reactors reached 48 % from the initial methane content of 66 % due to the dilution of hydrogen. The increase of methane content in reactor SS2 was relatively faster than in reactor SS1. The methane content in reactor SS2 reached 87 % on day 7 as hydrogen dropped to 4.2 %. On the other hand, the maximum methane content on reactor SS1 was achieved on day 14 at 78 %. The biomethanation extent reached the maximum value of around 90 % in biomethanation reactor SS1, which is 20 % higher compared to the reactor control SS.

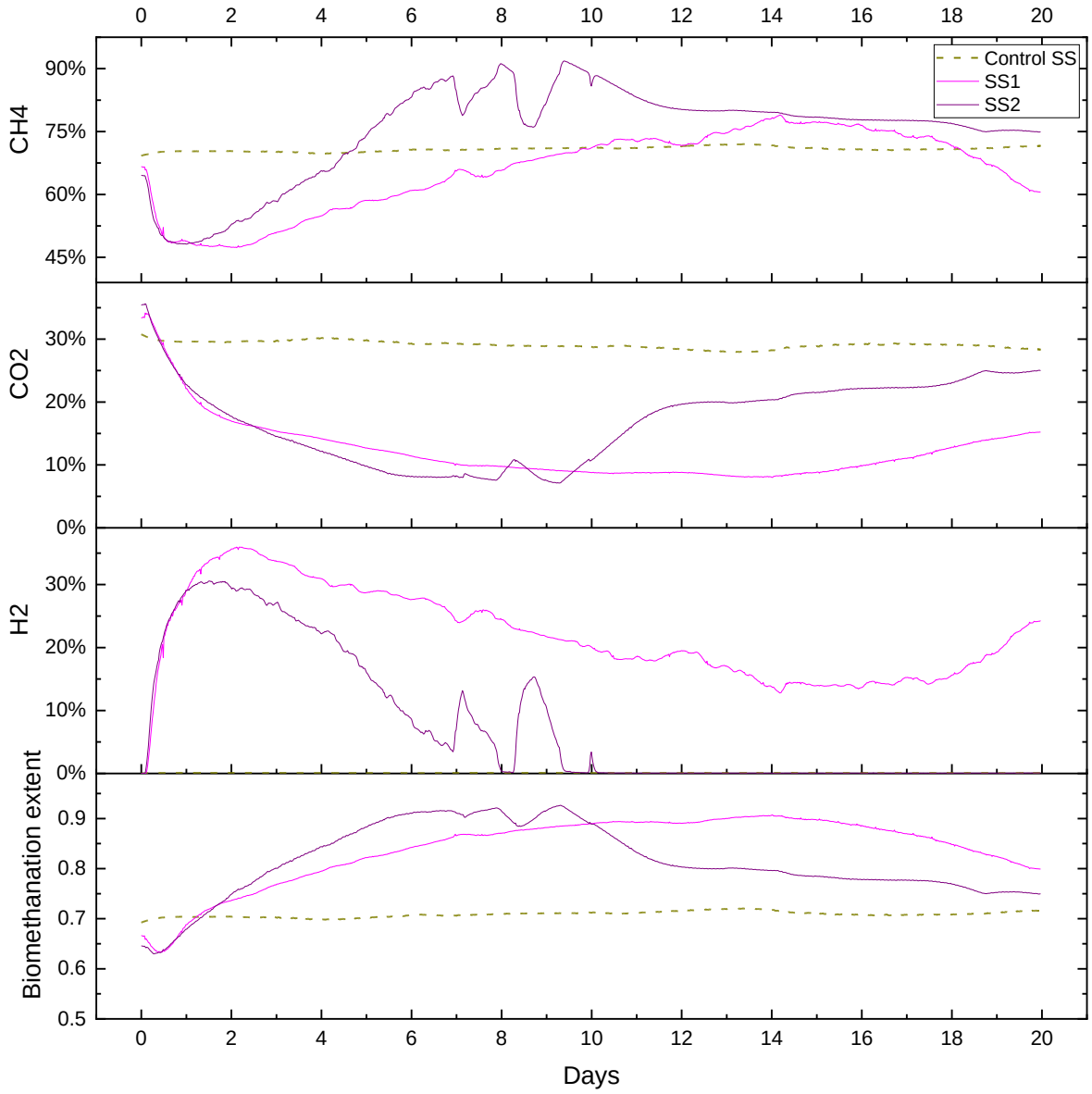

Figure 5-37 Gas composition and biomethanation extent during the in-situ biomethanation of sewage sludge with the additional sparger and higher mixing rate.

The hydrogen conversion in reactor SS1 could reach the maximum value of 95 %. The rapid increase of hydrogen conversion in reactor SS2 was due to low gas production flow resulting in high gas retention time, as the alkalinity ratio was recorded high, which could lead to inhibition.

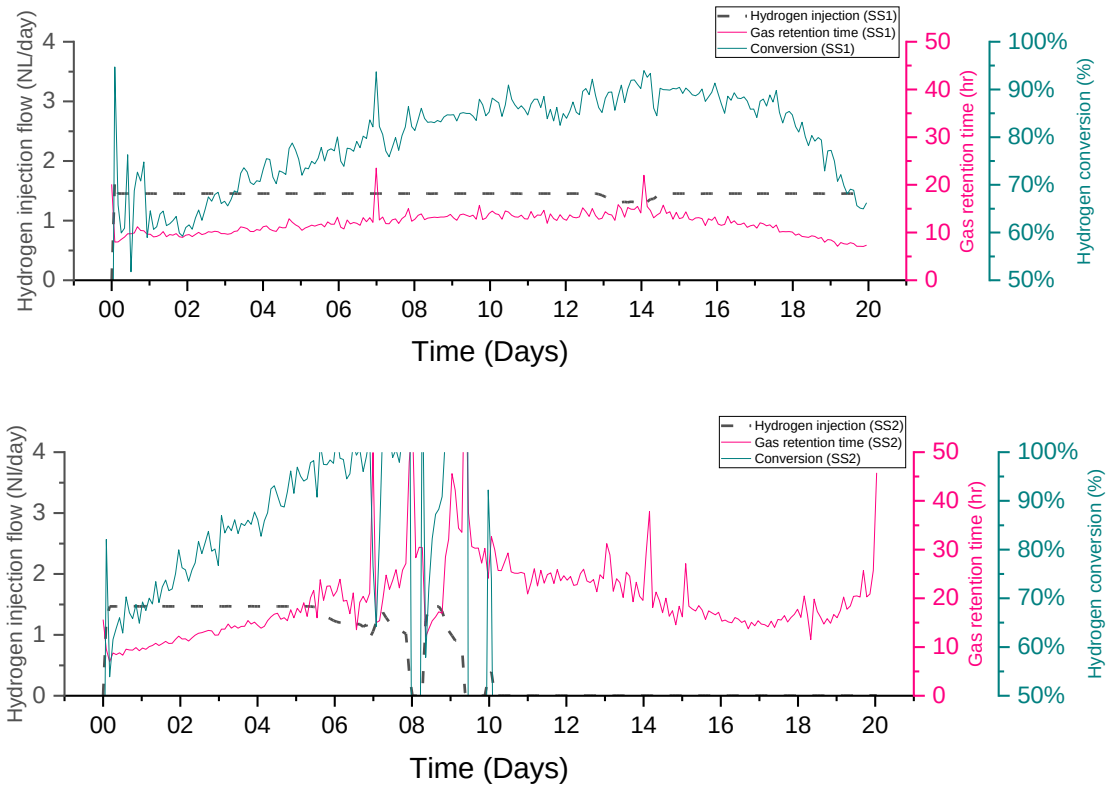

Figure 5-38 The hydrogen conversion in relation to the gas retention time and hydrogen injection during the in-situ biomethanation of food waste with the additional sparger and higher mixing rate.

In the literature, the positive correlation of increasing mixing rate to the increased gas-liquid mass transfer has been reported previously by Luo (Luo and Angelidaki, 2012a) and the linear relationship between mixing rate and hydrogen conversion was reported by Wahid and Horn (2021).

5.5.3 Effect of reducing the OLR using sewage sludge (OP3_SS)

Increasing the gas retention time could improve the gas-liquid mass transfer. The strategy for increasing the gas retention time is to reduce the flow of biogas as well as the hydrogen injection flow. In this period, the experiment was continued from the previous experiment by reducing the organic loading rate from 2 to 1 gVS L^{-1} day^{-1}. Reducing the OLR to 1 gVS L-1 day-1 also reduces the daily hydrogen requirement by 50 %. The hydrogen injection flow setpoint was then reduced by 50 %, while the other set points were set at similar values to the previous experiment.

The experiment was run for 18 days. The OLR profiles were stable in the reactor control SS

and SS1 with an average OLR of 0.88 gVS L^{-1} day^{-1} (control SS) and 0.88 gVS L^{-1} day^{-1} (SS1), while the OLR on the reactor SS2 slightly oscillated with an average OLR of 0.99 gVS L^{-1} day^{-1}. The gas outflow on the reactor control was recorded to be stable with an average flow rate of 0.4 NL day^{-1}. In comparison, the average gas outflow in the reactor biomethanation SS1 and SS2 has a similar average outflow with 0.6 NL day^{-1}, see Figure 5-39. The hydrogen injection was observed stable with 0.73 NL day^{-1}, and no feedback controls were activated in this period.

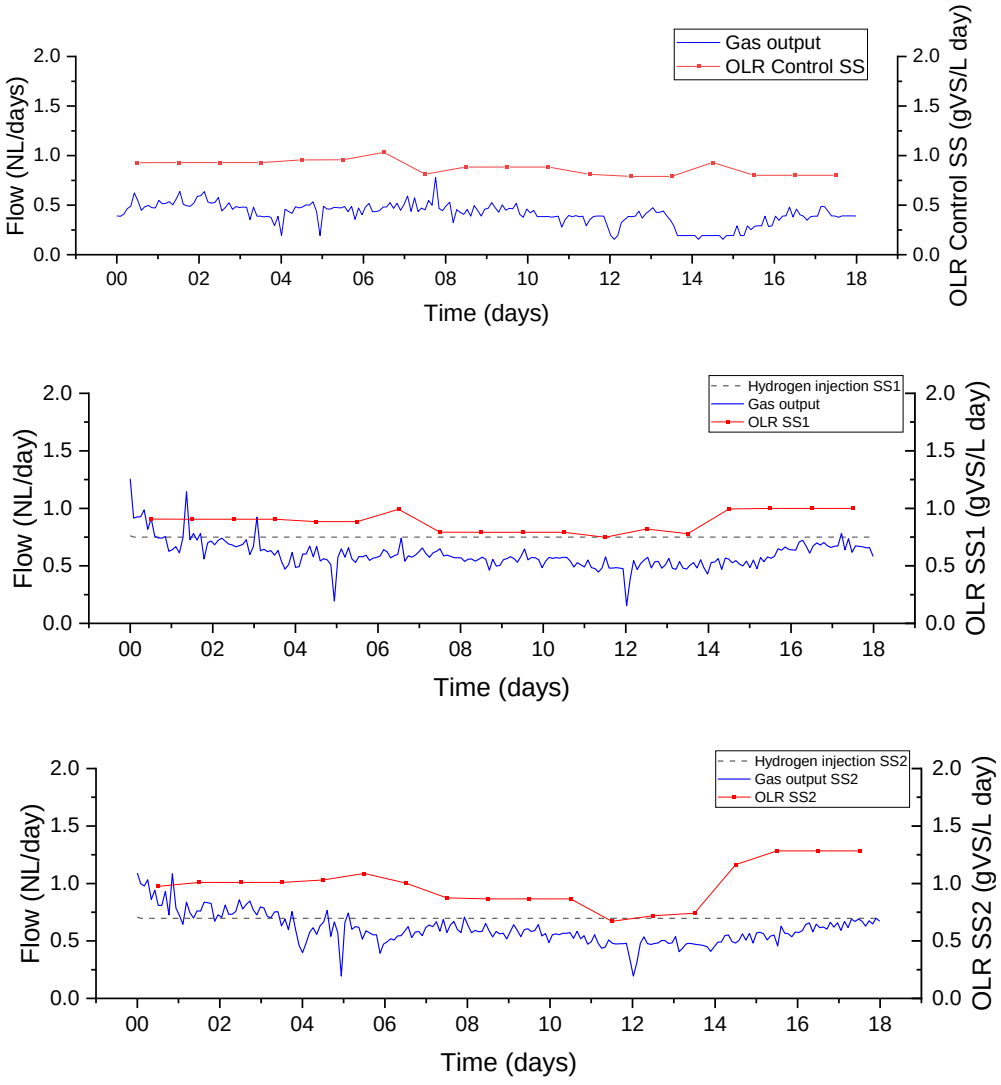

Figure 5-39 Gas flow, OLR and hydrogen injection from in-situ biomethanation of sewage sludge, at gas recirculation rate of 120rpm and with additional sparger on recirculation line, and higher mixing rate at OLR 1 gVS L^{-1} day^{-1}. SS: control reactor; SS1 and SS2 duplicate biomethanation reactors.

Similar to the previous period, the initial pH on the SS1 and SS2 was observed to be slightly lower than that of the control SS. The initial pH was 7.47 on the SS1 and 7.36 on the SS2,

while the reactor control SS had an initial pH of 7.56. There were no issues with the initial value of the alkalinity, where the alkalinity ratio in all the reactors was observed below 0.2.

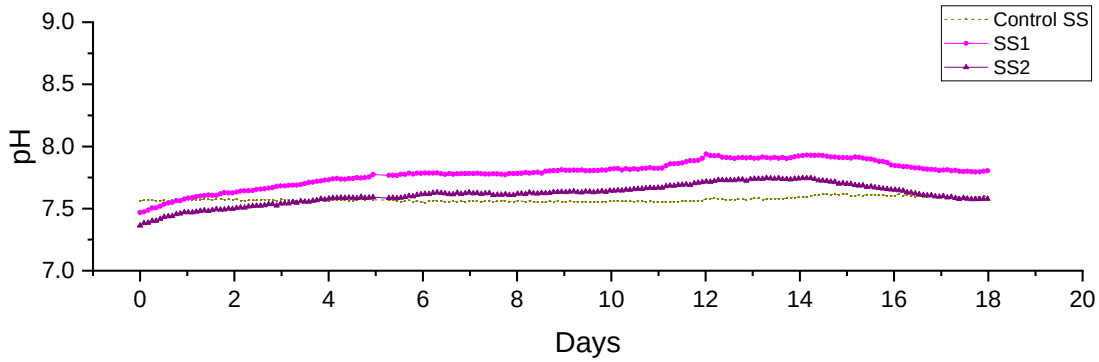

Figure 5-40 The pH profile during the in-situ biomethanation of food waste with the additional sparger, higher mixing rate and at OLR 1 gVS L^{-1} day^{-1}

The initial value of methane content was around 75 %, dropping immediately as soon as hydrogen was injected to 60 % on reactor SS1 and 68 % on reactor SS2. After that, the hydrogen content increased and reached the maximum hydrogen content of around 11.7 % (SS2) and 17.2 % (SS1) in just one day before slowly declining. The minimum hydrogen content achieved on the SS1 and SS2 were 4.6 % and 2.3 %, respectively. The maximum methane content that was able to be achieved was around 85 %, with the methane content average in SS1 and SS2 being 77.6 % and 80.8 %. The highest biomethane extent reached around 90 % in both reactors, or 17 % higher relative to the reactor control.

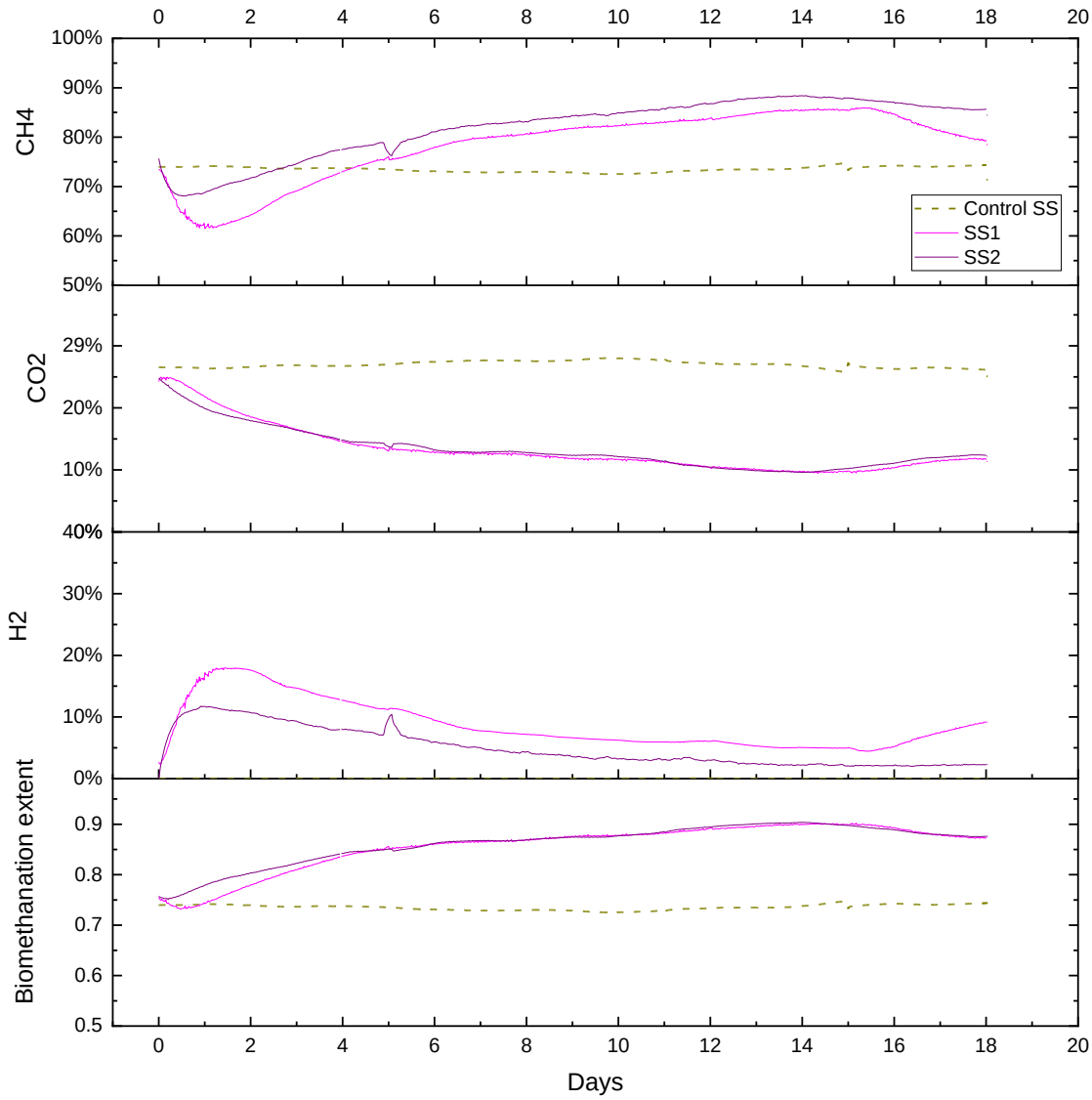

Figure 5-41 The gas composition and biomethanation extent during the in-situ biomethanation of sewage sludge with the additional sparger, higher mixing rate and at OLR 1 gVS L^{-1} day^{-1}

Compared to all the previous periods, the hydrogen level achieved in this period was the lowest, on the other hand achieving the highest hydrogen conversion. Almost all the hydrogen is consumed with an average hydrogen conversion of 92.4 % on the SS1 and 95.5 % on the SS2, see Figure 5-42. On day 15, the hydrogen content was recorded to have increased due to the overfeeding. Interestingly, the flow plays a critical role in increasing retention time, leading to increasing hydrogen conversion.

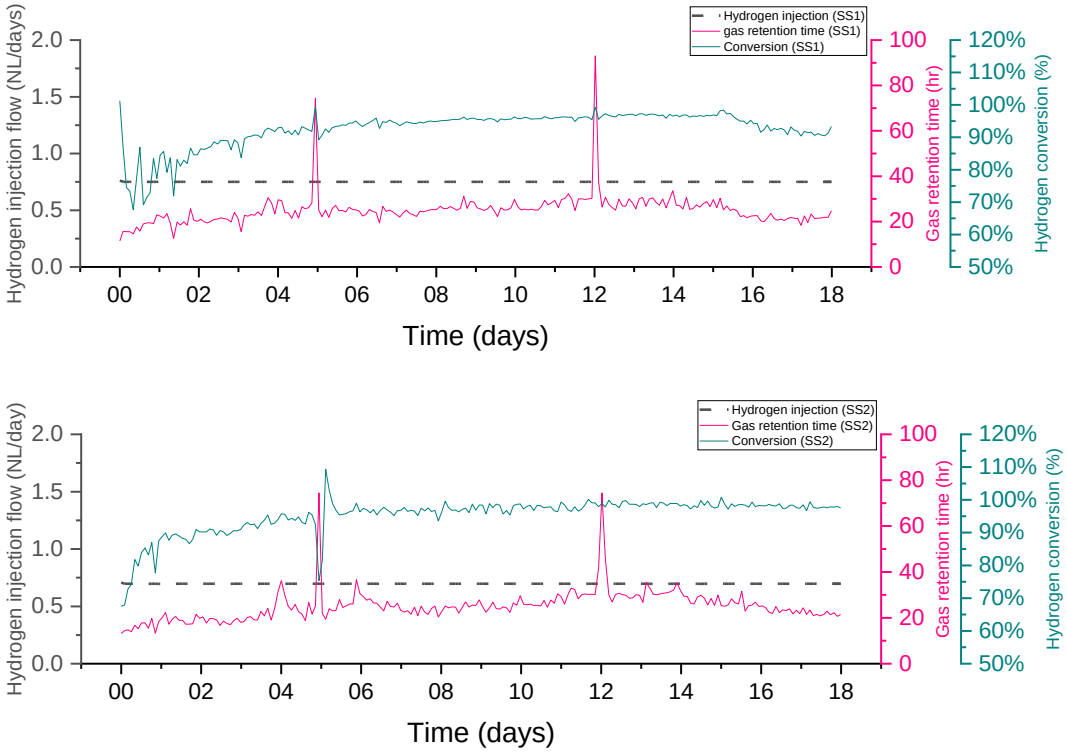

Figure 5-42 The hydrogen conversion in relation to the gas retention time and hydrogen injection during the in-situ biomethanation of food waste with the additional sparger, higher mixing rate and at OLR 1 gVS L^{-1} day^{-1}

The change in the biogas flow is related to the improvement in hydrogen conversion, as seen in Figure 5.39. The hydrogen conversion tended to increase gradually until it was found to be stable after day 4 at 95 % on the SS1 and 97 % on the SS2.

5.5.4 Comparison of process optimisation in the in-situ biomethanation using sewage sludge

An improvement in the strategies in order to increase the gas-liquid mass transfer provided a positive impact by increasing the hydrogen conversion. Table 5.6 shows that the hydrogen conversion increases from the period OP1_SS to OP2_SS as well as OP3. The highest improvement occurs in the period OP3_SS, which increases to around 20 % relative to OP1_SS, while the increase on OP2_SS was only around 4 % relative to OP1_SS. The highest methane content also could be achieved at OP3, where the average methane content could reach around 80 %.

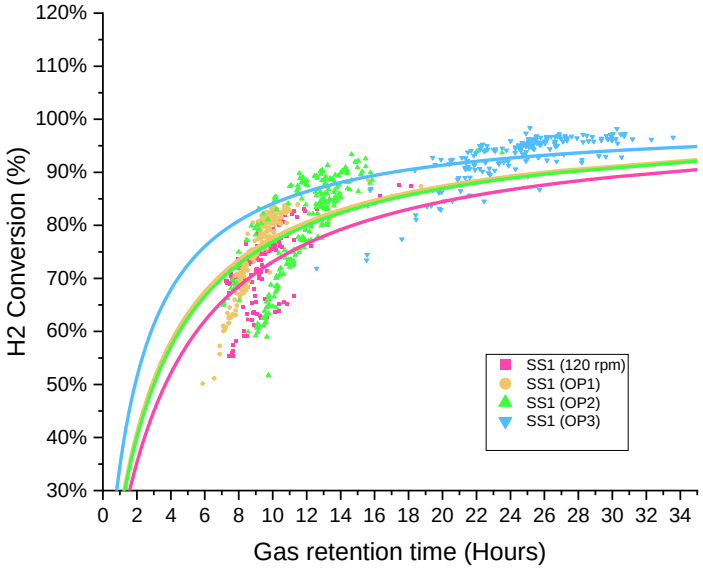

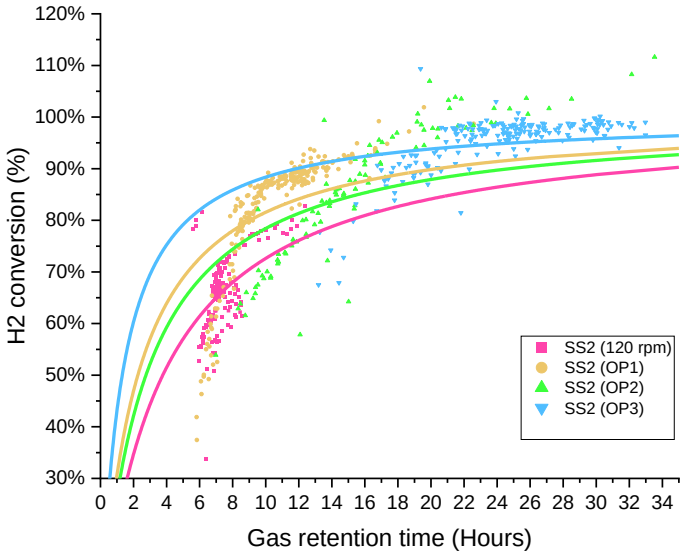

Figure 5-43 Scatter plot of the retention time and hydrogen conversion on the SS1 and the SS2 at different optimisation periods.

A scatter plot distribution shows that the hydrogen conversion in each period increased, see Figure 5-43. With the same gas retention time, the additional sparger on the recirculation line was able to increase the hydrogen conversion. On the other hand, an increasing mixing rate on the OP2 was able to increase the gas retention time, but there was not much difference in the hydrogen conversion. The greatest improvement was

shown in the period OP3, where the hydrogen conversion reached almost 100 %. This was due to the lower biogas production that produced a higher gas retention time.

Table 5.6 Summary of the in-situ biomethanation using sewage sludge at different optimisation periods.

		R_{120} SS			OP1 SS			OP2 SS			OP3 SS		
		Control	SS1	SS2	Control	SS1	SS2	Control SS	SS1	SS2	Control SS	SS1	SS2
Time	Days	12	12	12	19	19	19	20	20	10	18	18	18
Hydrogen injection flow setpoint	ml/min		1.02	1.02					2.14	2.38			
Average OLR	gVS/ L day^{-1}	1.93	1.89	2.03	1.94	1.85	1.79	2.12	2.07	2.10	0.88	0.88	0.99
Actual hydrogen Injection supplied	L day^{-1}		1.44	1.45		1.46	1.44		1.45	1.22		0.73	0.73
Total gas out	L/gVS	0.39	0.49	0.56	0.43	0.50	0.47	0.29	0.37	0.28	0.27	0.4	0.36
Specific CH_4 production rate	L/gVS	0.27	0.28	0.32	0.30	0.32	0.33	0.21	0.24	0.19	0.20	0.31	0.29
Specific CO_2 in output gas	L/gVS	0.12	0.08	0.10	0.14	0.07	0.06	0.08	0.05	0.04	0.07	0.05	0.05
Hydrogen consumption rate	L day^{-1}		1.03	0.96		1.12	1.19		1.16	1.04		0.38	0.7
H_2 Conversion	%		71.41	66.32		76.68	82.82		79.96	85.74		92.53	95.55
Average retention time	hr		9.42	7.63		9.42	10.91		11.89	19.75		25.06	25.11
Methane evolution rate (MER)	L/L_r day			0.14		0.16	0.18		0.16	0.14		0.10	0.10
Average pH		7.23	7.32	7.48	7.74	7.78	8.01	7.43	7.59	7.24	7.57	7.78	7.62
Average CH4	%	68.50	59.47	58.80	67.90	65.36	71.49	69.92	66.22	72.05	71.1	77.62	80.90
Average CO2	%	29.63	15.56	16.80	31.11	13.95	12.51	28.75	12.41	13.24	25.60	12.84	12.90
Average H2	%	0.11	25.28	24.63	0.12	21.32	15.99	0.08	22.14	14.37	0.03	8.63	4.92
Average TS	%	2.34	2.38	2.53	3.02	3.19	3.37	2.59	2.37	2.72	2.48	2.24	2.31
Average VS	%	1.30	1.47	1.58	1.63	1.75	1.87	1.24	1.31	1.45	1.29	1.25	1.24
Average Ammonia		0.37	0.38	0.31	0.41	0.42	0.38	0.17	0.41	0.63	0.14	0.14	0.15
Average Alkalinity ratio	[gTAN/kg_{sub}	1.46	1.36	1.56	1.60	1.59	1.53	1.38	1.46	1.45	1.51	1.53	1.57
Average Acetate	g kg_{sub}^{-1}	0.38	0.25	0.12	0.94	2.11	2.94	0.95	2.00	2.25	0.31	0.23	0.40
Average total VFA	g kg_{sub}^{-1}	3.34	2.55	2.35	2.40	3.27	4.04	2.61	3.62	3.08	1.01	0.58	0.79

5.6 Process optimisation of in-situ biomethanation to improve gas-liquid mass transfer on food waste digester

5.6.1 Effect of the additional sparger on the recirculation line using food waste (OP1_FW)

During this period, the experiment was observed for 32 days. The OLR was at the set point of 2 gVS L^{-1} day^{-1}. However, the feeding profile was oscillating, and some experienced very low feeding, with the average OLR being 1.79 gVS L^{-1} day^{-1} (control FW), 2.01 gVS L^{-1} day^{-1} (FW1) and 2.06 gVS L^{-1} day^{-1} (FW2). The average gas outflow in the reactor control FW was recorded at 2.14 NL day^{-1}, while the biomethanation reactor on FW1 and FW2 were 2.77 and 2.91 NL day^{-1}, respectively.

Hydrogen injection rate in reactor FW1 was strongly influenced by the feedback control, while hydrogen injection in FW2 was relative stable, see Figure 5-44. The average hydrogen injection in the biomethanation reactor was 2.35 NL day^{-1} on reactor FW1 and 2.43 NL day^{-1} on reactor FW2. The activation of the feedback control on FW 1 is due to the hydrogen content that reached the constraint. The hydrogen content increased as soon as the hydrogen was injected into the reactor, and it reached the maximum of 34 % in one day. Therefore, the feedback control parameter was activated, which was caused by the hydrogen when the hydrogen content in the headspace reached 33.6 %. During the period, the hydrogen level tended to be stable in the 33 to 34 % range, which is around the limit of the feedback control activation. This is why the feedback control was activated throughout this period on the FW1.

On day 13, the OLR on FW1 dropped to 0.67gVS L^{-1} day^{-1} due to technical issues. This caused the biogas flow to decrease significantly from around 4 NL day^{-1} to around 2 NL day^{-1}. The lower biogas flow would affect the increase in the gas retention time, leading to an increase in the hydrogen conversion, see Figure 5-47. The higher conversion affected the pH on day 13 and formed a peak in the bicarbonate consumption. In addition, this confirmed that the carbon dioxide content decreased and showed the opposite trend, see Figure 5-46.

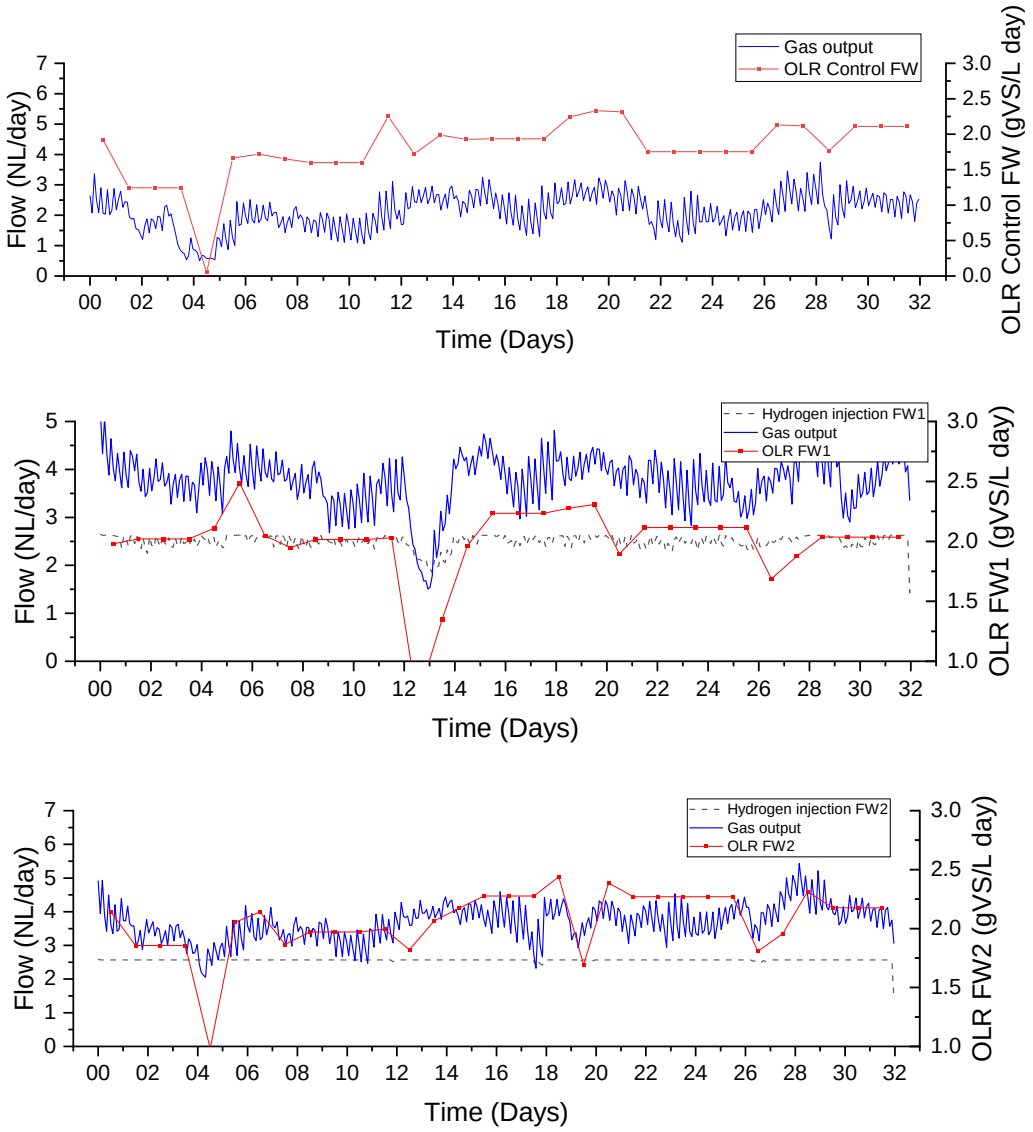

Figure 5-44 Gas flow, OLR and hydrogen injection from in-situ biomethanation of food waste, at gas recirculation rate of 120rpm and with additional sparger on recirculation line. FW: control reactor; FW1 and FW2 duplicate biomethanation reactors.

The initial value of pH in all reactors was around 7.7. Similar to other periods, the pH profile increased as soon as the hydrogen was injected. The pH looked stable throughout the experiment, with an average pH of 8.18 on FW1 and 8.10 on FW2, while in reactor control FW remained stable at pH 7.7, see Figure 5-45.

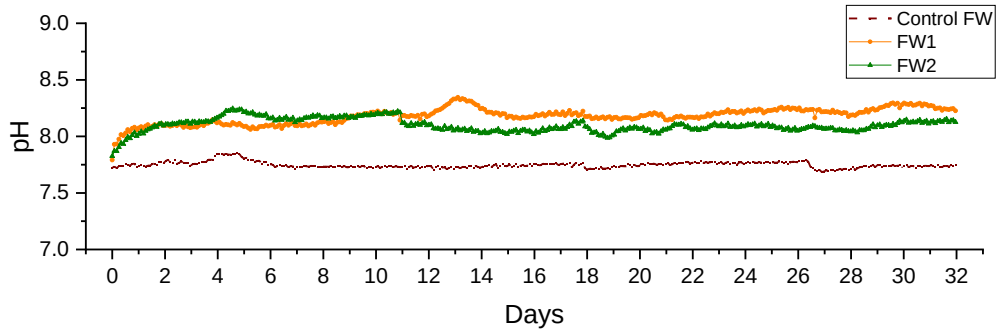

Figure 5-45 The pH profile during in-situ biomethanation of food waste on the additional sparger.

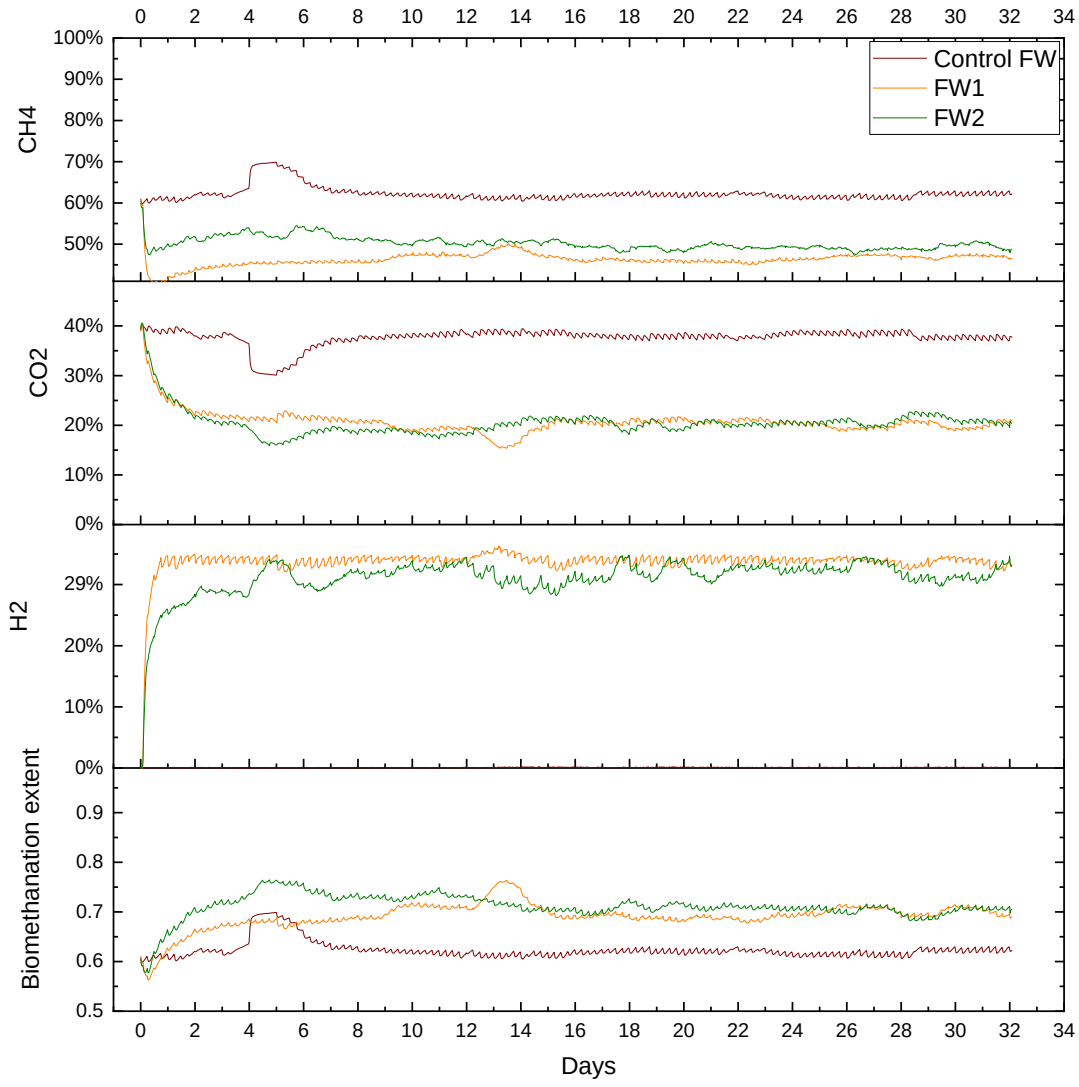

Figure 5-46 Gas composition and biomethanation extent during the in-situ biomethanation of food waste with the additional sparger.

The gas composition was shown to be relatively stable during the experiment. The hydrogen content in the FW1 was observed to be stable at around 33 % from the beginning

of the period, while the FW2 was observed to be slightly oscillatory but still relatively stable at around 30 %. Also, the stable hydrogen content was shown in the methane and carbon dioxide content. The methane content in reactor FW1 was observed to be stable at 46 %, while in reactor FW was 48 %. The average hydrogen conversion was relatively low compared to the previous periods, with only 49 % in reactor FW1 and 56 % in reactor FW2. The biomethanation extent was found to be similar in both biomethanation reactors, with around 70 % or 8 % higher relative to the reactor control.

The average hydrogen conversion was observed higher at reactor FW2 with 56 % compared to the reactor FW1 with 50 %, see Figure **5-47**.

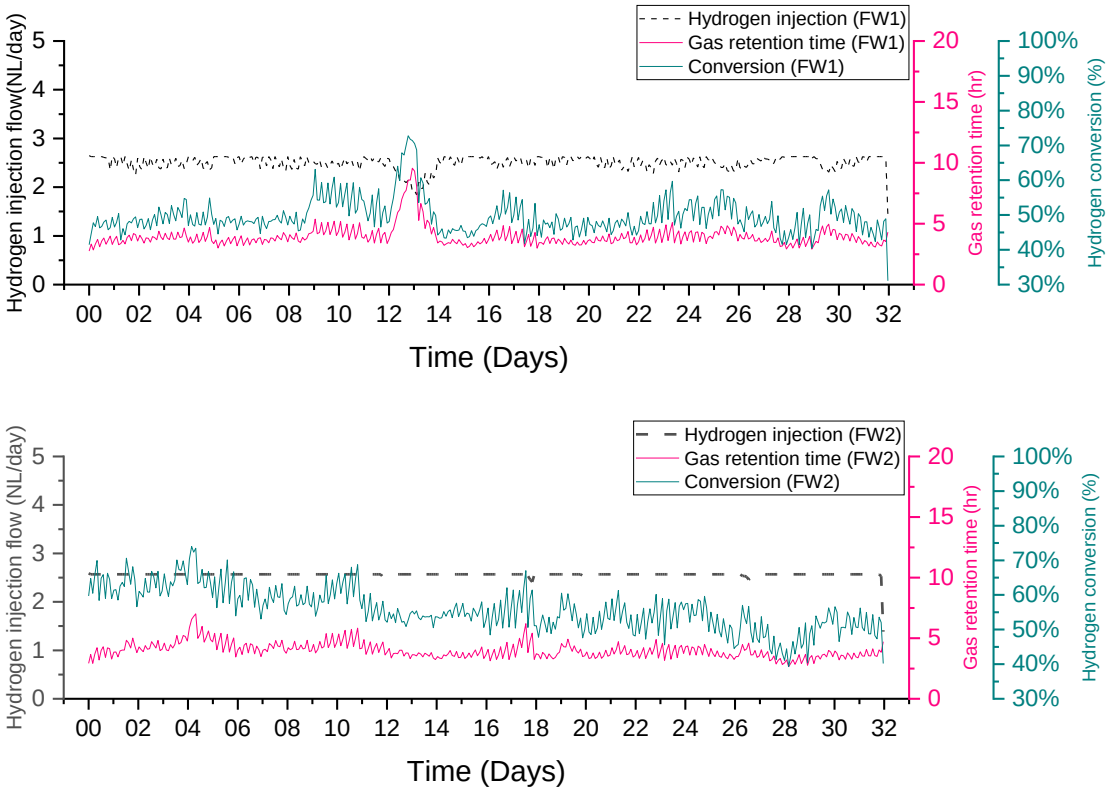

Figure 5-47 The hydrogen conversion in relation to the gas retention time and hydrogen injection during the in-situ biomethanation of food waste with the additional sparger.

5.6.2 Effect of the additional sparger on the recirculation line and the increased mixing rate using food waste (OP2_FW)

The period with higher mixing rates using food waste was observed for 20 days. The average OLR on the FW1 and the FW2 was more than 10 % lower than the feeding setting with 1.64 gVS L^{-1} day^{-1} on the FW1 and 1.71 gVS L^{-1} day^{-1} on the FW2, while the reactor

control SS has an average of 2.05 gVS L^{-1} day^{-1}. Hydrogen injection average on the reactor was recorded at 2.3 NL day^{-1} on reactor FW1 and 2.43 NL day^{-1} on reactor FW2.

There was an issue found on the feeding pump that made it have a lower feeding on day 3. The lower feeding on that day caused the biogas flow to decrease until day 6 slowly. Unfortunately, the daily feeding was not monitored daily during the weekend. Therefore, the feeding quantity at the weekend was measured based on the average three days from Friday to Sunday. Unfortunately, the case of feeding failure happened at the weekend. Since the feeding monitoring is done manually, it is hard to be sure when exactly the issue happened. However, it still can be tracked from the gas flow profile.

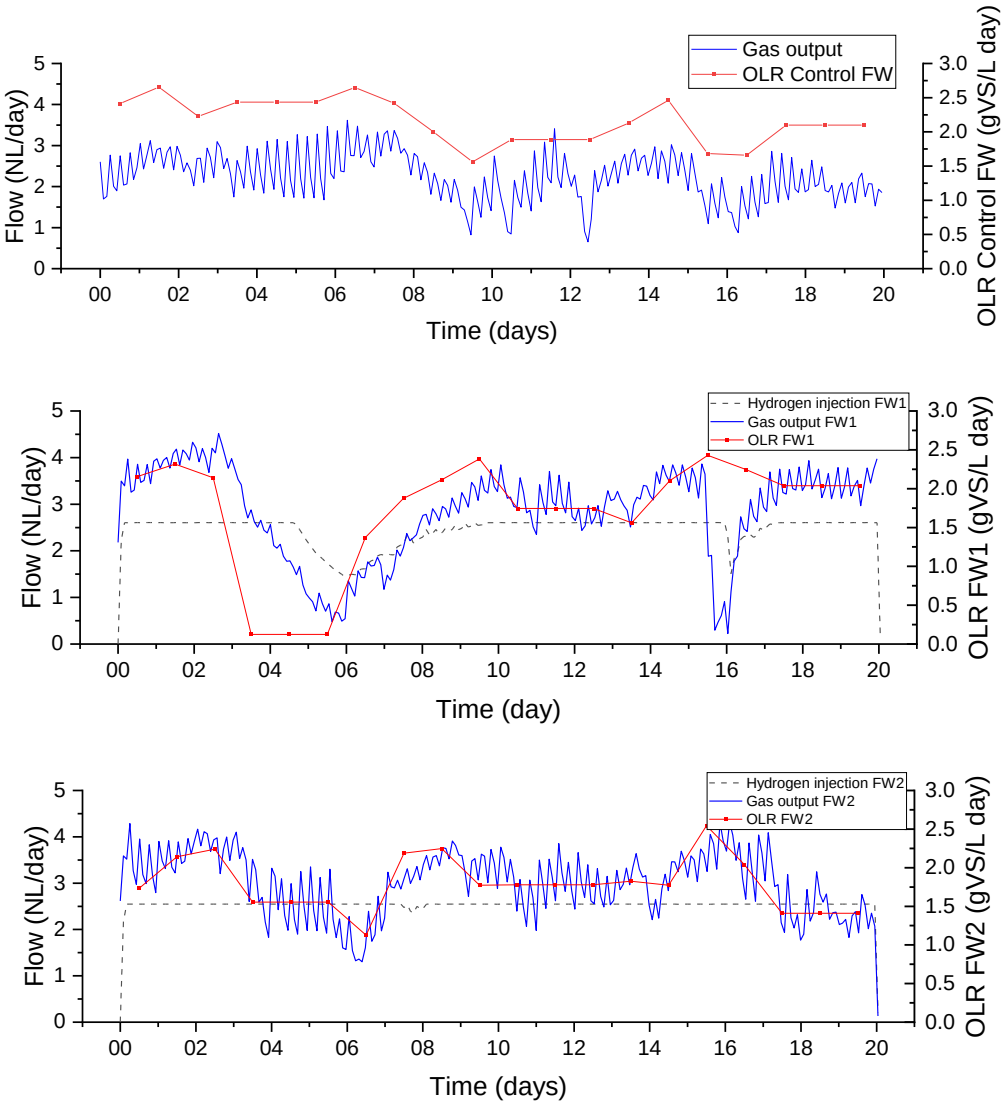

Figure 5-48 Gas flow, OLR and hydrogen injection from in-situ biomethanation of food waste, at gas recirculation rate of 120rpm and with additional sparger on recirculation line, and higher mixing rate. FW: control reactor; FW1 and FW2 duplicate biomethanation reactors.

The record showed that there is almost no feeding during the weekend on the FW1; thus, the gas outflow suffered a huge drop from 4.5 NL day^{-1} on day 3 to around 0.5 NL day^{-1} on day 6. The biogas flow increased as soon as the feeding was added. However, the very low flow affected the feedback control activation due to the higher conversion from the hydrogen in the headspace during this time.

Figure 5-49, the initial pH in all reactors was around 7.5, and it was stable at reactor control. In biomethanation reactors, the pH in reactor FW2 was relatively stable compared to reactor FW1. The average pH in reactor FW1 and FW2 were similar at 8.2.

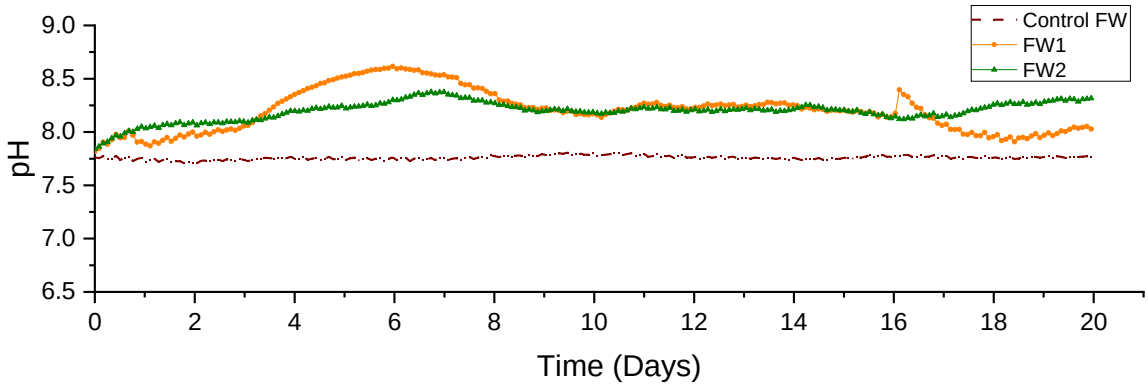

Figure 5-49 The pH profile during the in-situ biomethanation of food waste on the additional sparger and higher mixing rate.

As observed in Figure 5-50, the hydrogen content decreased along with the increase in the methane content. There was a less organic matter to be degraded, thus less carbon dioxide production. This makes the carbon dioxide in the form of bicarbonate in the liquid be consumed, and this causes the pH to increase.

The methane content dropped to around 45 % on day 1 due to the dilution of hydrogen. The methane content was increased to the maximum of 75 % on day 6 on reactors FW1 due to the drop in OLR. The drop of OLR increased the hydrogen conversion as this corresponded to the hydrogen content drop to 17 % on day 6. Carbon dioxide content was relatively stable in both reactors, with an average of 17 % in reactor FW1 and 18 % in reactor FW2. The biomethane extent was observed at 76 % in both reactors in stable

conditions. The interruption of gas composition occurred on day 16, which will explain below.

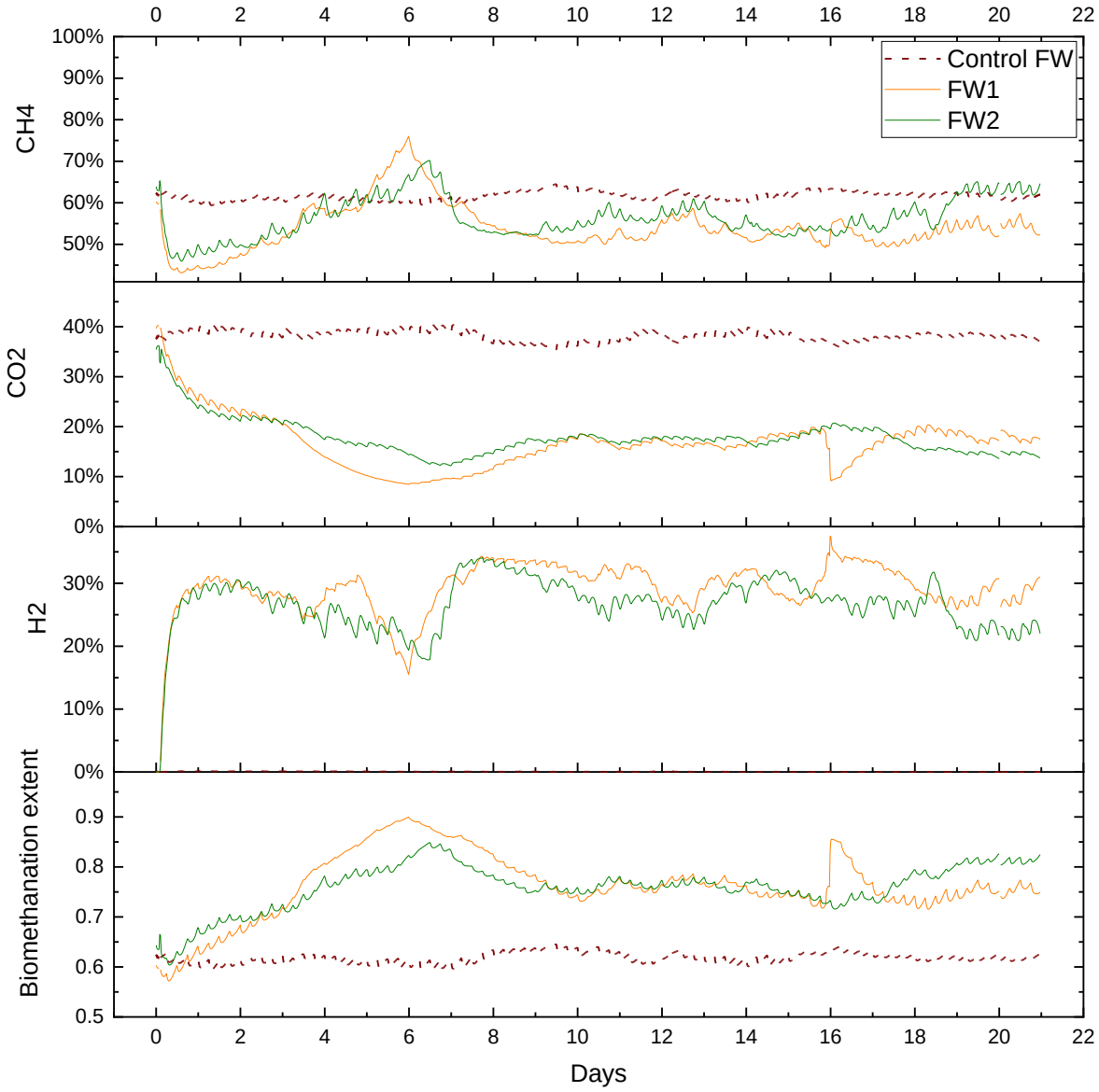

Figure 5-50 The gas composition and biomethanation extent during the in-situ biomethanation of food waste with the additional sparger and higher mixing rate.

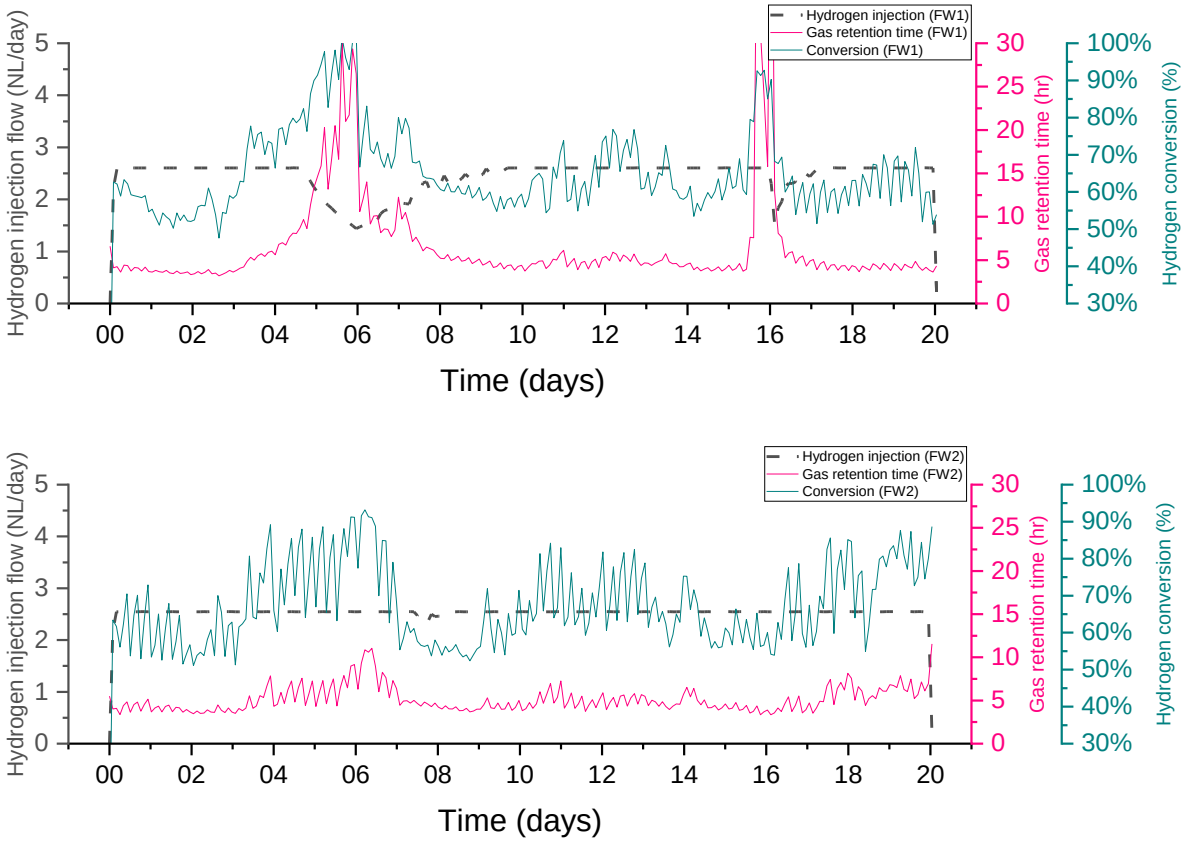

Figure 5-51 The hydrogen conversion in relation to the gas retention time and hydrogen injection during the in-situ biomethanation of food waste with the additional sparger and higher mixing rate.

In normal operation, the high pressure in the headspace does not create any problems because the gas was released through the flow meter by at least 5 mbar. However, as mentioned in the methodology chapter, the rig configuration was designed for a continuous experimental investigation when no user was present (unattended operation). Therefore, a liquid outlet was employed in order to avoid overpressure, which can occur when a gas outlet is fully or partially blocked. Although this configuration was designed as a safety feature, when the pressure inside the reactor is high, the gas will push the liquid out through the liquid outlet. Therefore, the pressure will be maintained low. If this happens, the digestate that is pushed out through the liquid outlet will be collected in the effluent tank.

This safety feature, unfortunately, does not discharge some of the digestate out of the reactor into the effluent tank. This occurred on FW1 on day 15, when the effluent was discharged out of the reactor, and this decreased the liquid volume. As a result, as shown in Figure 5-48, the biogas flow reduced in the middle of day 15, and the headspace was

filled by the hydrogen, causing the hydrogen content to increase (Figure 5-50). At the same time, due to the reduction in the flow, the gas retention time increased, and this resulted in the hydrogen conversion increase (Figure 5-51), and some of the bicarbonate in the liquid was consumed, which resulted in the pH increasing (Figure 5-49). Fortunately, the performance of the digester was able to recover by placing the digestate back in the reactor and ensuring no blockage in the biogas line. As observed, once the system was back to normal, all the parameters returned to the level before the issue occurred.

5.6.3 Effect of reducing OLR using food waste (OP3_FW)

The period OP3_FW was performed for 18 days. The average OLR was 0.95 gVS L^{-1} day^{-1} on the reactor control FW, 0.97 gVS L^{-1} day^{-1} on FW1, and 0.99 gVS L^{-1} day^{-1} on FW2 see Figure 5-52. The flow was relatively stable throughout the period, but there was a decrease in the biogas flow on the FW1 on day 7 due to less feeding during this time. The average gas output on reactor control FW was recorded at 0.78 NL day^{-1}, and the average gas outflow on biomethanation reactor FW1 and FW2 was recorded as quite similar average gas outflow with 0.78 NL day^{-1} and 0.75 NL day^{-1}. With this value, it seems that the hydrogen injected into the biomethanation rectors is fully converted. Hydrogen injection was stable throughout the experiment and maintained the hydrogen supply with the hydrogen injection flow around 2.4 NL day^{-1}.

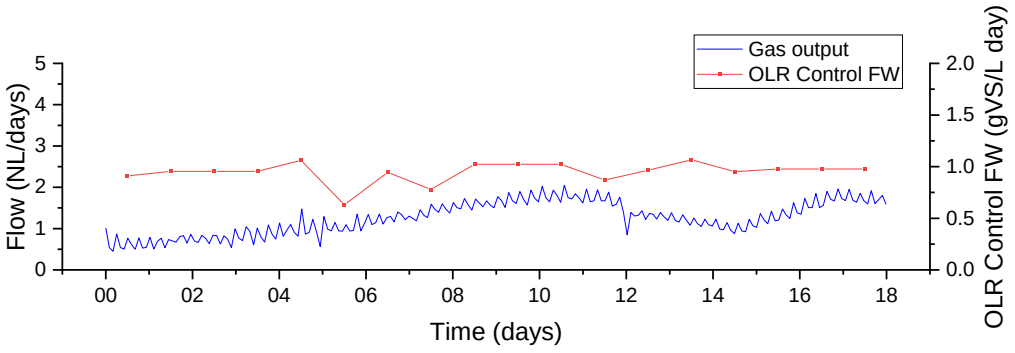

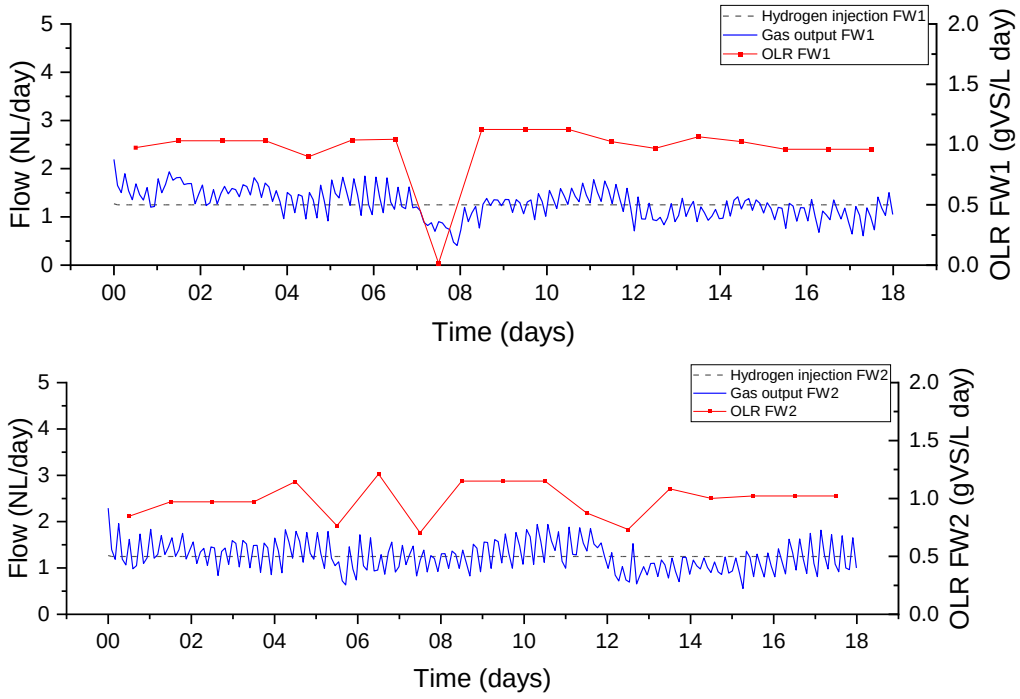

Figure 5-52. Gas flow, OLR and hydrogen injection from in-situ biomethanation of food waste, at gas recirculation rate of 120rpm and with additional sparger on recirculation line, and higher mixing rate at OLR 1 gVS L^{-1} day^{-1}. FW: control reactor; FW1 and FW2 duplicate biomethanation reactors.

The initial pH of the biomethanation reactor was already high, which was an influence of the previous period. The initial pH recorded on reactor FW1 and FW2 was 7.8 and 8, respectively. And because it was already high, the increase of hydrogen injection due to biomethanation to the pH was not as high as we had seen in the other period. The pH profile was quite stable throughout the period, with the average pH on the FW1 and FW2 being 8.13 and 8.25, respectively, which are higher compared to reactor control FW, which had an average pH of 7.69, see Figure 5-53.

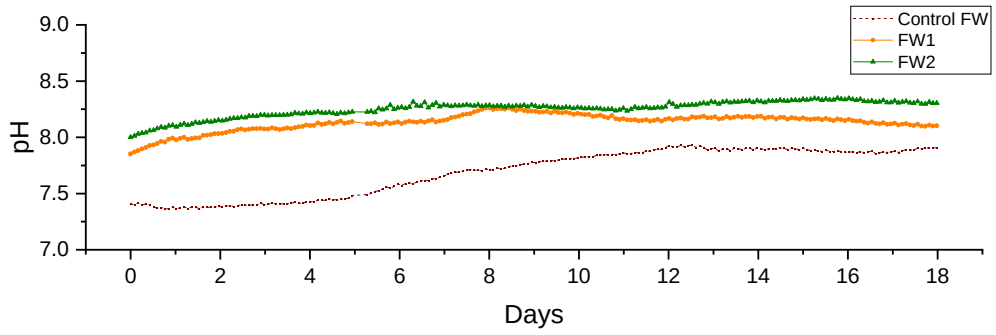

Figure 5-53 The pH profile during the in-situ biomethanation of food waste at period OP3_FW.

The methane content was slightly dropped to 57 % on the FW1 and 59 % on the FW2 at the beginning of hydrogen being injected into the reactor as the effect of hydrogen dilution. After that, the methane content was gradually increased until it was found to be stable at around 73-74 % at the end of the period. In reactor FW2, the methane content was influenced by the drop of OLR on day 12; this caused a gas output flow decrease from 1.5 NL day^{-1} to around 1 NL day^{-1}. The decreasing flow of gas output caused the hydrogen content to increase as hydrogen injection remained stable, and methane content decreased due to the dilution effect. The biomethanation extent was found stable at around 79 % in biomethanation reactor FW1 and around 82 % in reactor FW2.

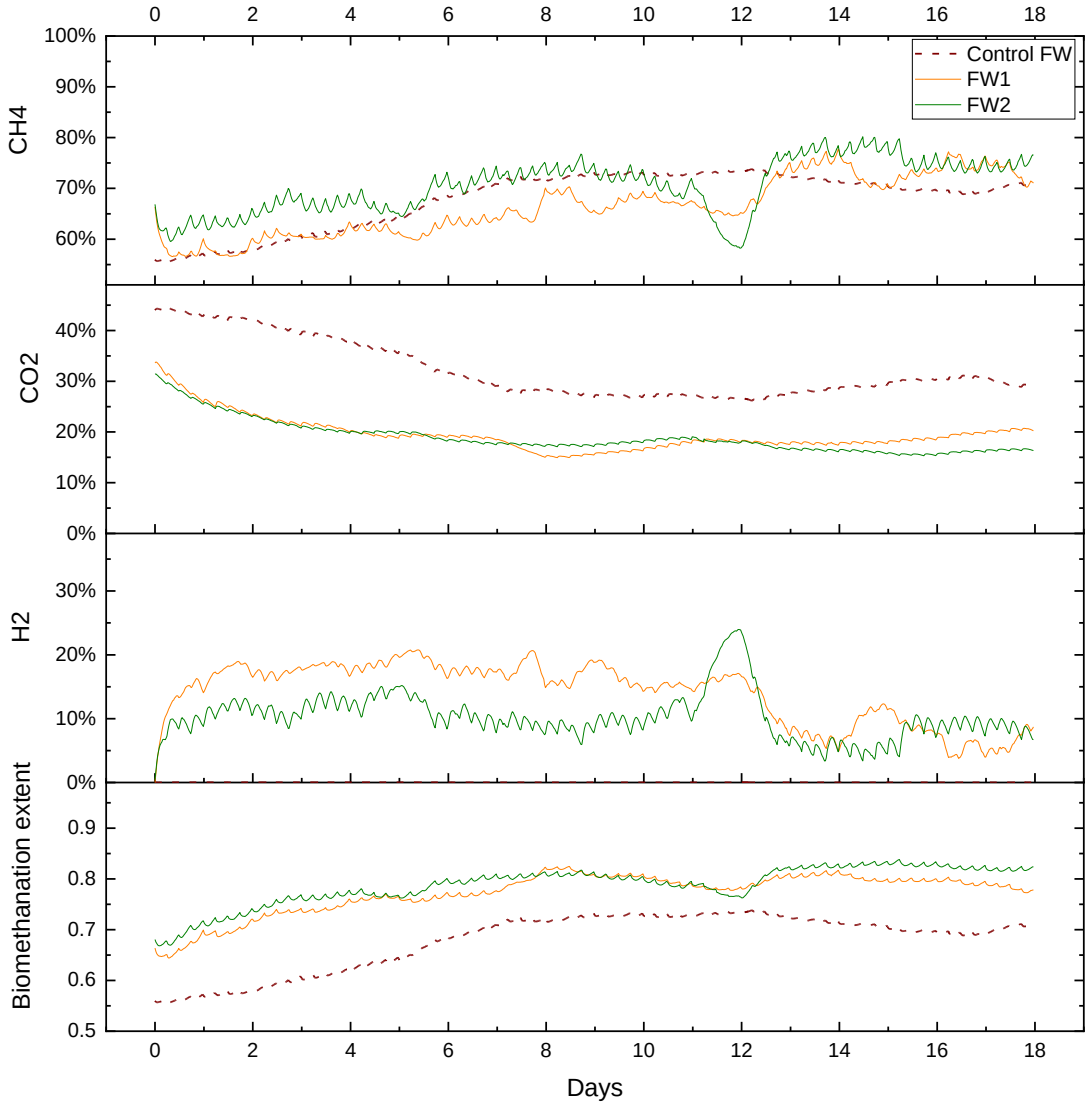

Figure 5-54 The gas composition and biomethanation extent during the in-situ biomethanation of food waste with the additional sparger and higher mixing rate at OLR 1 gVS L^{-1} day^{-1}

The hydrogen conversion was the highest compared to other periods, with an average hydrogen conversion in FW1 and FW2 being 85 % and 89 %, respectively.

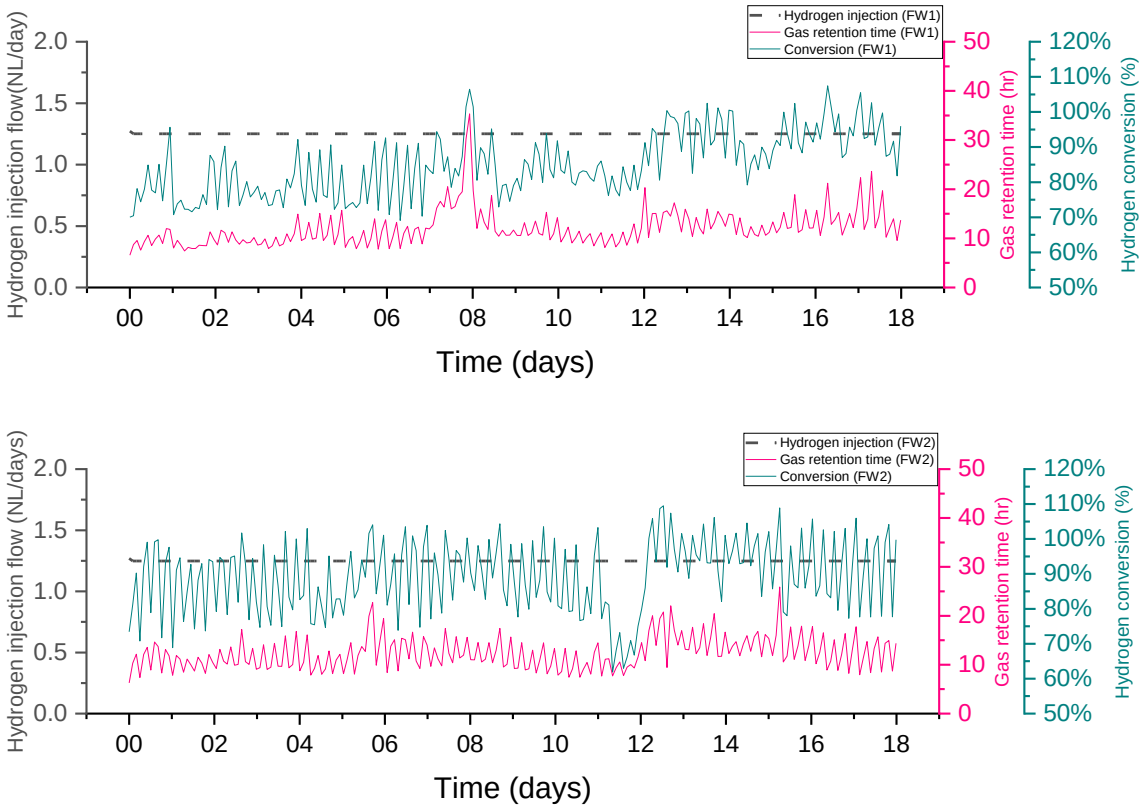

Figure 5-55 The hydrogen conversion in relation to the gas retention time and hydrogen injection during the in-situ biomethanation of food waste with the additional sparger and higher mixing rate at OLR 1gVS L^{-1} day^{-1}.

5.6.4 Comparison of process optimisation in the in-situ biomethanation using food waste

Table 5.7 shows the indicators comparison from OP1 to OP3 and also compared with the R_{120}. The additional sparger to the food waste reactor did not produce an improvement in the hydrogen conversion. In fact, the average conversion appears to be lower than in the period R_{120} with no additional sparger. In the period OP1, the average feeding or OLR on the FW1 and FW2 were relatively higher compared to the R_{120}_FW and OP2_FW. A higher OLR increases the biogas production rate, resulting in a lower gas retention time. This could be an indication of why the hydrogen conversion on the OP1 was found to be lower than the R_{120}_FW and OP2_FW.

In the period OP1, it was also observed that the ammonia level increased from around 3.7 gTAN $kg_{substrate}^{-1}$ to 3.9 gTAN $kg_{substrate}^{-1}$ in both the FW1 and the FW2 during the period OP1 _FW. Also, for the first time, the foam was detected in that period. There are numerous causes for the foaming in the anaerobic digestion systems, such as improper mixing, fluctuations in the OLR, and substrate types (Yang *et al.*, 2021). In addition, the accumulation of the VFA and the total ammonia may contribute to the foam formation by reducing the surface tension and increasing the foam stability (He *et al.*, 2017).

The levels of VFA and alkalinity ratio in the biomethanation reactors were, on average, comparable to the levels in the control reactors. This indicates that there was no noticeable The highest hydrogen conversion was achieved in the period OP3 FW when the reactors operated at the lowest OLR of 1 gVS/L^{-1} d^{-1}, 87 %.

Similar to the OP3_SS, the highest improvement in the hydrogen conversion was achieved in period OP3_FW, with the average conversion on each reactor reaching more than 85 %. Again this was due to the higher gas retention time as an effect of the lower biogas production and the lower hydrogen injection rate.

The distribution of the hydrogen conversion as a function of the gas retention time was shown in Figure 5-56. The distribution of the conversion was relatively similar between the R_{120} and OP1_FW. However, with the increased mixing rate in the reactor, a higher conversion was achieved in both the FW1 and the FW2. As mentioned before in section 5.7.1, it was observed that foam was detected in period OP1. Having a higher mixing rate then could help make the foam in a more unstable formation.

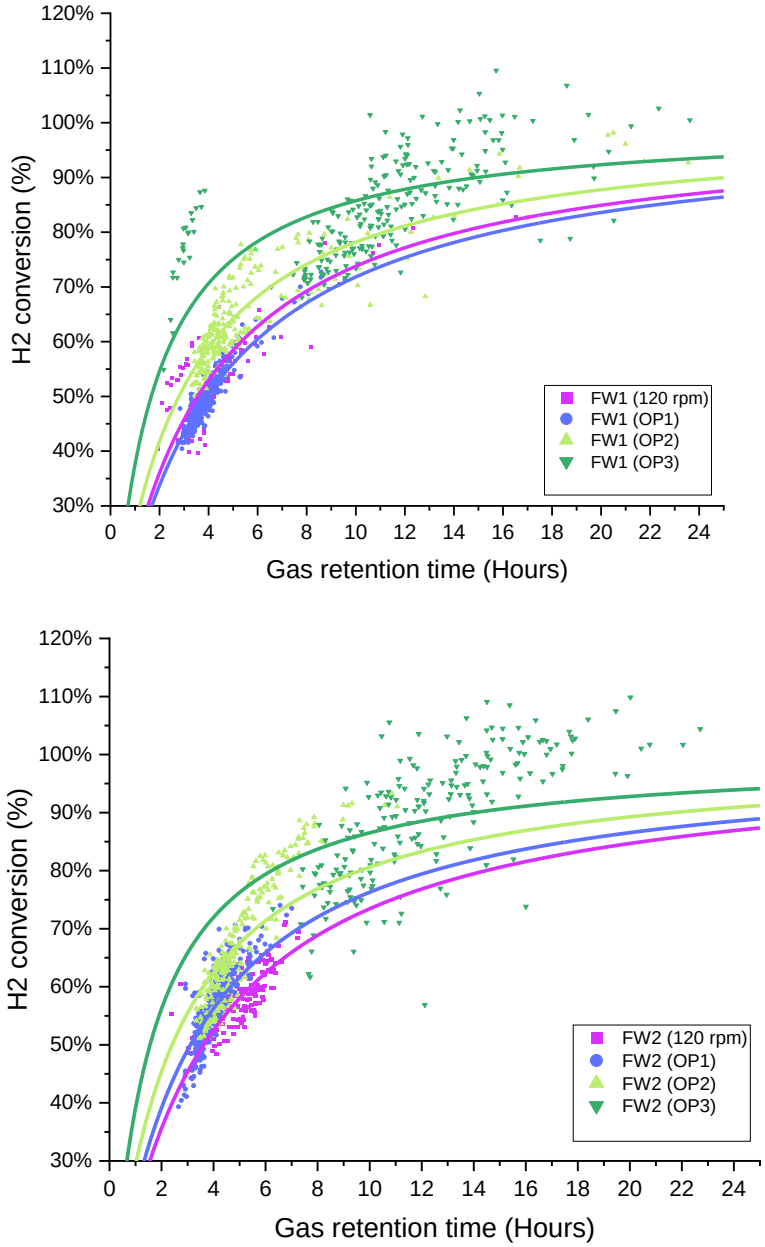

Figure 5-56 Scatter plot of the retention time and hydrogen conversion on the FW1 and the FW2 at different optimisation periods.

Table 5.7**.** Summarises the in-situ biomethanation using food waste at different optimisation periods.

		R_{120} FW			OP1 FW			OP2 FW			OP3 FW		
		Control FW	FW1	FW2	Control FW	FW1	FW2	Control FW	FW1	FW2	Control FW	FW1	FW2
Time	Days	9	4	9	32	32	32	20	20	20	18	18	18
Hydrogen injection flow setpoint	ml min^{-1}		1.79	1.79									
Average OLR	gVS/ L day^{-1}	1.70	1.88	1.63	1.79	2.01	2.06	2.05	1.64	1.71	0.95	0.97	0.99
Actual hydrogen Injection supplied	L day^{-1}		2.31	2.25		2.50	2.56		2.35	2.43		1.26	1.31
Total gas out	L gVS^{-1}	0.58	0.89	0.99	0.69	1.12	1.06	0.61	1.00	1.00	0.78	0.78	0.75
Specific CH_4 production rate	L gVS^{-1}	0.36	0.42	0.48	0.43	0.52	0.53	0.38	0.52	0.55	0.54	0.51	0.53
Specific CO_2 in output gas	L gVS^{-1}	0.21	0.42	0.48	0.26	0.23	0.22	0.24	0.18	0.18	0.24	0.15	0.14
Hydrogen consumption rate	L day^{-1}		1.39	1.35		1.24	1.43		1.53	1.64		1.08	1.18
H_2 Conversion	%		60.02	59.71		49.65	56.06		64.99	67.62		85.11	89.82
Average retention time	hr		7.83	5.29		3.94	3.99		6.67	5.08		12.06	12.33
Methane evolution rate (MER)	L L_r^{-1} day^{-1}		0.20	0.20		0.18	0.21		0.22	0.24		0.16	0.17
Average pH		7.71	7.86	n.a	7.75	8.18	8.10	7.76	8.20	8.20	7.69	8.13	8.25
Average CH4	%	62.45	47.96	49.67	61.96	46.79	50.20	61.54	54.50	56.05	67.37	66.26	70.56
Average CO2	%	36.33	20.26	17.67	37.48	20.94	20.45	37.97	16.95	18.03	31.84	19.51	18.93
Average H2	%	0.12	32.82	33.56	0.12	34.96	30.45	0.05	29.45	26.80	0.02	14.04	10.23
Average TS	%	2.38	2.29	2.24	3.04	2.83	2.92	2.91	2.78	2.74	2.72	2.54	2.55
Average VS	%	1.59	1.55	1.58	2.11	1.99	2.07	2.00	1.92	1.90	1.84	1.65	1.75
Average Ammonia	[gTAN/kg_{sub}	3.80	3.62	3.50	3.84	3.95	3.87	4.10	3.86	4.14	4.32	3.45	4.22
Average Alkalinity ratio		0.39	0.35	0.34	0.31	0.30	0.28	0.29	0.28	0.21	0.61	0.14	0.21
Average Acetate	g kg_{sub}^{-1}	0.47	0.53	0.51	0.84	0.84	0.88	2.01	1.86	0.65	4.42	0.61	0.35
Average total VFA	g kg_{sub}^{-1}	0.80	0.86	0.83	1.19	1.15	1.17	3.11	3.02	1.12	6.88	1.20	0.74

5.7 Comparison of hydrogen conversion, methane evolution rate and kLa in all periods.

An increase in gas recirculation rate to the in-situ biomethanation using sewage sludge gives a positive correlation to the hydrogen conversion methane evolution rate and kLa, as shown in Figure 5-57a, Figure 5-58a, Figure 5-59a. All three indicators increased along with the increase in gas recirculation rate. The increase of gas recirculation leads to increased gas hold-up and finally on the surface area through which the gas-liquid transfer happens. In the case of food waste, the effect of gas recirculation in the period R_{120} and R_{280} was not showing a significant difference in terms of hydrogen conversion, around 59 %. It should be noted that in period $R_{20,}$ the OLR was lower. Therefore, the hydrogen conversion in that period was also influenced by the high gas retention time due to lower gas flow. This was the reason that the experiment in periods OP1, OP2 and OP3 was not operated at a higher gas recirculation rate, by taking into consideration of the energy consumption on operating at a higher rate.

The hydrogen conversion tended to increase along with the increase of the gas recirculation rate. The additional sparger with a gas recirculation rate of 120 rpm to the recirculation line improved the hydrogen conversion even more than hydrogen conversion at recirculation 280 rpm (without additional sparger to the gas recirculation line). The effect of increasing the mixing rate did not significantly improve the hydrogen conversion.

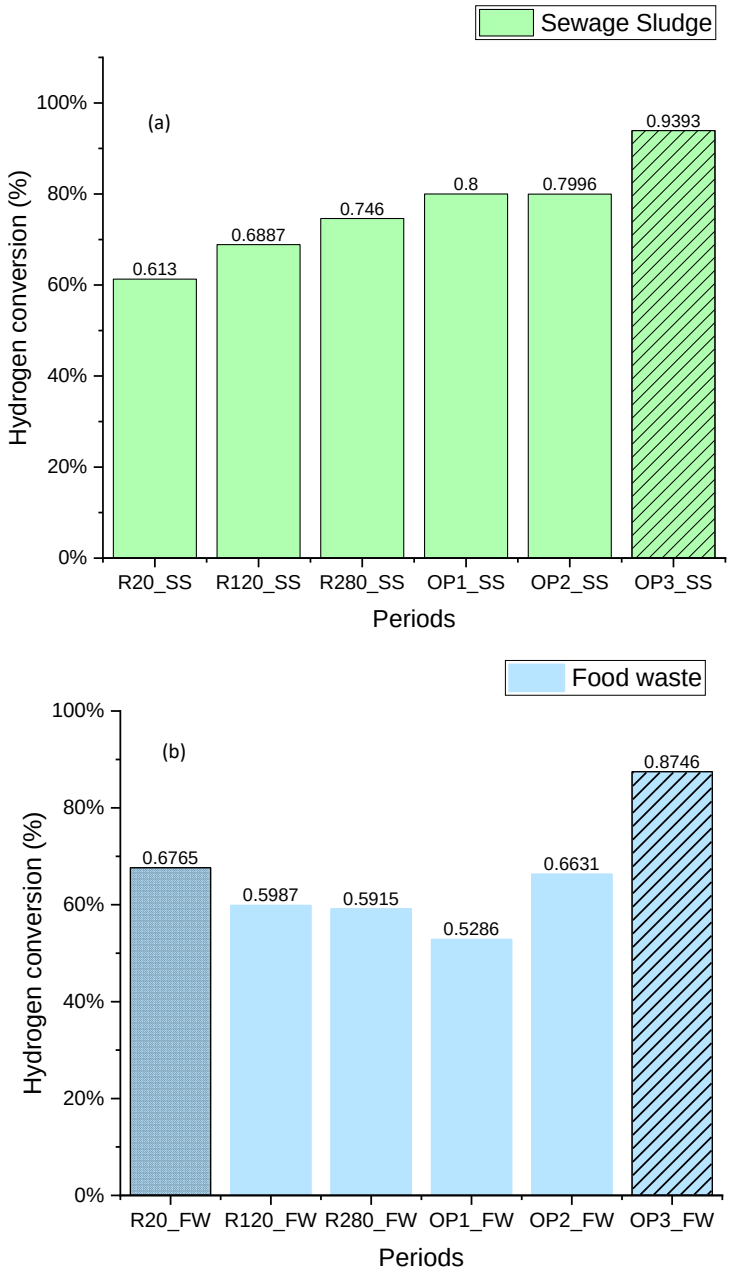

Figure 5-57 The hydrogen conversion of in-situ biomethanation in all periods using (a) sewage sludge and (b) Food waste Column with patterns indicate lower OLR values (at 1.5 (R20_FW) and 1 OLR (OP3_FW)

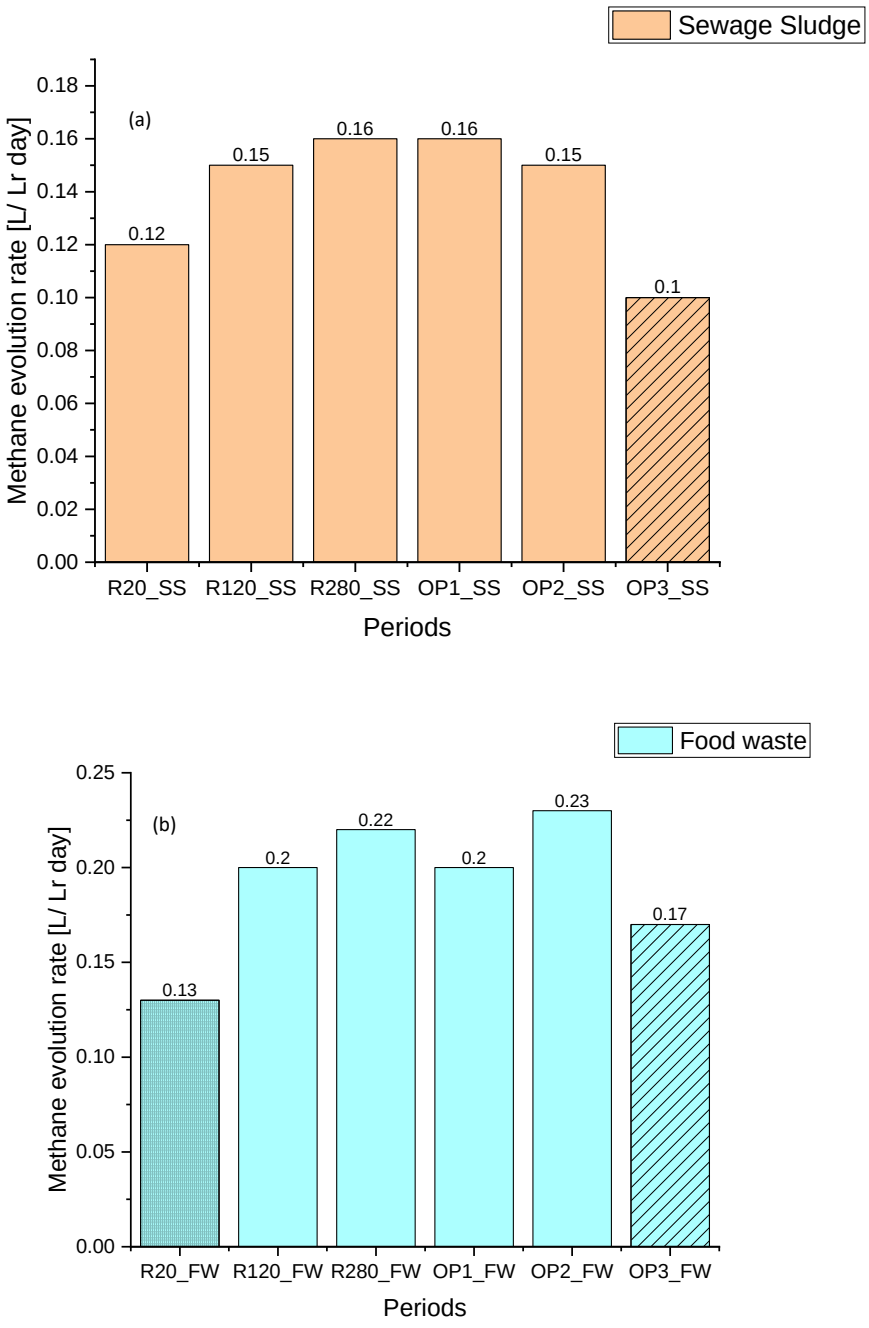

Figure 5-58 Methane evolution rate of in-situ biomethanation in all periods using (a) sewage sludge and (b) Food waste Column with patterns indicate lower OLR values (at 1.5 (R20_FW) and 1 OLR (OP3_FW)

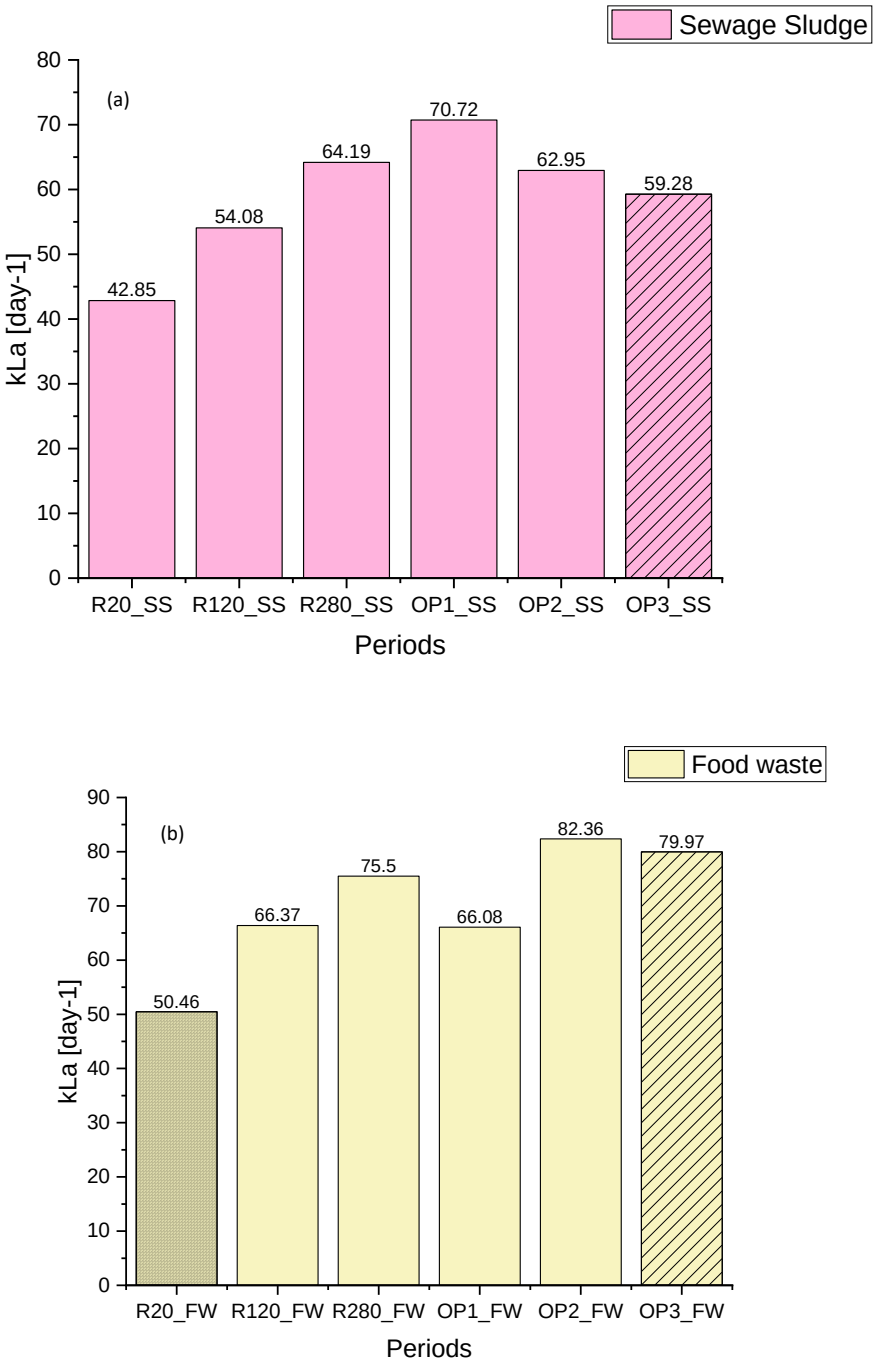

Figure 5-59 Gas-liquid mass transfer coefficient (kLa) of in-situ biomethanation in all periods using (a) sewage sludge and (b) Food waste Column with patterns indicate lower OLR values (at 1.5 (R20_FW) and 1 OLR (OP3_FW)

5.8 Disturbance due to reducing the organic loading rate.

The OLR showed a strong influence on the biomethanation process and performance. This was shown experimentally both during short feeding disturbances during the experiments and by comparing experiments carried out at different average OLR values. In this study, the use of an automatic feeding system illustrated the application of the feeding system in the practical application, where OLR, in some cases, has fluctuated or the quality of the feedstock was changed. The effect of the reduction of OLR in the continuous in-situ biomethanation system was summarised based on the phenomena that we have in the periods that occurred in the period below, see Table 5.8.

Table 5.8 The list of the case study of the event of reducing OLR

Period	Reactor	Days	Feedback control activated
R280	FW2	10-12	Yes
OP1	SS2	13	Yes
OP1	FW1	12	Yes
OP1	FW2	4	No
OP3	FW1	7	No

In the event of decreasing OLR, the immediate effect is that the gas flow rate will be decreased due to less degradation of OLR. The drop in gas flow will increase the gas retention time and lead to higher hydrogen conversion, resulting in a higher biomethanation extent. At the same time, the hydrogen will continue injecting and will cause the hydrogen content to increase. Due to the dilution effect of hydrogen injection and less additional biogas produced, the methane content and carbon dioxide content will decrease. The hydrogen conversion will decrease carbon dioxide, even more, followed by the increased pH due to the consumption of CO_2 in the liquid phase (bicarbonate, dissolved CO_2). On the other hand, the effect of hydrogen conversion will increase the methane content.

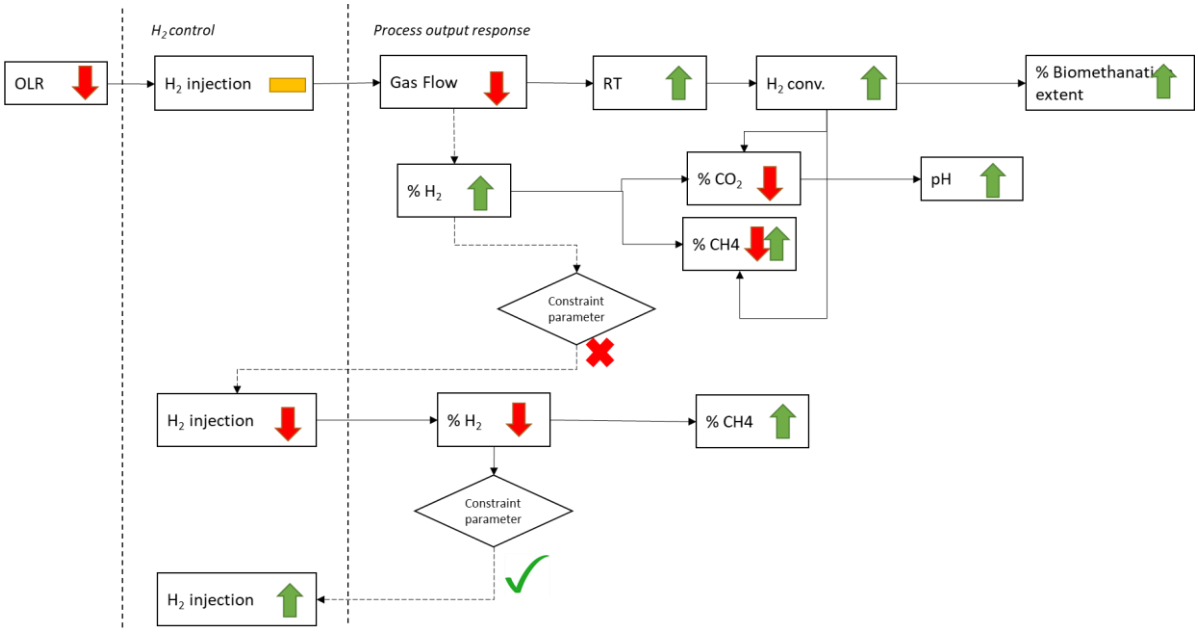

Figure 5-60 Schematic diagram of the effect of OLR reduction on the in-situ biomethanation process.

Due to the increase of hydrogen content as the consequence of reducing gas flow, there is a possibility that the increase of hydrogen is followed by the activation of feedback control (gas composition or pH). Then, the hydrogen injection rate will decrease. In this case, the change in the gas compositions is only due to the hydrogen conversion. It will result in a decrease in hydrogen and carbon dioxide along with an increase in methane. As soon as the constraint parameters are "*satisfied*", the hydrogen injection will back.

5.9 Conclusion

In all experiments, hydrogen tended to increase in the headspace after the start of the injection, from 11 % up to 36 % vol.; the increase of the hydrogen concentration as a "driving force" will lead to an increase in the gas-liquid mass transfer. The hydrogen concentration will increase until reaching an equilibrium with the injection rate, finally resulting in stable H_2 content in the headspace.

The highest methanation rate was achieved for;

- Sewage sludge (SS): an average of 0.16 L L^{-1} day^{-1} at period R_{280} and period OP1 correspond to the average gas composition of 63.3 % CH_4, 14.9 % CO_2, and 20.3 % H_2 at R280. 68.4 % CH_4, 13.2 % CO_2, and 18.6 % H_2 at period OP1.
- Food waste (FW), an average of 0.23 L L^{-1} day^{-1} at period OP2, corresponds to the gas composition of 55.3 % CH_4, 17.5 % CO_2, and 28.1 % H_2.

The greatest biomethanation extent was achieved in the following conditions:

- Sewage sludge (SS): an average value of 90 % at periods OP1 and OP3.
- Food waste (FW); an average value of 82 % at period OP3.

The average H_2 content was 22.5 % and 30.8 % at OLR of 2 in SS and FW, respectively, when injecting hydrogen at a stoichiometric requirement, while it was 6.8 % and 12.1 % at OLR1. This shows again how higher H_2 injection rates (at higher OLRs) require a higher driving force for the gas-liquid transfer to be in equilibrium.

Gas recirculation produced clear evidence of improvement in the biomethanation performance by showing a positive result in increasing the gas recirculation rate in both the sewage sludge and food waste digester. This is a further indication of the gas-liquid transfer limitations of the process, as increases in gas recirculation directly lead to an increase in a gas hold-up and finally on the surface area through which the gas-liquid transfer happens. The sewage sludge digester performed a better hydrogen conversion compared to the food waste digester in all periods. This was due to the lower biogas production, which affects the lower hydrogen injection rate. As a result, this increases the gas retention time, and having a higher gas retention time increases the gas-liquid mass transfer.

The OLR showed a strong influence on the biomethanation process and performance. This was shown experimentally both during short feeding disturbances during the experiments and by comparing experiments carried out at different average OLR values. Short disturbances (reductions) of OLR led to a clear pattern in in-situ biomethanation: first, a reduction of gas outflow; followed by an increase of H_2 content in the headspace; an increase of gas residence time; an increase of H_2 conversion; a decrease in CO_2 content and related increase of pH. As described in chapter five, the eventual intervention of the

feedback control in reducing the H_2 injection rate would also lead to an increase in the CH_4 content.

One of the most effective ways to increase the gas retention time is by reducing the organic loading rate. Reducing the OLR does not only reduce the biogas production but also reduces the hydrogen injection rate. As a result, this increases the contact time between the gas and the liquid. The maximum methane content in the headspace that can be reached in this period was up to 85 % in the sewage sludge digester and 76 % in the food waste digester, which was the highest compared to the other periods.

The levels of VFA and alkalinity ratio in the biomethanation reactors were, on average, comparable to the levels in the control reactors. This indicates that there was no noticeable accumulation of dissolved H_2 in the liquid phase, as it would happen in case of a biological process limitation; in that case, inhibition of acetogenesis would occur, as it would have happened in case of reaching high levels of dissolved H_2 in the liquid.

The monitoring and feedback control effectively maintained the biomethanation within the desired operational limits, depending on gas quality and pH levels. The feedback control was activated on most occasions after a disturbance on the substrate feeding rate to reduce the hydrogen injection rate in order to maintain the process outputs, mainly pH and H_2 content, below the process constraints

6. TECHNO-ECONOMIC ANALYSIS OF IN-SITU BIOMETHANATION: UK CASE STUDY

This chapter presents a techno-economic analysis of the in-situ biomethanation, and it employs an alternative approach to purchasing electricity based on the wholesale electricity price. The purchased electricity is used to produce hydrogen in order to fulfil the hydrogen requirement in the in-situ biomethanation process. A model was simulated to prioritise the purchase of electricity when the electricity is cheap.

6.1 Introduction

As mentioned in the literature review, the cost of electricity in power to gas applications, especially biological methanation, becomes a major contributor to the total operational cost, which could reach up to 80 % of the total operational expenses (OPEX). A flexible operation of an electrolyser to produce hydrogen could be a strategy to reduce the cost of electricity. Hydrogen production could be maximised when the price of electricity is low and reduced hydrogen production when the price of electricity is high. However, the description of this flexible operation of power to methane systems requires a more sophisticated model and techno-economic framework, particularly regarding the description of the electricity price fluctuations and the criteria for flexible operation of the electrolyser.

Participation in the wholesale electricity market could be a strategy to manage the electricity purchased in order to reduce the cost. For example, the production could be scheduled only when the price of electricity is low. However, the price of electricity has to be known in advance in order to avoid speculation about when hydrogen is needed to be produced. Participating in a day-ahead electricity market could be the answer to this issue, where electricity can be traded for the next 24 hours. Then hydrogen production could be scheduled one day before.

In order to take advantage of the hydrogen production when the electricity price is low, it will require hydrogen storage that could store excess hydrogen production that is not used

for biomethanation. In addition, the hydrogen in the hydrogen storage could be utilised when the electricity price is high. Therefore, the risk of producing hydrogen when the electricity price is high could be minimised.

The aim of this research is to develop an understanding of the key factors affecting the economic feasibility of biomethanation as a power to methane technology in the current market conditions in the UK.

Thus, the objectives of this study are as follows:

- Assess the yearly wholesale electricity price covered by the N2EX spot market and a comparison with the retail price.
- Evaluate the economic impact of the trade-off between flexible operation and reduced capacity factor of the electrolyser vs the H_2 storage and greater electrolyser utilisation as strategies for allowing continuous production of biomethane given the variation in the electricity purchase price.
- Compare the different scales and feedstock biomass (e.g. food waste vs farm manure systems) in relation to the different electricity markets they can be accessed (e.g. wholesale, vs supplier with flexible tariffs).
- Assess the effect of the variability in the electricity prices.

6.2 Methodology

6.2.1 System boundaries and scenarios definition

The system boundaries of the in-situ biomethanation techno-economic study consist of one anaerobic digestion system that is connected with a water electrolysis system to produce hydrogen (Figure 6-1). The main components of the system are the electrolyser, the H_2 storage and the AD system. The electrolysis system involves the supply of deionised (DI) water as a source to run the electrolyser. As mentioned in the literature review, this study will compare the economics of using an alkaline electrolyser and a PEM electrolyser. Both electrolysers have different operational performances that influence the amount of hydrogen produced as well as energy consumed. Therefore, it is interesting to explore the

key factors that may affect the economics of hydrogen production in relation to in-situ biomethanation applications.

The electrolyser is powered by the electricity that is purchased from the national grid. The electrolyser produces hydrogen and oxygen. The oxygen will be distributed or stored for selling at a later date, while the hydrogen will be connected with the hydrogen buffer storage before being injected into the anaerobic digester. Hydrogen buffer storage is required to balance the supply of hydrogen with the (fairly steady) demand for biomethanation in the AD system and allows storage of the excess daily hydrogen requirement, which can be used as reserve hydrogen during the higher electricity price. The maximum pressure of the hydrogen storage is assumed to be similar to the outlet pressure of the electrolyser (30bar). Therefore, the compressor is considered to be not necessary. The hydrogen then is injected into the anaerobic digester system to produce biomethane (in-situ biomethanation). The feedstock of the anaerobic digester is assumed to be of consistent quality and quantity, leading to the steady production of biogas. No revenue is considered from the effluent digestate, and its use on nearby farmland is assumed, with costs and benefits assumed external to the system analysed. The hydrogen from the electrolyser and the carbon dioxide from the anaerobic digestion process then is converted to methane. Therefore, the methane concentration in the biogas increases to more than 90 %. As a result, the biomethane produced can be injected into the national gas grid. The calorific value enrichment is required to comply with the regulations of injection biomethane, and blending biomethane with propane is included in this study, which is also a common method to increase the calorific value to meet the national gas standard (Bright *et al.*, 2011). If the methane quality does not meet the standard quality of the national gas grid, then the biomethane will be utilised as a vehicle fuel as an alternative utilisation.

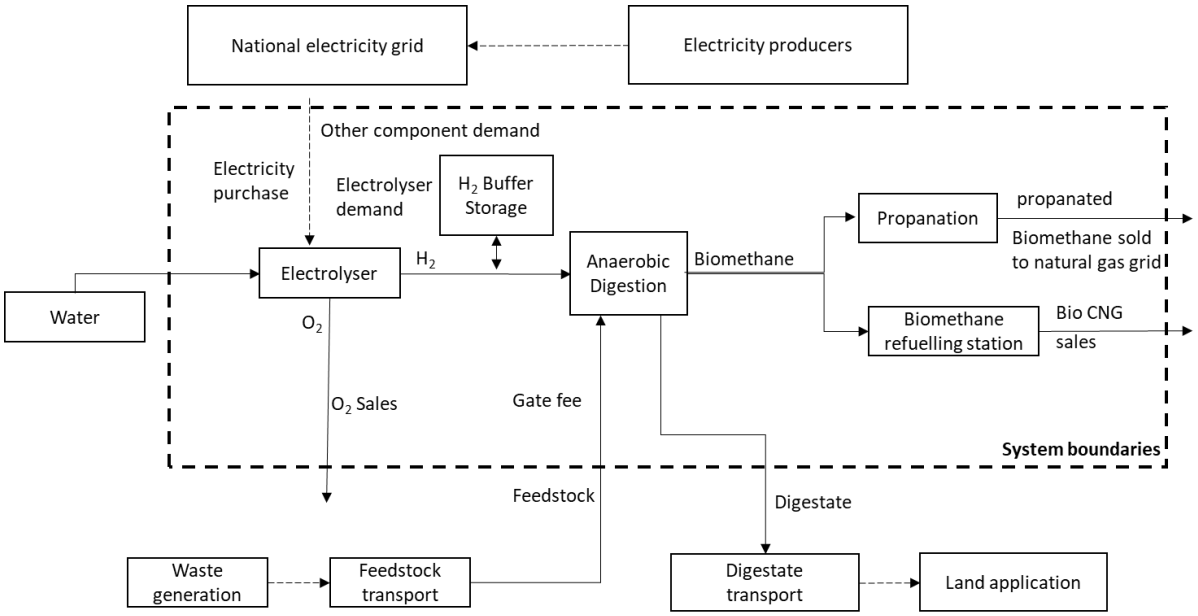

Figure 6-1 Schematic diagram of the techno-economic study of in-situ biomethanation.

In order to evaluate the influence of the flexible operation of electrolyser in reducing the operational cost of electricity, six different scenarios were designed to explore various possible conditions in the in-situ biomethanation process, as can be seen in

Table 6.1. The scenarios vary based on a) the utilisation of different electrolyser (proton exchange membrane electrolyser (PEMEL) or alkaline electrolyser (AEL)), b) different sizes of the electrolyser-based capacity factor, c) different sizes of the digester and its potential alternative utilisation of biomethane. For all scenarios, the hydrogen is produced through the electrolyser that is powered by the electricity that is purchased from the national electricity grid. The electricity price used in all scenarios is based on the wholesale electricity price in 2019, and parameters in scenario 2 were used as a baseline scenario. The dynamic electrolyser operation applied is based on the wholesale electricity prices, and the Capacity factor is defined as the annual energy consumption of the electrolyser capacity installed, as described in equation 6-1 :

$$Capacity\ factor\ (CF) = \frac{Annual\ power\ consumption\ in\ electrolyser}{Maximum\ annual\ electricity\ consumption\ by\ the\ electrolyser} \quad \text{Equation 6-1}$$

Table 6.1 Description of the scenarios.

	AD feedstock	Scale of AD (tpa)	Electrolyser type	Capacity factor	Biomethane utilisation
Scenario 1	Food waste	25,000	AEL	80 %	Gas grid
Scenario 2	Food waste	25,000	PEM	80 %	Gas grid
Scenario 3	Food waste	25,000	PEM	60 %	Gas grid
Scenario 4	Food waste	25,000	PEM	100 %	Gas grid
Scenario 5	Manure	7,500	PEM	80 %	Gas grid
Scenario 6	Manure	7,500	PEM	80 %	refuelling station

In-situ biomethanation has more challenging process compared to ex-situ biomethanation. During the biomethanation process, the conversion of carbon dioxide to methane distorts the bicarbonate buffering system, increases the pH and changes the activity of the microorganism (Tao *et al.*, 2019). Furthermore, injecting hydrogen into the anaerobic digester could also change the domination of the methanogenic pathways (Bassani *et al.*, 2015). In addition, the hydrogen mass-liquid transfer remains the biggest challenge in this process (Voelklein, Rusmanis and Murphy, 2019). In the literature, it is reported that the in-situ biomethanation process can upgrade the methane content by up to 95 % (Luo and Angelidaki, 2013; Díaz *et al.*, 2015). This study assumed that the CO_2 conversion into methane would be 95 %, also considered by Seifert, Rittmann and Herwig (2014).

As a baseline for the anaerobic digestion system, the anaerobic digestion plant was set to process 25,000 tpa of food waste with an annual biogas potential of 3,997,241 m^3/a and methane and carbon dioxide composition being 58 % and 42 %, respectively. For the farm-scale anaerobic digester plant, the capacity of the plant is assumed to be 7,500 tpa of manure. The biogas potential in the farm-scale AD is 475,000 m3/a, with 60 % and 40 % methane and carbon dioxide compositions, respectively. The characteristics and calculation of the AD system are based on AD modelling tools from the Bioenergy and

Organic Resource Research Groups (BORRG) at the University of Southampton (Banks *et al.*, 2015). Both scales of AD plants were selected based on the actual plant size in the UK according to the NNFCC database (NNFCC, 2020). To simplify the analysis, the biogas production and biogas composition are assumed to be constant all the time for both AD systems. Therefore, the annual requirement of hydrogen that is required for biological methanation can be calculated stoichiometrically according to the Sabatier reaction in the proportion H_2:CO_2 is 4:1 based on the CO2 production, and the target biomethane composition in the resulting biogas (95 %).

The data and assumptions for the techno-economic analysis were provided based on peer-reviewed literature. The wholesale electricity price was provided by N2EX Nord Pool day-ahead price in the UK from 2018-2020.

6.2.2 Modelling the Dynamic operation of the electrolyser

The basis of the electrolyser's dynamic operation is that, generally, hydrogen is produced when the electricity is cheaper. In order to model this in the TEA, a hypothetical scenario was considered where the electricity is purchased from the wholesale day-ahead market. Where participants can sell or buy electricity in the next 24 hours. This will allow the operation of hydrogen production scheduled at least one day before. This study assumed that the plant owner has access to the wholesale day-ahead electricity market. Nowadays, it is possible that customers can purchase electricity based on the wholesale electricity market. For example, one of the energy providers in the UK (Octopus Energy) has introduced and operates an agile smart tariff, where the customer could have access to half-hourly pricing of the wholesale market rates (Steele, 2019). The customer then has potentially saving cost by the consumed electricity when the electricity is low or even have an advantage of being paid for using the electricity when the electricity goes negative.

The electrolyser is assumed to be operated at 8760 hr/year without shutting down in order to maintain the temperature of the electrolyser. However, the production is managed to be operated at maximum load or minimum load based on the day-ahead electricity price. In this case, the electrolyser is assumed to be able to switch from maximum to minimum load rapidly. The electrolyser produces hydrogen at maximum load by prioritising the lower

price until the daily requirement is fulfilled. Once the hydrogen requirement is fulfilled, the electrolyser operates at the minimum load. In order to maximise the use of hydrogen storage, even though the daily requirement is fulfilled, the electrolyser will be operated at maximum load when the wholesale electricity price is below a threshold price. In all scenarios, the threshold price was set to be £43/MWh, which is 50 % of the average annual electricity price in 2019. This approach could save production costs by reducing energy usage when the electricity price is high.

In this study, the minimum load of the PEM electrolyser was assumed to be 5 % of the maximum load and 30 % for the Alkaline electrolyser (Lehner *et al.*, 2014; Götz *et al.*, 2016) (Table 6.2). According to the literature, the specific electricity consumption for PEM is in the range of 4.2-5.6 kWh/m^3H_2 and 4.2-5.9 kWh/m^3H_2 for the alkaline electrolyser (Carmo *et al.*, 2013). In this study, the specific electricity consumption for the PEM and Alkaline were assumed to be 5.13 and 4.59 kWh/m^3H_2, respectively (Matute, Yusta and Correas, 2019). Furthermore, in this study, the efficiency was assumed to be similar for the same type of electrolyser (e.g. in scenarios 2,3 and 4). In this study, the water consumption was assumed to be 15 L/m^3 H_2 produced, which was considered the same between AEL and PEM electrolyser (Matute, Yusta and Correas, 2019).

Table 6.2 Technical assumptions for scenarios 1 (Alkaline) and 2 (PEM).

Parameters	Unit	PEM	Alkaline	Ref
Specific electricity consumption	kWh/m^3H2	5.13	4.59	(Matute, Yusta and Correas, 2019)
Electrolyser efficiency (HHV)	%	69.24	77.39	(Carmo *et al.*, 2013)
DI water consumption	L/m^3H_2	15	15	(Matute, Yusta and Correas, 2019)
Stack lifetime	hours	50,000	90,000	(Schmidt *et al.*, 2017; Matute, Yusta and Correas, 2019)
Minimum load	%	5	30	(McDonagh *et al.*, 2018)
Electrolyser outlet pressure	bar	30	30	(Bertuccioli *et al.*, 2014)
H2 storage loses	%	2	2	This study
Hydrogen storage	m^3	9,119	9,119	This study
Propane adjustment	% of biomethane	4	4	(ADBA, 2020)

The hydrogen that is produced above the hydrogen daily requirement is called excess hydrogen production. At the baseline scenarios, the hydrogen storage size was assumed to be able to store 50% of the daily hydrogen requirement, which is 9,119 m^3.

The excess hydrogen that is produced during the minimum load production is collected in hydrogen buffer storage. The idea of the use of hydrogen buffer storage is for short-term storage. Therefore, the storage material is as simple as tank storage.

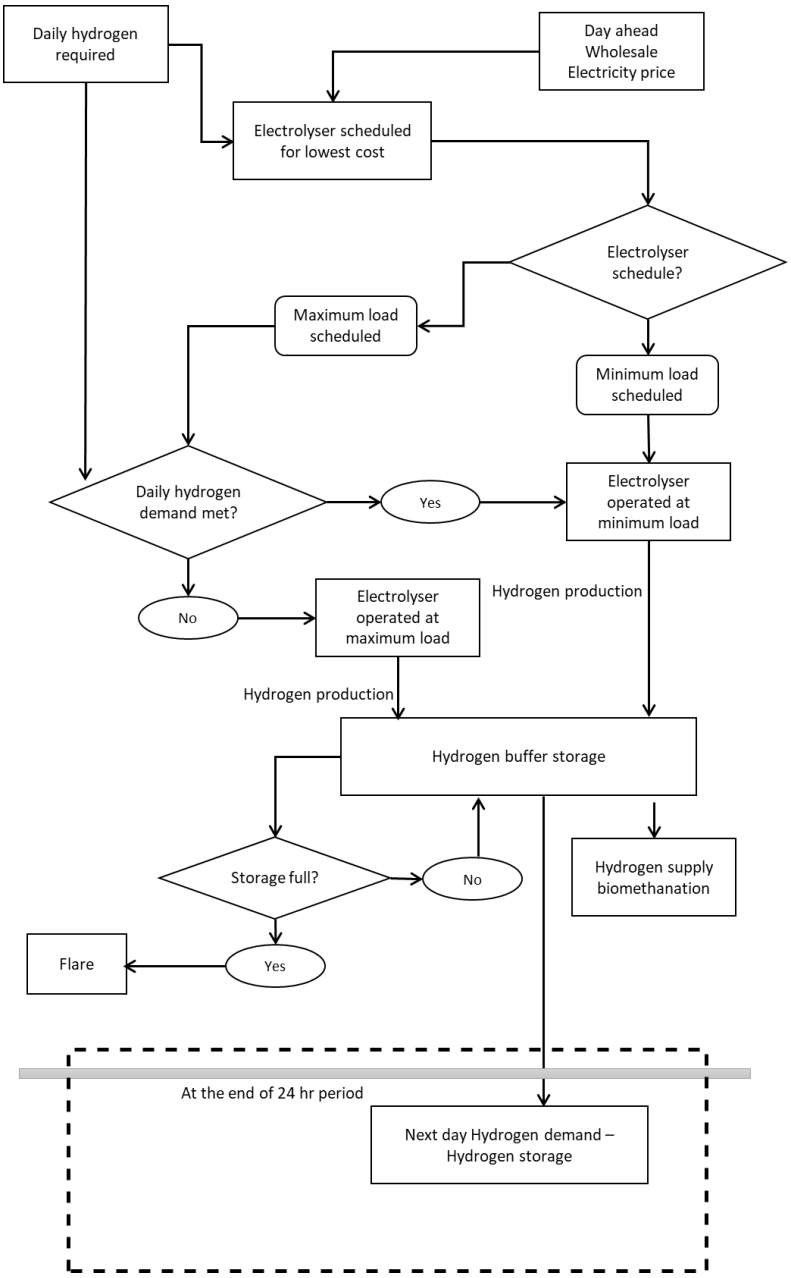

Figure 6-2 Decision tree for the running of the electrolyser based on the electricity price.

The amount of hydrogen in the buffer storage is calculated as the subtraction of the daily requirement for the next day and so on. This approach could minimise the hydrogen at the maximum production when the electricity price is higher and given by:

$$H_{2\,req} = H_{2\,bio} - H_{2\,storage} \qquad \text{Equation 6-2}$$

Where,

$H_{2\,req} = Hydrogen\ daily\ requirement$

$H_{2\,bio} = Hydrogen\ that\ is\ required\ for\ biomethanation$

$H_{2\,storage} = Hydrogen\ that\ is\ available\ in\ the\ hydrogen\ storage$

The electrolyser daily schedule is calculated on an hourly basis in order to deliver the daily requirement of hydrogen (minus hydrogen available in the storage from the previous day) at the cheapest cost. A daily simulation follows the time frame on a wholesale day-ahead market, which starts from 00.00 and ends at the same time on the next day. The hydrogen is produced based on an hourly basis according to the capacity of the electrolyser to produce hydrogen in m^3/hr. When the daily requirement of hydrogen is fulfilled, the hydrogen then will be produced on a minimum load. The extra daily production of hydrogen is categorised as an excess production that will be considered as a reduction of daily requirements for the next day's production. For instance, the hydrogen requirement for today's production will be the daily hydrogen production for biomethanation minus the hydrogen that is available in the hydrogen storage (if any). The hydrogen is (continuously) taken from the storage tank to meet the immediate demand of the in-situ biomethanation; excess hydrogen production is stored in hydrogen buffer storage unless it is full, in which case the hydrogen will be flared. Once the hydrogen demand is met, and according to the electrolyser schedule, the electrolyser operates at the minimum load for the remainder of the day. In addition, there is also the command to produce hydrogen on the maximum load when the wholesale price is below a certain threshold. In this study, the default threshold price is an average of the annual wholesale price.

The potential of the hydrogen losses during the distribution to the digester was assumed to be 2 % of the total hydrogen production on a daily basis. In addition, carbon dioxide is required to keep the chemical balance in the anaerobic digester system. In this study, it was assumed that 95 % of the CO_2 and H_2 that is injected into the digester was converted into methane (Voelklein, Rusmanis and Murphy, 2019). The biogas production process was assumed to be stable, and thus the demand for hydrogen for the in-situ biomethanation was also stable to achieve the required output biomethane quality.

6.2.3 Economic analysis

In the economic analysis, the main objective was to evaluate the economic feasibility study of implementing in-situ biomethanation in six different scenarios, based on the type and size of the electrolyser and the size of the anaerobic digestion plant.

The Capital Expenses (CAPEX) and Operational Expenses (OPEX) were estimated based on the literature by considering the scaling and inflation rate to the year of study (2019) in order to achieve the best estimates. The investment in the AD plant was assumed to be equal to the installed AD plant, including the equipment and construction. In this study, the investment cost of the anaerobic digestion plant to process the 25,000 tpa of food waste plant was estimated based on the literature data (SKM Enviros, 2011) and considering an inflation rate of 2 %. The investment cost of the electrolyser was assumed to be an installed electrolyser with the assumption of 950 (£/kW) for the PEM and 600 (£/kW) for the Alkaline electrolyser with a scaling factor of 0.75 for both cases (Götz *et al.*, 2016; IRENA, 2018). Finally, the hydrogen storage cost was calculated according to the literature with a scaling factor of 0.7 (Pääkkönen, Tolvanen and Rintala, 2018). The scaling method of the calculation is defined in equation 6-3 as follows:

$$C_b = C_a \left(\frac{S_b}{S_a}\right)^f \qquad \text{Equation 6-3}$$

Where,

$C_b = actual\ cost$
$C_a = base\ cost$
$S_b = actual\ capacity$
$S_a = base\ capacity$
$f = scaling\ factor$

The general economic assumption can be seen in Table 6.3.

Table 6.3 General economic assumption.

Parameter	Value	Unit	Reference
Project lifetime	20	Years	(Carmo *et al.*, 2013)
Inflation rate	2	%	(Statista, 2020)
Discount rate	10	%	(McDonagh *et al.*, 2018)

As the base case scenario, the electricity cost for the electrolyser was calculated using a day-ahead hourly data of the wholesale electricity price in 2019 in the UK. According to the Ofgem data, the wholesale price could be made up to 32.36 % of the household's total electricity bills (Ofgem, no date). In other references, the wholesale electricity price contributed in the range of 36 to 42 % of the total tariff (Helm, 2017). The objective of this study was to provide the demand of hydrogen requirement for in-situ biomethanation by using the cheapest electricity price in the day-ahead scheme. This approach simulates a large consumer with access to a variable tariff influenced by the wholesale market. However, other cost elements such as network cost, operating cost, VAT, etc., are still assumed to be applied. In this study, the wholesale price was assumed to be 36 % of the total tariff.

The hydrogen storage was assumed to be a steel tank. The investment of this buffer storage tank was estimated according to the literature (Pääkkönen, Tolvanen and Rintala, 2018) in the equation 6-4 as follows:

$$Storage\ investment\ cost = 5800 + 1600\ (S)^n \qquad \text{Equation 6-4}$$

Where,

S is the size of storage (m^3), and n is the scaling factor (n=0.7)

Table 6.4 Base case of the economic assumption for the electrolysis.

Parameter	Unit	PEM	Alkaline	Reference
Installed cost electrolyser	£/kW	950	600	(Schmidt *et al.*, 2017)
Insurance cost	% of CAPEX	0.7	0.7	(Vo *et al.*, 2018)
Maintenance cost	% of CAPEX	2	2	(McDonagh *et al.*, 2018)
Water purchase price	£/m3	0.87	0.87	(Michailos *et al.*, 2020)
Stack replacement cost	% of installed cost	30	45	(IRENA, 2018)
Cost of propane	p/kWh	4.65	4.65	(Breyer *et al.*, 2015)
Oxygen selling price	£/ton	70	70	(Michailos *et al.*, 2020)

The project's revenue was obtained from the sold biomethane to the grid or through a local refuelling station. Also, the sold oxygen was considered as an additional benefit from the electrolyser of 70 £/ton (Breyer *et al.*, 2015). The incentive, either Renewable Heat Incentive (RHI) or Renewable Transport Fuel Certificate (RTFC), were included as sources of revenue with the value of 62.0 £/MWh (ADBA, 2020; Michailos *et al.*, 2020) for the RHI and 54.72 £/MWh (ADBA, 2020) for the RTFO.

The economic evaluation was based on the Levelised cost of energy (*LCOE*) as calculated in equation 6-5 as follows:

$$LCOE = \frac{\sum_{i=0}^{n} \frac{total\ cost in\ year\ i}{(1+r)^i}}{\sum_{i=0}^{n} \frac{MWh\ of\ gas\ produced\ in\ year\ i}{(1+r)^i}} \qquad \text{Equation 6-5}$$

In scenarios 5 and 6, the alternative utilisation of biomethane required different investment values, operational costs, and revenue. Therefore, the economic evaluation is calculated based on the net present value (NPV). The NPV is calculated based on the equation 6-6 as follows:

$$\text{NPV} = -Initial\ investment + \sum_{i=1}^{T} \frac{C_i}{(1+r)^i} \qquad \text{Equation 6-6}$$

where C is the cash flow in the year *i*, *r* is the discount rate, and *T* is the economic lifetime, and all revenues and costs were discounted based on the discount rate *r*.

6.2.4 Sensitivity analysis

The most critical parameter in the biomethanation project is the electricity price to produce hydrogen using the electrolyser (Lehner *et al.*, 2014). The electricity price has the biggest uncertainty factor that will be difficult to predict. Sensitivity analysis allows the evaluation of the effect of electricity price on the net present value and payback period. The input of electricity price will change based on data in 2019, with the option to simulate if the data in 2019 will increase or decrease by 25 %. In addition, a synthetic dataset was also made to simulate the fluctuation of electricity in the future and see how this input will influence the result of the feasibility study. The sensitivity analysis includes other uncertainty parameters, such as the price of installed electrolyser, discount rate, electricity price, and electrolyser efficiency.

6.3 Results and Discussion

6.3.1 Variability of the cost of electricity and calculation of retail price

The summary of daily day-ahead wholesale electricity price characteristics during 2018 and 2020 can be seen in Table 6.5. In general, the average daily wholesale electricity price in 2018 is £57.44/MWh, which is higher compared to 2019 and 2020 with £42.94/MWh and £35.25/MWh. A daily day-ahead price is basically an average of an hourly day-ahead price. In order to show the distribution in detail, the hourly wholesale electricity price is presented in Figure 6-3.

Table 6.5 Summary of wholesale electricity price distribution between 2018-2020.

Wholesale daily electricity price (GBP/MWh)	2018	2019	2020
Average	57.44	42.94	35.25
Maximum	92.57	75.53	77.88
Minimum	40.47	26.55	-10.13
Mean	57.44	42.94	35.28
Median	56.57	41.85	33.59

In 2018, the highest day-ahead hourly wholesale electricity price distribution was found in the range of £46-50/MWh, with 17.8 % of the total distribution. However, 96 % of the

distribution in 2018 was found above £40/MWh, and that makes the cost of electricity in 2018 the highest of the three years considered; for comparison, the distribution of prices above £40/MWh in 2019 and 2020 are 55 % and 23 %, respectively. In addition, it can be seen that the yearly average in 2018 was also the highest at £57.44/MWh, and the lowest was in the year 2020 with an average of £35.28/MWh.

Surprisingly, the cost of electricity in 2018 has the smallest range (£182/MWh) of the distribution between the maximum and minimum values compared to 2019 (£279/MWh, the biggest range) and 2020 (£231/MWh). Interestingly, in 2020 about 1 % of the price was found to be negative, which could benefit consumers (although consumers cannot directly access this wholesale market). According to the profile of electricity price distribution during 2018-2020 (Figure 6-3), the power to gas project could face financial challenges due to large fluctuations (uncertainty) in electricity price. The data that is shown in the figure is on a daily basis of day-ahead hourly wholesale electricity price, including the daily minimum, maximum and average. The trend of wholesale electricity price in 2019 is lower than wholesale electricity price in 2018 but higher than in 2020. For this reason, the wholesale electricity price in 2019 is used as a baseline of wholesale electricity in this study.

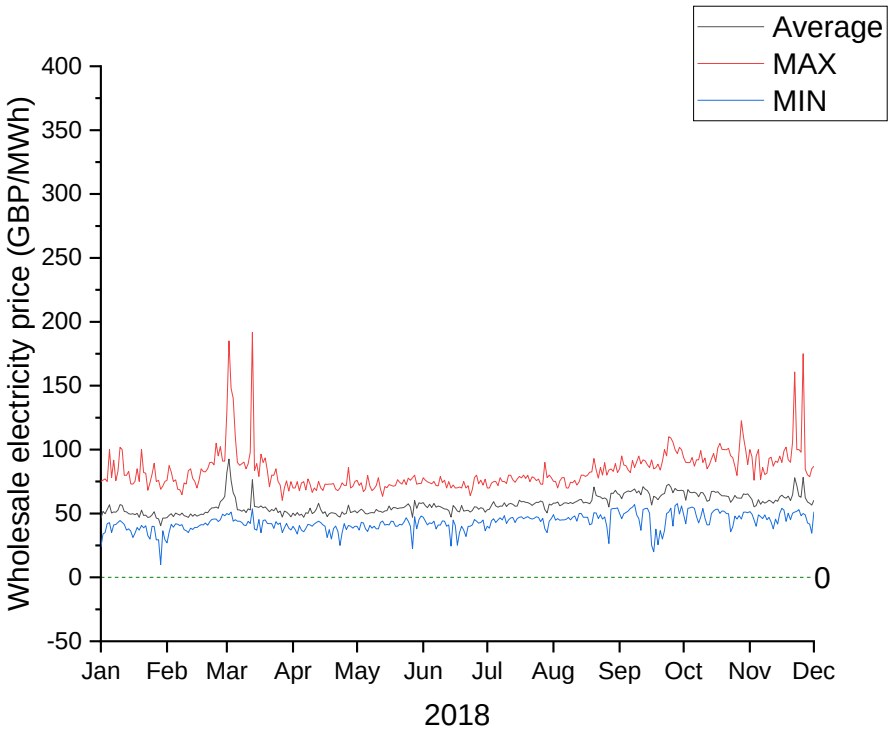

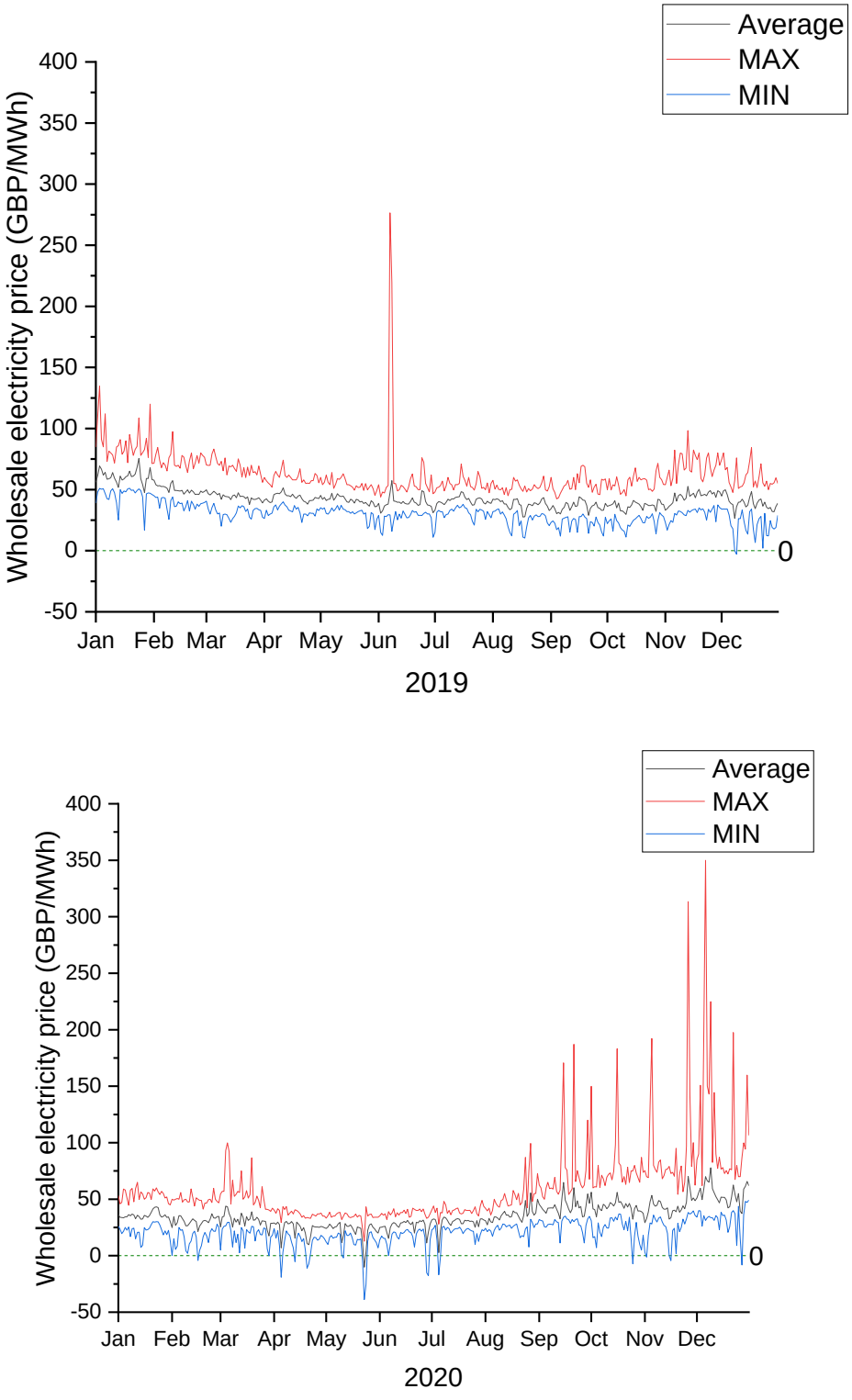

Figure 6-3 Wholesale electricity price distribution during the years 2018-2020.

The proportion of the wholesale price to the total tariff can be studied by comparing the wholesale price and the retail price. One of the distributors (Octopus Energy) has introduced agile pricing based on wholesale electricity. This means that the consumer can

use their electricity when the wholesale price is cheaper, thus avoiding the use of electricity when the demand is high. This saves on the consumer's energy bills.

A comparison between the wholesale and retail electricity prices based on the 2019 price can be seen in Figure 6.4. On average, the wholesale price contributes 41.83 % to the total retail electricity price (Octopus energy). Other cost elements, such as distribution, operating, profit, and taxes, are still unclear. The distribution cost varies depending on the location, while the operating cost and profit depend on the distributor company. However, the proportion of wholesale electricity price to the electricity retail price gives a figure of the contribution of wholesale electricity price to the retail price. In this study, the assumption of the synthetic wholesale price that is calculated based on the retail price for the economic evaluation is 50 %, with the assumption that 7 % of the distributor profit can be cut due to the direct participation in the wholesale market (Business electricity price, 2021).

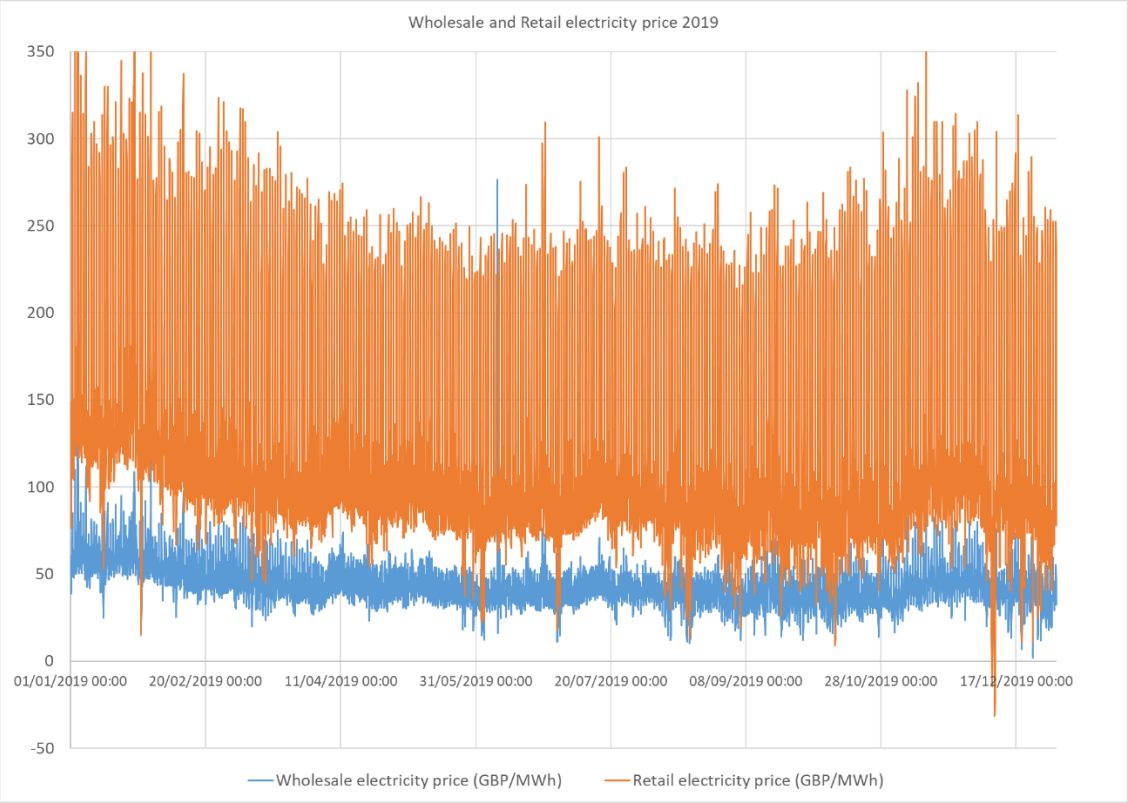

Figure 6-4 Wholesale Nord pool electricity price vs Octopus retail electricity price distribution in 2019.

6.3.2 Variability of hydrogen production cost

The effect of the electricity price on the cost of electricity in relation to the fluctuating wholesale electricity price between 2018 and 2020 can be seen in Table 6.5. The evaluation was performed with the assumption that there was an 80 % of capacity factor.

To study the effect of electricity price on hydrogen production cost, the annual hydrogen requirement is calculated according to the reaction stoichiometry (equation 2-8) (Jürgensen *et al.*, 2015). Theoretical annual biogas production from 25,000 tpa of food waste in an anaerobic digestion plant is 3,997,241 m^3 or about 456 m^3/hr (Banks *et al.*, 2015). With a volumetric composition of CH_4:CO_2 is 58 %: 48 %, the amount of CO_2 available for biomethanation would be 1,678,841 m^3/year. Therefore, the amount of hydrogen required is 6,715,366 m^3/year or 18,398 m^3/day. The hydrogen storage design is assumed to store the hydrogen sufficient for at least twelve hours of daily hydrogen requirement, which is 9,119 m^3. The scheduling of the electrolyser on a daily basis was calculated using the decision tree in Figure 6-2.

To produce the required amount of hydrogen with 80 % of the capacity factor, the use of wholesale price in 2018 was unable to fulfil the annual hydrogen requirement due to higher electricity prices and the use of the same threshold to produce the maximum load. With higher prices, the chance to save hydrogen production on daily basis at low electricity prices is smaller than in 2019 and 2020. Furthermore, with the same size of electrolyser, using the wholesale electricity price was not able to maximise the production of hydrogen by keep producing hydrogen at maximum load when the electricity price is cheaper than the threshold of 43 £/MWh. On the other hand, the electrolyser forces to produce the hydrogen even when the electricity price is high to fulfil daily hydrogen requirements.

Table 6.6 Cost of the electricity using different wholesale electricity prices.

Wholesale price year	Unit	2018	2019	2020
Electrolyser size	MW	4.18	4.92	4.92
Hydrogen production	m^3	5,719,357	6,716,564	6,720,210
Hydrogen produced	% requirement	85.17 %	100.02 %	100.07 %
Energy consumption	MWh	29,340	34,456	34,475
Cost of electricity	£	3,197,301	2,797,488	2,240,329
Maximum load hours	hr	6,914	6,907	6,911
Minimum load hours	hr	1,846	1,853	1,849
Average price paid	£/MWh	53.41	39.78	31.84

Looking at the energy consumption, the cost of electricity using the price of electricity in 2018 is the highest compared to 2019 and 2020, and this is with even only 29,340 MWh of energy consumed, which is around 15 % lower compared to 2019 and 2020. The average hourly wholesale electricity price in 2018 was 53.41 £/MWh. This is enough to explain why the price distribution in 2018 increased hydrogen production costs.

6.3.3 Using AEL and PEM to produce hydrogen for in-situ biomethanation

The use of different electrolyser technologies was explored: AEL (scenario 1) and PEM (scenario 2). These are commonly used as electrolysers in the application of power to gas (Götz *et al.*, 2016; IRENA, 2018). The technical parameters of electrolysers are mentioned in Table 6.2.

To compare the in-situ biomethanation performance indicators using AEL and PEM, both the electrolysers were simulated to produce similar hydrogen requirements (6,715,366 m^3 or 18,398 m^3/day), hydrogen storage (9,119 m^3) and with a capacity factor of 80 %. The simulation was performed using wholesale electricity data in 2019. As per the decision tree (Figure **6-2**), the daily set point for electrolyser usage is determined by the daily demand and the amount of stored hydrogen; as can be seen in Table 6.7, the maximum hydrogen in the storage was 73.0 % in the scenario 1, while in the scenario 2 was 58.9 %.

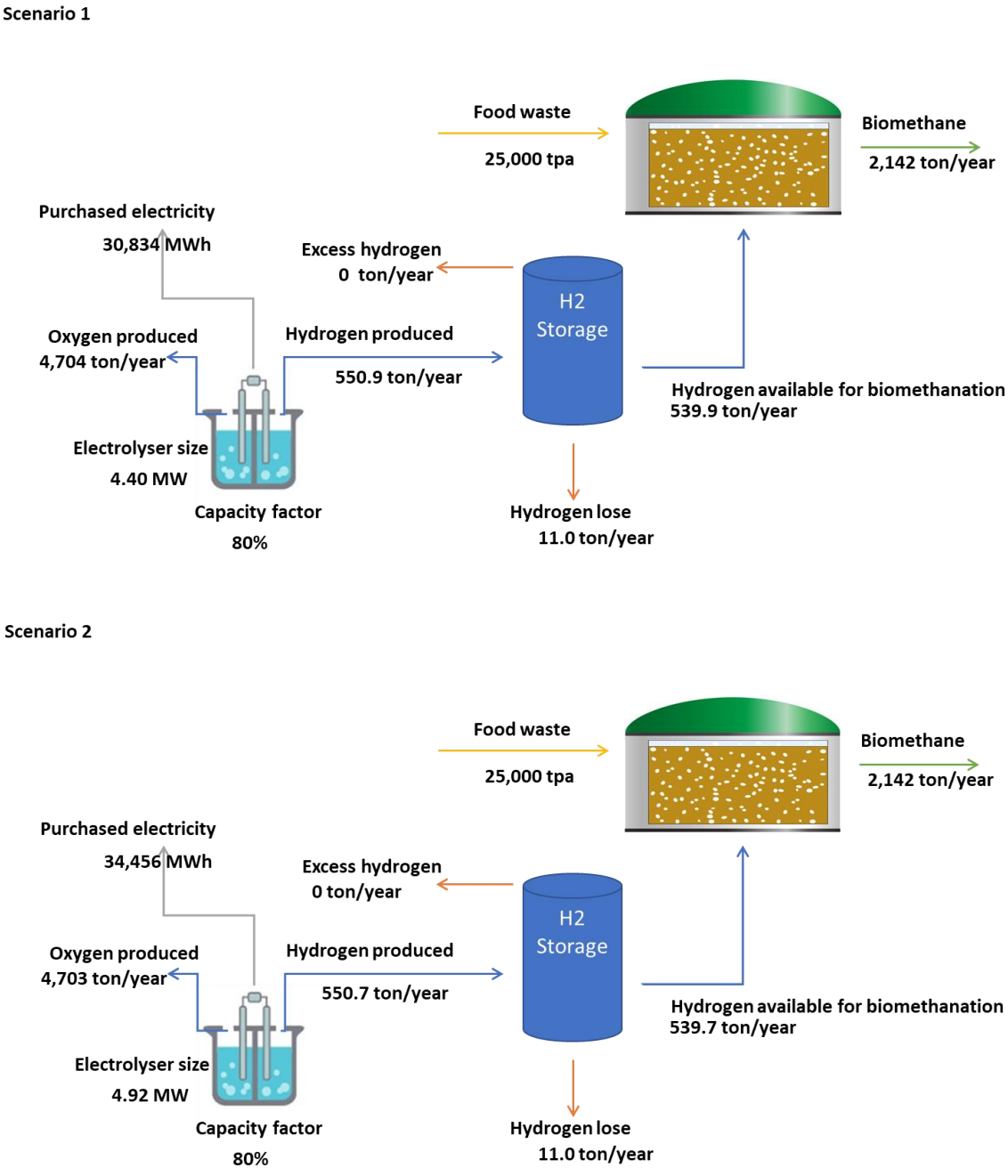

Figure 6-5 Schematic of the basic mass balance for the scenarios 1 (AEL) and 2 (PEM).

AEL has a higher efficiency than PEM electrolyser (IRENA, 2018), so the size of AEL is smaller than PEM's at the same capacity factor. Higher efficiency of the electrolyser also affected the energy consumption, where PEM required 11.7 % more electricity to produce the same hydrogen demand. No excess hydrogen is released during the production, meaning that the hydrogen storage size is big enough to store the hydrogen produced. In scenario 1 (AEL), the hydrogen produced by the electrolyser is slightly higher than the hydrogen

produced in scenario 2 (PEM). This is due to the higher electrolyser efficiency of AEL compared to PEM electrolyser.

Less energy required to produce hydrogen means savings on the cost of electricity. Table 6.6 shows that the annual electricity consumption in scenario 1 was still lower compared to scenario 2. This is because the PEM electrolyser has a lower energy requirement when operating at the minimum load (Bertuccioli *et al.*, 2014). The proportion of the time operating at maximum load in scenario 1 was 71 % (6,256 hr), which was lower than that for scenario 2, which was 79 % (6,907 hr). In this case, the PEM in scenario 2 must work harder to produce hydrogen at the maximum load. On the other hand, the operation on the minimum load is the second priority, meaning that the electricity price when operating at the minimum load could be higher than when operating at the maximum load. However, the benefit of using the PEM in scenario 2 was still not able to compete with the AEL in order to save on the annual electricity cost as the hydrogen production by using AEL, where the use of the PEM in scenario 2 has a 10.4 % higher electricity cost compared to the use of the AEL electrolyser in scenario 1, and that was due to the lower energy usage.

Table 6.7 Summary of the hydrogen production using different electrolysers.

	Unit	Scenario 1 (AEL)	Scenario 2 (PEM)
Capacity factor	%	80 %	80 %
Electrolyser size	MW	4.40	4.92
Hydrogen produced	% of requirement	100.16 %	100.09 %
Maximum load hours	hr	6,256	6,907
Minimum load hours	hr	2,504	1,853
Maximum hydrogen in the storage	m^3	6,717	5,421
Minimum hydrogen in the storage	m^3	2,195	291
Electricity consumption	MWh	30,834	34,456
Annual Cost of electricity	£	3,447,832	3,807,208
Average daily cost of electricity	£/ day	9,446	10,431

The maximum and minimum hydrogen in the storage that is presented in Table 6.7 is the amount of daily minimum and maximum hydrogen in the storage in one year of production (2019).

The use of hydrogen storage in scenario 2 could be reduced to 50 % of the storage capacity, where 92 % of the time, the hydrogen capacity was within a range from 0-50 %. On the other hand, in scenario 1, the hydrogen storage appears to be more utilised for about 75 % of the capacity, where it was used about 97 % of the time within the range 0-50 %. However, there is a potential saving of capital investment by reducing the size of the electrolyser. However, the amount of the savings was not significant, which is only 0.3 % compared to the total CAPEX.

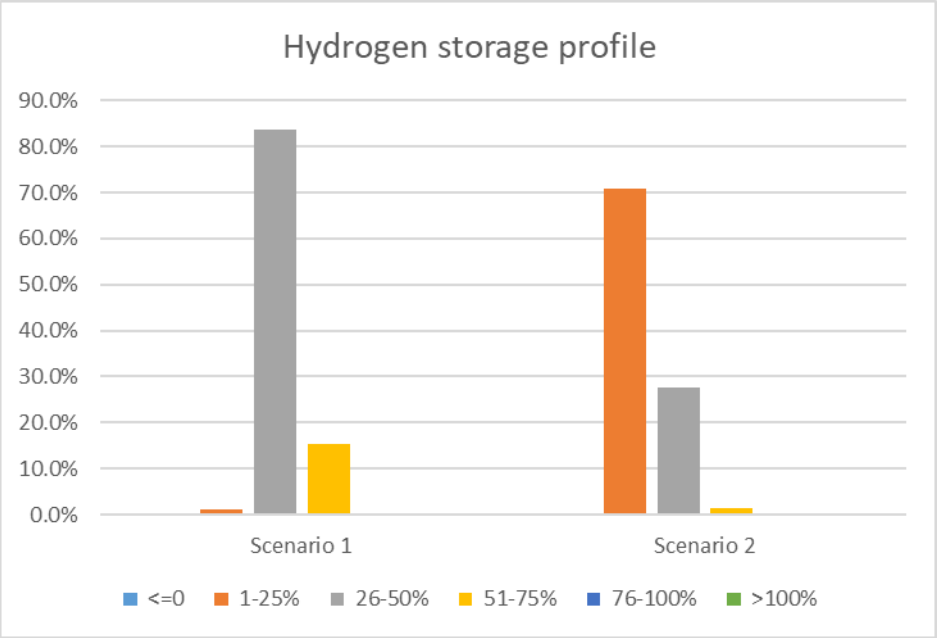

Figure 6-6 Hydrogen storage profile in scenarios 1 and 2.

From this evaluation, it is concluded that the efficiency of the electrolyser plays a significant role in reducing the use of energy and the electricity cost. Therefore, it appears that the use of the AEL in scenario 1 is more promising than the use of the PEM in scenario 2. Moreover, the investment cost of the AEL is significantly lower than that of the PEM (Götz *et al.*, 2016; IRENA, 2018). However, in the application of the in-situ biomethanation, the PEM electrolyser is preferable in terms of the flexibility in the operating range and also has a shorter response time that is required in this application (Eichman, Townsend and Melaina, 2016).

6.3.4 Using different capacity factors for the PEM electrolyser to produce hydrogen for in-situ biomethanation

The capacity factor determines the size of the electrolyser. In this part, the study compares the effect of capacity factor and electrolyser size on the overall operational cost, in the 60 % CF (scenario 3), based on the hourly day-ahead electricity price. The simulation was selected when the electrolyser was running at maximum load or when running at minimum load. In scenario 4, at 100 % CF, the electrolyser effectively runs at maximum capacity all of the time to produce the required hydrogen.

The benefit of using the lower capacity factor was to reduce the time of the operation on the maximum load and maximise the use of hydrogen storage. As can be seen in Figure 6.7 and Table 6.6, the size of the electrolyser in scenario 3 is 33.3 % bigger than the size in scenario 2. On the other hand, the size of the electrolyser in scenario 4 was 20 % lower than that in scenario 2.

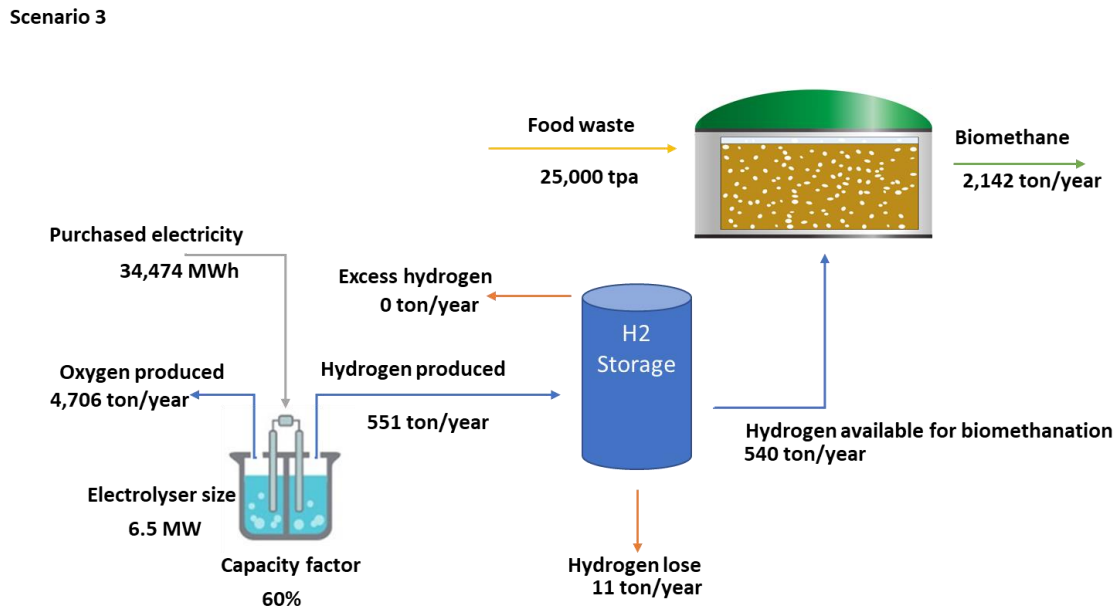

Scenario 4

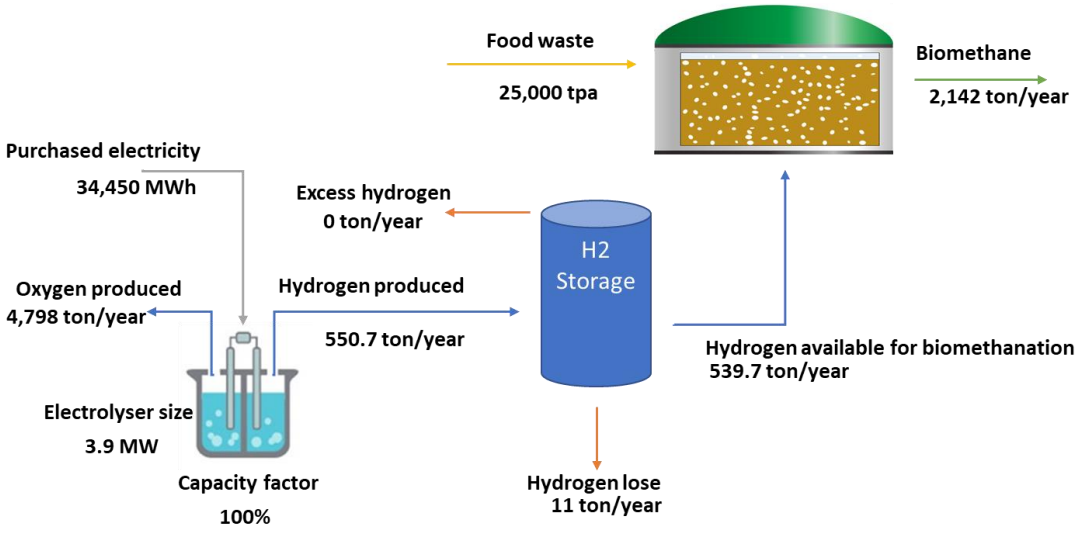

Figure 6-7 Schematic of the basic mass balance of scenario 3 (60 % CF) and scenario 4 (100 % CF).

As discussed in the methodology, the hydrogen production approach prioritised the production of hydrogen at a lower price. However, when the daily requirement was fulfilled, the load in the production changed to the minimum load in order to minimise the hydrogen production without shutting down the system. This was when the hydrogen storage took a role in storing the excess hydrogen production to be utilised on the next production day. By having a bigger size electrolyser, it will benefit from producing more hydrogen at a minimum price compared to the smaller size electrolyser. This allows the fulfilment of the daily hydrogen requirement faster than the smaller size electrolyser, meaning that the electrolyser can switch to be operated at minimum load faster, and this leads to the reduction in the cost of electricity because we do not have to produce hydrogen at maximum load when the price of hydrogen is higher.

Table 6.8 Summary of the hydrogen production using different capacity factors

	Unit	Scenario 2	Scenario 3	Scenario 4
Capacity factor	%	80 %	60 %	100 %
Electrolyser size (MW)	MW	4.92	6.56	3.93
Hydrogen produced (% of requirement)	%	100.09 %	100.07 %	100.00 %
Maximum load hours	hr	6,907	5,072	8,760
Minimum load hours	hr	1,853	3,688	0
Maximum hydrogen in the storage	m^3	5,421	10,683	0
Minimum hydrogen in the storage	m^3	291	729	0
Electricity consumption	MWh	34,456	34,475	34,450
Annual Cost of electricity	£	3,807,208	3,596,241	4,109,431
Average daily cost of electricity	£/ day	10,431	9,853	11,258

In Table 6.8, the maximum load hours in scenario 3 have a proportion of 58 % of the operation time. On the other hand, full operation at maximum load has happened in scenario 4. This would indicate that in scenario 4, the hydrogen must be produced at maximum load no matter the prices, as we can see that the highest cost of electricity is obtained in scenario 4. In the case when the electricity price is cheap, and most of the time, the price is lower than the threshold price (£ 43/MWH). Therefore, the electrolyser will maintain producing hydrogen at maximum load. In this situation, it is possible to have excess hydrogen where hydrogen storage capacity is unable to store hydrogen. In that situation, the hydrogen was assumed to be flared.

In scenarios 2, 3 and 4, the hydrogen production was almost similar, see Figure 6-8. However, hydrogen storage will play a significant role in the operation at a minimum load.

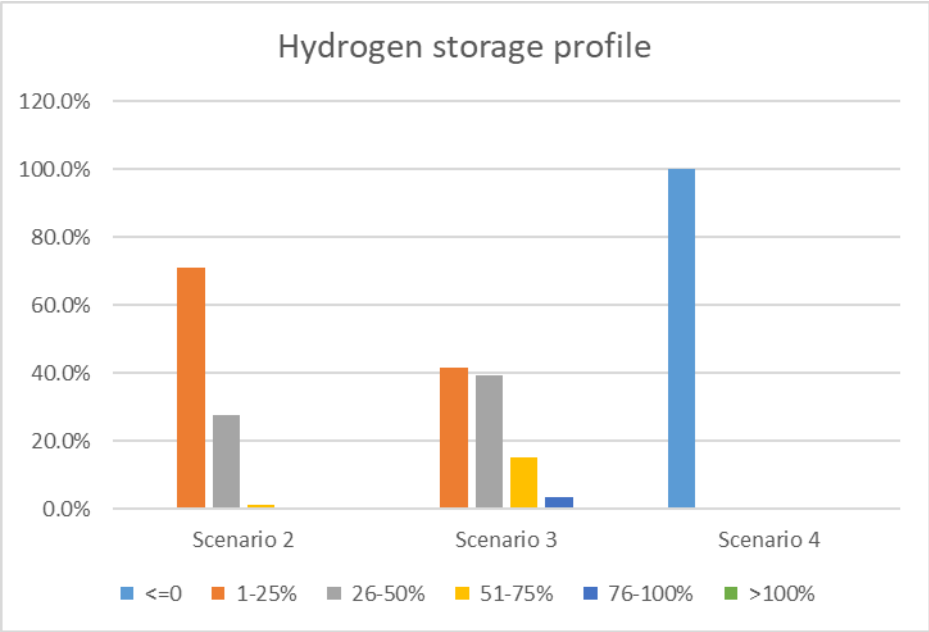

Figure 6-8. The use of hydrogen storage volume capacity in different capacity factors.

As we can see in the profile of hydrogen storage in Figure 6-8, The profile of the usage of hydrogen storage by using the 80 % capacity factor in scenario 2 shows a potential reduction of hydrogen storage. Around 90 % of the time, hydrogen storage is only used at 50 % of its capacity. On the other hand, the size of hydrogen storage shows more efficiency when using the 60 % capacity factor of electrolyser in scenario 3. Contrarily, in scenario 4, hydrogen storage is not required in this scenario since the supply and demand for hydrogen are matched.

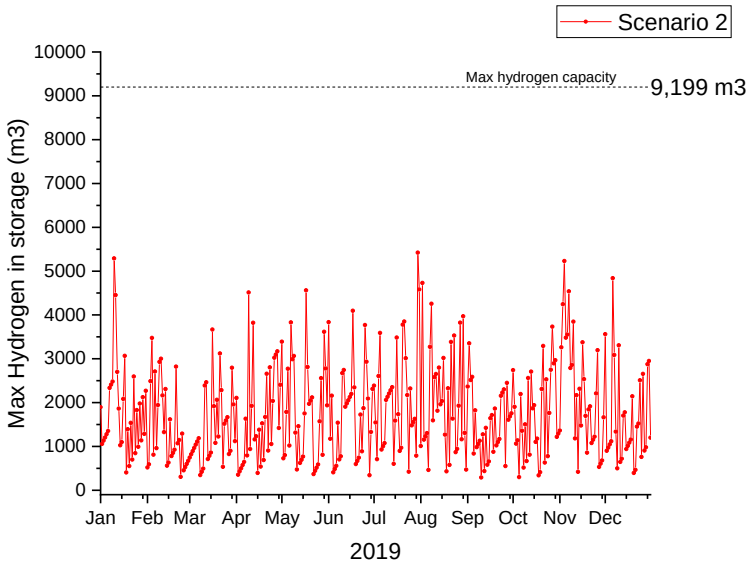

Figure 6-9 Profile of the daily hydrogen in the storage in scenario 2 (PEM, 80 % CF).

Hydrogen storage plays a significant role in order to reduce electricity costs. There will be a benefit when hydrogen production is maximised when the electricity price is cheaper and hydrogen storage is required to store excess hydrogen produced on a minimum load. Therefore, the size of hydrogen storage is not required to be bigger. In Figure **6-9**, the maximum hydrogen stored in the storage was 5,421 m^3 (58.9 % of the full storage capacity). However, 71.0 % of the time, the hydrogen stored in the storage is below 25 % (2,300 m^3) of the total storage capacity (9,200 m^3). In this case, the option to invest in bigger storage is not efficient.

6.3.5 Economic Evaluation

The daily purchase of electricity to produce hydrogen for biomethanation fluctuates depending on the electricity price and the production dynamics. For instance, in scenario 2 (PEM 80 % CF), the daily cost of electricity is within a range of £4,500 to £19,140, which is a huge range to produce a similar daily hydrogen requirement as is shown in, Figure 6-10

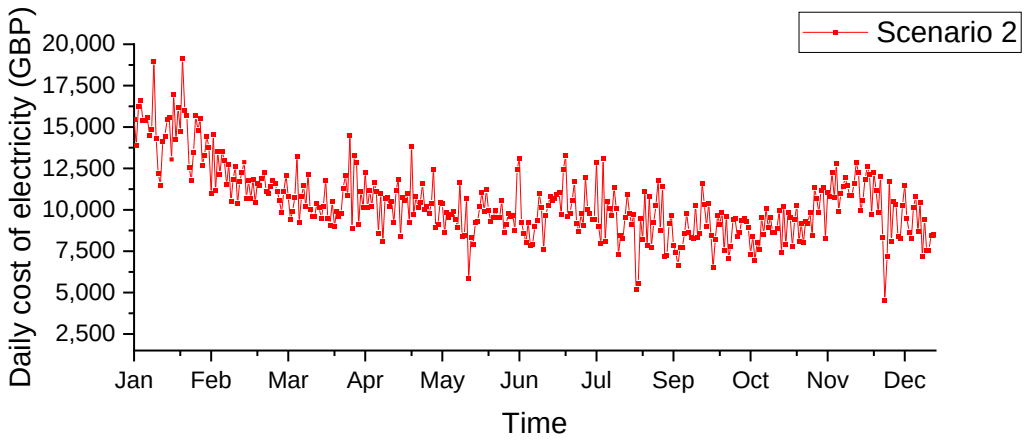

Figure 6-10 Daily costs of electricity in 2019.

According to the wholesale electricity price in 2019, the hourly electricity cost was higher in the winter since, in this period, the demand increased. Due to the different dynamic production of hydrogen, the hourly cost of electricity seems volatile, with a huge range of differences in scenarios 1 and 4. Having a higher electrolyser efficiency, the maximum hourly cost of electricity using the AEL in scenario 1 was the lowest compared to all the scenarios that have been investigated that use the PEM electrolyser. In addition, this fact can be seen in Figure 6-11, where the lowest energy consumption was provided in scenario

1 throughout the year. In comparison, only a small cost saving was provided by reducing the capacity factor between scenario 2 and scenario 3. On the other hand, there were huge consequences in scenario 4, where the purchase of the electricity was at any price. Fortunately, some of the savings obtained in scenario 4 required a smaller electrolyser and no hydrogen buffer storage is required.

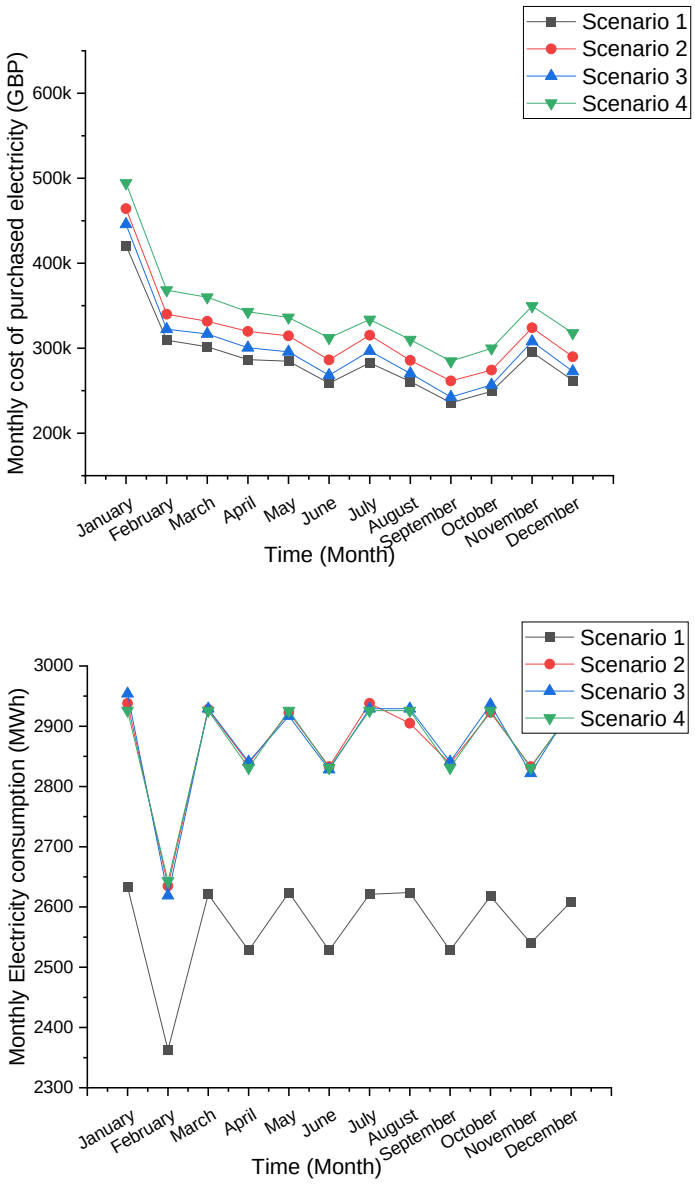

Figure 6-11 Monthly costs and electricity consumption in scenarios 1,2,3, and 4.

Table 6.7 shows the results of the economic analysis against scenarios 1-4. In all the scenarios investigated, the electricity cost contributed around 80 % (73 % to 83 %) of the OPEX. This case was similar to some other studies related to the power to gas or biological

methanation (Michailos *et al.*, 2020) that the electricity cost is a major contributor to the operational cost. Different capacity factors do not give a linear relationship. Scenario 2 (CF 80 %) gives a slightly higher LCOE compared to the scenario 3 (CF 60 %); in comparison of scenario 2 (CF 80 %) and scenario 4 (CF 100 %), see Table 6.9. In this case, the higher capacity of the electrolyser could contribute to the electricity cost reduction. However, the investment cost of having a bigger electrolyser was not able to compete with the smaller size electrolyser. On the other hand, in scenario 4, even though this scenario could save the investment cost with a smaller size of electrolyser, and also no hydrogen buffer storage was required. However, with no option to purchase electricity at a cheap price, the cost of biomethane production was still higher compared to scenario 2.

Table 6.9 Summary of the economic results for each scenario.

	Scenario 1	Scenario 2	Scenario 3	Scenario 4
Short name	AEL_80 % CF	PEM_80 % CF	PEM_60 % CF	PEM_100 % CF
CAPEX (M£)	16.75	17.19	18.52	16.21
OPEX(M£)	4.37	4.77	4.58	5.07
LCOE (£/MWh)*)	94	105	104	109
Maximum hourly cost (£)	1,014	1,203	1,474	3,020

*) The LCOE include the RHI payment

According to the Department of Energy and Climate change, UK, the average non-domestic natural gas price is £24/MWh (SKM Enviros, 2011). The LCOE shown in Table 6.9 included the government renewable heat incentive (RHI). The LCOE was almost four times higher for all the cases investigated compared to the natural gas price. As mentioned before, despite the higher investment of the electrolyser in scenario 3 compared with scenario 2 and scenario 4, the lower annual electricity cost showed a reduced cost of biomethane production. For scenarios 1-4, the LCOE is almost four times higher than the natural gas price. From the economic point of view, it is difficult for the project owner to find the benefit of biomethanation. Therefore, as with many other renewable energy projects, government incentive is required to make the project's application more attractive.

6.3.6 In-situ biomethanation on a small-scale anaerobic digestion

The application of in-situ biomethanation to small-scale anaerobic digestion explores the potential of using in-situ biomethanation in farm-scale plants. The annual feedstock of 7,500 tons would give the capacity of the plant 340kW (Banks *et al.*, 2015). The plant would have potential carbon dioxide for about 190,000 m^3/year, which would require 760,000 m^3/year of hydrogen for in-situ biomethanation, according to stoichiometric. In Figure 6-12, the size of the electrolyser that is required was 0.556 MW to cover the annual hydrogen requirement with an 80 % capacity factor. According to the wholesale electricity price in 2019, the electrolyser consumed 3,899 MWh of electricity to produce around 62 tons of hydrogen with an annual cost of £ 431,125 or an average price of £110.56/MWh, which contributes to around 70 % of the total OPEX.

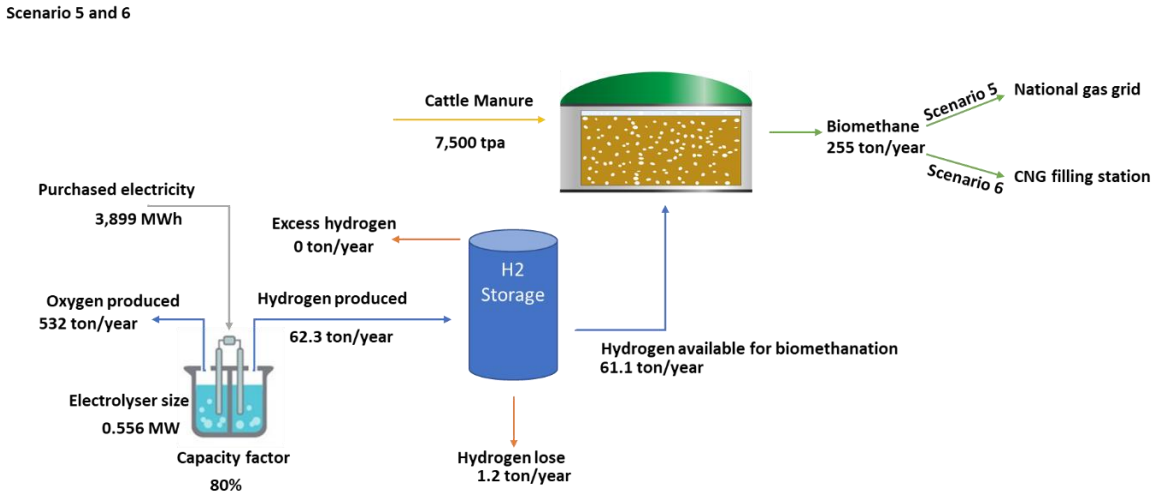

Figure 6-12 Schematic of the basic mass balance of scenarios 5 and 6.

In this study, the incentive of RHI was assumed to be £62/MWh, and RTFO was assumed to be £54.7/MWh (ADBA, 2020). The LCOE of biomethane including the RHI in scenario 5 was £110/MWh. The alternative of biomethane utilisation is to be used as vehicle fuel. The CAPEX of additional infrastructure in scenario 6 is reduced to 82 % compared to CAPEX in scenario 5, resulting in the LCOE in scenario 6 to £93/MWh (including RTFO). However, the LCOE is still much higher compared to the natural gas price. In order to analyse the minimum selling price, the potential revenue is included to see the potential to compete with the natural gas price. The minimum selling price is defined as the minimum acceptable price that is expressed as the value where the NPV is equal to 0 during the project lifetime.

The oxygen produced from the electrolysis process would have a value of £70/ton (Breyer *et al.*, 2015). As mentioned before, another source of revenue would be related to the government policy as an incentive. In this case, using biomethane to be injected into the natural gas grid will receive a renewable heat incentive (RHI) in scenario 5. In contrast, the biomethane utilisation to gas refuelling stations will receive a renewable transport fuel obligation (RTFO) in scenario 6.

Table 6.10 Summary of the economic results for scenarios 5 and 6.

	Unit	Scenario 5	Scenario 6
Capacity factor	%	80	80
Electrolyser size (MW)	MW	0.556	0.556
Hydrogen produced (% of requirement)	%	100.01	100.01
Maximum load hours	hr	6,918	6,918
Minimum load hours	hr	1,842	1,842
Maximum hydrogen in the storage	m^3	658	658
Minimum hydrogen in the storage	m^3	33	33
Electricity consumption	MWh	3,899	3,899
Cost of electricity	£	431,125	431,125
Average cost of electricity	£/ day	1,181	1,181
CAPEX (M£)	M£	5.47	4.46
OPEX(M£)	M£	0.66	0.62
LCOE *)	(£/MWh)	110	93

*) The LCOE include the RHI and RTFO payment

With the project's lifetime of 20 years, including the incentives, the minimum selling price for utilising through injection to the natural gas grid in scenario 5 would be £162.3/MWh. On the other hand, an alternative utilisation of using biomethane for vehicle fuel in scenario 6 could achieve a minimum selling price of £148.02/MWh. With these two scenarios of utilising in-situ biomethanation in a small-scale anaerobic digestion plant, the project appears unable to compete with the price of natural gas. The high investment cost was not met with sufficient return to break even, and this result was in line with the result that was reported in the ADBA report (ADBA, 2020), which shows that AD plants with capacities less than 500 kW will never be profitable with 20 years of project lifetime.

6.3.7 Sensitivity analysis

A sensitivity analysis was carried out for parameters with a high degree of uncertainty. Parameters such as electric price, discount rate, electrolyser electricity and electrolyser capital were selected to be varied in relation to the LCOE. The percentage variation varied to ±50 % for the installed cost of the electrolyser. The electricity price and discount rate varied by ±25 %, and the electrolyser efficiency varied by ± 15 %. It should be noted that the value of LCOE included the government incentives (RHI). Different percentages of variation on each parameter were expected to change in the future significantly. Hence, the percentage of uncertainty is higher. For instance, the variation of change in the installed cost of electrolyser was expected to be higher than the variation of change in electricity price.

Figure 6-13 shows that wholesale electricity and electrolyser efficiency had the greatest impact on the levelised cost of energy (LCOE). As discussed before, electricity price has a major effect on the operational cost of in-situ biomethanation. It has the highest level of uncertainty that will determine the project's profitability. On the other hand, the effect of discount rate and installed cost of electrolyser was shown to have a lower influence on the LCOE. The electrolyser efficiency gives a higher influence than the discount rate and cost of the electrolyser but is less significant compared to the electricity price.

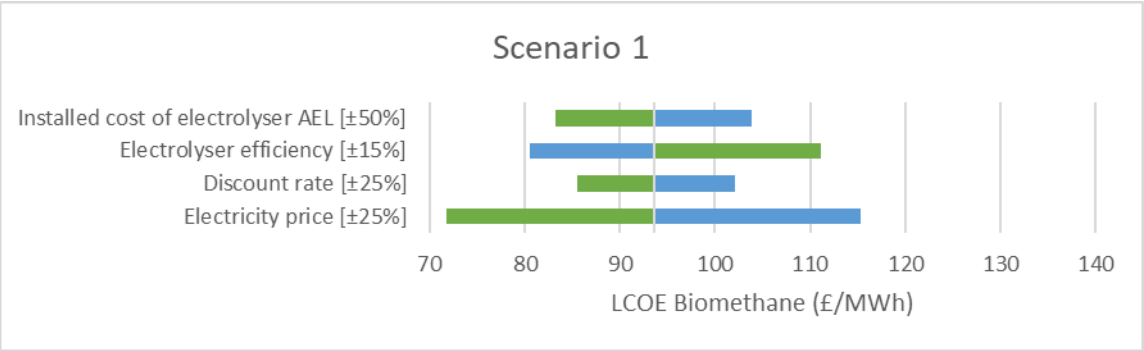

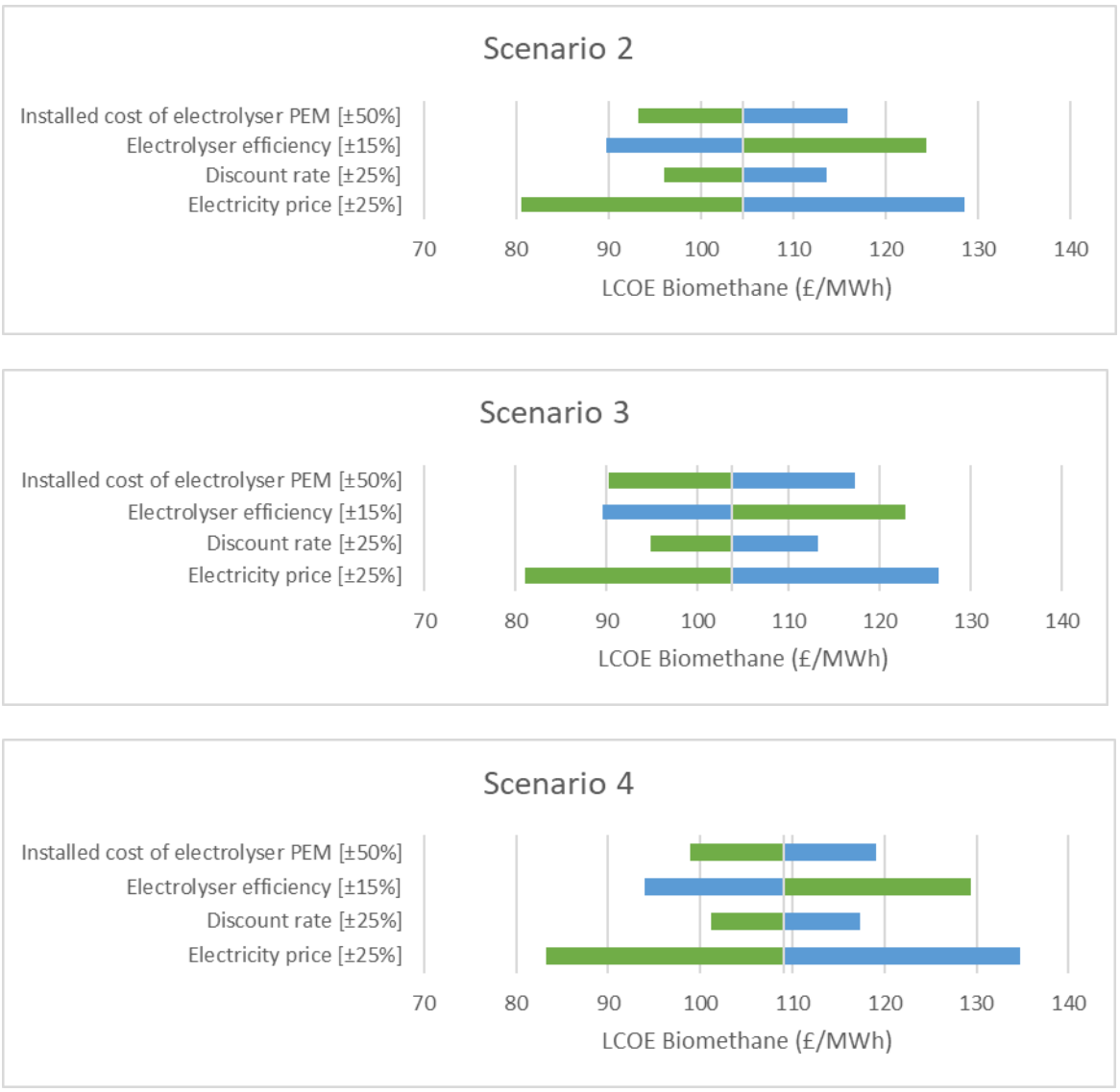

Figure 6-13 Sensitivity analysis of LCOE biomethane in scenarios 1,2,3, and 4.

6.4 Conclusions

A techno-economic framework was developed to allow the analysis of a biomethanation system using a hypothetical variable-priced electricity tariff. Day-ahead electricity prices from the UK from 2018-2020 were used to estimate the variation in cost for such a consumer tariff and the purchase price profile. Day-ahead foresight was used to schedule the electrolyser for the lowest cost of operation.

Techno-economic analysis of an in situ biomethanation system operating alongside a 25,000 tpa food waste anaerobic digester resulted in a CAPEX of £16.21-18.52M and OPEX

of £4.37-5.07 per year. The lowest LCOE for the produced biomethane was £94/MWh, which is significantly greater than the current wholesale price of natural gas of £24/MWh

On performing techno-economic analysis, electricity cost still becomes a major contributor that influences the LCOE of biomethane, covering up to 80 % (78 % to 83 %) of the total OPEX across all scenarios explored.

In order to minimise the cost, the efficiency of the electrolyser significantly impacts electricity consumption, which will lead to reducing the electricity cost. In this case, using an alkaline electrolyser could give lower LCOE (£94/MWh) compared to the PEM electrolyser due to AEL's higher operating efficiency (77 % for AEL and 69 % for PEM) despite the beneficial operational flexibility of the PEM electrolyser leading to a large reduction in over-generation of hydrogen.

Variation of the capacity factors of PEM electrolyser (60-100 %) does not significantly impact the LCOE (£104-109 /MWh). Lower capacity factors have an advantage as it allows greater temporal flexibility leading to reduced average electricity cost. However, this benefit is approximately offset by the higher investment cost to the electrolyser.

Sensitivity analysis on the techno-economic analysis showed the results were most sensitive to the average purchase price of the electricity and the CAPEX of the electrolyser. Given future trends in electrify price variability (greater), and cost of electrolysis technology (lower), the financial viability of in situ biomethanation is expected to improve over time.

7. CONCLUSION AND FUTURE WORKS

7.1 Conclusions

The application of in-situ biomethanation as a technology for the decarbonisation of future energy systems is multiple: it is a biogas upgrading technology, which could be retrofitted to existing AD plants for the production of biomethane and the consequent decarbonisation of the gas grid; it is a way to improve the carbon efficiency and methane production from the anaerobic digestion of biowastes, up to 100 % higher when considering biogas with 50 % content of carbon dioxide; and it is an enabler of power-to-gas systems, thereby favouring the stabilisation of the electrical grid, using excess renewables, and favouring long-term storage of electricity in the form of high-density energy fuel.

The use of existing anaerobic digesters for in situ biomethanation gives this technology a potential practical and economic advantage compared to ex-situ approaches which would require the installation of additional and separate reactors. However, the technical readiness of in-situ biomethanation is still considered low, with only a few pilot demonstrations and yet without a commercial deployment; on the other hand, ex-situ biomethanation has already achieved commercial implementation with a few plants installed in Germany, Denmark and Switzerland. The dynamics of biowaste degradation and CO_2 production; the need to control H_2 injection into the digester based on both process stability and biogenic CO_2 availability; and the low solubility of H_2 in the liquid phase: this complex interrelationship between different phenomena constitutes an engineering challenge and the main technical reason for the relatively low commercial advancement of this technology. From an economic perspective, the sustainability of in-situ biomethanation relies on the possibility to adapt a continuous process (i.e. biowaste digestion) to the dynamics of the electricity market prices; in other words, on the trade-off between high capacity factors and the use of electricity during periods of excess renewables and low market prices.

This PhD work attempted to advance the understanding of in-situ biomethanation, using a combined lab-based experimental and desk-based techno-economic approach and

implementing the following framework, which could be relevant to the industrial application of the process:

Use of realistic feedstock.

Realistic substrates were used for in-situ biomethanation laboratory reactors. Food waste was sourced from the University of Sheffield canteen, and its composition was adapted to the average UK household food waste composition reported by WRAP statistics. Sewage sludge was sourced from the existing United Utilities wastewater plant (mixed sewage sludge). The type of substrate directly affects biomethanation performance, as it directly determines the dynamics and the amount of CO_2 production, the concentration of potential inhibitors such as ammonia, and hydrodynamic characteristics influencing gas-liquid transfer.

Continuous biomethanation process.

Theoretically, the biomethanation process could be designed as a combination of batch and continuous processes. For instance, both substrate and hydrogen could be batch-fed and allow them a suitable reaction time; substrate could be fed continuously and gas batch-fed, etc. The experimental work of this PhD implemented a configuration that would result from the retrofit of existing industrial AD reactors without affecting either the typical plants' operational strategies or gas storage characteristics. In other words, the AD reactor would receive the feedstock semi-continuously (i.e. a certain number of feedings per day), while a suitable injection system would deliver the hydrogen into the reactor in a continuous way. The storage of gas in the headspace would remain constant, and therefore, the flow of biomethane would result continuously.

Process control.

The hydrogen injection rate directly influences the resulting biomethane composition and can also affect the process stability. This project implemented a simple feedback process control of the hydrogen injection (based on a gain-scheduling concept) to maintain the process within safe operational limits.

Economic Scenario.

Relevant scenarios were built and analysed to evaluate the economic sustainability of the in-situ biomethanation. In particular, a focus on UK scenarios was adopted, considering realistic biogas plants for food waste and manure-based anaerobic digestion.

Experimental development of in-situ biomethanation

The first part of the PhD work consisted of the development of a suitable experimental setup involving the following tasks:

- Sizing and selection of components
- Online and high-frequency measurement of gas composition, gas flow, pH, temperature and pressure.
- Monitoring and control system implemented in Labview
- Safety measures in case of H_2 leak or excessive pressure

The rig, consisting of four biomethanation reactors and two control anaerobic digesters, together with the monitoring and control system, was successfully built and commissioned during the PhD work.

The gas-liquid mass transfer was the main process limitation for in-situ biomethanation experiments. The various experiments carried out in both chapter 4 and chapter 5 highlighted the importance of H_2 gas-liquid mass transfer on the performance of biomethanation, namely on either the methane evolution rate or biomethane enrichment.

The following experimental observations can demonstrate the process limitation by gas-liquid mass transfer:

- In all experiments, H_2 tended to increase in the headspace after the start of the injection, up to 11 %-36 % vol.; this would result in an increase of the gas-liquid transfer via an increase of the concentration “driving force” until reaching an equilibrium with the injection rate and therefore finally resulting into stable H_2 content in the headspace.
- The levels of VFA and alkalinity ratio in the biomethanation reactors were, on average, comparable to the levels in the control reactors. This indicates that there was no noticeable accumulation of dissolved H_2 in the liquid phase, as it would

happen in case of a biological process limitation; in that case, inhibition of acetogenesis would occur, as it would have happened in case of reaching high levels of dissolved H_2 in the liquid.

The highest methanation rate was achieved for;

- Sewage sludge (SS): an average of 0.16 L L^{-1} day^{-1} at period R_{280} and period OP1 correspond to the average gas composition of 63.3 % CH_4, 14.9 % CO_2, and 20.3 % H_2 at R280. 68.4 % CH_4, 13.2 % CO_2, and 18.6 % H_2 at period OP1.
- Food waste (FW): an average of 0.23 L L^{-1} day^{-1} at period OP2 correspond to the gas composition of 55.3 % CH_4, 17.5 % CO_2, and 28.1 % H_2.

The highest biomethanation extent was achieved in the following conditions:

- Sewage sludge (SS): an average value of 90 % at periods OP1 and OP3.
- Food waste (FW); an average value of 82 % at period OP3.

The average H_2 content was 22.5 % and 30.8 % at OLR of 2 in SS and FW, respectively, when injecting hydrogen at a stoichiometric requirement, while it was 6.8 % and 12.1 % at OLR1. This shows again how higher H_2 injection rates (at higher OLRs) require a higher driving force for the gas-liquid transfer to be in equilibrium.

Effect of H_2 injection system.

Chapter4 showed how a porous sparger improved the biomethanation performance compared to a simple open tubing injector. In particular, the reactor with porous sparger achieved MER values across all experiments that were 56 % higher on average compared to the tubing injector.

This can be explained by an increase of the gas-liquid interfacial area due to smaller bubble diameter achieved when hydrogen is injected through a porous sparger. All the experiments in Chapter 5 implemented the use of the porous sparger.

Effect of H_2 partial pressure.

The maximum H_2 content in the headspace could be controlled in the experiments through the monitoring and control system (which was constrained by the feedback control). This is a design decision, and it affects the quality of biomethane that would be produced.

Ideally, the amount of H_2 in the headspace, and therefore appearing in the product gas, would need to be compatible with the regulation on the local natural gas grid to allow its immediate application.

The research has demonstrated how increasing values of H_2 content in the headspace (thereby partial pressure) would be needed to achieve higher hydrogen injection and methane evolution rates. This is a consequence of the dependence of the gas-liquid mass transfer rate on the concentration driving force (as explained above).

In chapter 4 – an increase of the allowed H_2 content from 5 % to 10 % allowed an increase in the H_2 injection rate from 12 % stoichiometric to 39 % stoichiometric for sewage sludge and 9 % to 25 % for food waste.

In chapter 5 – the average H_2 content was 22.5 % and 30.8 % at OLR of 2 in SS and FW, respectively, when injecting hydrogen at a stoichiometric requirement, while it was 6.8 % and 12.1 % at OLR1. This shows again how higher H_2 injection rates (at higher OLRs) require a higher driving force for the gas-liquid transfer to be in equilibrium.

The dilution of the product gas with hydrogen, and this apparently being a requirement for allowing mass transfer of the hydrogen, seems to be one of the most important limitations on the possibility that continuous in-situ biomethanation could produce biomethane with grid quality without the need of further down-stream processing. However, it is noted that in full-scale systems, with liquid depths in the order of several metres, this could become irrelevant and may simply be an artefact of the small-scale testing done in this research.

<u>Effect of gas recirculation.</u>

Gas recirculation produced clear evidence of improvement in the biomethanation performance. This is a further indication of the gas-liquid transfer limitations on the process, as increases in gas recirculation directly lead to an increase in gas hold-up and finally on the surface area through which the gas-liquid transfer happens. In both SS and FW, each increase in gas recirculation rate produced an increase in MER and kLa.

While gas recirculation can be an effective method to enhance in-situ biomethanation, its energy footprint may be considerable. In this regard, the volumetric recycling range

employed in this work (12-155 L L^{-1} day^{-1}) compared to typical gas mixing rates in industrial anaerobic digesters between 10-20 L L^{-1} day^{-1}.

Effect of OLR variation.

The OLR showed a strong influence on the biomethanation process and performance. This was shown experimentally both during short feeding disturbances during the experiments and by comparing experiments carried out at different average OLR values.

Short disturbances (reductions) of OLR led to a clear pattern in in-situ biomethanation: first, a reduction of gas outflow; followed by an increase of H_2 content in the headspace; an increase of gas residence time; an increase of H_2 conversion; a decrease in CO_2 content and related increase of pH. As described in Chapter5, the eventual intervention of the feedback control in reducing the H_2 injection rate would also lead to an increase in the CH_4 content.

Specific experiments were carried out to ascertain the effect of OLR at different average OLR. The highest H_2 conversion was achieved for both SS and FW in reactors operated at the lowest OLR of 1 gVS L^{-1} d^{-1}, at 94 % for SS and 87 % for FW.

The effect of OLR on the H_2 conversion was shown to be directly related to the gas Retention Time (RT), as calculated in Chapter 5. In particular, a positive correlation between RT and H_2 conversion was shown for all experiments.

Feedback control and safe operational limits

The monitoring and feedback control effectively maintained the biomethanation within the desired operational limits, depending on gas quality and pH levels. The feedback control was activated on most occasions after a disturbance on the substrate feeding rate to reduce the hydrogen injection rate in order to maintain the process outputs, mainly pH and H_2 content, below the process constraints.

The highest pH was achieved at 8.1 for sewage sludge and 8.6 for food waste. These pH levels seem not to affect the biomethanation process, as demonstrated by previous literature. The constraint on the minimum CO_2 level (5 % vol.) was not achieved in any experimental condition.

Techno-economic assessment

A techno-economic framework was developed to allow the analysis of a biomethanation system using a hypothetical variable-priced electricity tariff. Day-ahead electricity prices from the UK from 2018-2020 were used to estimate the variation in cost for such a consumer tariff. The purchase price profile, with day-ahead foresight, was used to schedule the electrolyser for the lowest cost of operation.

Techno-economic analysis of an in situ biomethanation system operating alongside a 25,000 tpa food waste anaerobic digester (AD) resulted in a CAPEX of £16.21-18.52M and OPEX of £4.37-5.07 M per year. The lowest LCOE for the produced biomethane was 94£/MWh which is significantly greater than the current wholesale price of natural gas of £24/MWh

On performing techno-economic analysis, electricity cost still becomes a major contributor that influences the LCOE of biomethane, covering up to 80 % (78 % to 83 %) of the total OPEX across all scenarios explored.

In order to minimise the cost, better efficiency of electrolyser gives a significant impact in order to reduce electricity consumption that will lead to reducing the electricity cost. In this case, using an alkaline electrolyser could give lower LCOE (94 £/MWh) compared to the PEM electrolyser due to AEL's higher operating efficiency (77 % for AEL and 69 % % for PEM) despite the beneficial operational flexibility of the PEM electrolyser leading to a large reduction in over-generation of hydrogen.

Variation of the capacity factors of PEM electrolyser (60-100 %) does not significantly impact to the LCOE (104-109£/MWh). There is an advantage of lower capacity factors as it allows greater temporal flexibility leading to reduced average electricity cost; however, this benefit is approximately offset by the higher investment cost to the electrolyser.

Sensitivity analysis on the techno-economic analysis showed the results were most sensitive to the average purchase price of the electricity and the CAPEX of the electrolyser. Given future trends in electrify price variability (greater), and cost of electrolysis technology (lower), the financial viability of in situ biomethanation is expected to improve over time.

7.2 Future works

In this project, a novel configuration was designed to improve the performance of in-situ biomethanation. Based on the result and experience during the experimental work, the future perspective on improving this work and suggestions for the continuation of this thesis are as follows:

- Better gas-liquid mass transfer

  In the case of using a continuous stirred tank reactor (CSTR), the stirring mechanism can be improved by using the stirrer with an impeller in order to increase the gas-liquid interface area.
- Improve the control of OLR in the developed rig.

  In this study, it was quite challenging to control the OLR due to the characteristic of the feedstock and the pump mechanism. The suggestion to overcome this issue would be to perform a better feeding control that could increase the stability of the feeding.
- An optimal level of gas recirculation

  A wider range of the effect of gas recirculation rate could be useful in order to gain better knowledge of the correlation between the benefit and cost of energy.
- A model-based analysis in order to have a better understanding of the trade-offs between OLR, H_2 conversion and gas Retention Time.
- In general – operational and design guidance should be developed, with recommendations based on whether the process is biological or mass-transfer limited.
- A deeper investigation of the microbial activity during the in-situ biomethanation process would be beneficial to make a better understanding in mechanism of the process. In particular, the activity of the microbial community can also directly increase the gas-liquid mass transfer rate compared to the purely abiotic process. This occurs due to the microbial conversion of the absorbed gas in the stagnant liquid layer (around the gas bubbles) and thereby increases the diffusional gradient. This phenomenon is generally known as “microbial enhancement of the gas-liquid mass transfer”. In some of the experiments presented in Chapter 5, it can be noted how the H_2 content tends to decrease after reaching a maximum, without particular effects due to changes in OLR. It can be speculated that this may be due to a higher and more

active microbial population developing during the experiment, thus leading to microbial enhancement of the mass transfer.

- The effect of the gas-liquid transfer due to the characteristics of different substrates could be further investigated. This is an aspect that could not be explored sufficiently in this work. However, substrates with higher total solids are expected to perform relatively higher gas-liquid transfer than more aqueous substrates.
- Finally, a pilot study would be necessary to study several process conditions on a larger reactor scale, where the gas-liquid mass transfer will be largely affected by different hydrodynamic characteristics.

Regarding the techno-economic part of the study, the following consideration could guide future work, and techno-economic assessment could be extended to consider the following factors:

- Additional future financial incentives for low carbon energy, energy storage, demand turn-up etc.;
- more accurate modelling and optimisation of electrolyser scheduling considering multi-day demand matching, variable turn-up, turn-down and complete shutdown periods;
- variation in storage requirements;
- combined biomethanation and conventional biogas upgrading, linking the analysis with future projections on electricity price volatility and future variable rate tariff availability.

Combining these factors may increase the relevance and realism of the results generated.

REFERENCES

ADBA (2020) *Biomethane: The pathway to 2030*. Available at: https://adbioresources.org/news/adba-launches-biomethane-the-pathway-to-2030-report.

Adekunle, K. F. and Okolie, J. A. (2015) 'A Review of Biochemical Process of Anaerobic Digestion', *Scientific Research Publishing Inc.*, 6(March), pp. 205–212. doi: http://dx.doi.org/10.4236/abb.2015.63020.

Agneessens, L. M. *et al.* (2017) 'In-Situ Biogas Upgrading with Pulse H2 Additions: the Relevance of Methanogen Adaption and Inorganic Carbon Level', *Bioresource Technology*, 233, pp. 256–263. doi: 10.1016/j.biortech.2017.02.016.

Ahern, E. P. *et al.* (2015) 'A perspective on the potential role of renewable gas in a smart energy island system', *Renewable Energy*, 78, pp. 648–656. doi: 10.1016/j.renene.2015.01.048.

Alfaro, N. *et al.* (2018) 'Evaluation of process performance, energy consumption and microbiota characterization in a ceramic membrane bioreactor for ex-situ biomethanation of H2 and CO2', *Bioresource Technology*, 258(February), pp. 142–150. doi: 10.1016/j.biortech.2018.02.087.

Alfaro, N. *et al.* (2019) 'H2 addition through a submerged membrane for in-situ biogas upgrading in the anaerobic digestion of sewage sludge', *Bioresource Technology*, 280(December 2018), pp. 1–8. doi: 10.1016/j.biortech.2019.01.135.

Alitalo, A., Niskanen, M. and Aura, E. (2015) 'Biocatalytic methanation of hydrogen and carbon dioxide in a fixed bed bioreactor', *Bioresource Technology*, 196, pp. 600–605. doi: 10.1016/j.biortech.2015.08.021.

Altfeld, K. and Pinchbeck, D. (2013) 'Admissible hydrogen concentrations in natural gas systems', *Gas for Energy*, March/2013, pp. 1–16. Available at: www.gas-for-energy.com.

Amaral, A. *et al.* (2019) 'Modelling gas–liquid mass transfer in wastewater treatment: When current knowledge needs to encounter engineering practice and vice versa', *Water Science and Technology*, 80(4), pp. 607–619. doi: 10.2166/wst.2019.253.

Angelidaki, I. *et al.* (2011) 'Biomethanation and its potential', *Methods in Enzymology*. 1st edn, 494, pp. 327–351. doi: 10.1016/B978-0-12-385112-3.00016-0.

Angelidaki, I. *et al.* (2018) 'Biogas upgrading and utilization: Current status and perspectives', *Biotechnology Advances*, 36(2), pp. 452–466. doi: 10.1016/j.biotechadv.2018.01.011.

Angelidaki, I. and Ahring, B. K. (1994) 'Anaerobic thermophilic digestion of manure at different ammonia loads: Effect of temperature', *Water Research*, 28(3), pp. 727–731. doi: 10.1016/0043-1354(94)90153-8.

Angelidaki, I., Ellegaard, L. and Ahring, B. K. (1993) 'A mathematical model for dynamic simulation of anaerobic digestion of complex substrates: Focusing on ammonia inhibition', *Biotechnology and Bioengineering*, 42(2), pp. 159–166. doi:

10.1002/bit.260420203.

Angelidaki, I. and Sanders, W. (2004) 'Assessment of the anaerobic biodegradability of macropollutants', *Reviews in Environmental Science and Biotechnology*, 3(2), pp. 117–129. doi: 10.1007/s11157-004-2502-3.

Arnold E. Greenberg, L. S. C. and A. D. E. (1992) *APHA Method 2320: Standard Methods for the Examination of Water and Wastewater*. WASHINGTON, D.C.

Banks, C. J. *et al.* (2012a) 'Trace element requirements for stable food waste digestion at elevated ammonia concentrations', *Bioresource Technology*, 104, pp. 127–135. doi: 10.1016/j.biortech.2011.10.068.

Banks, C. J. *et al.* (2012b) 'Trace element requirements for stable food waste digestion at elevated ammonia concentrations', *Bioresource Technology*, 104, pp. 127–135. doi: 10.1016/j.biortech.2011.10.068.

Banks, C. J. *et al.* (2015) *ADAT - Anaerobic digestion assessment tool*. Available at: http://www.bioenergy.soton.ac.uk/AD_software_tool.htm (Accessed: 1 February 2021).

Bassani, I. *et al.* (2015) 'Biogas Upgrading via Hydrogenotrophic Methanogenesis in Two-Stage Continuous Stirred Tank Reactors at Mesophilic and Thermophilic Conditions', *Environmental Science and Technology*, 49(20), pp. 12585–12593. doi: 10.1021/acs.est.5b03451.

Bassani, I. *et al.* (2017) 'Optimization of hydrogen dispersion in thermophilic up-flow reactors for ex situ biogas upgrading', *Bioresource Technology*, 234, pp. 310–319. doi: 10.1016/j.biortech.2017.03.055.

Bassani, I., Kougias, P. G. and Angelidaki, I. (2016) 'In-situ biogas upgrading in thermophilic granular UASB reactor: key factors affecting the hydrogen mass transfer rate', *Bioresource Technology*, 221, pp. 485–491. doi: 10.1016/j.biortech.2016.09.083.

Batstone, D. J. *et al.* (2002) 'The IWA Anaerobic Digestion Model No 1 (ADM1).', *Water Science and Technology*, 45(10), pp. 65–73. doi: 10.2166/wst.2008.678.

Bensmann, A. *et al.* (2014) 'Biological methanation of hydrogen within biogas plants: A model-based feasibility study', *Applied Energy*, 134, pp. 413–425. doi: 10.1016/j.apenergy.2014.08.047.

Bertuccioli, L. *et al.* (2014) 'Study on development of water electrolysis in the EU, Fuel Cells and hydrogen Joint Undertaking', *Fuel Cells and hydrogen Joint Undertaking*, 1(February), pp. 1–160. Available at: https://www.fch.europa.eu/sites/default/files/FCHJUElectrolysisStudy_FullReport (ID 199214).pdf.

Bilitewski, B. *et al.* (1997) *Waste management with 126 tables*, *Waste-to-Energy Research and Technology Council*. Springer. Available at: http://www.wtert.eu/default.asp?Menue=13&ShowDok=12 (Accessed: 11 April 2017).

Bochmann, G. and Montgomery, L. F. R. (2013) 'The Biogas Handbook', in *The Biogas*

Handbook, pp. 85–103. doi: 10.1533/9780857097415.1.85.

Boe, K., Batstone, D. J. and Angelidaki, I. (2007) 'An Innovative Online VFA Monitoring System for the Anerobic Process, Based on Headspace Gas Chromatography', *Biotechnology and Bioengineering*, 96(4), pp. 712–721. doi: 10.1002/bit.21131.

Böhm, H. *et al.* (2018) *Innovative large-scale energy storage technologies and Power-to-Gas concepts after optimization: Report on experience curves and economies of scale*.

Breyer, C. *et al.* (2015) 'Power-to-gas as an emerging profitable business through creating an integrated value chain', *Energy Procedia*, 73, pp. 182–189. doi: 10.1016/j.egypro.2015.07.668.

Bright, A. *et al.* (2011) 'An Introduction to the Production of Biomethane Gas and Injection to the National Grid', *Advantage West Midlands and Waste and Resources Action Programme*, (July), p. 80. Available at: http://www.wrap.org.uk/sites/files/wrap/AWM Biomethane to Grid 05 07 11.pdf.

Bugante, E. C. *et al.* (1989) 'Methane production from hydrogen and carbon dioxide and monoxide in a column bioreactor of thermophilic methanogens by gas recirculation', *Journal of Fermentation and Bioengineering*, 67(6), pp. 419–421. doi: 10.1016/0922-338X(89)90148-7.

Business electricity price (2021) *Wholesale Electricity Price Guide*. Available at: https://www.businesselectricityprices.org.uk/retail-versus-wholesale-prices/ (Accessed: 3 February 2021).

Buswell, A. M. (1936) 'Anaerobic Fermentators', *State Water Survey. University of Illinois*, 32(32), p. 58.

Buswell, A. M. and Mueller, H. F. (1952) 'Mechanism of Methane Fermentation', *Industrial & Engineering Chemistry*, 44(3), pp. 550–552. doi: 10.1021/ie50507a033.

Carmo, M. *et al.* (2013) 'A comprehensive review on PEM water electrolysis', *International Journal of Hydrogen Energy*, 38(12), pp. 4901–4934. doi: 10.1016/j.ijhydene.2013.01.151.

Chen, Y., Cheng, J. J. and Creamer, K. S. (2008) 'Inhibition of anaerobic digestion process: A review', *Bioresource Technology*, 99(10), pp. 4044–4064. doi: 10.1016/j.biortech.2007.01.057.

Choi, D. *et al.* (2010) 'A techno-economic analysis of polyhydroxyalkanoate and hydrogen production from syngas fermentation of gasified biomass', *Applied Biochemistry and Biotechnology*, 160(4), pp. 1032–1046. doi: 10.1007/s12010-009-8560-9.

Chong, S. A., Subramaniam, M. and Ng, L. L. (2015) 'Power to gas trial to inject hydrogen into Australia's gas grid', *Australian Renewable Energy Agency*, August. Available at: https://www.imh.com.sg/uploadedFiles/Newsroom/News_Releases/23Mar15_WiSE Study Results.pdf.

Chow, W. L. *et al.* (2020) 'Anaerobic Co-Digestion of Wastewater Sludge : A Review

of Potential Co-Substrates and Operating', *Processes*, 8(1)(39), pp. 1–21.

Christou, M. L. *et al.* (2021) 'Ammonia-induced inhibition of manure-based continuous biomethanation process under different organic loading rates and associated microbial community dynamics', *Bioresource Technology*, 320(PA), p. 124323. doi: 10.1016/j.biortech.2020.124323.

Costa, K. C., Lie, T. J. and Jacobs, M. A. (2013) 'H2 independent growth Methanococcus maripaludis', *Microbiology*, 4(2), pp. 1–7. doi: 10.1128/mBio.00062-13.Editor.

Van Dael, M. *et al.* (2018) 'Techno-economic assessment of a microbial power-to-gas plant – Case study in Belgium', *Applied Energy*, 215(February), pp. 416–425. doi: 10.1016/j.apenergy.2018.01.092.

Dai, X. *et al.* (2017) 'Impact of a high ammonia-ammonium-pH system on methane-producing archaea and sulfate-reducing bacteria in mesophilic anaerobic digestion', *Bioresource Technology*, 245(August), pp. 598–605. doi: 10.1016/j.biortech.2017.08.208.

Dauwalder, O. *et al.* (2016) 'Does bacteriology laboratory automation reduce time to results and increase quality management?', *Clinical Microbiology and Infection*, 22(3), pp. 236–243. doi: 10.1016/j.cmi.2015.10.037.

Demirel, B. and Scherer, P. (2008) 'The roles of acetotrophic and hydrogenotrophic methanogens during anaerobic conversion of biomass to methane: A review', *Reviews in Environmental Science and Biotechnology*, 7(2), pp. 173–190. doi: 10.1007/s11157-008-9131-1.

Demirel, B. and Scherer, P. (2011) 'Trace element requirements of agricultural biogas digesters during biological conversion of renewable biomass to methane', *Biomass and Bioenergy*, 35(3), pp. 992–998. doi: 10.1016/j.biombioe.2010.12.022.

Derbal Kerroum, Bencheikh-LeHocine Mossaab, M. A. H. (2012) 'Production of Biogas from Sludge Waste and Organic Fraction of Municipal Solid Waste', in Kumar, S. (ed.) *Biogas*. Croatia: InTech, pp. 152–172.

Deublein, D. and Steinhauser, A. (2008) 'Biogas from waste and renewable resources', in *Choice: Current Reviews for Academic Libraries*, pp. 98-99,391. doi: 10.1002/9783527632794.

Díaz, I. *et al.* (2015) 'A feasibility study on the bioconversion of CO2 and H2 to biomethane by gas sparging through polymeric membranes', *Bioresource Technology*, 185, pp. 246–253. doi: 10.1016/j.biortech.2015.02.114.

Diekert, G. and Wohlfarth, G. (1994) 'Metabolism of homoacetogens', *Antonie van Leeuwenhoek*, 66(1–3), pp. 209–221. doi: 10.1007/BF00871640.

Durbin, D. J. and Malardier-Jugroot, C. (2013) 'Review of hydrogen storage techniques for on board vehicle applications', *International Journal of Hydrogen Energy*, 38(34), pp. 14595–14617. doi: 10.1016/j.ijhydene.2013.07.058.

Eichman, J., Townsend, A. and Melaina, M. (2016) 'Economic Assessment of Hydrogen Technologies Participating in California Electricity Markets Economic

Assessment of Hydrogen Technologies Participating in California Electricity Markets', *National Renewable Energy Laboratory*, (February), p. 31. Available at: www.nrel.gov/publications.%0Ahttps://www.nrel.gov/docs/fy16osti/65856.pdf%0Ahttps://www.nrel.gov/docs/fy16osti/65856.pdf.

Facchin, V. *et al.* (2013) 'Effect of trace element supplementation on the mesophilic anaerobic digestion of foodwaste in batch trials : The influence of inoculum origin', *Biochemical Engineering Journal*, 70, pp. 71–77. doi: 10.1016/j.bej.2012.10.004.

Fletcher, K. (2017) *European Biogas Association reports 17,376 biogas plants in EU*, *Biomass Magazine*. Available at: http://biomassmagazine.com/articles/14141/european-biogas-association-reports-17-376-biogas-plants-in-eu (Accessed: 8 August 2017).

Fotidis, I. A. *et al.* (2013) 'Effect of ammonium and acetate on methanogenic pathway and methanogenic community composition', *FEMS Microbiology Ecology*, 83(1), pp. 38–48. doi: 10.1111/j.1574-6941.2012.01456.x.

Fotidis, I. A., Karakashev, D. and Angelidaki, I. (2013) 'The dominant acetate degradation pathway/methanogenic composition in full-scale anaerobic digesters operating under different ammonia levels', *International Journal of Environmental Science and Technology*, 11(7), pp. 2087–2094. doi: 10.1007/s13762-013-0407-9.

Fu, L., Song, T. and Lu, Y. (2015) 'Snapshot of methanogen sensitivity to temperature in Zoige wetland from Tibetan plateau', *Frontiers in Microbiology*, 6(FEB), pp. 1–9. doi: 10.3389/fmicb.2015.00131.

Fukuzaki, S. *et al.* (1990) 'Inhibition of the fermentation of propionate to methane by hydrogen, acetate, and propionate', *Applied and Environmental Microbiology*, 56(3), pp. 719–723.

Garcia-Robledo, E. *et al.* (2016) 'Micro-scale H2-CO2 dynamics in a hydrogenotrophic methanogenic membrane reactor', *Frontiers in Microbiology*, 7(AUG), pp. 1–10. doi: 10.3389/fmicb.2016.01276.

Gebreeyessus, G. and Jenicek, P. (2016) 'Thermophilic versus Mesophilic Anaerobic Digestion of Sewage Sludge: A Comparative Review', *Bioengineering*, 3(2), p. 15. doi: 10.3390/bioengineering3020015.

Götz, M. *et al.* (2016) 'Renewable Power-to-Gas: A technological and economic review', *Renewable Energy*, pp. 1371–1390. doi: 10.1016/j.renene.2015.07.066.

Grosser, A. (2018) 'Determination of methane potential of mixtures composed of sewage sludge, organic fraction of municipal waste and grease trap sludge using biochemical methane potential assays. A comparison of BMP tests and semi-continuous trial results', *Energy*, 143, pp. 488–499. doi: 10.1016/j.energy.2017.11.010.

Hansen, K. H., Angelidaki, I. and Ahring, B. K. (1998) 'Anaerobic digestion of swine manure: Inhibition by ammonia', *Water Research*, 32(1), pp. 5–12. doi: 10.1016/S0043-1354(97)00201-7.

Hao, L. P. *et al.* (2012) 'Shift of pathways during initiation of thermophilic

methanogenesis at different initial pH', *Bioresource Technology*, 126, pp. 418–424. doi: 10.1016/j.biortech.2011.12.072.

Hawkes, F. R. *et al.* (1994) 'On-line monitoring of anaerobic digestion: application of a device for continuous measurement of bicarbonate alkalinity', *Water Science and Technology*, pp. 1–10.

He, Q. *et al.* (2017) 'Investigation of foaming causes in three mesophilic food waste digesters: Reactor performance and microbial analysis', *Scientific Reports*, 7(1), pp. 1–10. doi: 10.1038/s41598-017-14258-3.

Helm, D. (2017) *Great Britain Cost of Energy Review*.

Ho, D., Jensen, P. and Batstone, D. (2014) 'Effects of temperature and hydraulic retention time on acetotrophic pathways and performance in high-rate sludge digestion', *Environmental Science and Technology*, 48(11), pp. 6468–6476. doi: 10.1021/es500074j.

Holliger, C. *et al.* (2016) 'Towards a standardization of biomethane potential tests', *Water Science and Technology*, 74(11), pp. 2515–2522. doi: 10.2166/wst.2016.336.

Holmes, M. E. *et al.* (2015) 'CO2 and CH4 isotope compositions and production pathways in a tropical peatland', *Global Biogeochemical Cycles*, 29(1), pp. 1–18. doi: 10.1002/2014GB004951.

Horn, M. A. *et al.* (2003) 'Hydrogenotrophic methanogenesis by moderately acid-tolerant methanogens of a methane-emitting acidic peat', *Applied and Environmental Microbiology*, 69(1), pp. 74–83. doi: 10.1128/AEM.69.1.74-83.2003.

Huiliñir, C. *et al.* (2017) 'Biochemical methane potential from sewage sludge: Effect of an aerobic pretreatment and fly ash addition as source of trace elements', *Waste Management*, 64, pp. 140–148. doi: 10.1016/j.wasman.2017.03.023.

IEA (2016) 'Key World Energy Statistics 2016', *Statistics*, p. 80. doi: 10.1787/9789264039537-en.

IEA (2020) *Current limits on hydrogen blending in natural gas networks and gas demand per capita in selected locations*. Available at: https://www.iea.org/data-and-statistics/charts/current-limits-on-hydrogen-blending-in-natural-gas-networks-and-gas-demand-per-capita-in-selected-locations (Accessed: 15 September 2021).

IRENA (2018) *Hydrogen From Renewable Power: Technology outlook for the energy transition*. Available at: www.irena.org.

Jarrell, K. F., Saulnier, M. and Ley, A. (1987) 'Inhibition of methanogenesis in pure cultures by ammonia, fatty acids, and heavy metals, and protection against heavy metal toxicity by sewage sludge', *Canadian Journal of Microbiology*, 33(6), pp. 551–554. doi: 10.1139/m87-093.

Jee, H. A. E. S., Nishio, N. and Nagai, S. (1987) 'Influence of redox potential on biomethanation of H2 and CO2 by Methanobacterium thermoautotrophicum in E(h)-stat batch cultures', *General & Applied Microbiology*, 33, pp. 401–408. doi: 10.2323/jgam.33.401.

Jee, H. S. *et al.* (1987) 'Biomethanation of H2 and CO2 by Methanobacterium thermoautotrophicum in membrane and ceramic bioreactors', *Journal of Fermentation Technology*, 65(4), pp. 413–418. doi: 10.1016/0385-6380(87)90137-3.

Jee, H. S., Nishio, N. and Nagai, S. (1988) 'Continuous methane production from hydrogen and carbon dioxide by Methanobacterium thermoautotrophicum in a fixed-bed reactor', *J. Ferment. Technol.*, 66(2), pp. 235–238. doi: 10.1016/0385-6380(88)90054-4.

Jensen, M. B. *et al.* (2018) 'Venturi-type injection system as a potential H2 mass transfer technology for full-scale in situ biomethanation', *Applied Energy*, 222(October 2017), pp. 840–846. doi: 10.1016/j.apenergy.2018.04.034.

Jensen, M. B., Ottosen, L. D. M. and Kofoed, M. V. W. (2021) 'H2 gas-liquid mass transfer: A key element in biological Power-to-Gas methanation', *Renewable and Sustainable Energy Reviews*, 147, p. 111209. doi: 10.1016/j.rser.2021.111209.

Jerry A. Nathanson (2022) *Wastewater treatment - Sludge treatment and disposal*, *Britannica*. Available at: https://www.britannica.com/technology/wastewater-treatment/Sludge-treatment-and-disposal (Accessed: 6 May 2022).

Ju, D. H. *et al.* (2008) 'Effects of pH conditions on the biological conversion of carbon dioxide to methane in a hollow-fiber membrane biofilm reactor (Hf-MBfR)', *Desalination*, 234(1–3), pp. 409–415. doi: 10.1016/j.desal.2007.09.111.

Jürgensen, L. *et al.* (2015) 'Dynamic biogas upgrading based on the Sabatier process: Thermodynamic and dynamic process simulation', *Bioresource Technology*, 178, pp. 323–329. doi: 10.1016/j.biortech.2014.10.069.

Kanellopoulos, K., Busch, S. and M, D. F. (2022) *Blending hydrogen from electrolysis into the European gas grid*. doi: 10.2760/908387.

Karakashev, D. *et al.* (2006) 'Acetate oxidation is the dominant methanogenic pathway from acetate in the absence of Methanosaetaceae', *Applied and Environmental Microbiology*, 72(7), pp. 5138–5141. doi: 10.1128/AEM.00489-06.

Kayhanian, M. (1994) 'Performance of a high-solids anaerobic digestion process under various ammonia concentrations', *Journal of Chemical Technology & Biotechnology*, 59(4), pp. 349–352. doi: 10.1002/jctb.280590406.

Kayhanian, M. (1999) 'Ammonia inhibition in high-solids biogasification: An overview and practical solutions', *Environmental Technology (United Kingdom)*, 20(4), pp. 355–365. doi: 10.1080/09593332008616828.

Khanh Nguyen, V. *et al.* (2021) 'Review on pretreatment techniques to improve anaerobic digestion of sewage sludge', *Fuel*, 285(August 2020), p. 119105. doi: 10.1016/j.fuel.2020.119105.

Kim, J. H., Chang, W. S. and Pak, D. (2015) 'Factors affecting biological reduction of CO2 into CH4 using a hydrogenotrophic methanogen in a fixed bed reactor', *Korean Journal of Chemical Engineering*, 32(10), pp. 2067–2072. doi: 10.1007/s11814-015-0023-0.

Kotsyurbenko, O. R. *et al.* (2007) 'Shift from acetoclastic to H2-dependent

methanogenesis in a West Siberian peat bog at low pH values and isolation of an acidophilic Methanobacterium strain', *Applied and Environmental Microbiology*, 73(7), pp. 2344–2348. doi: 10.1128/AEM.02413-06.

Kougias, P. G. *et al.* (2017) 'Ex-situ biogas upgrading and enhancement in different reactor systems', *Bioresource Technology*, 225, pp. 429–437. doi: 10.1016/j.biortech.2016.11.124.

Krakat, N. *et al.* (2017) 'Methods of ammonia removal in anaerobic digestion: A review', *Water Science and Technology*, 76(8), pp. 1925–1938. doi: 10.2166/wst.2017.406.

L. E. Ripley, W. C. B. and J. C. C. (1986) 'Improved Alkalimetric Monitoring for Anaerobic Digestion of High-Strength Wastes', *Water Pollution Control Federation*, 58(5), pp. 406–411.

Labatut, R. A., Angenent, L. T. and Scott, N. R. (2014) 'Conventional mesophilic vs. thermophilic anaerobic digestion: Atrade-off between performance and stability?', *Water Research*, 53, pp. 249–258. doi: 10.1016/j.watres.2014.01.035.

Latif, M. A., Mehta, C. M. and Batstone, D. J. (2017) 'Influence of low pH on continuous anaerobic digestion of waste activated sludge', *Water Research*, 113, pp. 42–49. doi: 10.1016/j.watres.2017.02.002.

Lebaz, N. *et al.* (2015) 'Population balance approach for the modelling of enzymatic hydrolysis of cellulose', *Canadian Journal of Chemical Engineering*, 93(2), pp. 276–284. doi: 10.1002/cjce.22088.

Lebranchu, A. *et al.* (2019) 'Pilot-scale biomethanation of cattle manure using dense membranes', *Bioresource Technology*, 284(April), pp. 430–436. doi: 10.1016/j.biortech.2019.03.140.

Lecker, B. *et al.* (2017) 'Biological hydrogen methanation – A review', *Bioresource Technology*, 245(August), pp. 1220–1228. doi: 10.1016/j.biortech.2017.08.176.

Lee, J. C. *et al.* (2012) 'Biological conversion of CO2 to CH4 using hydrogenotrophic methanogen in a fixed bed reactor', *Journal of Chemical Technology and Biotechnology*, 87(6), pp. 844–847. doi: 10.1002/jctb.3787.

Lehner, M. *et al.* (2014) *Power-to-Gas: Technology and Business Models*, *Power-to-Gas: Technology and Business Models*. doi: 10.1007/978-3-319-03995-4.

Leonzio, G. (2016) 'Process analysis of biological Sabatier reaction for bio-methane production', *Chemical Engineering Journal*, 290, pp. 490–498. doi: 10.1016/j.cej.2016.01.068.

Lettinga, G., Rebac, S. and Zeeman, G. (2001) 'Challenge of psychrophilic anaerobic wastewater treatment', *Trends in Biotechnology*, 19(9), pp. 363–370. doi: 10.1016/S0167-7799(01)01701-2.

Li, D. *et al.* (2017) 'Instability mechanisms and early warning indicators for mesophilic anaerobic digestion of vegetable waste', *Bioresource Technology*, 245(13), pp. 90–97. doi: 10.1016/j.biortech.2017.07.098.

Linville, J. L. *et al.* (2016) 'Impact of trace element additives on anaerobic digestion of sewage sludge with in-situ carbon dioxide sequestration', *Process Biochemistry*, 51(9), pp. 1283–1289. doi: 10.1016/j.procbio.2016.06.003.

Luo, G. *et al.* (2012a) 'Simultaneous hydrogen utilization and in situ biogas upgrading in an anaerobic reactor', *Biotechnology and Bioengineering*, 109(4), pp. 1088–1094. doi: 10.1002/bit.24360.

Luo, G. *et al.* (2012b) 'Simultaneous hydrogen utilization and in situ biogas upgrading in an anaerobic reactor', *Biotechnology and Bioengineering*, 109(4), pp. 1088–1094. doi: 10.1002/bit.24360.

Luo, G. and Angelidaki, I. (2012a) 'Co-digestion of manure and whey for in situ biogas upgrading by the addition of H2: Process performance and microbial insights', *Applied Microbiology and Biotechnology*, 97(3), pp. 1373–1381. doi: 10.1007/s00253-012-4547-5.

Luo, G. and Angelidaki, I. (2012b) 'Integrated biogas upgrading and hydrogen utilization in an anaerobic reactor containing enriched hydrogenotrophic methanogenic culture', *Biotechnology and Bioengineering*, 109(11), pp. 2729–2736. doi: 10.1002/bit.24557.

Luo, G. and Angelidaki, I. (2013) 'Hollow fiber membrane based H2 diffusion for efficient in situ biogas upgrading in an anaerobic reactor', *Applied Microbiology and Biotechnology*, 97(8), pp. 3739–3744. doi: 10.1007/s00253-013-4811-3.

Mahdy, A. *et al.* (2017) 'Ammonia tolerant inocula provide a good base for anaerobic digestion of microalgae in third generation biogas process', *Bioresource Technology*, 225, pp. 272–278. doi: 10.1016/j.biortech.2016.11.086.

Martín-González, L., Font, X. and Vicent, T. (2013) 'Alkalinity ratios to identify process imbalances in anaerobic digesters treating source-sorted organic fraction of municipal wastes', *Biochemical Engineering Journal*, 76, pp. 1–5. doi: 10.1016/j.bej.2013.03.016.

Matute, G., Yusta, J. M. and Correas, L. C. (2019) 'Techno-economic modelling of water electrolysers in the range of several MW to provide grid services while generating hydrogen for different applications: A case study in Spain applied to mobility with FCEVs', *International Journal of Hydrogen Energy*, 44(33), pp. 17431–17442. doi: 10.1016/j.ijhydene.2019.05.092.

Mccarty, P. L. and Mckinney, R. E. (1961) 'Salt Toxicity in Anaerobic Digestion', *Water Pollution Control Federation*, 33(4), pp. 399–415. doi: 10.2307/25034396.

McCrone, A. *et al.* (2016) *Global Trends in Renewable Energy investment*, *UNEP's Division of Technology*. Frankfurt. Available at: http://www.actu-environnement.com/media/pdf/news-26477-rapport-pnue-enr.pdf.

McDonagh, S. *et al.* (2018) 'Modelling of a power-to-gas system to predict the levelised cost of energy of an advanced renewable gaseous transport fuel', *Applied Energy*, 215(November 2017), pp. 444–456. doi: 10.1016/j.apenergy.2018.02.019.

McDonald, Z. (2020) *Injecting hydrogen in natural gas grids could provide steady*

demand the sector needs to develop, *ELECTRIC POWER | NATURAL GAS*. Available at: https://www.spglobal.com/platts/en/market-insights/blogs/natural-gas/051920-injecting-hydrogen-in-natural-gas-grids-could-provide-steady-demand-the-sector-needs-to-develop (Accessed: 29 June 2021).

Mesbah, N. M. and Wiegel, J. (2008) 'Life at extreme limits: The anaerobic halophilic alkalithermophiles', *Annals of the New York Academy of Sciences*, 1125(April), pp. 44–57. doi: 10.1196/annals.1419.028.

Michailos, S. *et al.* (2020) 'A techno-economic assessment of implementing power-to-gas systems based on biomethanation in an operating waste water treatment plant', *Journal of Environmental Chemical Engineering*, (November), p. 104735. doi: 10.1016/j.jece.2020.104735.

Miguel, C. V. *et al.* (2015) 'Direct CO2 hydrogenation to methane or methanol from post-combustion exhaust streams - A thermodynamic study', *Journal of Natural Gas Science and Engineering*, 22, pp. 1–8. doi: 10.1016/j.jngse.2014.11.010.

Mulat, D. G. *et al.* (2016) 'Changing Feeding Regimes To Demonstrate Flexible Biogas Production : Effects on Process Performance , Microbial Community Structure , and Methanogenesis Pathways', *Applied and Environmental Microbiology*, 82(2), pp. 438–449. doi: 10.1128/AEM.02320-15.Editor.

NNFCC (2020) *Biogas Map | Anaerobic Digestion*. Available at: https://www.biogas-info.co.uk/resources/biogas-map/ (Accessed: 1 February 2021).

Nord Pool (2016) *Trading Appendix 1 / Clearing Appendix 1 N2EX Physical Market Nord Pool AS*.

Ofgem (no date) *Infographic: Bills, prices and profits | Ofgem*. Available at: https://www.ofgem.gov.uk/publications-and-updates/infographic-bills-prices-and-profits (Accessed: 3 February 2021).

Ohrel, R. L. and Register, K. M. (2006) 'Voluntary Estuary Monitoring Manual', in *Volunteer Estuary Monitoring, A Methods Manual*. Second edi. Washingtong DC: U.S. Environmental Protection Agency Office of Wetlands, Oceans, and Watersheds Volunteer Monitoring, pp. 1–13. Available at: http://water.epa.gov/type/oceb/nep/upload/2009_03_13_estuaries_monitor_chap9.pdf.

Ostrem, K. M., Millrath, K. and Themelis, N. J. (2004) 'Combining Anaerobic Digestion and Waste-to-Energy', *12th Annual North American Waste-to-Energy Conference*, pp. 265–271. doi: 10.1115/NAWTEC12-2231.

Pääkkönen, A., Tolvanen, H. and Rintala, J. (2018) 'Techno-economic analysis of a power to biogas system operated based on fluctuating electricity price', *Renewable Energy*, 117, pp. 166–174. doi: 10.1016/j.renene.2017.10.031.

Pablo-Romero, M. del P. *et al.* (2017) 'An overview of feed-in tariffs, premiums and tenders to promote electricity from biogas in the EU-28', *Renewable and Sustainable Energy Reviews*, 73(January), pp. 1366–1379. doi: 10.1016/j.rser.2017.01.132.

Paudel, S. R. *et al.* (2017) 'Pretreatment of agricultural biomass for anaerobic

digestion: Current state and challenges', *Bioresource Technology*, 245(September), pp. 1194–1205. doi: 10.1016/j.biortech.2017.08.182.

Pauss, A. *et al.* (1990) 'Liquid-to-Gas mass transfer in anaerobic processes: Inevitable transfer limitations of methane and hydrogen in the biomethanation process', *Applied and Environmental Microbiology*, 56(6), pp. 1636–1644.

Peillex, J.-P., Fardeau, M.-L. and Belaich, E.-P. (1990) 'Growth of Methanobacterium thermoautotrophicum on H2-CO2: High CH 4 Productivities in Continuous Culture', *Biomass*, 21, pp. 315–321.

Petersson, A. and Wellinger, A. (2009) *Biogas upgrading technologies–developments and innovations*, *IEA Bioenergy*. doi: 10.1016/j.wasman.2011.09.003.

Polag, D. *et al.* (2015) 'Online monitoring of stable carbon isotopes of methane in anaerobic digestion as a new tool for early warning of process instability', *Bioresource Technology*, 197, pp. 161–170. doi: 10.1016/j.biortech.2015.08.058.

Polizzi, C., Alatriste-Mondragón, F. and Munz, G. (2018) 'The role of organic load and ammonia inhibition in anaerobic digestion of tannery fleshing', *Water Resources and Industry*, 19(April 2017), pp. 25–34. doi: 10.1016/j.wri.2017.12.001.

Rajagopal, R., Massé, D. I. and Singh, G. (2013) 'A critical review on inhibition of anaerobic digestion process by excess ammonia', *Bioresource Technology*, 143, pp. 632–641. doi: 10.1016/j.biortech.2013.06.030.

Raposo, F. *et al.* (2006) 'Influence of inoculum to substrate ratio on the biochemical methane potential of maize in batch tests', *Process Biochemistry*, 41(6), pp. 1444–1450. doi: 10.1016/j.procbio.2006.01.012.

Raposo, F. *et al.* (2012) 'Anaerobic digestion of solid organic substrates in batch mode: An overview relating to methane yields and experimental procedures', *Renewable and Sustainable Energy Reviews*, 16(1), pp. 861–877. doi: 10.1016/j.rser.2011.09.008.

Raposo, F. *et al.* (2013) 'First international comparative study of volatile fatty acids in aqueous samples by chromatographic techniques: Evaluating sources of error', *TrAC - Trends in Analytical Chemistry*, 51, pp. 127–143. doi: 10.1016/j.trac.2013.07.007.

Rebecca Markillie (2013a) *Injection of Hydrogen into the German Gas Distribution Grid | ITM Power*, *ITM Power*. Available at: http://www.itm-power.com/news-item/injection-of-hydrogen-into-the-german-gas-distribution-grid (Accessed: 28 March 2018).

Rebecca Markillie (2013b) *Injection of Hydrogen into the German Gas Distribution Grid | ITM Power*, *ITM Power*. Available at: http://www.itm-power.com/news-item/injection-of-hydrogen-into-the-german-gas-distribution-grid (Accessed: 11 April 2018).

Remigijus Lapinskas (2017) *2017 outlook: A global future for bioenergy*, *Bioenergy Insight Magazine*. Available at: http://www.bioenergy-news.com/display_news/11808/2017_outlook_a_global_future_for_bioenergy/ (Accessed: 16 July 2017).

Rittmann, S., Seifert, A. and Herwig, C. (2015) 'Essential prerequisites for successful bioprocess development of biological CH 4 production from CO 2 and H 2', *Critical Reviews in Biotechnology*, 32(September), pp. 141–151. doi: 10.3109/07388551.2013.820685.

Savvas, S. *et al.* (2017) 'Biological methanation of CO2 in a novel biofilm plug-flow reactor: A high rate and low parasitic energy process', *Applied Energy*, 202, pp. 238–247. doi: 10.1016/j.apenergy.2017.05.134.

Schmidt, J. E. and Ahring, B. K. (1993) 'Effects of hydrogen and formate on the degradation of propionate and butyrate in thermophilic granules from an upflow anaerobic sludge blanket reactor', *Applied and Environmental Microbiology*, 59(8), pp. 2546–2551.

Schmidt, O. *et al.* (2017) 'Future cost and performance of water electrolysis: An expert elicitation study', *International Journal of Hydrogen Energy*, 42(52), pp. 30470–30492. doi: 10.1016/j.ijhydene.2017.10.045.

Schnürer, A. and Nordberg, Å. (2008) 'Ammonia, a selective agent for methane production by syntrophic acetate oxidation at mesophilic temperature', *Water Science and Technology*, 57(5), pp. 735–740. doi: 10.2166/wst.2008.097.

Schunurer, A. and Jarvis, A. (2009) 'Microbiological Handbook for Biogas Plants', *Waste Management*, p. 138.

Seifert, A. H., Rittmann, S. and Herwig, C. (2014) 'Analysis of process related factors to increase volumetric productivity and quality of biomethane with Methanothermobacter marburgensis', *Applied Energy*, 132, pp. 155–162. doi: 10.1016/j.apenergy.2014.07.002.

Siriwongrungson, V., Zeng, R. J. and Angelidaki, I. (2007) 'Homoacetogenesis as the alternative pathway for H2 sink during thermophilic anaerobic degradation of butyrate under suppressed methanogenesis', *Water Research*, 41(18), pp. 4204–4210. doi: 10.1016/j.watres.2007.05.037.

SKM Enviros (2011) *Department of Energy and Climate Change COMBUSTION FOR HEAT , ELECTRICITY AND TRANSPORT AND BIOMETHANE PRODUCTION Department of Energy and Climate Change*.

Smolinka, T. (2011) 'WATER ELECTROLYSER FOR HYDROGEN STORAGE SYSTEMS – STUDY ON STATE OF THE ART OF THE technology and future development trends', (Ihres).

Statista (2020) *United Kingdom: Inflation rate from 1986 to 2026*.

Steele, P. (2019) *Agile pricing explained | Octopus Energy*. Available at: https://octopus.energy/blog/agile-pricing-explained/ (Accessed: 3 February 2021).

Strömberg, S., Nistor, M. and Liu, J. (2014) 'Towards eliminating systematic errors caused by the experimental conditions in Biochemical Methane Potential (BMP) tests', *Waste Management*, 34(11), pp. 1939–1948. doi: 10.1016/j.wasman.2014.07.018.

Sustainable Agribusiness Forum (2020) *The number and total capacity of biogas*

plants in Europe continued to grow. Available at: https://saf.org.ua/en/news/906/ (Accessed: 8 January 2022).

Svensson, K. *et al.* (2018) 'Feeding frequency influences process performance and microbial community composition in anaerobic digesters treating steam exploded food waste', *Bioresource Technology*, 269(August), pp. 276–284. doi: 10.1016/j.biortech.2018.08.096.

Szuhaj, M. *et al.* (2016) 'Conversion of H2 and CO2 to CH4 and acetate in fed-batch biogas reactors by mixed biogas community: a novel route for the power-to-gas concept', *Biotechnol Biofuels*, 9, p. 102. doi: 10.1186/s13068-016-0515-0.

Taherzadeh, M. J. and Karimi, K. (2008) *Pretreatment of lignocellulosic wastes to improve ethanol and biogas production: A review*, *International Journal of Molecular Sciences*. doi: 10.3390/ijms9091621.

Tanimu, M. I. *et al.* (2014) 'Effect of Carbon to Nitrogen Ratio of Food Waste on Biogas Methane Production in a Batch Mesophilic Anaerobic Digester', *International Journal of Innovation, Management and Technology*, 5(2), pp. 116–119. doi: 10.7763/IJIMT.2014.V5.497.

Tao, B. *et al.* (2019) 'Simultaneous biomethanisation of endogenous and imported CO2 in organically loaded anaerobic digesters', *Applied Energy*, 247(March), pp. 670–681. doi: 10.1016/j.apenergy.2019.04.058.

Tao, B. *et al.* (2020) 'Predicting pH rise as a control measure for integration of CO2 biomethanisation with anaerobic digestion', *Applied Energy*, 277(April), p. 115535. doi: 10.1016/j.apenergy.2020.115535.

Thema, M. *et al.* (2019) 'Biological CO2-methanation: An approach to standardization', *Energies*, 12(9), pp. 0–32. doi: 10.3390/en12091670.

Tian, G. *et al.* (2020) 'Characteristics and mechanisms of H2S production in anaerobic digestion of food waste', *Science of the Total Environment*, 724, p. 137977. doi: 10.1016/j.scitotenv.2020.137977.

TNO Biobased and Circular Technologies (2022) *Phyllis2: Database for the physico-chemical composition of (treated) lignocellulosic biomass, micro- and macroalgae, various feedstocks for biogas production and biochar*. Available at: https://phyllis.nl/ (Accessed: 23 January 2022).

Tom, Q. and Andrew, P. (2017) *Household Food Waste in the UK, 2015*, *Wrap*. Available at: http://www.wrap.org.uk/sites/files/wrap/Household_food_waste_in_the_UK_2015_Report.pdf.

Tom, Q. and Hannah, J. (2009) *Household Food and Drink Waste in the UK 2007*. Wrap. Available at: www.wrap.org.uk/foodanddrinkwaste.

UK Houses of Parliament (2017) *Decarbonising the Gas Network*. Available at: www.parliament.uk/post.

Usack, J. G., Spirito, C. M. and Angenent, L. T. (2012) 'Continuously-stirred Anaerobic Digester to Convert Organic Wastes into Biogas: System Setup and Basic Operation',

Journal of Visualized Experiments, (65), pp. 1–9. doi: 10.3791/3978.

Vo, T. T. Q. *et al.* (2018) 'Techno-economic analysis of biogas upgrading via amine scrubber, carbon capture and ex-situ methanation', *Applied Energy*, 212(November 2017), pp. 1191–1202. doi: 10.1016/j.apenergy.2017.12.099.

Voelklein, M. A. *et al.* (2016) 'Assessment of increasing loading rate on two-stage digestion of food waste', *Bioresource Technology*, 202, pp. 172–180. doi: 10.1016/j.biortech.2015.12.001.

Voelklein, M. A., Rusmanis, D. and Murphy, J. D. (2019) 'Biological methanation : Strategies for in-situ and ex-situ upgrading in anaerobic digestion', *Applied Energy*, 235(October 2018), pp. 1061–1071. doi: 10.1016/j.apenergy.2018.11.006.

Wahid, R. and Horn, S. J. (2021) 'The effect of mixing rate and gas recirculation on biological CO2 methanation in two-stage CSTR systems', *Biomass and Bioenergy*, 144(November 2020), p. 105918. doi: 10.1016/j.biombioe.2020.105918.

Wang, B. *et al.* (2014) 'Determination of methane yield of cellulose using different experimental setups', *Water Science and Technology*, 70(4), pp. 599–604. doi: 10.2166/wst.2014.275.

Wang, H., Fotidis, I. A. and Angelidaki, I. (2015) 'Ammonia effect on hydrogenotrophic methanogens and syntrophic acetate-oxidizing bacteria', *FEMS Microbiology Ecology*, 91(11), pp. 1–8. doi: 10.1093/femsec/fiv130.

Wang, W. *et al.* (2013) 'Performance and microbial community analysis of the anaerobic reactor with coke oven gas biomethanation and in situ biogas upgrading', *Bioresource Technology*, 146, pp. 234–239. doi: 10.1016/j.biortech.2013.07.049.

Wang, X. *et al.* (2014) 'Effects of temperature and Carbon-Nitrogen (C/N) ratio on the performance of anaerobic co-digestion of dairy manure, chicken manure and rice straw: Focusing on ammonia inhibition', *PLoS ONE*, 9(5), pp. 1–7. doi: 10.1371/journal.pone.0097265.

Wang, X. *et al.* (2018) 'Evaluation of artificial neural network models for online monitoring of alkalinity in anaerobic co-digestion system', *Biochemical Engineering Journal*, 140(August), pp. 85–92. doi: 10.1016/j.bej.2018.09.010.

Westerholm, M., Levén, L. and Schnürer, A. (2012) 'Bioaugmentation of syntrophic acetate-oxidizing culture in biogas reactors exposed to increasing levels of ammonia', *Applied and Environmental Microbiology*, 78(21), pp. 7619–7625. doi: 10.1128/AEM.01637-12.

Xu, F. *et al.* (2018) 'Anaerobic digestion of food waste – Challenges and opportunities', *Bioresource Technology*, 247(September 2017), pp. 1047–1058. doi: 10.1016/j.biortech.2017.09.020.

Xu, H. *et al.* (2015) 'High-rate hydrogenotrophic methanogenesis for biogas upgrading: the role of anaerobic granules.', *Environmental technology*, 36(1–4), pp. 529–37. doi: 10.1080/09593330.2014.979886.

Yang, P. *et al.* (2021) 'Foaming mechanisms and control strategies during the anaerobic digestion of organic waste: A critical review', *Science of the Total*

Environment, 779(174). doi: 10.1016/j.scitotenv.2021.146531.

Yang, S.-L. *et al.* (2015) 'Effect of sulfate addition on methane production and sulfate reduction in a mesophilic acetate-fed anaerobic reactor', *Applied Microbiology and Biotechnology*, 99(7), pp. 3269–3277. doi: 10.1007/s00253-014-6235-0.

Yenigün, O. and Demirel, B. (2013) 'Ammonia inhibition in anaerobic digestion: A review', *Process Biochemistry*, 48(5–6), pp. 901–911. doi: 10.1016/j.procbio.2013.04.012.

Yu, D. *et al.* (2016) 'Biogas-pH automation control strategy for optimizing organic loading rate of anaerobic membrane bioreactor treating high COD wastewater', *Bioresource Technology*, 203, pp. 62–70. doi: 10.1016/j.biortech.2015.12.010.

Zamanzadeh, M. *et al.* (2016) 'Anaerobic digestion of food waste - Effect of recirculation and temperature on performance and microbiology', *Water Research*, 96, pp. 246–254. doi: 10.1016/j.watres.2016.03.058.

Zhang, C. *et al.* (2014) 'Reviewing the anaerobic digestion of food waste for biogas production', *Renewable and Sustainable Energy Reviews*, 38, pp. 383–392. doi: 10.1016/j.rser.2014.05.038.